Title	Design and development of polymeric transfection vectors for gene delivery in Recessive Dystrophic Epidermolysis Bullosa
Author(s)	Aied, Ahmed
Publication Date	2014-07-23
Item record	http://hdl.handle.net/10379/4569

Design and Development of Polymeric Transfection Vectors for Gene Delivery in Recessive Dystrophic Epidermolysis Bullosa

A thesis submitted to the National University of Ireland for the degree of Doctor of Philosophy

By

Ahmed Aied

April 2014

Network of Excellence for Functional Biomaterials

National University of Ireland, Galway

Research Supervisor: Doctor Wenxin Wang

TABLE OF CONTENTS

Chapter 3: Polymer transfection efficiency analysis *in vitro*

LIST OF APPENDICES

LIST OF FIGURES

Chapter 5

LIST OF TABLES

ACKNOWLEDGEMENTS

ABBREVIATIONS

AA	Ascorbic Acid
ADA-SCID	Adenosine deaminase - severe combined immunodeficiency
ANOVA	Analysis of variance
ATRP	Atom transfer radical polymerization
BMZ (DEJ)	Basement membrane zone
Br	Bromine
CAGR	Compound Annual Growth Rate
C7	Collagen VII
C4	Collagen IV
Cl	Chloride
CMV	Cytomegalovirus
Col7α1	Collagen VII alpha 1 gene
Col7α1-/-	Collagen VII null/knockout mouse
CPPs	Cell penetrating peptides
CTL	Cytotoxic T lymphocyte
DAPI	4', 6-diamidino-2-phenylindole
DE-ATRP	Deactivation-Enhanced Atom Transfer Radical Polymerisation
DMAEMA	Dimethylamino ethyl mythacrylate
DMD	Multi-knot polymer
DMF	Dimethylformamide
DMSO	Dimethyl sulfoxide
EB	Epidermolysis Bullosa
EBIB	ethylbromoisobutyrate
EDC	ethyl(dimethylaminopropyl) carbodiimide
EEPs	Endosomal escape peptides
EGDMA	Ethylene glycol dimethyl amine
FDA	Food and drug administration
FACS	Fluorescence-activated cell sorting
GAPDH	Glyceraldehyde 3-phosphate dehydrogenase

GAG	Glycoaminoglycan
GPC	Gel Permeation chromatography
hADSCs	human adipose-derived stem cells
HD	heterozygote
HeLa	Henrietta lacks cells (cervical cancer cell line)
HIV	Human immunodeficiency virus
His-LPIE	Histidinylated linear PEI
HM_w	High molecular weight
HPAE	Hyper branched poly (β-amino esters)
HPMA	N-(2-Hydroxypropyl) methacrylamide
HSV	Herpes simplex virus
INF7	Interferon 7
kDa	kilo daltons
LAM-β3	Laminin beta 3
LDL	Low density lipoprotein
LM_w	Low molecular weight
LSCT	Lower critical solution temperature
MLV	Marine leukaemia virus
MVM	Multivinyl monomer
NC1	Non collagenous domain 1
NF_kB	Nuclear factor kappa-light-chain-enhancer of activated B cells
NLS	Nuclear localizing signal
NMR	Nuclear magnetic resonance
N/P	Nitrogen to Phosphate ratio
PAMAM	Poly (amidoamine)
PBS	Phosphate buffered saline
PEEDEPE	2-{[2-(prop-2-enoyloxy) ethyl] disulfanyl-4-ethyl prop-2-enoate
PEG	Polyethylene glycol
PEI	Polyethyleneimine
PG	PicoGreen®

PFA	Paraformaldehyde
PTC	Premature termination codons
rAAV	Adeno-associated retroviral vectors
RAFT	Reversible addition-fragmentation chain Transfer
RDEB	Recessive dystrophic epidermolysis bullosa
SD	Standard deviation
SCC	Squamous cell carcinoma
SEs	Skin equivalents
siRNA	Small interfering RNA
SV40	Simian vacuolating virus 40
TEM	Transmission electron microscopy
tRNA	Transfer RNA
WT	Wild type animal

ABSTRACT

Recessive Dystrophic Epidermolysis Bullosa (RDEB) is caused by mutations in the collagen VII gene (COL7A1) that lead to an alteration of function or a reduction in the amounts of collagen VII protein (C7). Any of these mutations will impair C7 assembly into anchoring fibrils that anchor the basement membrane zone (BMZ) to the underlying dermis. This in turn causes reduced skin resistance to mild trauma making the patients suffer from severe blistering and scarring in the skin and mucosa. Intensive efforts are being made to restore the anchoring protein at the BMZ as a means of providing a lasting cure for the disease. One of the methods examined as potential therapy utilizes viral vectors for genetic correction of the C7 expressing cells. However, toxicity and immunogenicity concerns have halted progress using viral vectors for gene therapy in many clinical trials. As a result, non-viral methods of delivery have attracted great interest as a replacement. The overall aim of this project was to develop a safe and efficient polymer based gene delivery method to encourage the production of functional C7 protein and restore the mechanical stability at the BMZ in RDEB mouse skin. We focused on one of the more versatile methods of non-viral based delivery that utilizes a dense polycation synthesized from deactivation-enhanced atom transfer radical polymerisation (multi-knot) or Michael addition (hyperbranched poly (β-amino ester)). The polymers were created to deliver the therapeutic C7 plasmid DNA to RDEB keratinocytes and fibroblasts. The focus was mainly on keratinocytes and fibroblasts since they are the predominant cells found in the upper dermis and epidermis, and perhaps contribute more to C7 expression than any other group of cells. Using specially designed cationic polymers, we were able to restore some of the C7 expression *in vitro* and in RDEB skin equivalents (SEs) (3D organ cultures). SEs are being used to test for toxicity and effectiveness of many drugs, reducing the need for pre-clinical trials. Unfortunately, SEs do not fully replicate natural tissues, because they lack the complexity and array of cells and proteins found in natural tissue. In addition, the presence of immune response capability and blood circulation in pre-clinical models will give a more accurate account of the drug's safety. This encouraged us to test the effectiveness of polymer vectors for COL7A1 delivery in an *in vivo* pre-clinical model of RDEB. We used Col7α1 null RDEB (Col7α1-/-) knockout mice

(developed from immune-competent mice by targeted inactivation of Col7α1) to test our hypothesis. Clinically, these mice showed severe blistering and detachment of the epidermis from the dermis after birth similar to the human phenotype. We successfully observed expression of the therapeutic transgene product (C7) in the mice after intradermal injection of the HPAE/COL7A1 complex into the mouse paws and ventral region, although there was a noticeable inflammatory response around the injected area. This new approach has proved that it is possible to restore the expression of the missing protein C7 in RDEB skin using a polymer based gene delivery. Full restoration of the skin's mechanical stability requires further investigation into the delivery system, areas of injection and addressing the adverse effects of the delivery agents.

CHAPTER 1

Introduction

1.1. Recessive Dystrophic Epidermolysis Bullosa

1.1.1. Background

The term epidermolysis bullosa (EB) describes a group of 30 different clinical entities characterized by the mechanical fragility of the epithelial tissue leading to blistering and formation of open and non-healing wounds [1]. Classification of the EB subtypes is based on the identification of the distinct differences in the ultrastructural components of the blisters [2]. Although the subtypes can be hard to distinguish at the initial inspection, there are more than 13 genes involved in all the different clinical forms of EB [3-6]. The final classification is based on the mode of inheritance which can be dominant or recessive, of which the latter is the more severe.

Recessive dystrophic epidermolysis bullosa (RDEB), of which severe generalized RDEB-sv is the most common, is characterized by the severe blistering and scarring of the skin. The disease manifests at birth or during neonatal development with an estimated prevalence of less than 1 per million worldwide [7]. The blisters are not limited to the skin but spread to the oral and gastrointestinal regions. Joint contractures further limit the movement of the limbs while dental caries and esophageal strictures are frequent. All these factors, especially the oral, esophageal and anal involvement, induce a state of chronic malnutrition which contributes to growth retardation typical of the disease. Another serious complication is the development of squamous cell carcinoma (SCC) [8] which is the leading cause of death among RDEB patients that survive into adulthood. As a result, most patients have life expectancies lower than half of that of an average person. The disease is incurable and management is preventive. Protective padding is used to reduce trauma and blistering to the skin and routine wound care is necessary to prevent scarring. Iron deficiency and anemia are improved with iron supplements and transfusions. In some cases surgery is required to treat severe deformities or SCC.

RDEB is caused by mutations in the collagen VII gene (COL7A1) [9, 10] that lead to an alteration of function or a reduction in the amounts of collagen VII protein (C7). This impairs collagen VII assembly into

anchoring fibrils that anchor the basement membrane to the underlying dermis. This in turn causes reduced skin resistance to mild trauma (Figure 1.1). A range of mutations are responsible for RDEB which may result in expression of full length C7 variants with altered stability and/or function or non-expression caused by the premature termination codons (PTCs).

Collagen VII alpha 1 (COL7A1) is an 8.8kb coding sequence segmented into 118 axons and codes for C7 protein [11]. The protein is composed of three identical alpha 1 chains characterized by Gly-x-y amino acid sequences. These are flanked by a large 145kDa amino terminal non-collagenous domain (NC1) and a small 34kDa carboxyl-terminal non-collagenous domain (NC2). In the extracellular space, C7 forms anti-parallel dimers stabilized by disulfide bonds. The dimers aggregate laterally to form anchoring fibrils with large globular NC1 domains at both ends of the structure and extend from the lamina densa to the underlying dermis immobilizing the epithelia to the underlying dermis [12].
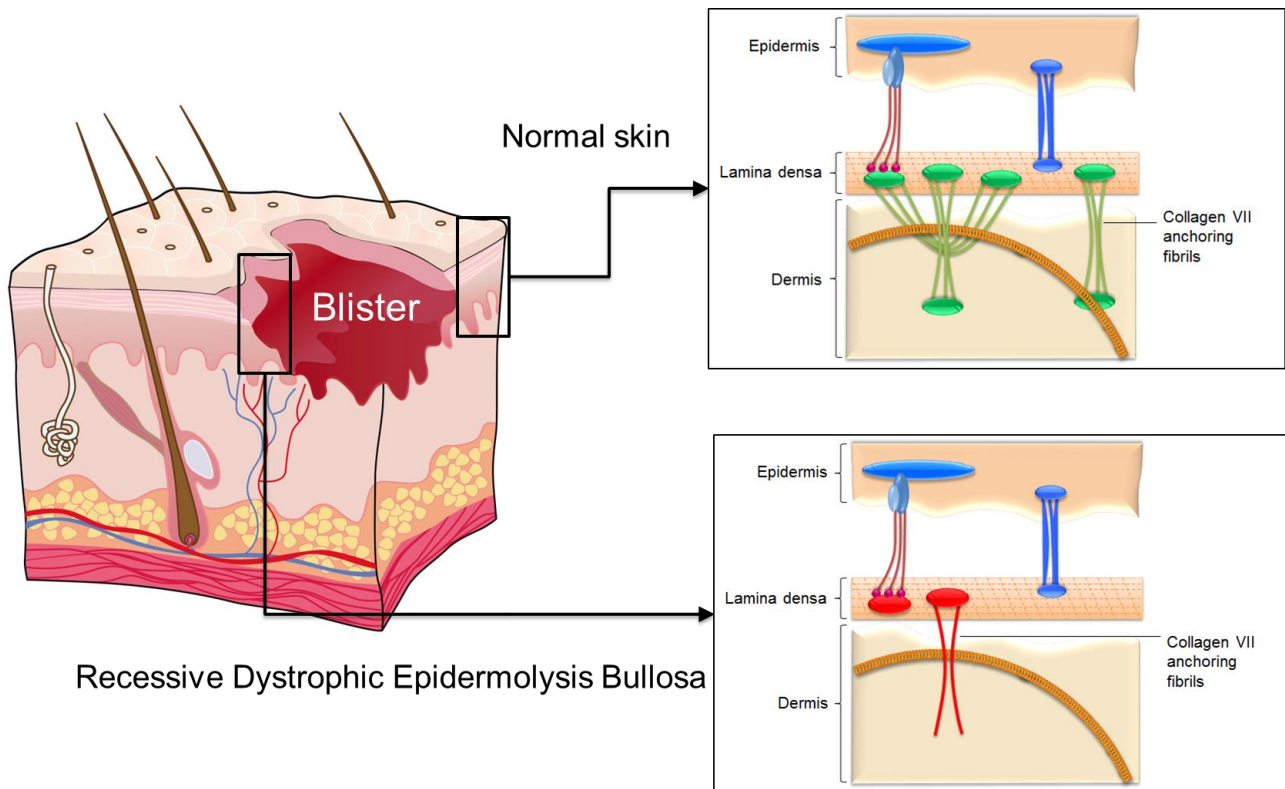
Figure 1.1: Schematic comparison between normal and RDEB skin at the ultrastructural level. In normal skin, functional C7 assembles into fibrils that anchor the lamina densa to the dermis. In RDEB skin, mutations in the COL7A1 gene produce impaired or lower amounts of C7 which increases the chances of detachment of the lamina densa and epidermis from the dermis.

1.1.2. Current progress in RDEB therapy

With no current effective cure for RDEB, interest in the disease has increased rapidly over the years with many approaches being proposed, from genetic correction to direct protein delivery (Table 1.1). *Ex vivo* genetic correction is one indirect method that has been investigated because it provides more controlled environment for gene delivery. Gene corrected keratinocytes and fibroblasts have successfully been used to generate skin equivalents capable of restoring C7 in the basement membrane zone (BMZ) and subsequently adhering the epidermis to the underlying dermis in mice [13]. Similarly, epidermal grafts generated from genetically corrected epidermal stem cells restored LAM-β3 in a patient with junctional EB [14]. Success with gene therapy has been limited mainly due to delivery issues and risks of insertional mutagenesis which was observed in some clinical trials [15]. Alternatively, direct intradermal injection of allogeneic fibroblasts into RDEB patients has been examined and the results showed increased levels of C7 although its capability to form functional anchoring fibrils was not confirmed [16]. More encouraging results were obtained from bone marrow transplantation of allogeneic stem cells in young RDEB patients. Five out of seven patients who received the treatment showed increased C7 deposition and sustained presence of donor cells, but two died because of toxicity issues [17]. The most direct approach is the intradermal injection of the recombinant protein, which has shown promising results, and is currently being tested on RDEB patients.

To date, there has been little to no effective method of treatment of the disease while clinical prevention is limited to wound care. Here we look at the potential of cationic polymers as delivery agents for genetic correction of RDEB by direct *in situ* application. Before that, we give a brief background on gene therapy; discuss the various viral delivery methods, and evaluate the hurdles facing polymer gene delivery today.

Table 1.1: The major reported milestones in RDEB research.

Year of publication	Lead author(s)	Model	Therapy type	Journal	Findings	Reference
1986-7	Sakai Keene	-	-	The Journal of Cell Biology	C7 is the major structural component of anchoring fibrils	[18, 19]
1992	Ryynänen	-	-	Journal of Investigative Dermatology	Expression of C7 is mainly found in epidermal keratinocytes	[20]
1991	Uitto	Human	-	Proceedings of the National Academy of Sciences USA	First mapping of the COL7A1 gene	[10]
1999	Uitto	Human	-	Matrix Biology	Mutation analysis of EB	[21]
2000	O'Toole, Woodley	Human DEB keratinocytes	Retrovirus	The Journal of Biological Chemistry	First minigene C7	[22]
2000	Cheah	Transgenic mice	Injection	Gene Therapy	First whole C7 gene therapy	[23]
2002	Barrandon	RDEB keratinocytes	Microinjection	Human Gene Therapy	Firs PAC derived C7 therapy	[24]
2002	Khavari	SCID Mice	phi C31 bacteriophage integrase	Nature Medicine	First phi C31 bacteriophage integrase therapy	[25]
2002	Woodley	SCID Mice	Lentivirus	Nature Genetics	First lentiviral vector delivery of whole C7	[26]
2003	Khavari	SCID Mice	Corrected fibroblasts	Journal of Clinical Investigation	First fibroblast cell therapy	[27]
2003	Meneguzzi	RDEB Dog	Retrovirus	Human Molecular Genetics	First canine therapy	[28]
2003	Chen, Woodley	SEs on SCID mice	Normal/corrected Fibroblasts	Journal of Investigative Dermatology	First RDEB organotypic culture	[29]
2004	Chen, Woodley	SEs on SCID mice	C7 protein injection	Nature Medicine	First C7 protein injection	[30]
2004	Chen, Woodley	SEs on nude SCID mice	SIN-lentivirus	Molecular Therapy	Combination of viral gene therapy and organoypic cultures	[31]
2004	Meneguzzi	SEs	Retrovirus	Human Gene Therapy	First retroviral therapy on SEs	[32]
2006	Shimizu	Nude Rats	Retrovirus corrected RDEB fibroblasts	Journal of Investigative Dermatology	Showed fibroblasts can express more C7 than keratinocytes in-vivo	[33]
2007	Chen, Woodley	SCID Mice	Intravenously injected human fibroblasts	Molecular Therapy	First intervenous injection cell therapy	[34]

2008	McGrath	Humans with RDEB (5)	Intradermal injection of fibroblasts extracted from unaffected arease	Journal of Investigative Dermatology	First human fibroblast therapy	[16]
2009	Balzar	Mouse	Wild type bone marrow transplantation	Blood	First study with bone marrow WT	[35]
2009	Chen, Uitto, Woodley	C7 null mice	C7 protein injection	Molecular Therapy	-	[36]
2009	Bruckner-Tuderman	Collagen VII hypomprph mouse model	Intradermal injection of RDEB fibroblast (WT)	Molecular Therapy	-	[37]
2009	Shimizu	C7 knockout mouse	Rescue by cross breeding	American Journal of Pathology	C7 knockout mouse rescued by cross breeding with heterozygous mouse expressing human C7	[38]
2010	Hovnanian	SEs	SIN Retrovirus	Molecular Therapy	RDEBKs and RDEBFs corrected with SIN retrovirus	[13]
2010	Khavari	SEs grafted on SCID mice	Retrovirus	Human Gene Therapy	-	[39]
2010	Meneguzzi, Buer	SEs	Retroviral transduction of tran-spliced C7 DNA	Journal of Investigative Dermatology	Selected populations were used to develop SEs	[40]
2010	Tolar	Human patients with RDEB	Bone marrow transplantation	New England Journal of Medicine	5 out of seven patients survived with some progression	[41]
2011	Blazar	SEs	Corrected RDEB iPS cells	Journal of Investigative Dermatology	RDEB reverted to iPS developed normal human SEs	[42]
2011	Meneguzzi	RDEB Dog	Corrected RDEB keratinocytes	Journal of Investigative Dermatology	Corrected RDEB cells used to generate SEs grafted onto back of SCID mice	[43]
2013	Chen	SEs on SCID mice	Topical application of recombinant type VII collagen VII onto wounds	Molecular Therapy	applying rC7 onto RDEB grafts with wounds restored C7 and anchoring fibrils (AFs) at the DEJ	[44]

1.2. Gene therapy

Gene therapy has been hailed as the new breakthrough in molecular medicine as it allows the treatment of diseases at the genetic level. It involves the insertion of therapeutic genes in individual's cells or tissues to treat genetic diseases in which deleterious genetic mutations have occurred. The first gene therapy trial was carried out in 1990 at the National Institutes of Health clinical center using a retrovirus to genetically correct white blood cells into producing adenosine deaminase *in vitro*. Gene therapy has the potential to treat many other diseases including cystic fibrosis, low density lipoprotein (LDL)-receptor deficiency, haemophilia A and B, alpha-1-antitrypsin deficiency, and Gaucher's disease, many malignancies and viral infections such as Acquired Immunodeficiency Syndrome [45]. Although viral vectors are the most efficient nanoparticles for gene delivery, there is still a big concern over safety to patients, as viral vectors tend to replicate and invade other tissues and organs leading to immunogenicity and toxicity. The death of an arthritis patient after gene therapy clinical trial has prompted the United States Food and Drug Administration (FDA) to halt any further clinical trials using viral vectors. This was a major drawback for the gene therapy field, which shifted the focus to non-viral approaches. Since then, a variety of non-viral approaches have been developed, including (but not limited to): naked DNA, gene gun, liposomes, polycations and electroporation [46].

1.3.   Viral gene delivery

Since the discovery of the role of chromosomal DNA as a main storage information unit that codes for most life forms, it was hypothesized that by replacing protein coding regions of the chromosome in inherent or acquired diseases, it is possible to reprogram the cell into producing normal functional proteins that can reverse the disease [47]. Effective delivery to the cells and nucleus has been the sole challenge for achieving successful gene therapy in many diseases. At the forefront of methods used for delivery, are modified viruses (viral vectors).

Viruses are capable of infecting their host with high efficiency because of their unique structure and composition. A virus is mainly made of two or three components depending on its origin. Firstly, all viruses carry a DNA or RNA sequence known as the viral genome. This can be regarded as the most important viral component. Secondly, a protein cover, known as capsid, encapsulates the viral genome to protect it from enzymatic degradation. In some viruses, such as the retrovirus, a third component, made from host cell lipid bilayer, coats the capsid and can have glycoproteins which helps the virus to identify specific cells by binding to the cellular membrane receptors [48]. Naturally occurring strains will infect their host by depositing their viral genome into the host's cells and change the genomic configuration of the cell making it a temporary virus factory. It's not the fact that viruses can replicate in cells that drew the attention of scientists, but the way these viruses are capable of effectively overcoming the cellular barriers, infect a wide range of cells, and force the cells into producing new proteins. This concept is the basis of gene therapy and has been for more than 20 years [49]. The first successful viral transduction based gene therapy trial took place in 1990 to cure a four year old patient from ADA-SCID, a severe immunodeficiency disease [50]. Since then, over 600 clinical trials involving viral vectors have been carried out with the majority of them being successful.

1.3.1. From virus to viral vector

To harness the transduction efficiency of viruses without inducing widespread infection and immunogenicity, all sequences that give the virus its replication capability after transduction have to be removed [51, 52]. The transgenic expression cassette is then cloned into the genome to create the first construct known as the viral genome. This is flanked by inverted terminal repeats and *cis* acting sequences required for genome encapsulation. The second construct contains the sequences that code for viral structural proteins and proteins that are required for replication of the vector DNA. All of which are produced and expressed by the packaging cell [53].

1.3.2. Types of viruses

Retroviral vectors

Retroviruses belong to the viral family *retroviridae* and carry genetic material in the form of RNA. Structurally, these viruses are encapsidated and enveloped with a loading capacity between 8-11kb of genetic material depending on the type of virus. The RNA carried by this virus is transcribed into DNA upon cellular infection which is then integrated into the host genome allowing for persistent and lasting protein expression which is one of the major advantages of retroviral vectors [54]. However, the risk of oncogenesis is substantial in some cases due to their DNA integrating potential that can result in insertional mutagenesis [55]. In addition, they are only capable of transducing dividing cells, which limits their application in clinical settings. Murine Leukemia Virus (MLV) based γ-retroviral vectors were used successfully to treat immunodeficiency disorders [56]. However, complications from adverse oncogenesis caused by retroviral vector integration into target genome [57] led to a decline in their applications especially after the development in other types of viral vectors such as lentiviral vectors.

Lentiviral vectors

Like retroviral vectors, lentiviral vectors are enveloped and carry genetic material in the form of RNA, in fact, they carry two RNA molecules in

addition to enzymes including protease, RNase, integrase and reverse transcriptase. The first lentiviral vectors were developed based on the HIV-1 virus but other viruses soon emerged from various strains including simian immunodeficiency virus and non-primate viruses such as the visna virus. Their popularity stems from their capability of transducing non-dividing cells with high efficiency, but like retroviral vectors, they can only carry small RNA molecules (~8kb).

Herpes simplex viral vectors (HSV)

HSV belongs to the family herpeviridae of which HSV-1 is the most used for gene therapy and is characterized by its high transduction efficiency in sensory neurons. Although the transduction is episomal (because HSV's carry genetic material in the form of dsDNA), gene expression is persistent in neuronal cells. Another advantage of vectors from HSV is the gene packaging capacity which can range from 40kb-150kb, substantially greater than other viral vectors. HSV-1 replication-defective vectors have been successfully tested for the treatment of epilepsy, [58] chronic pain (in phase I clinical trial), [59] and many other neuropathological disorders. Exploration of immune response, however, yielded induction of innate and adaptive immune responses in HSV infected hosts [60].

Adenoviral vectors

Adenoviruses were first isolated from adenoid tissue in 1953 with more than 50 serotypes being identified since. Their genome is composed of double-stranded DNA like HSV-1 viruses but can only carry between 30-40 kb. They can transduce a broad range of cell types by episomal transduction with very high efficiency. The major problem with adenoviruses is that they induce potent toxicity and immune response caused by both, their capsids and gene products; this is especially true in early generation vectors. High efficiency adenoviral vectors have been extensively used in the treatment of many cancers in humans through targeted suicide gene therapy. Among the clinical targets being investigated on human patients are prostate cancer [61] head and neck cancer renal cell carcinoma, and chronic lymphocytic leukemia [62].

Recombinant *adeno-associated viral vectors (rAAV)*

Adeno-associated viral vectors carry genetic material in the form of single stranded DNA which is less than 5kb in length. They can transfect a broad range of cell types including non-dividing cells and achieve integrated transduction (<10%) at a specific site on chromosome 19 with near 100% certainty. Because these vectors completely lack viral genomes they are considered non-inflammatory and non-pathogenic but very difficult to produce. rAAV is defective which means co-transfection with a helper virus is required (e.g. adenovirus). Delivery of these vectors to mouse muscle showed no cytotoxic T lymphocyte (CTL) response or CD4+ T helper activation [63]. However, intraperitoneal, intravenous and subcutaneous administration all lead to significant CTL response. Despite these findings, rAAVs have been successfully used to correct the behavior of rodent models with Parkinson's disease for up to 12 months [64].

Table 1.2: The five most common types of viral vectors used in gene therapy and their characteristics.

Viral vector	Genetic material	Integration	Capacity	Toxicity	dividing/non-dividing cells
Lentivirus	RNA	Yes	8kb	-	Both
Retrovirus	RNA	Yes	8kb	-	Dividing cells only
Adeno-associated virus	ssDNA	No	5kb	-	Both
Adenovirus	dsDNA	No	30kb	+	Both
Herpes-simplex virus	dsDNA	No	40kb	++	High efficiency in neuronal cells

1.4. Polymer based gene delivery

The immunogenic and cytotoxic fallout of viral vectors led to the emergence of cationic polymers specifically synthesized for gene delivery, of which, Polyethylinimine (PEI) showed the greatest promise [65]. However, it was quickly realized that PEI had major drawbacks, including high toxicity [66-68] attributed to its high cationic charge and limited transfection efficiency in non-dividing cells. Many alternatives have since been synthesized that outperform PEI in transfection efficacy and maintaining cell viability [69-71] most of which are cationic in nature so that they can be taken up by the cells when they interact with the negatively charged plasma membrane (Figure 1.2). This excess positive charge also helps DNA escape the endosomal compartment during endocytosis through the "proton sponge" effect (Refer to section 1.4.5. of this chapter) [72, 73]. However, this property tends to kill cells as an excess of positive charges can interact with biological membranes and lead to the inhibition of crucial cellular processes [70]. Additionally, interactions with anionic molecules in the blood or surrounding tissue are inevitable in systematic administration. To overcome these obstacles, scientists are working towards constructing multifunctional polymeric gene vectors that can carry out a multitude of tasks in a single application, from overcoming the cellular membrane to the safe release of the cargo inside the cell.
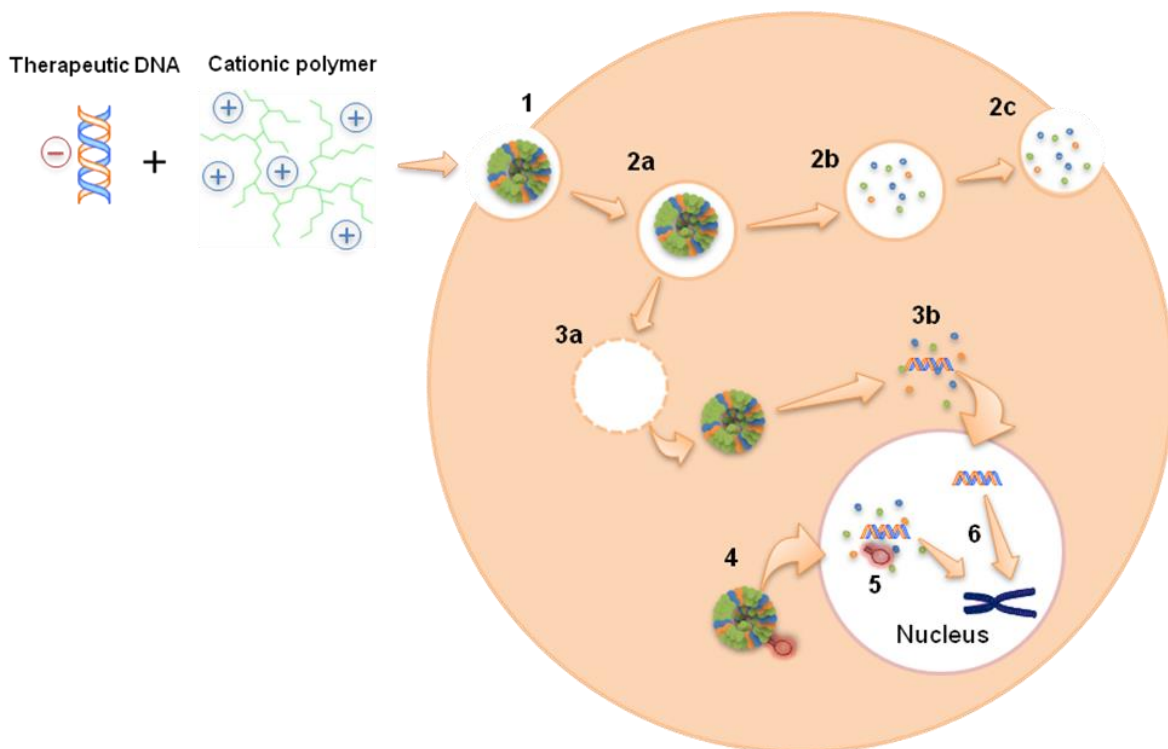
Figure 1.2: The known stages in intracellular gene delivery:

1. Polyplex interaction with cell membrane results in the internalisation of the polyplex by, Macropinocytosis, Phagocytosis and Receptor mediated endocytosis (Caveolae or clathrin). 2. Formation of early endosome (2a). Polyplexes trapped in the endosome are digested in the late endosome/lysosome (2b) and removed from the cell by exocytosis (2c). 3. Alternatively, if the polyplex induces endosomal escape (3a) via the proton sponge method it travels through the cytoplasm where the polymer is gradually degraded by cytoplasmic or intracellular enzymes (3b). 4. The polyplexes can also be internalized directly into the nucleus via nuclear localization peptides (NLS). 5. Disintegration of the polyplex and DNA release into the nucleus. 6. Finally, the DNA is inserted into the host genome.

1.4.1. Polymer structure

The molecular weight and chain length have a significant effect on cellular uptake, endosomal escape, DNA un-packing and nuclear internalization. High molecular weight polymers show better DNA binding, cellular uptake and transfection efficiency, while low molecular weight (LM_W) polymers show less cytotoxicty and better DNA un-packing [74, 75].

Artursson *et al*. studied the effect of low molecular weight chitosan (<5 kDa) related to physical shape and stability for gene delivery *in vitro* and *in vivo*. Globular structures increased with increasing chain length of the chitosan oligomer. Gene transfection efficiencies *in vitro* and *in vivo* were related to the physical shape and stability of the complexes (Figure 1.3). An optimal M_W has to be used depending on the polymer structure and charge density. Several approaches have been utilized to increase cellular uptake and stability of low molecular weight polymers or decrease cytotoxity and increase DNA un-packing of high molecular weight (HM_W) polymers. Both approaches are feasible and have demonstrated improved cellular uptake and reduced cytotoxicity [76]. Reduction of the polymer size upon internalization by degradation [77] or modification with a hydrophilic moieties [78, 79] has been shown to reduce cytotoxicity of HM_W polymers. Based on the theory that low molecular weight polymers form less stable complexes with DNA than higher molecular weight polymer, it seems that incorporation of degradable functionality into LM_W polymers is theoretically incorrect. However, a recent publication by Wu *et al*. [80] emphasized on the high transfection efficiency of LM_W (7 kDa) disulfide-PEI compared with HM_W (400 kDa) disulfide-PEI, 25k-PEI and Lipofectamine®2000. The optimization of the molecular weight is important and unique for each type of polymer. Slight modifications to the polymer structure affect the optimal molecular weight for transfection. An example of this is the self-branched trisaccharide-substituted chitosans, which show superior colloidal stability, efficient internalization, low cytotoxicity and high transfection efficiency compared to their linear counterparts [81].

A more thorough investigation was carried out by Anderson *et al*. The group developed a polymer library of over 2000 poly(β-aminoesters) in which the M_W varied from 2000 to 50000 Da [82]. Because these polymers contain ester groups, they degrade via hydrolysis within hours under physiological conditions. The study showed that diacrylate monomer terminated polymers were unable to promote cellular uptake and the optimal formulations were composed of polymers greater than 10,000 Da. The most interesting, however, was the effect of minor polymer composition changes had on the overall efficacy of the polymer. The diacrylate and amine alcohol formulations were the best in terms of cell viability and transfection efficiency [83]. Further modification of these polymers by end-capping with diamines increased transfection efficiency to levels comparable to adenovirus [84]. Interestingly, minor changes to the diamine end-capping monomers also had a large influence on transfection efficiency. There is currently a surge of interest in poly (β-aminesters) as gene delivery agents with new structures emerging in literature regularly. Saltzman *et al.* have recently reported on a new class of degradable amine-co-ester terpolymers which show great promise in tumor targeting and suppression [85]. The optimization of polymer molecular weight is thus vital for improving polymer/DNA complex stability, reducing cytotoxicity and increasing transfection in mammalian cells.
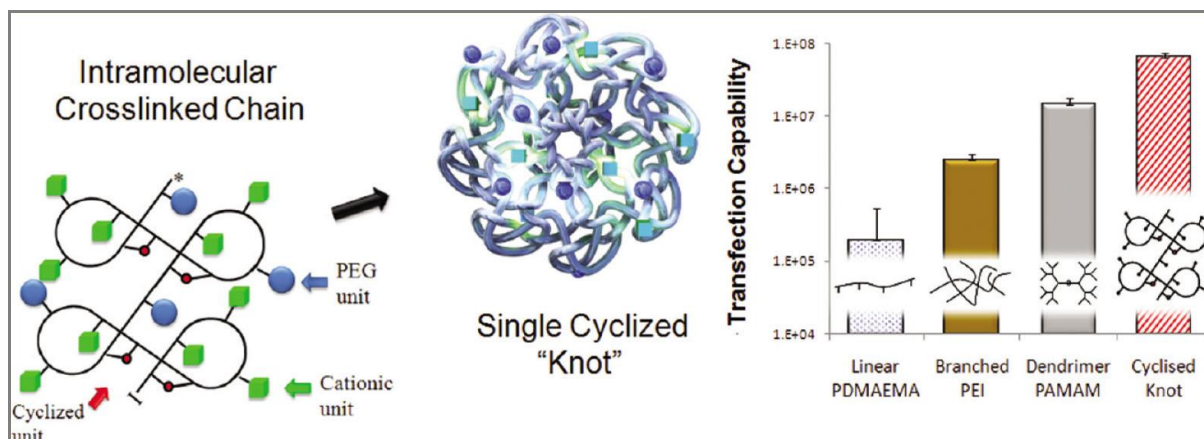
Figure 1.3: Structure of single cyclized polymer knot synthesized from free radical polymerization. This newly developed polymer shows better transfection efficiency and cytotoxicity over its linear, branched and dendritic polymers [86].

1.4.2. DNA Packaging

The efficient packaging of DNA prior to delivery into cells is a major step for successful transfection using polymer based delivery vectors. The polymers have to have DNA binding properties in order to bind to DNA and prevent it from enzymatic degradation and promote cellular uptake [87, 88] . It is well known that binding usually occurs by hydrophobic and electrostatic interactions between the phosphate groups (anionic) along the DNA backbone and cationic groups (usually amine groups) of the polymer agent [89]. However, a number of studies have shown that there are significant interactions between electronegative sites in the major and minor grooves of DNA and interactions via RNA bases in tRNA [90-92]. These findings further support the original perspective on the importance of charge density of cationic polymers in packaging DNA. Protonation is a common method of increasing the net positive charge of cationic polymers. It involves the addition of a proton to the amine functional groups of the polymers by lowering the pH of the polymer solution [93]. Cationic polymers seem to exhibit a pH-dependent interaction with DNA, considering an optimal nitrogen/phosphate ratio and polymer weight average molecular weight is reached [94]. Stolnik *et al*. demonstrated an increase in the binding constant of a dimethylaminoethyl methacrylate (DMAEMA) based polymer from 7.8×10^5 to 20.4×10^5 M^{-1} after decreasing the pH from 8 to 6.6 respectively [93]. The electrostatic interaction between the polymer and DNA forces the DNA to collapse into nanoparticles termed polyplexes whose size is largely influenced by the charge density of the polymer [95]. It is important to note that strong binding does not mean better transfection, in fact, it may hinder the transfection by preventing the un-packaging and release of DNA into the cytoplasm [96]. It is also important that the B-form of the natural cellular DNA structure is maintained after binding, as some lipid formulations have induced partial B to A and B to C conformational changes in the DNA structure [97]. These conformational changes refer to either the distance between the bonded base pairs or the orientation of the helical structure, right handed for B-form and left handed for Z-form.

1.4.3. Serum stability of polyplexes

Polymer gene delivery vectors have the important role of protecting the DNA from degradation by serum enzymes. This role is maintained as long as the DNA is tightly attached to the polymer and can travel freely to its target cell. Disassembly and release of the DNA from the polyplexes can occur after interaction of the latter with negatively charged serum proteins. Rapid blood elimination of polycation/DNA complexes results from binding to serum albumin and other proteins due to aggregation and accumulation of the complexes in fine capillary beds [98, 99]. Polyplex aggregation and clearance by phagocytic cells upon serum protein interaction is more prevalent especially in the case of cationic complexes. Modifications to the cationic polymers or polyplexes by addition of hydrophilic polymers such as Poly (ethylene glycol) can reduce aggregate formation or polyplex destabilization by hydrophilic shielding [99-104]. *In vivo* behavior of siRNA complexes, through pharmcokintetics and biodistribution, have been analyzed using non-invasive fluorescence fluctuation spectroscopy [103]. Superior stability of PEG/PEI complexed siRNA over free siRNA had been demonstrated as predicted, but disassembly of polyplexes upon liver passage hindered systematic administration. Although the binding strength of 'PEGylated' polymers is less than un-PEGylated polymers, the size of the complexes they form are the same. However, PEGylated polymers form neutral polyplexes while un-PEGylated polymers form highly charged polyplexes, relatively. Additionally, PEGylated polymers improve cell viability at the cost of reduction in cellular transfection efficiency both *in vitro* and *in vivo* (**Figure 1.4**). Other alternatives to PEGylation have been investigated including deoxycholate [105], HPMA [106-110], galactosylation [111], and various oligosaccharides [105, 112-117]. Proteins have also been used to improve polyplex stability *in vivo*. Human serum albumin has been electro-statically bound to polymer/DNA complexes to increase their tolerance against other serum proteins and bypass barriers such as cystic fibrosis airway secretions [118-120]. Nearly all of these compounds form neutral polyplexes that have increased tolerance against ionic strength. However, as stated earlier, neutral complexes have reduced

cellular membrane interaction ability thus lower uptake and transfection efficiency. To alleviate this problem, additional modifications, in terms of modification to the hydrophilic polymer structure or addition of cell-penetrating peptide moieties have been carried out [121-124]. Replacement of PEG with faster degrading P(EPE)-SS- maintained high colloidal stability with 2 orders of magnitude increase in transfection efficiency [100]. Avoiding serum proteins can be achieved through direct injection into target tissue bypassing the circulation system [125]. The extent of stabilization achieved by hydrophilic group addition to polyplexes depends on a number of factors which include but are not limited to: hydrophilic moiety chain length, ionic strength of the polymer, charge density and hydrophilic to polycation ratio used to assemble the polyplex.
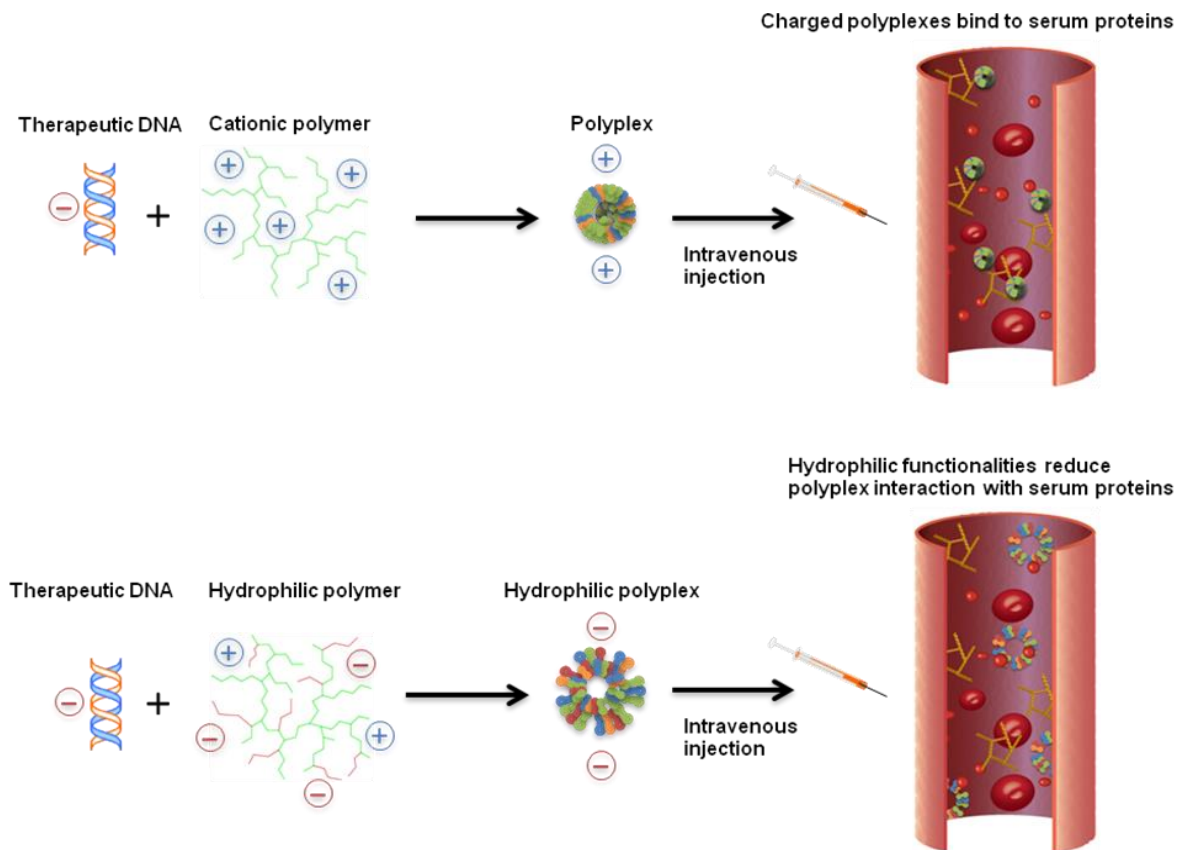
Figure 1.4: Polyplex stability in blood is largely influenced by the structure and charge density of the polymer. Cationic polymers with no hydrophilic functional groups interact with proteins reducing their gene delivery efficiency after intravenous injection. On the other hand, polymers functionalized with hydrophilic functional groups such as PEG, have higher stability in the blood because they do not interact with serum proteins making them more efficient gene carriers *in vivo*.

1.4.4. Cell internalization

Endocytosis is a process by which cells engulf extracellular molecules by forming invagination in the cell membrane. This process is energy dependent and is the main process by which most polyplexes are taken up by the cell. Endocytosis is an umbrella term, which comprises of macropinocytosis, phagocytosis and receptor mediated endocytosis [126, 127]. Phagocytosis is generally carried out by specialized cells like monocytes, macrophages and neutrophils [128]. Phagocytosis is not an ideal endocytic pathway of polyplex internalization as it is a process used by specialized cells to eliminate foreign particles. It can also be an obstacle for efficient delivery to target cells [129, 130]. Recent publications have highlighted the involvement of PAK1 dependent phagocytosis-like mechanism in uptake of cationic polymers [131, 132]. A more prevalent form of endocytosis is macropinocytosis, which involves the formation of large uncoated vesicles (~200nm-5μm) by the cell membrane much like phagocytosis. The similarity comes from the actin-rich pseudopod that makes a phagosome which is structurally similar to the ruffle that becomes a macropinosome. However, pseudopods are guided by targeting molecules on the surface in the case of phagocytosis and both vesicles are processed differently [133, 134]. Even though this is present in most spreading cells, this mechanism has not been fully characterized for its involvement in polycation uptake. Some characterization carried out by Jones *et al.* showed inhibition of cationic peptide uptake in A431 cells depleted of PAK-1 [135]. Moreover, the mechanism of macropinocytosis has been identified in the uptake of polyplexes and polymer based nanoparticles [136, 137]. Additionally, d-octaarginine-linked polymers showed a 25-fold increase in uptake over unmodified polymers, mainly through macropinocytosis. Although macropinocytosis has played a role in the uptake of several types of polyplexes, the predominant process of polyplex uptake is receptor mediated or dependent. Internalization of PEI carrying a splice-shifting oligonucleotide was inhibited partially by chlorpromazine (inhibitor of clathrin pathway) and almost completely by methyl-β-CD (inhibitor of lipid rafts or caveolae) suggesting that most polyplexes are taken up by lipid raft

mediated endocytosis [138]. Caveolae endocytosis of polyplexes has been the most studied of all the endocytic pathways as it bypasses the lysosome [139]. Histone H3 tail peptide conjugated PEI polyplexes were endocytosed by caveolin and transported through the golgi and endocytic reticulum before nuclear entry [140]. This mechanism seems to yield better transfection efficiency as a recent report suggests [141]. In this study, mouse myoblast cells were transfected with lipoplexes or histidine modified linear PEI (His-lPEI). Cells treated with polyplexes showed less transfection efficiency than cells treated with lipoplexes. The reason for this is explained in the different mechanisms of uptake. His-lPEI particles are internalized via the clathrin mediated endocytosis while lipoplexes are internalized through the caveolea as well as clathrin mediated endocytosis indicating that transfection efficiency is better correlated with the nature of the endocytic pathway than with uptake efficiency. The structure and composition of the polymer carrier also plays a role in determining the route of internalization [142]. Different cell lines utilize uptake pathways differently [143]. Although there is some indication that cationic polyplexes bypass the endosome, there still remains evidence to suggest otherwise [144]. Other key factors that influence the pathway of internalization are the polyplex size and charge. Large particles are internalized via micropinocytosis, smaller polyplexes (<200nm) are generally taken up through the clathrin pathway [145], although a recent report showed peptide modified polymer based nanoparticles, of the same size, internalized via the clathrin and caveolae pathways [146]. Positively charged or neutral polyplexes are internalized by electrostatic interactions or fluid phase transport while anionic polyplexes are up taken via the caveolea mediated endocytosis [147]. Interestingly, PEI was found to be taken up by ligand specific proteoglycans that facilitate its uptake via flotlin and dynamin [148]. Anionic polyplexes are usually composed of negatively charged polymers such as PEG. Anionic complexes made from such polymers do not bind to the cell membrane via electrostatic interactions and thus must internalize by other means. Coatings of targeting peptides or molecules such as the folate receptor allows for caveolae mediated uptake [149]. Different modifications can be used with PEG to optimized uptake [150]. It is clear that there is no

superior uptake mechanism of polyplexes and that many factors combined to improve uptake have to be utilized. It is also clear that the uptake mechanisms seem to work in conjunction with one another to facilitate the internalization of polyplexes [142].

1.4.5. Endosomal escape

Buffering capacity and the proton sponge effect

Cationic polymers can induce endosomal escape because of their net positive charge [151]. Endosomes maintain a certain pH which can be destabilized by protonable polymers such as PEI. As the polyplexes enter the cell and become trapped in endosomal vesicles, each of these endosomes have membrane bound ATPase ion channels that pump protons into the endosome. The polymers become protonated and prevent the acidification of the endosome. This resistance leads to continuous influx of protons and passive entry of chloride ions. As a result, water accumulates into the endosome which eventually leads to the rupture of the endosomal membrane (Figure 1.5). Polymers with higher buffering capacity showed better transfection efficiency with PEI being the best. It has also been shown that dextran conjugated PEI reduced transfection efficiency due to reduction in buffering capacity [152]. Although the theory of the 'proton sponge' effect has been previously challenged [153], it has now become widely accepted as the primary route of escape of cationic vectors and has been proven practically [154] and theoretically [155].
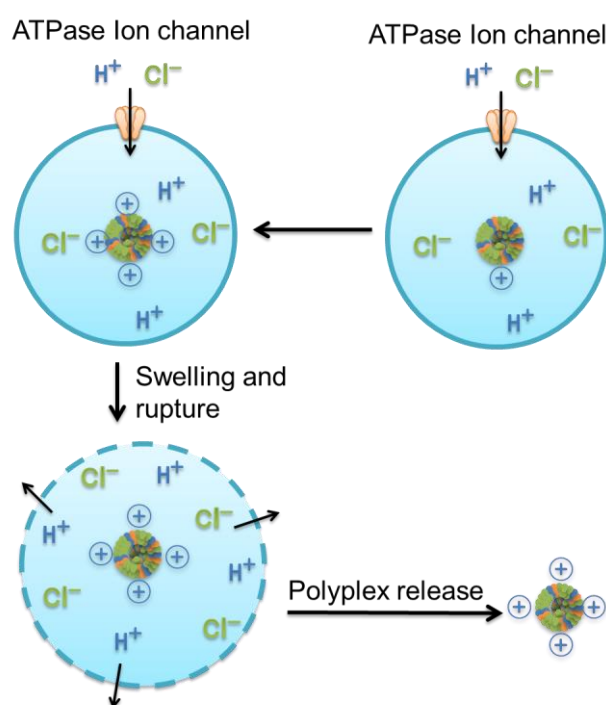
Figure 1.5: Endosomal escape of cationic polyplexes through the 'proton sponge' effect. Polyplexes, containing the protonable amine groups, distort the endosomal pH by preventing the acidification of the vesicle. Protons are actively pumped in to counter this resistance while chloride ions passively defuse in contributing to the increase in ionic concentration. As a result water also purges into the vesicle causing swelling and rupture of the endosomal membrane.

Peptides for endosomal escape

Endosomal escape can also be facilitated by vesicle disturbing peptides that are conjugated to the polyplex to enhance cytosol delivery. Diphtheria toxin T domain was conjugated to dual functionalized PEI, which enhanced gene expression [156]. This has also been shown with Polyethylene glycol-tetraacrylate functionalized with INF7 and H5WYG endosomal escape peptides (EEPs) [157, 158]. Additionally, PEI modified with melittin analogs showed enhanced gene expression over unmodified PEI but also increased toxicity possibly due to the capability of the polyplexes to disrupt other vesicles and the cell membrane [159]. Perhaps the most studied are the cell penetrating peptides (CCPs) used to promote endosomal escape of siRNA. Because siRNA delivery does not require entry to the nucleus, endosomal escape is a prerequisite for efficient knock down of genes, a process that mainly occurs in the cytosol. An effective method of peptide based membrane disruption involves hydrophobic peptides such as the endodomain of the HIV gp41 envelope glycoprotein which form pores in the cell membrane by adopting an amphipathic α-helical structure allowing the flow of biological material through the membrane [160]. A lot of the proposed peptides are obtained from viral components demonstrating the efficiency of viral vectors over polymer carrier systems. When the peptide fragment of the influenza virus haemagglutinin (IFN7-SGSC) is coupled with Poly (L-Lysine)/DNA polyplexes, transfection efficiency increased by 100-fold [161] demonstrating the effect of endosomal escape on transgene expression. Endosmal escape and nuclear entry were two main intracellular barriers which were crossed with endosomal escape and NLS peptides showing 2-3 fold increase in transfection efficiency over PEI [162].

Chemical agents

Certain chemical agents such as ammonium chloride, methylamine, spermine and monensin, which are weak bases, are known to induce pH buffering in the endosomal vesicles but do not seem to improve transgene expression. However, chloroquine, another weak base, has been shown to increase transgene expression when applied with Poly (L-Lysine)/DNA polyplexes [163]. It has been hypothesized that chloroquine has the

additional benefit of polyplex disassociation which leads to improved cell transfection [161]. Treating cells with chloroquine before and during transfection with Poly (L-Glutamic Acid)/PEI polyplexes enhanced gene expression but had a synergistic effect when coupled with the NLS histone [164]. Additionally, chloroquine effectiveness is dictated by the presence of endosomal vesicles and their acidity, for example, normal cells treated with chloroquine showed 2-fold higher gene expression than chloroquine treated cancer cells because the latter has less acidic endosomal vesicles [165]. The results further support the theory behind the method of endosomal escape by chloroquine and other weak bases.

Photochemical Endosomal escape

Another emerging method of inducing endosmal escape is photochemical vesicle escape, which is based on the chemical modification of photosensitizers, compounds that undergo molecular deformation when absorbing light at specific wavelengths. Some of these photosensitizers include aluminium phthalocyanine ($AlPcS_{2a}$) and meso-tetraphenylporphine [166, 167]. When absorbing light, the photosensitizer is converted to an excited singlet state that transfers its energy to molecular oxygen to what is named as singlet oxygen. This promotes the rupture of the endosomal vesicle releasing its contents into the cytosol [168]. Several groups have demonstrated that incorporation of photosensitizers with polymeric gene carriers significantly improved gene expression [166, 167, 169-171].

Polymer dissociation

Polyplexes are required to have high stability outside the cell to ensure the DNA is protected from degradation by enzymes, but are also required to disassemble upon entry into the cell to allow release and efficient integration of DNA into the host genome [172, 173]. A balance between polyplex stability and DNA release has to be achieved for efficient transfection. Shorter polycations have a higher probability of dissociating from DNA allowing for higher gene expression over a short period of time. The compromise is reduced stability in serum and salt solutions with higher molar ratio of polymer to DNA being required to maintain stability [174].

Chain length and polymer molecular weight play a significant role in dictating the efficiency of DNA release [175, 176]. Characterization of polymer/DNA binding is prerequisite for obtaining an optimal molecular weight and polymer to DNA ratio. Chen *et al.* showed correlation between polyplex unpacking kinetics and transfection efficiencies of polyethylenimine, polyphosphoramidate and chitosan when compared using quantitative image–based analysis [177]. Chitosan has been used extensively in gene therapy as it releases the DNA when glycosaminglycans are applied to the polyplex solution [174]. The efficiency of release depends on chitosan chain length and GAG properties. It is well known that longer polymer chains tend to form more stable polyplexes that do not dissociate efficiently in the cell. To overcome this, polymers with additional properties that allow easier DNA release have been synthesized. Reduction of the force of attraction between the polycation and DNA can be controlled using stimulus such as temperature [178, 179]. Temperature responsive polycations can change their properties depending on the physiological environment to reduce interaction with DNA. For example, poly (N-isopropylacrylamide)/poly (L-arginine)bioconjugate (PNIPArg), prepared by radical polymerization and EDC-activated coupling, dissociated from DNA above its lower critical solution temperature (LSCT) which increased its transfection efficiency [180]. Another group of stimuli responsive polymers are bioreducible polymers, which have attracted a significant amount of attention in recent years as they disassemble in physiological environments allowing efficient and quick release of DNA into the cytosol [181]. Bioreducible polymers, such as those that contain characteristic disulfide linkages, can be degraded through thiol-disulfide exchange reaction [182]. Disulfide bonds present in the structure of polyplexes are preserved in the predominantly oxidizing extracellular space while readily reduced in the glutathione and thioredoxin containing intracellular space. Incorporation of disulfide linkages in polycations increases their degradation rate in physiological environment allowing faster release of DNA. The hydrolytically degradable ester groups in polyaminoesters have also been thoroughly investigated displaying elevated transfection efficiency and reduced cytotoxicity due to their degradation and DNA un-packaging

capabilities [176, 183-185]. The fast degradation of the polymer is also beneficial to the cell due to the lowered risk of cationic charge induced cytotoxicity [186].

1.4.6. Nuclear internalization

The nucleus is the control center of the cell and contains the genomic information required for protein synthesis. It is enclosed by two membranes that allow the passage of small particles (<10nm) freely into and out of the cytoplasm [187]. Larger particles are transported by nuclear localization signals (NLS) [144]. Those membranes are important barriers to gene therapy and have to be taken into consideration for *in vitro* and *in vivo* gene delivery [188]. It has been established that proliferating cells are easier to transfect because they undergo mitosis regularly [189]. During this process, the nuclear membrane breaks down for a short period of time [187] exposing the genomic material and allowing foreign DNA to be integrated into host genome. However, primary mammalian cells proliferate at a much slower rate, triggering the need for alternative methods of nuclear internalization. NLS have been extensively used to improve nuclear localization of which the most widely used are the classical NLS from SV40 Large T-antigen (PKKKRKV) and the bipartite NLS in which the classical NLS is split into two halves (typically KKKX5-20RK) [190]. Additionally, Conjugation of nuclear localization signal peptides has been shown to improve nuclear entry and transfection in both, dividing and non-dividing cells [144, 191-193]. Direct microinjection of PEI polyplexes into the nucleus showed high levels of transgene expression as opposed to lipoplexes indicating the rapid disassembly of polyplexes inside the nucleus [194], but due to the differing roles of mammalian cells, gene expression efficiency is cell type dependent [195]. However, encouraging signs of progress are emerging. Modification of polymers with multifunctional peptides that drive the DNA from the lysosome to the nucleus has proven to be successful in a range of cell types [196]. Polymers seem to transfect better upon transport from outside the cell into the cytoplasm as a number of groups have demonstrated injection of PEI based polyplexes into the cytoplasm yielded lower protein expression than simple topical application

on a monolayer of cells. However, recent studies showed conjugation of lactose to PEI and subsequent microinjection into the cytoplasm increased transfection, independent of import-β nuclear import. This implies the presence of a connecting network between the cell membrane, cytoplasm and nucleus. The protein complex nuclear factor kappa-light-chain-enhancer of activated B cells (NF$_k$B), which controls the transcription of DNA, has been utilized to enhance nuclear import by using pluronic based non-ionic co-polymer. Other studies suggest that pluronics rapidly activate NF$_k$B, which bind cytosolic plasmid DNA that possesses promoters containing NF$_k$B binding sites, and consequently increase nuclear import of plasmid DNA through NF$_k$B nuclear translocation [197]. More recent studies suggest possible direct involvement of polymers in nuclear localization of DNA through its membrane disruptive properties which may also be the reason behind the cytotoxic side effects [198]. Contrary to the accepted theory that NLS peptides improve nuclear import of DNA, several groups have shown that direct conjugation of NLS-peptides to linear DNA did not improve transfection efficiency, regardless of whether it was free DNA [199] or bound to a polymer [200, 201]. Co-localization of polymers and DNA-bearing optimized kB motif to favor NFiB-driven nuclear import in the nucleus indicates the involvement of polymers in nuclear entry [202]. Additionally, poly (L-Lysine)-DNA complexes of diameters less than 25nm were successfully co-localized in the nucleus after nucleolin binding at the cell surface [203].

1.4.7. Future of polymer gene delivery
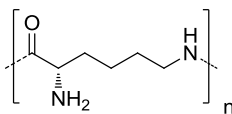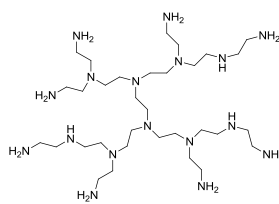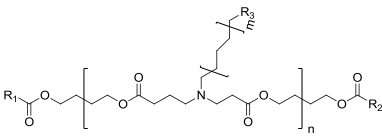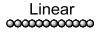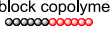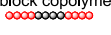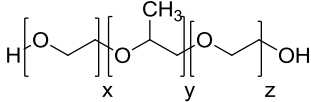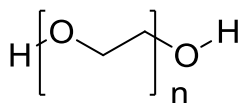
Firstly, polymer composition has been shown to play a vital role in regulating transfection, uptake, and cell viability [204]. Parameters including amount of amine groups, type of amine groups, charge density, hydrophilic and hydrophobic content have direct influence on gene delivery efficacy. So it is important to design polymeric gene delivery vectors with optimized parameters.
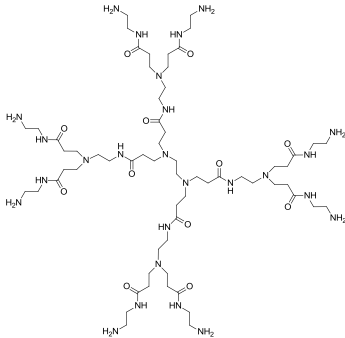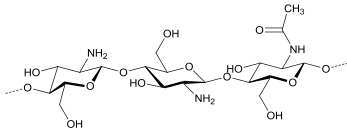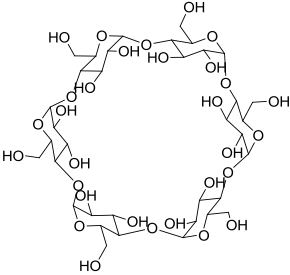
Secondly, dependence on single cationic monomers for polymeric gene delivery vector synthesis, such as DMAEMA (which has been extensively used for polymer synthesis using RAFT and ATRP), limits our

understanding of the effects of minor chemical structure changes have on transfection efficiency [69]. For future development of polycations, it is important to examine the best combination of elements that make an ideal gene vector carrier. An interesting and practical approach is to use combinatorial chemistry to analyze thousands of monomer combinations with different compositions like the method utilized by Anderson [205]. Polymer structure, which includes distances between different molecules in the polymer chains, overall chain length and branching density, contribute more to transfection efficiency than previously thought [206, 207]. Moreover, recent publications in the area of gene and drug delivery have pointed at the importance of combining several synthetic and natural polymers (namely proteins and peptides) for maximum transfection. A combination of cell and nuclear penetrating peptides, cationic endosomal buffering polymer, and hydrophilic functionality (for improved serum stability) in one delivery vector seem to overcome the significant barriers associated with conventional cationic polymer-based gene delivery vectors [208-210]. However, many of these delivery vectors fail to cross all the barriers and seem to only work in well studied and characterized cell lines. In addition, there still remain unanswered questions surrounding the fate of DNA in the cytoplasm and the nucleus. Progress in analytical methods of polyplex internalization and intercellular pathway is still ongoing and the requirement for unmasking further barriers is still there. The additional barriers of *in vivo* gene delivery that include 3-dimensional arrangement of cells in dense connective tissue [211], presence of serum proteins, and the acute immune response make it difficult to translate results to the *in vivo* environment. The future of polymer-based gene therapy should rely mostly on *in vivo* experiments to overcome the physical barriers that are slowing down the progress towards clinical studies and the development of an efficient gene therapy vector. This is evident from recent *in vivo* transfection and toxicity studies that expose the differences between the polymers attributes required for *in vivo* or *in vitro* transfection. Polymers containing hydrophilic groups [212, 213], low-molecular weight [214] or linear polymers [215-217] are superior to large-molecular weight, branched, and

highly charged polymers *in vivo*, completely opposite of what's observed *in vitro*.

Table 1.3: Commonly used gene delivery polymers and their modifications.

Name	Modifications	Basic structure	*In vitro* targets	*In vivo* targets	Ref.
Poly-L-Lysine (PLL)	Poly(ethylene glycol), Disulifde linkage, PAMAM Dendrimer		Various cell lines	Rabbit injured vessel	[218, 219]
Polyethylenimine (PEI)	Cyclodextrin, Targeting peptides, Succinylation, Dislufide linkage, Deacylation, Jeffamin	Linear : Branched:	Rat brain endothelium, embryonic neurons, mesenchymal stem cells, macrophages, and various cell lines	Newborn mouse brain, local/IP injection in tumor-bearing mice and reporter gene expression in vital organs	[220, 221]
Poly(β-aminoesters)	PEG, Branched/crosslinked, Thiol-reactive sidechains, spermine		Embryonic and adult stem cells, Adipose derived stromal cells, neuronal cells, and various cell lines	Reporter gene expression in mouse muscle, excisional wound and gene therapy in tumor bearing mice	[70, 183]
Poly(DMAEMA)	Cyclodextrin , PEG/HEMA, Redox-cleavable groups, IFN-7 peptides, TGN peptides, Additional ester groups		Mouse C3H myoblasts Various cell lines	Intravenous injection into mouse brain and tumor bearing mice	[87, 222]
Pluronic	Poly (ethylene glycol), PDMAEMA, Poly(propylene glycol), PEI, Solid lipid nanoparticles, Adeno-associated viral vector	Pluronic F-68	Sea urchin eggs, myoblasts, mouse macrophages and various cell lines	dystrophic mdx mice, gene therapy in muscle adipose tissue and tumor bearing mice	**[223]**
PEG	P(DMAEMA), Arginine, Cyclodextrin, PEI, Chitosan, Targeting peptides and proteins, Lipid carriers, PAMAM Dendrimers, Adnovirus, Folic acid		Brain capillary endothelial cells, Kupffer cells, Primary smooth muscle cells, macrophages and various cell lines	Gene therapy in tumor bearing mice and Wistar rats, Intramuscular gene silencing in mouse and reporter gene expression in vital organs	[102, 224]

Dendrimers (PAMAM)	PEG, Lactose, Targeting peptides and antibodies, Folic acid, Mannose, Arginine , Cholesterol, Targeting peptides and proteins	 G1	Mesenchymal stem cells, cytokine-activated primary human saphenous vein, endothelial cells and various cell lines	Intramuscular gene silencing in mouse, gene therapy in tumors	[225]
Chitosan	Poly-L-Lysine, Arginine, Guanidylated, PEG, Histindine, Cysteine, Glutathione, Glutamic acid, Galactose, Targeting peptides and proteins, Biotinylted, chondroitin sulphate, chitosan nanobubbles, PEI, Lipid shell, spermine		Macrophages, adipose derived mesenchymal stem cells and various cell lines	Antiapoptotic Bcl-2 gene knockdown in mice, autoimmune diabetes, aerosol delivery to mouse lung, reporter gene topical delivery to rat, reporter gene expression in endovascular rabbit organs	[226]
Cyclodextrin (CD)	Lipid, PEG, Arginine, PEI, Galactose , Targeting peptides and proteins, Histidine, Chitosan	 α-CD	Mesenchymal stem cells and various cell lines	EGFP transfected MSCs injected into rat tail vein and nude mice bearing SKOV-3 ovarian tumors	[227]

1.5.   Project rationale

Justification for choosing polymer based gene delivery over other methods:

Alternatives to polymer based gene delivery include: viral vectors, liposomes and physical delivery methods, all of which have their own unique attributes and have shown great success in the gene delivery field. In terms of flexibility, efficiency and clinical application, all of these methods have equally significant limitations, some of which can be exploited by the newly emerging polymer nanotechnology.

Advantages over viral vectors:

Polymeric based transfection agents have a critical selling point (like other non-viral vectors) over viral vectors that comes in the form of lowered risk of toxicity and immunogenesis [56], a highly influential risk factor in clinical settings. Additionally, viral vectors have limited packaging capability, especially for large genes like the COL7A1.

Advantages over liposomes:

Liposomal vectors greatly resemble polymer vectors in their transfection efficiency and ease of production, but lack of limited modification capability has given the lead to polymer agents. Where polymers can be synthesized with a wide scope of monomers producing an infinite range of chemical structures, liposomes are limited by their basic structure which is composed of hydrophilic and hydrophobic layers.

Advantages over physical methods:

Physical means of gene delivery are not restricted to polymers and liposomes, but can include; naked DNA injection [228], electroporation, gene gun [229], sonoporation [230] and magnetofection [231]. Naked DNA injection is impractical since it requires direct injection of DNA into one cell at a time, while electroporation and sonoporation induce mass cell shock in which most affected cells die. In addition, particles of these systems, including gene gun and magnetofection, have shallow penetration *in vivo*, a major drawback that limited their application to skin and superficial tissue [232].

Justification for using DE-ATRP, the multi-knot structure and the monomers, DMAEMA and PEEDEPE:

The DMAEMA monomer provides the positive charge required for DNA binding while the multi-knot structure increases the charge density of the individual polymer molecules. Having high charge density boosts transfection efficiency, because it improves binding strength to DNA and generates compact nanoparticles [233].

To encourage intracellular DNA release, a thiol degradable linker, in the form of PEEDEPE, is added to the structure. Disulfide bridges are reduced rapidly by intracellular glutathione [234].

The 3D multi-knot form is synthesized from controlled polymerization of DMAEMA and PEEDEPE, achievable only through the mechanism of DE-ATRP [235].

Justification for using hyperbranched poly (β-amino esters) for gene delivery in RDEB mice:

Poly (β-amino esters) (PAEs) are a group of cationic polymers with biodegradable polyester backbone with a capability of binding to DNA in acidic states. Herein, a hyperbranched version of the PAEs was used because hyperbranched structures are more efficient at gene delivery than their linear counterparts. In addition *in vitro* studies (carried out by Dr. Dezhong Zhao in our research lab) suggest the superiority of these polymers over the best of commercial agents in terms of viability and transfection efficiency (manuscript in preparation). Thus, the hyperbranched PAEs were used to complement the multi-knot polymer *in vivo* and because of the efficiency of PAE that has been reported previously by several groups.

1.6.   Project objectives and hypotheses

The ultimate goal of the project is to develop a safe and efficient polymer based gene delivery method to encourage the production of functional collagen type VII protein and restore the mechanical stability at the BMZ in RDEB mouse skin.

Phase I- Optimizing polymer properties (Chapter 2)

Hypothesis:

1. A multi-knot polymer with high charge density and disulfide reducible bonds can be synthesized from DE-ATRP.

2. A hyperbranched poly (β-amino ester) can be synthesized by Michael addition type reaction and by delaying the 'gelation point'. The polymer is degradable by ester hydrolysis.

3. The polymers will be able to bind to DNA efficiently forming nanoscale polyplexes for comprehensive cellular uptake.

4. The potential of the polymer to degrade will reduce cytotoxicity and encourage intracellular therapeutic DNA release.

Objectives:

1. Synthesize a multi-knot polymer from DMAEMA and PEEDEPE using the DE-ATRP method.

2. Synthesize a second polymer, (hyperbranched PAE) in the event that the multi-knot polymer does not meet the challenge of high efficacy *in vivo*.

3. Characterize the polymers in terms of molecular weight and atomic structure.

4. Characterize the polymers' DNA binding efficiency through polypex zeta size and zeta charge analysis.

Phase II- Polymer transfection efficiency analysis *in vitro* (Chapter 3)

Hypothesis:

The multi-knot and HPAE polymers can achieve high transfection efficiency and low cytotoxicity in a range of cell types and will outperform the gold standard and commercial transfection agents (e.g. Polyethylenimine and Lipofectamine®2000).

Objectives:

1. Optimize the transfection environment and compare protein expression and cytotoxicity levels to the commercial agents.

2. Test a range of polymer to DNA weight ratios on various cell types.

3. Find the range of DNA and polymer concentrations that complement high protein expression with minimal cytotoxicity.

Phase III- *Ex vivo* and *in vivo* analysis of gene delivery efficacy (RDEB model, Chapter 4)

Hypothesis: Polymer delivery of the therapeutic plasmid to *ex vivo* cultured skin equivalents or RDEB mice (Col7α1-/-) *in vivo* will promote expression of functional collagen VII protein and formation of anchoring fibrils allowing the skin to regain its structural integrity.

Objectives:

1. Examine the C7 plasmid delivery efficiency and protein expression capability of the multi-knot polymer in *ex vivo* 3D co-cultures (skin equivalents) of fibroblasts and keratinocytes.

2. Examine the C7 plasmid delivery efficiency and protein expression capability of the poly (β-amino esters) in an *in vivo* RDEB mouse model (Col7α1-/-).

3. Analyze C7 protein expression *in vivo* (RDEB mouse, Col7α1-/-) after intradermal injection of polyplexes into the blister region.

4. Investigate the inflammatory response and toxicity of the vector in terms of tissue necrosis, macrophage infiltration and swelling of the injected area.

1.7. References

1.   Pearson, R.W., Clinicopathologic Types of Epidermolysis Bullosa and Their Non-Dermatological Complications. *Arch Dermatol*, 1988. 124: p. 718.

2.   Pearson, R.W., Studies on the Pathogenesis of Epidermolysis Bullosa. *J Invest Dermatol*, 1962. 39: p. 551.

3.   Fine, J.D., R.A.J. Eady, E.A. Bauer, J.W. Bauer, L. Bruckner-Tuderman, A. Heagerty, H. Hintner, A. Hovnanian, M.E. Jonkman, I. Leigh, J.A. McGrath, J.E. Mellerio, D.E. Murrell, H. Shimizu, J. Uitto, A. Vahlquist, D. Woodley, and G. Zambruno, The classification of inherited epidermolysis bullosa (EB): Report of the Third International Consensus Meeting on Diagnosis and Classification of EB. *J Am Acad Dermatol*, 2008. 58: p. 931.

4.   McGrath, J.A., J.R. McMillan, C.S. Shemanko, S.K. Runswick, I.M. Leigh, E.B. Lane, D.R. Garrod, and R.A. Eady, Mutations in the plakophilin 1 gene result in ectodermal dysplasia/skin fragility syndrome. *Nat gen*, 1997. 17: p. 240.

5.   Pulkkinen, L., A.M. Christiano, T. Airenne, H. Haakana, K. Tryggvason, and J. Uitto, Mutations in the Gamma-2 Chain Gene (Lamc2) of Kalinin/Laminin-5 in the Junctional Forms of Epidermolysis-Bullosa. *Nat gen*, 1994. 6: p. 293.

6.   Schuilenga-Hut, P.H., P. Vlies, M.F. Jonkman, E. Waanders, C.H. Buys, and H. Scheffer, Mutation analysis of the entire keratin 5 and 14 genes in patients with epidermolysis bullosa simplex and identification of novel mutations. *Hum mut*, 2003. 21: p. 447.

7.   Pfendner, E., J. Uitto, and J.D. Fine, Epidermolysis bullosa carrier frequencies in the US population. *J Invest Dermatol*, 2001. 116: p. 483.

8.   South, A.P. and E.A. O'Toole, Understanding the Pathogenesis of Recessive Dystrophic Epidermolysis Bullosa Squamous Cell Carcinoma. *Dermatol Clin*, 2010. 28: p. 171.

9.   Titeux, M., J.E. Mejia, L. Mejlumian, S. Bourthoumieu, S. Mirval, L. Tonasso, M. Heller, C. Prost-Squarcioni, and A. Hovnanian, Recessive dystrophic epidermolysis bullosa caused by COL7A1 hemizygosity and a missense mutation with complex effects on splicing. *Hum mut*, 2006. 27: p. 291.

10. Uitto, J. and A.M. Christiano, Molecular-Basis for the Dystrophic Forms of Epidermolysis-Bullosa - Mutations in the Type-Vii Collagen Gene. *Arch Dermatol Res*, 1994. 287: p. 16.

11. Christiano, A.M., G.G. Hoffman, L.C. Chunghonet, S.B. Lee, W. Cheng, J. Uitto, and D.S. Greenspan, Structural Organization of the Human Type-Vii Collagen Gene (Col7a1), Composed of More Exons Than Any Previously Characterized Gene. *Genomics*, 1994. 21: p. 169.

12. Heinonen, S., M. Mannikko, J.F. Klement, D. Whitaker-Menezes, G.F. Murphy, and J. Uitto, Targeted inactivation of the type VII collagen gene (Col7a1) in mice results in severe blistering phenotype: a model for recessive dystrophic epidermolysis bullosa. *J Cell Sci*, 1999. 112: p. 3641.

13. Titeux, M., V. Pendaries, M.A. Zanta-Boussif, A. Decha, N. Pironon, L. Tonasso, J.E. Mejia, A. Brice, O. Danos, and A. Hovnanian, SIN Retroviral Vectors Expressing COL7A1 Under Human Promoters for Ex Vivo Gene Therapy of Recessive Dystrophic Epidermolysis Bullosa. *Mol Ther*, 2010. 18: p. 1509.

14. Mavilio, F., G. Pellegrini, S. Ferrari, F. Di Nunzio, E. Di Iorio, A. Recchia, G. Maruggi, G. Ferrari, E. Provasi, C. Bonini, S. Capurro, A. Conti, C. Magnoni, A. Giannetti, and M. De Luca, Correction of junctional epidermolysis bullosa by transplantation of genetically modified epidermal stem cells. *Nat Med*, 2006. 12: p. 1397.

15. Romano, G., I.R. Morino, F. Pentimalli, V. Adamo, and A. Giordano, Insertional Mutagenesis and Development of Malignancies Induced by Integrating Gene Delivery Systems: Implications for the Design of Safer Gene-Based Interventions in Patients. *Drug News Perspect*, 2009. 22: p. 185.

16. Wong, T., L. Gammon, L. Liu, J.E. Mellerio, P.J.C. Dopping-Hepenstal, J. Pacy, G. Elia, R. Jeffery, I.M. Leigh, H. Navsaria, and J.A. McGrath, Potential of fibroblast cell therapy for recessive dystrophic epidermolysis bullosa. *J Invest Dermatol*, 2008. 128: p. 2179.

17. Wagner, J.E., A. Ishida-Yamamoto, J.A. McGrath, M. Hordinsky, D.R. Keene, D.T. Woodley, M. Chen, M.J. Riddle, M.J. Osborn, T. Lund, M. Dolan, B.R. Blazar, and J. Tolar, Bone marrow transplantation for recessive dystrophic epidermolysis bullosa. *N Engl J Med*, 2010. 363: p. 629.

18.   Sakai, L.Y., D.R. Keene, N.P. Morris, and R.E. Burgeson, Type-Vii Collagen Is a Major Structural Component of Anchoring Fibrils. *J Cell Biol*, 1986. 103: p. 1577.

19.   Keene, D.R., L.Y. Sakai, G.P. Lunstrum, N.P. Morris, and R.E. Burgeson, Type-Vii Collagen Forms an Extended Network of Anchoring Fibrils. *J Cell Biol*, 1987. 104: p. 611.

20.   Ryynanen, J., S. Sollberg, M.G. Parente, L.C. Chung, A.M. Christiano, and J. Uitto, Type-Vii Collagen Gene-Expression by Cultured Human-Cells and in Fetal Skin - Abundant Messenger-Rna and Protein-Levels in Epidermal-Keratinocytes. *J Invest Dermatol*, 1992. 98: p. 399.

21.   Pulkkinen, L. and J. Uitto, Mutation analysis and molecular genetics of epidermolysis bullosa. *Matrix Biol*, 1999. 18: p. 29.

22.   Chen, M., E.A. O'Toole, Y.Y. Li, and D.T. Woodley, Development and characterization of a recombinant truncated type VII collagen "minigene": Implications for gene therapy of dystrophic epidermolysis bullosa. *J Invest Dermatol*, 1998. 110: p. 473.

23.   Sat, E., K.H. Leung, L. Bruckner-Tuderman, and K.S.E. Cheah, Tissue-specific expression and long-term deposition of human collagen VII in the skin of transgenic mice: implications for gene therapy. *Gene Ther*, 2000. 7: p. 1631.

24.   Mecklenbeck, S., S.H. Compton, J.E. Mejia, R. Cervini, A. Hovnanian, L. Bruckner-Tuderman, and Y. Barrandon, A microinjected COL7A1-PAC vector restores synthesis of intact procollagen VII in a dystrophic epidermolysis bullosa keratinocyte cell line. *Hum Gene Ther*, 2002. 13: p. 1655.

25.   Ortiz-Urda, S., B. Thyagarajan, D.R. Keene, Q. Lin, M. Fang, M.P. Calos, and P.A. Khavari, Stable nonviral genetic correction of inherited human skin disease. *Nat Med*, 2002. 8: p. 1166.

26.   Chen, M., N. Kasahara, D.R. Keene, L. Chan, W.K. Hoeffler, D. Finlay, M. Barcova, P.M. Cannon, C. Mazurek, and D.T. Woodley, Restoration of type VII collagen expression and function in dystrophic epidermolysis bullosa. *Nat gen*, 2002. 32: p. 670.

27.   Ortiz-Urda, S., Q. Lin, C.L. Green, D.R. Keene, M.P. Marinkovich, and P.A. Khavari, Injection of genetically engineered fibroblasts corrects regenerated human epidermolysis bullosa skin tissue. *J Clin Invest*, 2003. 111: p. 251.

28. Baldeschi, C., Y. Gache, A. Rattenholl, P. Bouille, O. Danos, J.P. Ortonne, L. Bruckner-Tuderman, and G. Meneguzzi, Genetic correction of canine dystrophic epidermolysis bullosa mediated by retroviral vectors. *Hum Mol Genet*, 2003. 12: p. 1897.

29. Woodley, D.T., G.G. Krueger, C.M. Jorgensen, J.A. Fairley, T. Atha, Y. Huang, L. Chan, D.R. Keene, and M. Chen, Normal and gene-corrected dystrophic epidermolysis bullosa fibroblasts alone can produce type VII collagen at the basement membrane zone. *J Invest Dermatol*, 2003. 121: p. 1021.

30. Woodley, D.T., D.R. Keene, T. Atha, Y. Huang, K. Lipman, W. Li, and M. Chen, Injection of recombinant human type VII collagen restores collagen function in dystrophic epidermolysis bullosa. *Nat Med*, 2004. 10: p. 693.

31. Woodley, D.T., D.R. Keene, T. Atha, Y. Huang, R. Ram, N. Kasahara, and M. Chen, Intradermal injection of lentiviral vectors corrects regenerated human dystrophic epidermolysis bullosa skin tissue in vivo. *Mol Ther*, 2004. 10: p. 318.

32. Gache, Y., C. Baldeschi, M. Del Rio, L. Gagnoux-Palacios, F. Larcher, J.P. Lacour, and G. Meneguzzi, Construction of skin equivalents for gene therapy of recessive dystrophic epidermolysis bullosa. *Hum Gene Ther*, 2004. 15: p. 921.

33. Goto, M., D. Sawamura, K. Ito, M. Abe, W. Nishie, K. Sakai, A. Shibaki, M. Akiyama, and H. Shimizu, Fibroblasts show more potential as target cells than keratinocytes in COL7A1 gene therapy of dystrophic epidermolysis bullosa. *J Invest Dermatol*, 2006. 126: p. 766.

34. Woodley, D.T., J. Remington, Y. Huang, Y.P. Hou, W. Li, D.R. Keene, and M. Chen, Intravenously injected human fibroblasts home to skin wounds, deliver type VII collagen, and promote wound healing. *Mol Ther*, 2007. 15: p. 628.

35. Tolar, J., A. Ishida-Yamamoto, M. Riddle, R.T. McElmurry, M. Osborn, L. Xia, T. Lund, C. Slattery, J. Uitto, A.M. Christiano, J.E. Wagner, and B.R. Blazar, Amelioration of epidermolysis bullosa by transfer of wild-type bone marrow cells. *Blood*, 2009. 113: p. 1167.

36. Remington, J., X.Y. Wang, Y.P. Hou, H. Zhou, J. Burnett, T. Muirhead, J. Uitto, D.R. Keene, D.T. Woodley, and M. Chen, Injection of Recombinant Human Type VII Collagen Corrects the Disease Phenotype in a Murine Model of Dystrophic Epidermolysis Bullosa. *Mol Ther*, 2009. 17: p. 26.

37.   Kern, J.S., S. Loeckermann, A. Fritsch, I. Hausser, W. Roth, T.M. Magin, C. Mack, M.L. Muller, O. Paul, P. Ruther, and L. Bruckner-Tuderman, Mechanisms of Fibroblast Cell Therapy for Dystrophic Epidermolysis Bullosa: High Stability of Collagen VII Favors Long-term Skin Integrity. *Mol Ther*, 2009. 17: p. 1605.

38.   Ito, K., D. Sawamura, M. Goto, H. Nakamura, W. Nishie, K. Sakai, K. Natsuga, S. Shinkuma, A. Shibaki, J. Uitto, C.P. Denton, O. Nakajima, M. Akiyama, and H. Shimizu, Keratinocyte-/Fibroblast-Targeted Rescue of Col7a1-Disrupted Mice and Generation of an Exact Dystrophic Epidermolysis Bullosa Model Using a Human COL7A1 Mutation. *Am J Pathol*, 2009. 175: p. 2508.

39.   Siprashvili, Z., N.T. Nguyen, M.Y. Bezchinsky, M.P. Marinkovich, A.T. Lane, and P.A. Khavari, Long-Term Type VII Collagen Restoration to Human Epidermolysis Bullosa Skin Tissue. *Hum Gene Ther*, 2010. 21: p. 1299.

40.   Murauer, E.M., Y. Gache, I.K. Gratz, A. Klausegger, W. Muss, C. Gruber, G. Meneguzzi, H. Hintner, and J.W. Bauer, Functional Correction of Type VII Collagen Expression in Dystrophic Epidermolysis Bullosa. *J Invest Dermatol*, 2011. 131: p. 74.

41.   J. Wagner, and J. Tolar, Bone Marrow Transplantation for Recessive Dystrophic Epidermolysis Bullosa. *New Engl J Med*, 2010. 363: p. 629.

42.   Tolar, J., L. Xia, M.J. Riddle, C.J. Lees, C.R. Eide, R.T. McElmurry, M. Titeux, M.J. Osborn, T.C. Lund, A. Hovnanian, J.E. Wagner, and B.R. Blazar, Induced Pluripotent Stem Cells from Individuals with Recessive Dystrophic Epidermolysis Bullosa. *J Invest Dermatol*, 2011. 131: p. 848.

43.   Gache, Y., D. Pin, L. Gagnoux-Palacios, C. Carozzo, and G. Meneguzzi, Correction of Dog Dystrophic Epidermolysis Bullosa by Transplantation of Genetically Modified Epidermal Autografts. *J Invest Dermatol*, 2011. 131: p. 2069.

44.   Wang, X.Y., P. Ghasri, M. Amir, B. Hwang, Y.P. Hou, M. Khilili, A. Lin, D. Keene, J. Uitto, D.T. Woodley, and M. Chen, Topical Application of Recombinant Type VII Collagen Incorporates Into the Dermal-Epidermal Junction and Promotes Wound Closure. *Mol Ther*, 2013. 21: p. 1335.

45.   Blaese, R.M., K.W. Culver, A.D. Miller, C.S. Carter, T. Fleisher, M. Clerici, G. Shearer, L. Chang, Y. Chiang, P. Tolstoshev, J.J. Greenblatt, S.A. Rosenberg, H. Klein, M. Berger, C.A. Mullen, W.J. Ramsey, L. Muul,

R.A. Morgan, and W.F. Anderson, T lymphocyte-directed gene therapy for ADA- SCID: initial trial results after 4 years. *Science*, 1995. 270: p. 475.

46. Gao, X., K.S. Kim, and D.X. Liu, Nonviral gene delivery: What we know and what is next. *Aaps J*, 2007. 9: p. E92.

47. Friedman.T and R. Roblin, Gene Therapy for Human Genetic Disease. *Science*, 1972. 175: p. 949.

48. Edward Karl Wagner, M., Joseph Hewlett, Basic Virology. 2004: Blackwell Science.

49. Ledley, F.D., H.E. Grenett, D.P. Bartos, and S.L.C. Woo, Retroviral Mediated Transfer and Expression of Human Alpha-1-Antitrypsin in Cultured-Cells. *Gene*, 1987. 61: p. 113.

50. Blaese, R.M., K.W. Culver, A.D. Miller, C.S. Carter, T. Fleisher, M. Clerici, G. Shearer, L. Chang, Y.W. Chiang, P. Tolstoshev, J.J. Greenblatt, S.A. Rosenberg, H. Klein, M. Berger, C.A. Mullen, W.J. Ramsey, L. Muul, R.A. Morgan, and W.F. Anderson, T-Lymphocyte-Directed Gene-Therapy for Ada(-) Scid - Initial Trial Results after 4 Years. *Science*, 1995. 270: p. 475.

51. Somia, N.V., M. Zoppe, and I.M. Verma, Generation of Targeted Retroviral Vectors by Using Single-Chain Variable Fragment - an Approach to in-Vivo Gene Delivery. *P Natl Acad Sci USA*, 1995. 92: p. 7570.

52. Shimotohno, K. and H.M. Temin, Loss of Intervening Sequences in Genomic Mouse Alpha-Globin DNA Inserted in an Infectious Retrovirus Vector. *Nature*, 1982. 299: p. 265.

53. Thomas, C.E., A. Ehrhardt, and M.A. Kay, Progress and problems with the use of viral vectors for gene therapy. *Nat Rev Genet*, 2003. 4: p. 346.

54. Miller, A.D., Retroviral Vectors. *Curr Top Microbiol*, 1992. 158: p. 1.

55. Nair, V., Retrovirus-induced oncogenesis and safety of retroviral vectors. *Curr Opin Mol Ther*, 2008. 10: p. 431.

56. Cavazzana-Calvo, M., S. Hacein-Bey, C.D. Basile, F. Gross, E. Yvon, P. Nusbaum, F. Selz, C. Hue, S. Certain, J.L. Casanova, P. Bousso, F. Le Deist, and A. Fischer, Gene therapy of human severe combined immunodeficiency (SCID)-X1 disease. *Science*, 2000. 288: p. 669.

57. Hacein-Bey-Abina, S., C. von Kalle, M. Schmidt, F. Le Deist, N. Wulffraat, E. McIntyre, I. Radford, J.L. Villeval, C.C. Fraser, M. Cavazzana-Calvo, and A. Fischer, A serious adverse event after successful

gene therapy for X-linked severe combined immunodeficiency. *New Engl J Med*, 2003. 348: p. 255.

58.   Paradiso, B., P. Marconi, S. Zucchini, E. Berto, A. Binaschi, A. Bozac, A. Buzzi, M. Mazzuferi, E. Magri, G.N. Mora, D. Rodi, T. Su, I. Volpi, L. Zanetti, A. Marzola, R. Manservigi, P.F. Fabene, and M. Simonato, Localized delivery of fibroblast growth factor-2 and brain-derived neurotrophic factor reduces spontaneous seizures in an epilepsy model. *P Natl Acad Sci USA*, 2009. 106: p. 7191.

59.   Wolfe, D., M. Mata, and D.J. Fink, A human trial of HSV-mediated gene transfer for the treatment of chronic pain. *Gene Ther*, 2009. 16: p. 455.

60.   Broberg, E.K. and V. Hukkanen, Immune response to herpes simplex virus and gamma134.5 deleted HSV vectors. *Curr gene ther*, 2005. 5: p. 523.

61.   Schenk, E., M. Essand, C.H. Bangma, and G.F. Consortium, Clinical Adenoviral Gene Therapy for Prostate Cancer. *Hum Gene Ther*, 2010. 21: p. 807.

62.   Castro, J.E., J. Melo-Cardenas, M. Urquiza, J.S. Barajas-Gamboa, R.S. Pakbaz, and T.J. Kipps, Gene Immunotherapy of Chronic Lymphocytic Leukemia: A Phase I Study of Intranodally Injected Adenovirus Expressing a Chimeric CD154 Molecule. *Cancer Res*, 2012. 72: p. 2937.

63.   Fisher, K.J., K. Jooss, J. Alston, Y.P. Yang, S.E. Haecker, K. High, R. Pathak, S.E. Raper, and J.M. Wilson, Recombinant adeno-associated virus for muscle directed gene therapy. *Nat med*, 1997. 3: p. 306.

64.   Shen, Y., S.I. Muramatsu, K. Ikeguchi, K.I. Fujimoto, D.S. Fan, M. Ogawa, H. Mizukami, M. Urabe, A. Kume, I. Nagatsu, F. Urano, T. Suzuki, H. Ichinose, T. Nagatsu, J. Monahan, I. Nakano, and K. Ozawa, Triple transduction with adeno-associated virus vectors expressing tyrosine hydroxylase, aromatic-L-amino-acid decarboxylase, and GTP cyclohydrolase I for gene therapy of Parkinson's disease. *Hum Gene Ther*, 2000. 11: p. 1509.

65.   Boussif, O., F. Lezoualch, M.A. Zanta, M.D. Mergny, D. Scherman, B. Demeneix, and J.P. Behr, A Versatile Vector for Gene and Oligonucleotide Transfer into Cells in Culture and in-Vivo - Polyethylenimine. *P Natl Acad Sci USA*, 1995. 92: p. 7297.

66.   Fischer, D., T. Bieber, Y.X. Li, H.P. Elsasser, and T. Kissel, A novel non-viral vector for DNA delivery based on low molecular weight, branched

polyethylenimine: Effect of molecular weight on transfection efficiency and cytotoxicity. *Pharmaceut Res*, 1999. 16: p. 1273.

67.   Florea, B.I., C. Meaney, H.E. Junginger, and G. Borchard, Transfection efficiency and toxicity of polyethylenimine in differentiated Calu-3 and nondifferentiated COS-1 cell cultures. *Aaps Pharmsci*, 2002. 4.

68.   Moghimi, S.M., P. Symonds, J.C. Murray, A.C. Hunter, G. Debska, and A. Szewczyk, A two-stage poly(ethylenimine)-mediated cytotoxicity: Implications for gene transfer/therapy. *Mol Ther*, 2005. 11: p. 990.

69.   Newland, B., H. Tai, Y. Zheng, D. Velasco, A. Di Luca, S.M. Howdle, C. Alexander, W. Wang, and A. Pandit, A highly effective gene delivery vector--hyperbranched poly(2-(dimethylamino)ethyl methacrylate) from in situ deactivation enhanced ATRP. *Chem Commun (Camb)*, 2010. 46: p. 4698.

70.   Zhou, J., J. Liu, C.J. Cheng, T.R. Patel, C.E. Weller, J.M. Piepmeier, Z. Jiang, and W.M. Saltzman, Biodegradable poly(amine-co-ester) terpolymers for targeted gene delivery. *Nat Mater*, 2012. 11: p. 82.

71.   Mastrobattista, E. and W.E. Hennink, Polymers for gene delivery: Charged for success. *Nat Mater*, 2012. 11: p. 10.

72.   Anderson, D.G., A. Akinc, N. Hossain, and R. Langer, Structure/property studies of polymeric gene delivery using a library of poly(beta-amino esters). *Mol Ther*, 2005. 11: p. 426.

73.   Creusat, G., A.S. Rinaldi, E. Weiss, R. Elbaghdadi, J.S. Remy, R. Mulherkar, and G. Zuber, Proton sponge trick for pH-sensitive disassembly of polyethylenimine-based siRNA delivery systems. *Bioconjug Chem*, 2010. 21: p. 994.

74.   Cai, J.G., Y.A. Yue, D. Rui, Y.F. Zhang, S.Y. Liu, and C. Wu, Effect of Chain Length on Cytotoxicity and Endocytosis of Cationic Polymers. *Macromolecules*, 2011. 44: p. 2050.

75.   Kunath, K., A. von Harpe, D. Fischer, H. Peterson, U. Bickel, K. Voigt, and T. Kissel, Low-molecular-weight polyethylenimine as a non-viral vector for DNA delivery: comparison of physicochemical properties, transfection efficiency and in vivo distribution with high-molecular-weight polyethylenimine. *J Control Release*, 2003. 89: p. 113.

76.   Neamnark, A., O. Suwantong, K.C.R. Bahadur, C.Y.M. Hsu, P. Supaphol, and H. Uludag, Aliphatic Lipid Substitution on 2 kDa Polyethylenimine

Improves Plasmid Delivery and Transgene Expression. *Mol Pharmaceut*, 2009. 6: p. 1798.

77.   Yu, J.H., J.S. Quan, J. Huang, J.W. Nah, and C.S. Cho, Degradable poly(amino ester) based on poly(ethylene glycol) dimethacrylate and polyethylenimine as a gene carrier: molecular weight of PEI affects transfection efficiency. *J Mater Sci-Mater M*, 2009. 20: p. 2501.

78.   Xu, F.J., Y. Ping, J. Ma, G.P. Tang, W.T. Yang, J. Li, E.T. Kang, and K.G. Neoh, Comb-shaped copolymers composed of hydroxypropyl cellulose backbones and cationic poly((2-dimethyl amino)ethyl methacrylate) side chains for gene delivery. *Bioconjug Chem*, 2009. 20: p. 1449.

79.   Venkataraman, S., W.L. Ong, Z.Y. Ong, S.C. Joachim Loo, P.L. Ee, and Y.Y. Yang, The role of PEG architecture and molecular weight in the gene transfection performance of PEGylated poly(dimethylaminoethyl methacrylate) based cationic polymers. *Biomaterials*, 2011. 32: p. 2369.

80.   Deng, R., Y. Yue, F. Jin, Y. Chen, H.F. Kung, M.C. Lin, and C. Wu, Revisit the complexation of PEI and DNA - how to make low cytotoxic and highly efficient PEI gene transfection non-viral vectors with a controllable chain length and structure? *J Control Release*, 2009. 140: p. 40.

81.   Malmo, J., K.M. Varum, and S.P. Strand, Effect of chitosan chain architecture on gene delivery: comparison of self-branched and linear chitosans. *Biomacromolecules*, 2011. 12: p. 721.

82.   Green, J.J., R. Langer, and D.G. Anderson, A combinatorial polymer library approach yields insight into nonviral gene delivery. *Accounts Chem Res*, 2008. 41: p. 749.

83.   Anderson, D.G., W.D. Peng, A. Akinc, N. Hossain, A. Kohn, R. Padera, R. Langer, and J.A. Sawicki, A polymer library approach to suicide gene therapy for cancer. *P Natl Acad Sci USA*, 2004. 101: p. 16028.

84.   Green, J.J., G.T. Zugates, N.C. Tedford, Y.H. Huang, L.G. Griffith, D.A. Lauffenburger, J.A. Sawicki, R. Langer, and D.G. Anderson, Combinatorial modification of degradable polymers enables transfection of human cells comparable to adenovirus. *Adv. Mater.*, 2007. 19: p. 2836.

85.   Zhou, J.B., J. Liu, C.J. Cheng, T.R. Patel, C.E. Weller, J.M. Piepmeier, Z.Z. Jiang, and W.M. Saltzman, Biodegradable poly(amine-co-ester) terpolymers for targeted gene delivery. *Nat Mat*, 2012. 11: p. 82.

86. Newland, B., Y. Zheng, Y. Jin, M. Abu-Rub, H. Cao, W. Wang, and A. Pandit, Single cyclized molecule versus single branched molecule: a simple and efficient 3D "knot" polymer structure for nonviral gene delivery. *J Am Chem Soc*, 2012. 134: p. 4782.

87. Dai, F. and W. Liu, Enhanced gene transfection and serum stability of polyplexes by PDMAEMA-polysulfobetaine diblock copolymers. *Biomaterials*, 2011. 32: p. 628.

88. Tiera, M.J., Q. Shi, F.M. Winnik, and J.C. Fernandes, Polycation-based gene therapy: current knowledge and new perspectives. *Curr Gene Ther*, 2011. 11: p. 288.

89. Sun, C.B., T. Tang, H. Uludag, and J.E. Cuervo, Molecular Dynamics Simulations of DNA/PEI Complexes: Effect of PEI Branching and Protonation State. *Biophys J*, 2011. 100: p. 2754.

90. Froehlich, E., J.S. Mandeville, L. Kreplak, and H.A. Tajmir-Riahi, Aggregation and Particle Formation of tRNA by Dendrimers. *Biomacromolecules*, 2011. 12: p. 2780.

91. Wang, Y.M. and J. Ziebarth, Multiscale molecular modeling and rational design of polymer based gene delivery vectors. *J Controlled Release*, 2011. 152: p. E174.

92. Ziebarth, J.D. and Y.M. Wang, Understanding the Protonation Behavior of Linear Polyethylenimine in Solutions through Monte Carlo Simulations. *Biomacromolecules*, 2010. 11: p. 29.

93. Rungsardthong, U., T. Ehtezazi, L. Bailey, S.P. Armes, M.C. Garnett, and S. Stolnik, Effect of polymer ionization on the interaction with DNA in nonviral gene delivery systems. *Biomacromolecules*, 2003. 4: p. 683.

94. Strand, S.P., S. Danielsen, B.E. Christensen, and K.M. Varum, Influence of chitosan structure on the formation and stability of DNA-chitosan polyelectrolyte complexes. *Biomacromolecules*, 2005. 6: p. 3357.

95. Tan, J.F., P. Ravi, H.P. Too, T.A. Hatton, and K.C. Tam, Association behavior of biotinylated and non-biotinylated poly(ethylene oxide)-b-poly(2-(diethylamino)ethyl methacrylate). *Biomacromolecules*, 2005. 6: p. 498.

96. Ketola, T.M., M. Hanzlikova, A. Urtti, H. Lemmetyinen, M. Yliperttula, and E. Vuorimaa, Role of polyplex intermediate species on gene transfer efficiency: polyethylenimine-DNA complexes and time-resolved fluorescence spectroscopy. *J Phys Chem B*, 2011. 115: p. 1895.

97.   Marty, R., C.N. N'Soukpoe-Kossi, D.M. Charbonneau, L. Kreplak, and H.A. Tajmir-Riahi, Structural characterization of cationic lipid-tRNA complexes. *Nucleic Acids Res*, 2009. 37: p. 5197.

98.   Dash, P.R., M.L. Read, L.B. Barrett, M. Wolfert, and L.W. Seymour, Factors affecting blood clearance and in vivo distribution of polyelectrolyte complexes for gene delivery. *Gene Ther*, 1999. 6: p. 643.

99.   Ogris, M., S. Brunner, S. Schuller, R. Kircheis, and E. Wagner, PEGylated DNA/transferrin-PEI complexes: reduced interaction with blood components, extended circulation in blood and potential for systemic gene delivery. *Gene Ther*, 1999. 6: p. 595.

100.   Lai, T.C., K. Kataoka, and G.S. Kwon, Bioreducible polyether-based pDNA ternary polyplexes: Balancing particle stability and transfection efficiency. *Colloids Surf B Biointerfaces*, 2012. 99: p. 27.

101.   Tsuchiya, A., Y. Naritomi, S. Kushio, J.H. Kang, M. Murata, M. Hashizume, T. Mori, T. Niidome, and Y. Katayama, Improvement in the colloidal stability of protein kinase-responsive polyplexes by PEG modification. *J Biomed Mater Res A*, 2012. 100: p. 1136.

102.   Weber, N.D., O.M. Merkel, T. Kissel, and M.A. Munoz-Fernandez, PEGylated poly(ethylene imine) copolymer-delivered siRNA inhibits HIV replication in vitro. *J Control Release*, 2012. 157: p. 55.

103.   Merkel, O.M., D. Librizzi, A. Pfestroff, T. Schurrat, K. Buyens, N.N. Sanders, S.C. De Smedt, M. Behe, and T. Kissel, Stability of siRNA polyplexes from poly(ethylenimine) and poly(ethylenimine)-g-poly(ethylene glycol) under in vivo conditions: effects on pharmacokinetics and biodistribution measured by Fluorescence Fluctuation Spectroscopy and Single Photon Emission Computed Tomography (SPECT) imaging. *J Control Release*, 2009. 138: p. 148.

104.   Itaka, K., K. Yamauchi, A. Harada, K. Nakamura, H. Kawaguchi, and K. Kataoka, Polyion complex micelles from plasmid DNA and poly(ethylene glycol)-poly(L-lysine) block copolymer as serum-tolerable polyplex system: physicochemical properties of micelles relevant to gene transfection efficiency. *Biomaterials*, 2003. 24: p. 4495.

105.   Anderson, K., A. Sizovs, M. Cortez, C. Waldron, D.M. Haddleton, and T.M. Reineke, Effects of trehalose polycation end-group functionalization on plasmid DNA uptake and transfection. *Biomacromolecules*, 2012. 13: p. 2229.

106. Oupicky, D., C. Konak, and K. Ulbrich, DNA complexes with block and graft copolymers of N-(2-hydroxypropyl) methacrylamide and 2-(trimethylammonio)ethyl methacrylate. *J Biomat Sci-Polym E*, 1999. 10: p. 573.

107. Oupicky, D., C. Konak, K. Ulbrich, M.A. Wolfert, and L.W. Seymour, DNA delivery systems based on complexes of DNA with synthetic polycations and their copolymers. *J Control Release*, 2000. 65: p. 149.

108. Seymour, L.W., Passive Tumor Targeting of Soluble Macromolecules and Drug Conjugates. *Crit Rev Ther Drug*, 1992. 9: p. 135.

109. Vasey, P.A., S.B. Kaye, R. Morrison, C. Twelves, P. Wilson, R. Duncan, A.H. Thomson, L.S. Murray, T.E. Hilditch, T. Murray, S. Burtles, D. Fraier, E. Frigerio, and J. Cassidy, Phase I clinical and pharmacokinetic study of PK1 [N-(2-hydroxypropyl)methacrylamide copolymer doxorubicin]: first member of a new class of chemotherapeutic agents-drug-polymer conjugates. Cancer Research Campaign Phase I/II Committee. *Clin Cancer Res*, 1999. 5: p. 83.

110. Burke, R.S. and S.H. Pun, Synthesis and characterization of biodegradable HPMA-oligolysine copolymers for improved gene delivery. *Bioconjug Chem*, 2010. 21: p. 140.

111. Morimoto, K., M. Nishikawa, S. Kawakami, T. Nakano, Y. Hattori, S. Fumoto, F. Yamashita, and M. Hashida, Molecular weight-dependent gene transfection activity of unmodified and galactosylated polyethyleneimine on hepatoma cells and mouse liver. *Mol Ther*, 2003. 7: p. 254.

112. He, W., Z.H. Guo, Y.T. Wen, Q. Wang, B.M. Xie, S.F. Zhu, and Q.M. Wang, Alginate-Graft-PEI as a Gene Delivery Vector with High Efficiency and Low Cytotoxicity. *J Biomat Sci-Polym E*, 2012. 23: p. 315.

113. Burckbuchler, V., V. Wintgens, C. Leborgne, S. Lecomte, N. Leygue, D. Scherman, A. Kichler, and C. Amiel, Development and characterization of new cyclodextrin polymer-based DNA delivery systems. *Bioconjug Chem*, 2008. 19: p. 2311.

114. Sun, K., J. Wang, J. Zhang, M. Hua, C.S. Liu, and T.Y. Chen, Dextran-g-PEI nanoparticles as a carrier for co-delivery of adriamycin and plasmid into osteosarcoma cells. *Int J Biol Macromol*, 2011. 49: p. 173.

115. Thomas, J.J., M.R. Rekha, and C.P. Sharma, Dextran-protamine polycation: An efficient nonviral and haemocompatible gene delivery system. *Colloid Surface B*, 2010. 81: p. 195.

116. Needham, C.J., A.K. Williams, S.A. Chew, F.K. Kasper, and A.G. Mikos, Engineering a Polymeric Gene Delivery Vector Based on Poly(ethylenimine) and Hyaluronic Acid. *Biomacromolecules*, 2012. 13: p. 1429.

117. Patnaik, S., A. Aggarwal, S. Nimesh, A. Goel, M. Ganguli, N. Saini, Y. Singh, and K.C. Gupta, PEI-alginate nanocomposites as efficient in vitro gene transfection agents. *J Control Release*, 2006. 114: p. 398.

118. Rhaese, S., H. von Briesen, H. Rubsamen-Waigmann, J. Kreuter, and K. Langer, Human serum albumin-polyethylenimine nanoparticles for gene delivery. *J Control Release*, 2003. 92: p. 199.

119. Liu, N., Y.L. Hao, Z. Yin, M.S. Ma, L. Wang, and X.N. Zhang, Self-assembled human serum albumin-coated complexes for gene delivery with improved transfection. *Pharmazie*, 2012. 67: p. 174.

120. Carrabino, S., S. Di Gioia, E. Copreni, and M. Conese, Serum albumin enhances polyethylenimine-mediated gene delivery to human respiratory epithelial cells. *J Gene Med*, 2005. 7: p. 1555.

121. Dash, P.R., M.L. Read, K.D. Fisher, K.A. Howard, M. Wolfert, D. Oupicky, V. Subr, J. Strohalm, K. Ulbrich, and L.W. Seymour, Decreased binding to proteins and cells of polymeric gene delivery vectors surface modified with a multivalent hydrophilic polymer and retargeting through attachment of transferrin. *J Biol Chem*, 2000. 275: p. 3793.

122. Blessing, T., M. Kursa, R. Holzhauser, R. Kircheis, and E. Wagner, Different strategies for formation of PEGylated EGF-conjugated PEI/DNA complexes for targeted gene delivery. *Bioconjugate Chem*, 2001. 12: p. 529.

123. Lee, K.M., Y.B. Lee, and I.J. Oh, Evaluation of PEG-Transferrin-PEI Nanocomplex as a Gene Delivery Agent. *J Nanosci Nanotechno*, 2011. 11: p. 7078.

124. Ward, C.M., M. Pechar, D. Oupicky, K. Ulbrich, and L.W. Seymour, Modification of pLL/DNA complexes with a multivalent hydrophilic polymer permits folate-mediated targeting in vitro and prolonged plasma circulation in vivo. *J Gene Med*, 2002. 4: p. 536.

125. Grzelinski, M., B. Urban-Klein, T. Martens, K. Lamszus, U. Bakowsky, S. Hobel, F. Czubayko, and A. Aigner, RNA interference-mediated gene silencing of pleiotrophin through polyethylenimine-complexed small

interfering RNAs in vivo exerts antitumoral effects in glioblastoma xenografts. *Hum Gene Ther*, 2006. 17: p. 751.

126. Kirkham, M. and R.G. Parton, Clathrin-independent endocytosis: new insights into caveolae and non-caveolar lipid raft carriers. *Biochim Biophys Acta*, 2005. 1746: p. 349.

127. Langel, U., Handbook of Cell-Penetrating Peptides, Second Edition (Pharmacology and Toxicology: Basic and Clinical Aspects). 2 ed, ed. U. Langel. 2007: Taylor and Francis.

128. Dale, D.C., L. Boxer, and W.C. Liles, The phagocytes: neutrophils and monocytes. *Blood*, 2008. 112: p. 935.

129. Besheer, A., J. Vogel, D. Glanz, J. Kressler, T. Groth, and K. Mader, Characterization of PLGA nanospheres stabilized with amphiphilic polymers: hydrophobically modified hydroxyethyl starch vs pluronics. *Mol Pharmaceut*, 2009. 6: p. 407.

130. Noga, M., D. Edinger, W. Rodl, E. Wagner, G. Winter, and A. Besheer, Controlled shielding and deshielding of gene delivery polyplexes using hydroxyethyl starch (HES) and alpha-amylase. *J Control Release*, 2012. 159: p. 92.

131. Vercauteren, D., M. Piest, L.J. van der Aa, M. Al Soraj, A.T. Jones, J.F. Engbersen, S.C. De Smedt, and K. Braeckmans, Flotillin-dependent endocytosis and a phagocytosis-like mechanism for cellular internalization of disulfide-based poly(amido amine)/DNA polyplexes. *Biomaterials*, 2011. 32: p. 3072.

132. Kopatz, I., J.S. Remy, and J.P. Behr, A model for non-viral gene delivery: through syndecan adhesion molecules and powered by actin. *J Gene Med*, 2004. 6: p. 769.

133. Kerr, M.C. and R.D. Teasdale, Defining macropinocytosis. *Traffic*, 2009. 10: p. 364.

134. Swanson, J.A. and S.C. Baer, Phagocytosis by zippers and triggers. *Trends Cell Biol*, 1995. 5: p. 89.

135. Gu, Z., E.H. Noss, V.W. Hsu, and M.B. Brenner, Integrins traffic rapidly via circular dorsal ruffles and macropinocytosis during stimulated cell migration. *J Cell Biol*, 2011. 193: p. 61.

136. Hsu, S.H., T.T. Ho, and T.C. Tseng, Nanoparticle uptake and gene transfer efficiency for MSCs on chitosan and chitosan-hyaluronan substrates. *Biomaterials*, 2012. 33: p. 3639.

137. Petrova, S., I. Kolev, S. Miloshev, M.D. Apostolova, and R. Mateva, Synthesis of amphiphilic [PEO(PCL)(2)] triarm star-shaped block copolymers: a promising system for in cell delivery. *J Mater Sci Mater Med*, 2012. 23: p. 1225.

138. Ming, X., K. Sato, and R.L. Juliano, Unconventional internalization mechanisms underlying functional delivery of antisense oligonucleotides via cationic lipoplexes and polyplexes. *J Control Release*, 2011. 153: p. 83.

139. Douglas, K.L., Toward development of artificial viruses for gene therapy: a comparative evaluation of viral and non-viral transfection. *Biotechnol Prog*, 2008. 24: p. 871.

140. Reilly, C., Polyplexes Traffic through Caveolae to the Golgi and Endoplasmic Reticulum en Route to the Nucleus. *Mol Pharmaceut*, 2012. 9: p. 1280.

141. Billiet, L., J.P. Gomez, M. Berchel, P.A. Jaffres, T. Le Gall, T. Montier, E. Bertrand, H. Cheradame, P. Guegan, M. Mevel, B. Pitard, T. Benvegnu, P. Lehn, C. Pichon, and P. Midoux, Gene transfer by chemical vectors, and endocytosis routes of polyplexes, lipoplexes and lipopolyplexes in a myoblast cell line. *Biomaterials*, 2012. 33: p. 2980.

142. van der Aa, M.A., U.S. Huth, S.Y. Hafele, R. Schubert, R.S. Oosting, E. Mastrobattista, W.E. Hennink, R. Peschka-Suss, G.A. Koning, and D.J. Crommelin, Cellular uptake of cationic polymer-DNA complexes via caveolae plays a pivotal role in gene transfection in COS-7 cells. *Pharmaceut Res*, 2007. 24: p. 1590.

143. von Gersdorff, K., N.N. Sanders, R. Vandenbroucke, S.C. De Smedt, E. Wagner, and M. Ogris, The internalization route resulting in successful gene expression depends on both cell line and polyethylenimine polyplex type. *Mol Ther*, 2006. 14: p. 745.

144. Hu, Q., J. Wang, J. Shen, M. Liu, X. Jin, G. Tang, and P.K. Chu, Intracellular pathways and nuclear localization signal peptide-mediated gene transfection by cationic polymeric nanovectors. *Biomaterials*, 2012. 33: p. 1135.

145. Benfer, M. and T. Kissel, Cellular uptake mechanism and knockdown activity of siRNA-loaded biodegradable DEAPA-PVA-g-PLGA nanoparticles. *Eur J Pharm Biopharm*, 2012. 80: p. 247.

146. Li, H., Y. Xiao, J. Niu, X. Chen, and Q. Ping, Preparation of a cationic nanoemulsome for intratumoral drug delivery and its enhancing effect on cellular uptake in vitro. *J Nanosci Nanotechnol*, 2011. 11: p. 8547.

147. Perumal, O.P., R. Inapagolla, S. Kannan, and R.M. Kannan, The effect of surface functionality on cellular trafficking of dendrimers. *Biomaterials*, 2008. 29: p. 3469.

148. Payne, C.K., S.A. Jones, C. Chen, and X. Zhuang, Internalization and trafficking of cell surface proteoglycans and proteoglycan-binding ligands. *Traffic*, 2007. 8: p. 389.

149. Dauty, E., J.S. Remy, G. Zuber, and J.P. Behr, Intracellular delivery of nanometric DNA particles via the folate receptor. *Bioconjug Chem*, 2002. 13: p. 831.

150. Xiao, K., Y. Li, J. Luo, J.S. Lee, W. Xiao, A.M. Gonik, R.G. Agarwal, and K.S. Lam, The effect of surface charge on in vivo biodistribution of PEG-oligocholic acid based micellar nanoparticles. *Biomaterials*, 2011. 32: p. 3435.

151. Kim, T.I., T. Rothmund, T. Kissel, and S.W. Kim, Bioreducible polymers with cell penetrating and endosome buffering functionality for gene delivery systems. *J Control Release*, 2011. 152: p. 110.

152. Tseng, W.C., T.Y. Fang, L.Y. Su, and C.H. Tang, Dependence of transgene expression and the relative buffering capacity of dextran-grafted polyethylenimine. *Mol Pharm*, 2005. 2: p. 224.

153. Funhoff, A.M., C.F. van Nostrum, G.A. Koning, N.M. Schuurmans-Nieuwenbroek, D.J. Crommelin, and W.E. Hennink, Endosomal escape of polymeric gene delivery complexes is not always enhanced by polymers buffering at low pH. *Biomacromolecules*, 2004. 5: p. 32.

154. Akinc, A., M. Thomas, A.M. Klibanov, and R. Langer, Exploring polyethylenimine-mediated DNA transfection and the proton sponge hypothesis. *J Gene Med*, 2005. 7: p. 657.

155. Yang, S. and S. May, Release of cationic polymer-DNA complexes from the endosome: A theoretical investigation of the proton sponge hypothesis. *J Chem Phys*, 2008. 129: p. 185105.

156. Kakimoto, S., T. Tanabe, H. Azuma, and T. Nagasaki, Enhanced internalization and endosomal escape of dual-functionalized poly(ethyleneimine)s polyplex with diphtheria toxin T and R domains. *Biomed Pharmacother*, 2010. 64: p. 296.

157. Lee, H., J.H. Jeong, and T.G. Park, PEG grafted polylysine with fusogenic peptide for gene delivery: high transfection efficiency with low cytotoxicity. *J Control Release*, 2002. 79: p. 283.

158. Moore, N.M., C.L. Sheppard, T.R. Barbour, and S.E. Sakiyama-Elbert, The effect of endosomal escape peptides on in vitro gene delivery of polyethylene glycol-based vehicles. *J Gene Med*, 2008. 10: p. 1134.

159. Boeckle, S., J. Fahrmeir, W. Roedl, M. Ogris, and E. Wagner, Melittin analogs with high lytic activity at endosomal pH enhance transfection with purified targeted PEI polyplexes. *J Control Release*, 2006. 112: p. 240.

160. Kwon, E.J., J.M. Bergen, and S.H. Pun, Application of an HIV gp41-derived peptide for enhanced intracellular trafficking of synthetic gene and siRNA delivery vehicles. *Bioconjugate Chem*, 2008. 19: p. 920.

161. Wolfert, M.A. and L.W. Seymour, Chloroquine and amphipathic peptide helices show synergistic transfection in vitro. *Gene Ther*, 1998. 5: p. 409.

162. Moore, N.M., C.L. Sheppard, and S.E. Sakiyama-Elbert, Characterization of a multifunctional PEG-based gene delivery system containing nuclear localization signals and endosomal escape peptides. *Acta biomat*, 2009. 5: p. 854.

163. Tanaka, K., T. Kanazawa, T. Ogawa, Y. Suda, Y. Takashima, T. Fukuda, and H. Okada, A novel, bio-reducible gene vector containing arginine and histidine enhances gene transfection and expression of plasmid DNA. *Chem Pharm Bull (Tokyo)*, 2011. 59: p. 202.

164. Deng, J., Y. Wen, C. Wang, S. Pan, H. Gu, X. Zeng, L. Han, Y. Zhao, M. Feng, and C. Wu, Efficient intracellular gene delivery using the formulation composed of poly (L-glutamic acid) grafted polyethylenimine and histone. *Pharm Res*, 2011. 28: p. 812.

165. Zhang, B. and S. Mallapragada, The mechanism of selective transfection mediated by pentablock copolymers; part II: nuclear entry and endosomal escape. *Acta Biomaterialia*, 2011. 7: p. 1580.

166. Cabral, H., M. Nakanishi, M. Kumagai, W.D. Jang, N. Nishiyama, and K. Kataoka, A photo-activated targeting chemotherapy using glutathione sensitive camptothecin-loaded polymeric micelles. *Pharmaceut Res*, 2009. 26: p. 82.

167. Nishiyama, N., A. Iriyama, W.D. Jang, K. Miyata, K. Itaka, Y. Inoue, H. Takahashi, Y. Yanagi, Y. Tamaki, H. Koyama, and K. Kataoka, Light-

induced gene transfer from packaged DNA enveloped in a dendrimeric photosensitizer. *Nat Mat*, 2005. 4: p. 934.

168. Bonsted, A., E. Wagner, L. Prasmickaite, A. Hogset, and K. Berg, Photochemical enhancement of DNA delivery by EGF receptor targeted polyplexes. *Methods in Molecular Biology*, 2008. 434: p. 171.

169. de Bruin, K.G., C. Fella, M. Ogris, E. Wagner, N. Ruthardt, and C. Brauchle, Dynamics of photoinduced endosomal release of polyplexes. *J Control Release*, 2008. 130: p. 175.

170. Ndoye, A., G. Dolivet, A. Hogset, A. Leroux, A. Fifre, P. Erbacher, K. Berg, J.P. Behr, F. Guillemin, and J.L. Merlin, Eradication of p53-mutated head and neck squamous cell carcinoma xenografts using nonviral p53 gene therapy and photochemical internalization. *Mol Ther*, 2006. 13: p. 1156.

171. Sauer, A.M., A. Schlossbauer, N. Ruthardt, V. Cauda, T. Bein, and C. Brauchle, Role of endosomal escape for disulfide-based drug delivery from colloidal mesoporous silica evaluated by live-cell imaging. *Nano Letters*, 2010. 10: p. 3684.

172. Pollard, H., J.S. Remy, G. Loussouarn, S. Demolombe, J.P. Behr, and D. Escande, Polyethylenimine but not cationic lipids promotes transgene delivery to the nucleus in mammalian cells. *J Biol Chem*, 1998. 273: p. 7507.

173. Schaffer, D.V., N.A. Fidelman, N. Dan, and D.A. Lauffenburger, Vector unpacking as a potential barrier for receptor-mediated polyplex gene delivery. *Biotechnol Bioeng*, 2000. 67: p. 598.

174. Danielsen, S., S. Strand, C. de Lange Davies, and B.T. Stokke, Glycosaminoglycan destabilization of DNA-chitosan polyplexes for gene delivery depends on chitosan chain length and GAG properties. *Biochimica et Biophysica Acta*, 2005. 1721: p. 44.

175. Strand, S.P., S. Lelu, N.K. Reitan, C. de Lange Davies, P. Artursson, and K.M. Varum, Molecular design of chitosan gene delivery systems with an optimized balance between polyplex stability and polyplex unpacking. *Biomaterials*, 2010. 31: p. 975.

176. Boussif, O., F. Lezoualc'h, M.A. Zanta, M.D. Mergny, D. Scherman, B. Demeneix, and J.P. Behr, A versatile vector for gene and oligonucleotide transfer into cells in culture and in vivo: polyethylenimine. *P Natl Acad Sci USA*, 1995. 92: p. 7297.

177.   Chen, H.H., Y.P. Ho, X. Jiang, H.Q. Mao, T.H. Wang, and K.W. Leong, Quantitative comparison of intracellular unpacking kinetics of polyplexes by a model constructed from quantum dot-FRET. *Mol Ther*, 2008. 16: p. 324.

178.   Kurisawa, M., M. Yokoyama, and T. Okano, Gene expression control by temperature with thermo-responsive polymeric gene carriers. *J Controll Release*, 2000. 69: p. 127.

179.   Sun, S., W. Liu, N. Cheng, B. Zhang, Z. Cao, K. Yao, D. Liang, A. Zuo, G. Guo, and J. Zhang, A thermoresponsive chitosan-NIPAAm/vinyl laurate copolymer vector for gene transfection. *Bioconjugate Chem*, 2005. 16: p. 972.

180.   Cheng, N., W. Liu, Z. Cao, W. Ji, D. Liang, G. Guo, and J. Zhang, A study of thermoresponsive poly(N-isopropylacrylamide)/polyarginine bioconjugate non-viral transgene vectors. *Biomaterials*, 2006. 27: p. 4984.

181.   Yamashita, A., D. Kanda, R. Katoono, N. Yui, T. Ooya, A. Maruyama, H. Akita, K. Kogure, and H. Harashima, Supramolecular control of polyplex dissociation and cell transfection: efficacy of amino groups and threading cyclodextrins in biocleavable polyrotaxanes. *J Control Release*, 2008. 131: p. 137.

182.   Soundara Manickam, D. and D. Oupicky, Polyplex gene delivery modulated by redox potential gradients. *J Drug Targeting*, 2006. 14: p. 519.

183.   Lynn, D.M. and R. Langer, Degradable poly(beta-amino esters): Synthesis, characterization, and self-assembly with plasmid DNA. *J Am Chem Soc*, 2000. 122: p. 10761.

184.   Arote, R.B., E.S. Lee, H.L. Jiang, Y.K. Kim, Y.J. Choi, M.H. Cho, and C.S. Cho, Efficient gene delivery with osmotically active and hyperbranched poly(ester amine)s. *Bioconjug Chem*, 2009. 20: p. 2231.

185.   Zhong, Z., Y. Song, J.F. Engbersen, M.C. Lok, W.E. Hennink, and J. Feijen, A versatile family of degradable non-viral gene carriers based on hyperbranched poly(ester amine)s. *J Control Release*, 2005. 109: p. 317.

186.   Dai, F.Y. and W.G. Liu, Enhanced gene transfection and serum stability of polyplexes by PDMAEMA-polysulfobetaine diblock copolymers. *Biomaterials*, 2011. 32: p. 628.

187.   DuPraw, E.J., Cell and molecular biology. 1968: New york, Academic press.

188. Wiethoff, C.M. and C.R. Middaugh, Barriers to nonviral gene delivery. *J Pharm Sci*, 2003. 92: p. 203.

189. Mortimer, I., P. Tam, I. MacLachlan, R.W. Graham, E.G. Saravolac, and P.B. Joshi, Cationic lipid-mediated transfection of cells in culture requires mitotic activity. *Gene Ther*, 1999. 6: p. 403.

190. McLane, L.M. and A.H. Corbett, Nuclear localization signals and human disease. *IUBMB Life*, 2009. 61: p. 697.

191. Yi, W.J., J. Yang, C. Li, H.Y. Wang, C.W. Liu, L. Tao, S.X. Cheng, R.X. Zhuo, and X.Z. Zhang, Enhanced nuclear import and transfection efficiency of TAT peptide-based gene delivery systems modified by additional nuclear localization signals. *Bioconjugate Chem*, 2012. 23: p. 125.

192. Shen, Y., H. Peng, S. Pan, M. Feng, Y. Wen, J. Deng, X. Luo, and C. Wu, Interaction of DNA/nuclear protein/polycation and the terplexes for gene delivery. *Nanotechnology*, 2010. 21: p. 045102.

193. Jeong, J.H., S.H. Kim, L.V. Christensen, J. Feijen, and S.W. Kim, Reducible poly(amido ethylenimine)-based gene delivery system for improved nucleus trafficking of plasmid DNA. *Bioconjugate Chem*, 2010. 21: p. 296.

194. Zabner, J., A.J. Fasbender, T. Moninger, K.A. Poellinger, and M.J. Welsh, Cellular and molecular barriers to gene transfer by a cationic lipid. *J Biol Chem*, 1995. 270: p. 18997.

195. James, M.B. and T.D. Giorgio, Nuclear-associated plasmid, but not cell-associated plasmid, is correlated with transgene expression in cultured mammalian cells. *Mol Ther*, 2000. 1: p. 339.

196. Ogris, M., R.C. Carlisle, T. Bettinger, and L.W. Seymour, Melittin enables efficient vesicular escape and enhanced nuclear access of nonviral gene delivery vectors. *J Biol Chem*, 2001. 276: p. 47550.

197. Yang, Z., G. Sahay, S. Sriadibhatla, and A.V. Kabanov, Amphiphilic Block Copolymers Enhance Cellular Uptake and Nuclear Entry of Polyplex-Delivered DNA. *Bioconjugate Chem*, 2008. 19: p. 1987.

198. Grandinetti, G., A.E. Smith, and T.M. Reineke, Membrane and nuclear permeabilization by polymeric pDNA vehicles: efficient method for gene delivery or mechanism of cytotoxicity? *Mol Pharm*, 2012. 9: p. 523.

199. Tanimoto, M., H. Kamiya, N. Minakawa, A. Matsuda, and H. Harashima, No enhancement of nuclear entry by direct conjugation of a nuclear

localization signal peptide to linearized DNA. *Bioconjugate Chem*, 2003. 14: p. 1197.

200. van der Aa, M., G. Koning, J. van der Gugten, C. d'Oliveira, R. Oosting, W.E. Hennink, and D.J. Crommelin, Covalent attachment of an NLS-peptide to linear dna does not enhance transfection efficiency of cationic polymer based gene delivery systems. *J Control Release*, 2005. 101: p. 395.

201. van der Aa, M.A., G.A. Koning, C. d'Oliveira, R.S. Oosting, K.J. Wilschut, W.E. Hennink, and D.J. Crommelin, An NLS peptide covalently linked to linear DNA does not enhance transfection efficiency of cationic polymer based gene delivery systems. *J Gene Med*, 2005. 7: p. 208.

202. Breuzard, G., M. Tertil, C. Goncalves, H. Cheradame, P. Geguan, C. Pichon, and P. Midoux, Nuclear delivery of NFkappaB-assisted DNA/polymer complexes: plasmid DNA quantitation by confocal laser scanning microscopy and evidence of nuclear polyplexes by FRET imaging. *Nucleic Acids Res*, 2008. 36: p. e71.

203. Chen, X., D.M. Kube, M.J. Cooper, and P.B. Davis, Cell surface nucleolin serves as receptor for DNA nanoparticles composed of pegylated polylysine and DNA. *Mol Ther*, 2008. 16: p. 333.

204. Hinton, T.M., C. Guerrero-Sanchez, J.E. Graham, T. Le, B.W. Muir, S. Shi, M.L. Tizard, P.A. Gunatillake, K.M. McLean, and S.H. Thang, The effect of RAFT-derived cationic block copolymer structure on gene silencing efficiency. *Biomaterials*, 2012. 33: p. 7631.

205. Goldberg, M., K. Mahon, and D. Anderson, Combinatorial and rational approaches to polymer synthesis for medicine. *Adv Drug Deliv Rev*, 2008. 60: p. 971.

206. Anderson, D.G., C.A. Tweedie, N. Hossain, S.M. Navarro, D.M. Brey, K.J. Van Vliet, R. Langer, and J.A. Burdick, A combinatorial library of photocrosslinkable and degradable materials. *Adv Mater*, 2006. 18: p. 2614.

207. Martello, F., M. Piest, J.F. Engbersen, and P. Ferruti, Effects of branched or linear architecture of bioreducible poly(amido amine)s on their in vitro gene delivery properties. *J Control Release*, 2012.

208. Lu, Z.X., L.T. Liu, and X.R. Qi, Development of small interfering RNA delivery system using PEI-PEG-APRPG polymer for antiangiogenic

vascular endothelial growth factor tumor-targeted therapy. *Int J Nanomed*, 2011. 6: p. 1661.

209. Reilly, M.J., J.D. Larsen, and M.O. Sullivan, Histone H3 Tail Peptides and Poly(ethylenimine) Have Synergistic Effects for Gene Delivery. *Mol Pharmaceut*, 2012. 9: p. 1031.

210. Hu, Q.L., J.L. Wang, J. Shen, M. Liu, X. Jin, G.P. Tang, and P.K. Chu, Intracellular pathways and nuclear localization signal peptide-mediated gene transfection by cationic polymeric nanovectors. *Biomaterials*, 2012. 33: p. 1135.

211. Sweeney, P., T. Karashima, H. Ishikura, S. Wiehle, M. Yamashita, W.F. Benedict, R.J. Cristiano, and C.P.N. Dinney, Efficient therapeutic gene delivery after systemic administration of a novel polyethylenimine/DNA vector in an orthotopic bladder cancer model. *Cancer Res*, 2003. 63: p. 4017.

212. Malek, A., O. Merkel, L. Fink, F. Czubayko, T. Kissel, and A. Aigner, In vivo pharmacokinetics, tissue distribution and underlying mechanisms of various PEI(-PEG)/siRNA complexes. *Toxicol Appl Pharm*, 2009. 236: p. 97.

213. Fitzsimmons, R.E. and H. Uludag, Specific effects of PEGylation on gene delivery efficacy of polyethylenimine: Interplay between PEG substitution and N/P ratio. *Acta Biomater*, 2012.

214. Roesler, S., F.P. Koch, T. Schmehl, N. Weissmann, W. Seeger, T. Gessler, and T. Kissel, Amphiphilic, low molecular weight poly(ethylene imine) derivatives with enhanced stability for efficient pulmonary gene delivery. *J Gene Med*, 2011. 13: p. 123.

215. Goyal, R., S.K. Tripathi, S. Tyagi, A. Sharma, K.R. Ram, D.K. Chowdhuri, Y. Shukla, P. Kumar, and K.C. Gupta, Linear PEI nanoparticles: efficient pDNA/siRNA carriers in vitro and in vivo. *Nanomedicine*, 2012. 8: p. 167.

216. Brissault, B., C. Leborgne, C. Guis, O. Danos, H. Cheradame, and A. Kichler, Linear topology confers in vivo gene transfer activity to polyethylenimines. *Bioconjug Chem*, 2006. 17: p. 759.

217. Bonnet, M.E., P. Erbacher, and A.L. Bolcato-Bellemin, Systemic delivery of DNA or siRNA mediated by linear polyethylenimine (L-PEI) does not induce an inflammatory response. *Pharm Res*, 2008. 25: p. 2972.

218. Fu, C., X. Sun, D. Liu, Z. Chen, Z. Lu, and N. Zhang, Biodegradable Tri-Block Copolymer Poly(lactic acid)-poly(ethylene glycol)-poly(l-lysine)(PLA-PEG-PLL) as a Non-Viral Vector to Enhance Gene Transfection. *Int J Mol Sci*, 2011. 12: p. 1371.

219. Pan, S., C. Wang, X. Zeng, Y. Wen, H. Wu, and M. Feng, Short multi-armed polylysine-graft-polyamidoamine copolymer as efficient gene vectors. *Int J Pharm*, 2011. 420: p. 206.

220. He, Y., G. Cheng, L. Xie, Y. Nie, B. He, and Z. Gu, Polyethyleneimine/DNA polyplexes with reduction-sensitive hyaluronic acid derivatives shielding for targeted gene delivery. *Biomaterials*, 2013. 34: p. 1235.

221. Patnaik, S. and K.C. Gupta, Novel polyethylenimine-derived nanoparticles for in vivo gene delivery. *Expert Opin Drug Deliv*, 2012.

222. Mathew, A., H. Cao, E. Collin, W. Wang, and A. Pandit, Hyperbranched PEGmethacrylate linear pDMAEMA block copolymer as an efficient non-viral gene delivery vector. *Int J Pharm*, 2012. 434: p. 99.

223. Fan, M.M., X. Zhang, J. Qin, B.J. Li, X. Sun, and S. Zhang, Self-Assembly Pluronic and beta-Cyclodextrin to Hollow Nanospheres for Enhanced Gene Delivery. *Macromol Rapid Commun*, 2011.

224. Uchida, S., K. Itaka, Q. Chen, K. Osada, T. Ishii, M.A. Shibata, M. Harada-Shiba, and K. Kataoka, PEGylated polyplex with optimized PEG shielding enhances gene introduction in lungs by minimizing inflammatory responses. *Mol Ther*, 2012. 20: p. 1196.

225. Ouyang, D., H. Zhang, H.S. Parekh, and S.C. Smith, The effect of pH on PAMAM dendrimer-siRNA complexation - Endosomal considerations as determined by molecular dynamics simulation. *Biophys Chem*, 2011. 158: p. 126.

226. Casettari, L., D. Vllasaliu, J.K.W. Lam, M. Soliman, and L. Illum, Biomedical applications of amino acid-modified chitosans: A review. *Biomaterials*, 2012. 33: p. 7565.

227. McMahon, A., M.J. O'Neill, E. Gomez, R. Donohue, D. Forde, R. Darcy, and C.M. O'Driscoll, Targeted gene delivery to hepatocytes with galactosylated amphiphilic cyclodextrins. *J Pharm Pharmacol*, 2012. 64: p. 1063.

228. Wolff, J.A. and V. Budker, The mechanism of naked DNA uptake and expression. *Adv Genet*, 2005. 54: p. 3.

229. Uchida, M., X.W. Li, P. Mertens, and H.O. Alpar, Transfection by particle bombardment: delivery of plasmid DNA into mammalian cells using gene gun. *Biochim Biophys Acta*, 2009. 1790: p. 754.

230. Zhong, W., W.H. Sit, J.M. Wan, and A.C. Yu, Sonoporation induces apoptosis and cell cycle arrest in human promyelocytic leukemia cells. *Ultrasound Med Biol*, 2011. 37: p. 2149.

231. Plank, C., O. Zelphati, and O. Mykhaylyk, Magnetically enhanced nucleic acid delivery. Ten years of magnetofection-progress and prospects. *Adv Drug Deliv Rev*, 2011. 63: p. 1300.

232. Denet, A.R. and V. Preat, Transdermal delivery of timolol by electroporation through human skin. *J Control Release*, 2003. 88: p. 253.

233. Eltoukhy, A.A., D.J. Siegwart, C.A. Alabi, J.S. Rajan, R. Langer, and D.G. Anderson, Effect of molecular weight of amine end-modified poly(beta-amino ester)s on gene delivery efficiency and toxicity. *Biomaterials*, 2012. 33: p. 3594.

234. Biaglow, J.E., J. Donahue, S. Tuttle, K. Held, C. Chrestensen, and J. Mieyal, A method for measuring disulfide reduction by cultured mammalian cells: relative contributions of glutathione-dependent and glutathione-independent mechanisms. *Anal Biochem*, 2000. 281: p. 77.

235. Wang W., Z.Y., Roberts E.,Duxbury C.,Ding L., Irvine D.,and Howdle S., Controlling chain growth: A new strategy to hyperbranched materials. *Macromolecules*, 2007. 40: p. 7184.

CHAPTER 2

Optimizing polymer properties

Parts of this chapter have been published or submitted for publication.

Aied, A., Zheng, Y., Pandit, A., and Wang, W. (2012) 'DNA Immobilization and detection on cellulose paper using a surface grown cationic polymer via ATRP'. *ACS Applied Materials and Interfaces*, 4, 826-831.

Aied, A., Glynn, B., Cao, H., Zheng, Y., Tai, H., Pandit, A., and Wang, W. (2012) 'A fluorescently labeled, hyperbranched polymer synthesized from DE-ATRP for the detection of DNA hybridization'. *Polymer Chemistry*, 3, 332-334.

Aied, A., Zheng, Y., Newland, B., and Wang, W. 'Combining 'Celtic' Knots: Multi-knot structured polymer for gene delivery'. *Journal of Investigative Dermatology*, 2014. (Submitted)

2.1. Introduction

Polymers used in gene delivery have a different structural and atomic composition from those used in detection of biological components. Important characteristics that a polymeric gene delivery vector must have include: charge, usually provided by amine groups, optimal molecular weight and the ability to protect DNA if delivered *in vivo*. One of the most critical traits is high electric charge, required for binding the polymer to the negatively charged DNA backbone and collapsing it into nano-sized particles [1]. Additionally, this high electric potential helps gene delivery by interacting with the negatively charged cellular membrane. The charge density of polycations is dictated by the number of primary, secondary or tertiary amines in the polymer chain. In designing a polymer for gene delivery, we hypothesised that having high charge density will increase DNA packaging quality, encourage particle uptake and disrupt the endosome to promote DNA release (proton sponge effect [2]). This will lead to elevated transfection and increase the levels of protein expression (Figure 2.1). To achieve this goal, amine content will be increased in the polymer backbone and additional primary amines will be conjugated to the polymer terminals by post modification reactions.

It has been reported that increasing the charge density will increase toxicity and may prevent DNA unpacking inside the cell (Figure 2.2). To compensate for this, a disulfide reduction mechanism was introduced into the polymer. Disulfide bridges are reduced intracellularly by glutathione, which reduces the polymer size and aid in the unpacking of DNA from the polymer [3]. We thus hypothesised that increased charge density and fast intracellular reduction capability will improve transfection properties of cationic polymers while maintaining high cell viability.

Charge density is not the sole contributor to determining the transfection efficiency. Better studies have shown a general trend of branching resulting in better transfection capability when analysing the structure-function relationship of polymer transfection vectors, which were previously limited to linear, branched and dendritic architectures. For example, star shaped 2-

dimethylaminoethyl methacrylate (DMAEMA) based polymers, with cationic tertiary amines showed better transfection capability than the linear control [4]. However, the transfection capability was overshadowed by the fact branched PEI which contains primary, secondary and tertiary amines through its structure. It is also worth noting that end-capping of polymers with additional amines can vastly alter the transfection performance. For example, tertiary amine containing poly (β-amino esters) show highly improved transfection traits, comparable to that of an adenovirus, when end-capped with primary amines [5].

Previous reports have shown that there is an optimal molecular weight for transfection and higher molecular weight does not mean better transfection [6, 7]. High molecular weight polymers show better DNA binding, cellular uptake and transfection efficiency, while low molecular weight polymers show less cytotoxicity and better DNA un-packaging [8, 9]. To this end, high molecular weight PEI polymers have been synthesized for a transfection capability, but which cleave upon cell entry, to yield low molecular weight degradation products and reduce the overall toxicity of the vector [10]. In addition Artursson *et al*. studied the effect of low molecular weight chitosan (<5 kDa) related to physical shape and stability for gene delivery *in vitro* and *in vivo*. The study showed globular structures increased with increasing chain length of the chitosan oligomer and gene transfection efficiencies *in vitro* and *in vivo* were related to the physical shape and stability of the complexes.

Until recently, the majority of polymerizations involving multi-vinyl monomers (MVMs) were carried out by using the co-polymerization system containing only a low percentage of MVMs. To overcome this bottle-neck, we have developed a deactivation enhanced strategy for ATRP that efficiently delayed the point of gelation in the homopolymerization of ethylene glycol dimethacrylate (EGDMA) to over 60% monomer conversion in a concentrated polymerization system [11-13]. With this method, termed *in situ* deactivation enhanced ATRP (*in situ* DE-ATRP, Figure 2.3), we produced a new 3D 'Single knot' molecule architecture that consisted of a single polymer chain cyclized within itself at the early stage

of reaction [11, 13]. Furthermore, we reported the use of 'Single knot' polymer for gene delivery applications through the preparation of a series of cationic transfection agents. We observed that the single knot gene vector interacts differently with plasmid DNA compared to conventional vectors and has a superior transfection profile in terms of both transfection capability and preservation of cell viability [11]. This ground breaking work has driven us to continue designing and exploring this new gene vector, as we believe that it can, in principle, be improved by higher cationic density and lowering the cytotoxicity. As the non-degradable single knot vector demonstrates that a high transfection performance can be achieved, it can be reasonably hypothesized that the advanced degradable 'multi-knot' polymer chain will out-perform currently available polymer structures in terms of efficacy, cell viability, and scalability.

For complex 3-dimentional environments, a hyperbranched poly (β-amino ester) (HPAE) was synthesized and tested (designed and tested by Dr. Dezhong Zhou) in parallel to the multi-knot polymer. PAEs have been previously tested *in vivo* and demonstrated excellent transfection efficiency on a number of occasions [6, 14] which is why it was selected as the transfection agent specifically for *in vivo* experiments.

2.2.   Materials

All reagents have been purchased from Sigma Aldrich unless otherwise stated. A comprehensive list of materials has been supplied in Appendix Y.

2.3.   Methods

2.3.1.   PEEDEPE monomer synthesis

All containers used in the reaction were washed with Tetrahydrofuran (THF) before the experiment. One hundred millilitres of THF was first added to the reaction flask with of acroylyl chloride added immediately after. The mixture was cooled down on ice and argon gas bubbled through the stirring solution. While bubbling on ice, triethylamine (TEA) was added slowly. Argon gas was bubbled through the solution for another 10 minutes before the hydroxy ethyl disulfide was added drop wise and stirred for 2

hours in the fume hood. The flask was closed and the reaction was allowed to progress for another 24 hours.

2.3.2. PEEDEPE monomer purification

A white solution was obtained after the reaction time is over. This white solution was then passed through filter paper (Whatman® cellulose filter paper) a number of times until the solution turn colourless. One hundred and fifty millilitres of dichloromethane and sodium carbonate were then added drop wise and the mixture was shaken vigorously to remove toxins and CO_2 gas. This was repeated 6 times to ensure all toxins have been removed. To remove sodium carbonate, 150ml of distilled water and 1-3 grams of sodium chloride were added and mixed vigorously for a couple of minutes. The solution was allowed to settle, a layer of dichloromethane and PEEDEPE monomer should form once the mixture is settled. This layer was poured out carefully. This step was repeated 3 times to insure all the sodium carbonate is removed. Adding anhydrous magnesium sulfate at 50% mass of the total monomer solution absorbs the water out. This compound was then passed through aluminum oxide and cotton wool with excess dichloromethane, which is later, removed by rotary evaporator.

2.3.3. Disulfide polymer synthesis (Multi-knot polymer)

The polymer was prepared in acetonitrile (the volume ratios of total monomers to solvent = 1:1) at 60°C with Schlenk line system, where argon was bubbled through the solutions to remove oxygen. Liquids were transferred by means of septa and syringes while under argon. A typical reaction procedure is described: 2-(Dimethylamino)ethyl methacrylate (DMAEMA) (5.4g), PEEDEPE (1g), Ethyl-α-bromoisobutyrate (Initiator) (0.186 g), *N*,*N*,*N*′,*N*″,*N*″-Pentamethyldiethylenetriamine (Ligand) (0.016 g), $CuCl_2$ (0.013 g) and acetonitrile (7ml) were transferred to a two necked round-bottom flask fitted with stopcocks. Argon was bubbled through the solution for 15 minutes to purge the oxygen. L-ascorbic acid was added into the flask to start the reaction, which was kept in an oil bath at 60°C and stirring at 600rpm. Samples were taken at different time points for chromatography analysis to monitor the monomer conversions by

comparing the peak areas for monomers and polymers. The reaction was stopped when the desired monomer to polymer ratio was obtained.

2.3.4. Polymer purification

After polymerization, the polymer was precipitated by adding the solution drop-wise into a large excess of hexane and diethyl ether (1:1) to remove excess DMAEMA and PEEDEPE monomers. The precipitated polymer was dissolved in acetone and passed through an aluminum oxide glass column to remove the copper. Acetone was removed by rotary evaporation and the polymer was dissolved in water for the next procedure.

2.3.5. Conjugate addition of diamine monomers and protonation

Unreacted vinyl groups of polymer were end-capped by adding 200mg (2mmol, dissolved in water) of the polymer to 40mg (50mmol, dissolved in water) of either 1,3-diaminopropane or ethylenediamine under argon at ambient temperature for 48 hours in the dark. The end-capped polymer solution was protonated to pH 5.5 by adding 1M HCL drop wise under stirring while constantly monitoring the pH using a pH meter (FiveEasy[TM], Mettler Toledo). Finally, the solution was freeze-dried and a white soft sponge was obtained.

2.3.6. Characterization of the polymer

The resultant polymer was characterized by gel permeation chromatography (GPC) and proton nuclear magnetic resonance (^{1}H NMR). Number average molecular weight (M_n), weight average molecular weight (M_w), and polydispersity (M_w/M_n) were obtained by GPC (920-LC Liquid Chromatograph, Varian) with a refractive index detector, column heater and evaporative light scattering (ELS) detector supplied by Varian. The columns (300×7.5 mm PolarGel-M Column, two in series) were eluted using DMF and calibrated with poly (methyl methacrylate) standards. All calibrations and analyses were performed at 60 °C and a flow rate of 1 mL/min. ^{1}H NMR was carried out on a 400 MHz JEOL NMR with DELTA processing software. The chemical shifts were referenced to the lock $(CD3)_2CO$. (GPC and NMR sample preparation in Appendix).

2.3.7. Polymer degradation analysis

The polymer was dissolved in water and combined with a glutathione solution in water. The final concentrations of the multi-knot polymer and glutathione were 1mg/ml and 5mM, respectively. The mixture was stirred and incubated at 37°C from 10 minutes to 60 minutes. Excess iodoacetic acid (10mM) was added to prevent further degradation during subsequent steps. The sample was then freeze dried and resuspended in 100µl of water topped up to 3ml with dimethylformamide (DMF). GPC measurements were then taken as described previously.

2.3.8. Polyplex preparation and characterisation

Polyplexes can be prepared from various polymers to DNA ratios, namely nitrogen to phosphate (N/P) or weight to weight (w/w) ratios. For the polymer used throughout this study, an N/P ratio of 20:1 (or w/w of 10:1) showed the best performance in terms of transfection efficiency. To prepare polyplexes with 1µg of plasmid DNA, 10µl of 0.1mg/ml plasmid DNA is added to a vial containing 100µl of 0.1mg/ml polymer solution. Table 3 shows the list of ratios tested.

NanoDrop®, Gel Electrophoresis and PicoGreen® assay: The DNA packaging efficiency of the polymer was analysed using the nanodrop, gel electrophoresis PicoGreen® assay.

(Detailed protocols of these experiments are available in Appendices F, E and G, respectively).

Size and Zeta potential: The hydrodynamic diameters and zeta (ζ) potentials of the multi-knot/plasmid DNA complexes were determined by light scattering and zeta potential analyser (Malvern instruments, Zetasizer Nano-ZS90). Polyplex solutions (1ml) containing 10µg of *gaussia* luciferase pcDNA were prepared at different weight ratios ranging from 0.5 to 100 after incubation at 25°C for 1 hour. Measured sizes and potentials were presented in the results as the average values of 5 runs. Optimal weight ratios were used for PEI and Superfect® as described by the manufacturer.

Transmission Electron Microscopy: Confirmation of polyplex size was obtained by examining the polyplexes under a transmission electron microscope (Hitachi H-7500 Transmission Electron Microscope) that utilises 80kV accelerating voltage, Gatan Inc. US1000 high resolution digital camera and Gatan Inc. Digital micrograph acquisition software v1.82.366. Ten microliters of polyplex solution at weight ratios of 5 and 10 containing 0.5μg of *gaussia* luciferase pcDNA were pipetted on to Graphene grids (Agar scientific, UK) and visualised after drying.

2.3.9. Synthesis of the 'hyperbranched poly (β-amino ester) (HPAE)

According to conventional statistical theory defined by Flory and Stockmayer (F-S theory), "A2+B3" type reaction would lead to the formation of insoluble cross-linked gel. We employed low monomer concentration (10%) and mild reaction temperature (90°C) to delay the "gelation point", at the same time end-capped the base polymers (acrylate terminated polymers) timely to overcome the limitation defined in the F-S theory and obtained a series of well-defined HPAEs. By varying the feed ratio of trimethylolpropane triacrylate (TMPTA) to bisphenol a ethoxylate diacrylate (BE), PAE structure was modulated from "A2+B2" type linear structure to "A2+B3/B2" type hybrid hyperbranched structure step by step (Figure 2.16).

2.4. Results and Discussion

2.4.1. PEEDEPE monomer synthesis and characterization

2-{[2-(prop-2-enoyloxy)ethyl]disulfanyl-4-ethyl prop-2-enoate or PEEDEPE was synthesized by nucleophilic addition/elimination of acrylate chloride and hydroxy ethyl with hydrochloric acid being the side product of the reaction (Figure 2.5). After purification, a light yellow and slightly viscous solution was obtained. Being highly reactive because of its divinyl groups, the monomer was always protected from light and stored at 4°C. The ^{1}H NMR spectrum confirmed the monomer structure and showed the presence of divinyl functional groups.

2.4.2. Disulfide polymer synthesis and amine conjugation

The multi-knot vectors were synthesized via *in situ* deactivation-enhanced atom transfer radical copolymerization of DMAEMA and PEEDEPE [15, 16], and post-functionalized by 1, 3-diaminopropane. The feed ratio of these two monomers was 90:10. The disulfide monomer, PEEDEPE, was synthesized by chlorine substitution of acroylyl chloride and hydroxy ethyle disulfide in the presence of triethylamine (TEA) as reported previously [17]. Gel permeation chromatography (GPC) and proton nuclear magnetic resonance (^{1}H NMR) were used to determine the polymer molecular weight and composition, respectively (Figure 2.7 and Figure 2.8 respectively). Firstly, the polymer chains display a linear-like growth, which is the increase of molecular weight, is linear with monomer conversion and PDI remaining low with unimodal molecular distribution (Figure 2.4). However, when the reaction reaches high monomer conversion, the single knot molecules start to combine into multi-knot molecules, along with a significant molecular weight increase. After 7 hours of reaction time at 60˚C, the DE-ATRP reaction was stopped resulting in a polymer with 40 kDa M_w (Table 2.4). The remaining vinyl groups were end-functionalized with 1, 3-diaminopropane by Michael Addition (Figure 2.9). It could reasonably be assumed that in addition, these vinyl groups could be subject to other post modifications for precise cell targeting or crossing *in vivo* or intracellular gene delivery barriers.

2.4.3. Polymer degradation

To investigate the degradation of the multi-knot polymer, the polymer was dissolved in 5mM glutathione solution, a disulfide reducing compound found at roughly that concentration in the intracellular space [18]. As a result, the polymer molecular weight reduced by 10 times within 20 minutes (Figure 2.10). This degradable property could be the sole factor for the reduced cytotoxicity of the polymer (discussed in the next chapter).

2.4.4. Polyplex characterization

Two of the most significant factors that affect polyplex uptake by cells are their cationic charge and hydrodynamic size [8, 9]. The binding efficiency

of the multi-knot polymer to nucleic acids was initially examined using the gel electrophoresis (Figure 2.11). All ratios (from 1:1-100:1) showed efficient binding of polymer to DNA. The polymer prevents DNA migration completely at 1:1. At higher ratios, the polyplexes seem to migrate in the opposite direction due to the positive charge of the polymer, but it is hindered by its size and thus does not migrate far through the tiny pores of the gel.

The charge and size of various polyplex ratios were evaluated using multimode measuring equipment that utilizes the DLS and charge properties of colloidal particles. Polyplexes formed monodisperse nanoparticles (<200nm) with high positive charge (~50mV) (Figure 2.13). The charge increased and the polyplex size decreased when the amount of polymer exceeded the amount of DNA as expected. However, this plateaued immediately after the ratio reached 5:1 indicating the presence of an optimal ratio at which the polyplexes reach maximum charge and minimum size. This is discussed further in the next chapter. At weight ratio of 1 (N/P 2:1) of the polymer, the polyplex size is higher and charge is lower than at higher ratios and also comparable to those of PEI (N/P 10:1).

Transmission electron microscopy (TEM) was used to obtain visual confirmation of particle sizes (Figure 2.12). The sizes and shapes of these particles are irregular but consistent with the zeta-size measurements that range from 100nm-300nm.

PicoGreen® Assay

PicoGreen® (PG) was chosen because it selectively binds double stranded DNA and remains relatively non-fluorescent when unbound [19]. Studies on PicoGreen® intercalation with DNA reveal that intramolecular dynamic fluctuation is the reason for quenching of PG in its free state [20]. PG has an excitation maximum at 480 nm and an emission peak at 520 nm. When bound to double stranded DNA, fluorescence enhancement of PG is exceptionally high; little background occurs since the unbound dye has virtually no fluorescence. PG is very stable to photo-bleaching, allowing longer exposure times and assay flexibility [21, 22].

PicoGreen® can detect the DNA bound to the polymer, although the signal is significantly reduced in comparison to naked DNA (Figure 2.14). Interestingly, PG fluorescence is more quenched at lower weight ratios (namely 2:1) than higher ratios possibly due to the repulsion of the positive charges which is enhanced at higher ratios. PEI polyplexes completely quenched the fluorescence of PG at all ratios. This could be due to the hyperbranched structure of PEI that prevents the PG from accessing the DNA [23].

Figure 2.15 shows the polyplexes formed by the polymer at three different ratios. These polyplexes were incubated with PG for 5 minutes. They can be clearly seen under FITC channel. These images show aggregation behaviour of polyplexes at high ratio (e.g. 30:1), an event that might hinder transfection [24]. In the same figure, polyplexes can be seen taken up by the cells with some residual green dots around the cellular membrane indicating positive interaction of the polyplexes with cell membrane.

2.4.5. Synthesis of the hyperbranched poly (β-amino ester) (HPAE)

Synthesis of PAEs is carried out using a Michael addition type reaction which is quite different from the synthesis procedure used in the making of the multi-knot polymer. Additionally, delaying of the gelation point in the predecessor yields a hyperbranched PAE, a unique polymer in its own right. There is no great difference in the number molecular weight (M_n) between the LPAE and HPAEs (around 3000 Da). Because of the difference in structure (linear versus hyperbranched) but similarity of the M_n, LPAE shows much lower molecular weight (M_w) than HPAEs. It is well-known that PDI generally correlates with polymer structure; compared to the LPAE, the much higher PDI of HPAEs indicates the formation of hyperbranched structure.
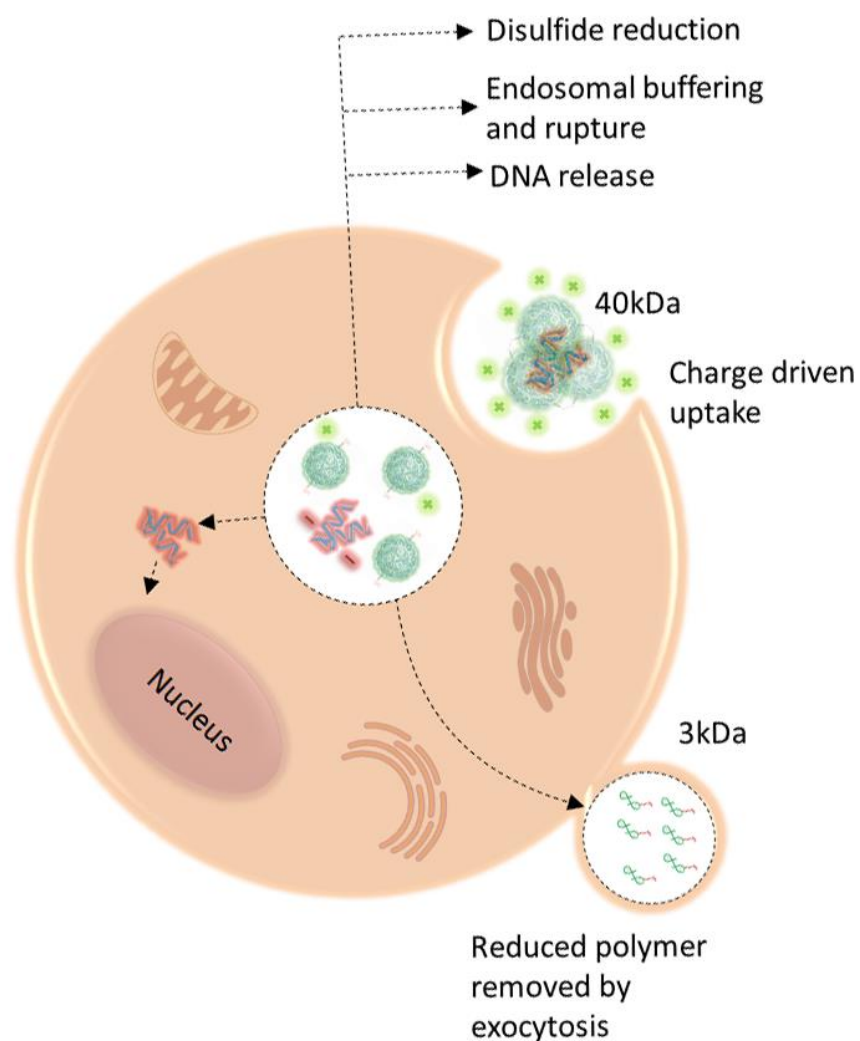
Figure 2.1: Schematic showing the properties of the multi-knot polymer that drive uptake and DNA release without inducing cytotoxicity. The ionic bond that forms between the cationic polyplexes and anionic cell wall is the predominant form of cell-particle interaction. Glutathione cleavage of the polymer's disulphide bonds breaks the polymer into low molecular weight polymer resulting in better DNA release.
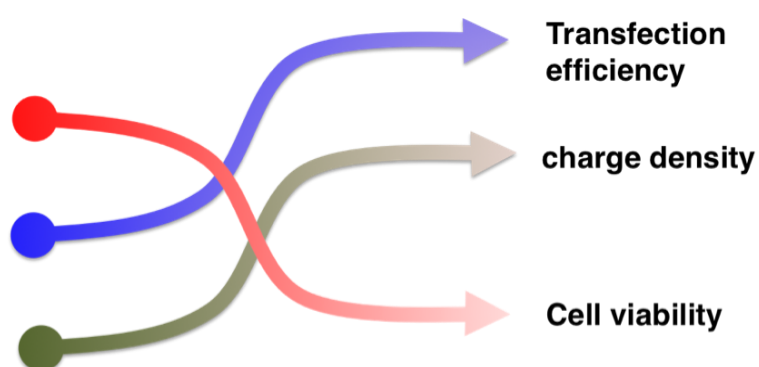
Figure 2.2: Relationship of charge density to cell viability and transfection efficiency. This image demonstrates that an increase in charge density results in increase transfection but reduces cell viability.

Reducing agent (**10%** of Cu^{II})

$$R-X + Cu^1-X/\text{Ligand} \underset{K_{deact}}{\overset{K_{act}}{\rightleftharpoons}} P_n^\bullet + Cu^{II}-X_2/\text{Ligand}$$

k_p
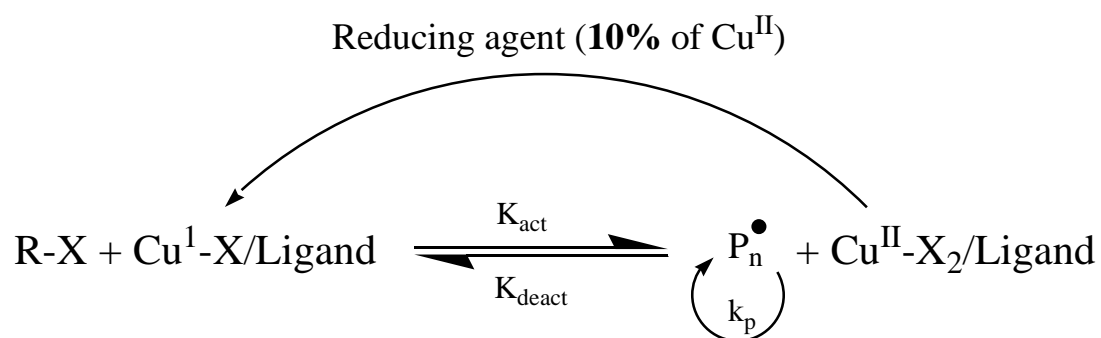
Figure 2.3: Mechanism of *in situ* DE-ATRP where X= Cl or Br. The reducing agent is usually ascorbic acid.
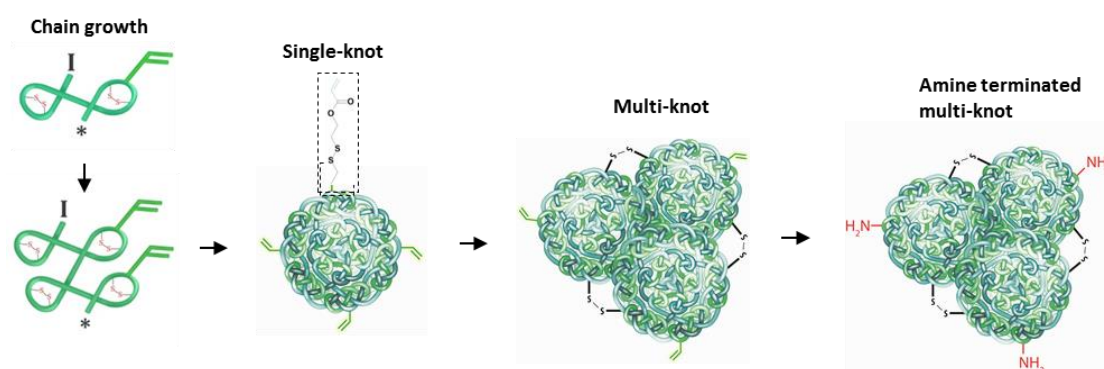
Figure 2.4: Polymer growth towards multi-knot structure. Excess vinyl groups are terminated with diamine monomer. Knotting occurs within the polymer chains due to close proximity of the reactive groups to each other to form a single-knot polymer. When single-knot molecules come in contact with each other towards the final stages of the reaction they form a multi-knot polymer. The initiator and free radical are represented by I and asterisk, respectively.

Table 2.1: Components required for the synthesis of the PEEDEPE monomer.

Monomer	Molar (mmol)	M_w (g/mol)	Density	Volume (ml)
Acroylyl chloride	320	90.51	1.114	25.8
Hydroxy ethyle disulfide	80	154.25	1.26	9.79
Tetrahydrofuran		72.11		200
Triethylamine	160	101	0.726	22.25

Table 2.2: Multi-knot polymer synthesis reactants and their ratios in the reaction pot. Molar ratio equates to feed ratio.

Monomer	Molar Ratio	M_w (g/mol)	Density	Mass(g)	Mass(mg)	Volume
DMAEMA	90	157.22	0.932	5		5.3ml
PEEDEPE	10	262		1		
Initiator	2.5	195	1.315	0.186	186	142ul
Ligand	0.25	173.3	0.83	0.016	16	19.3
CuCl$_2$	0.25	134.45		0.013	13	
AA	0.05	176.12		0.0034	3.4	
Solvent (Acetonitrile)	50% of total	72.11	0.805			7ml

Table 2.3: Making up polyplexes with different ratios

Polymer (ratio)	Concentration (mg/ml)	Polymer Mass (µg)	Polymer Volume (µl)	DNA Concentration (mg/ml)	DNA Mass (µg)	DNA Volume (µl)	Water (µl)
Polymer (1:1)	1	1	10	0.1	1	10	90
Polymer (2:1)	1	2	20	0.1	1	10	80
Polymer (5:1)	1	5	50	0.1	1	10	100
Polymer (10:1)	1	10	100	0.1	1	10	50
Polymer (15:1)	1	15	150	0.1	1	10	0
Naked DNA	-	-	-	0.1	1	10	150
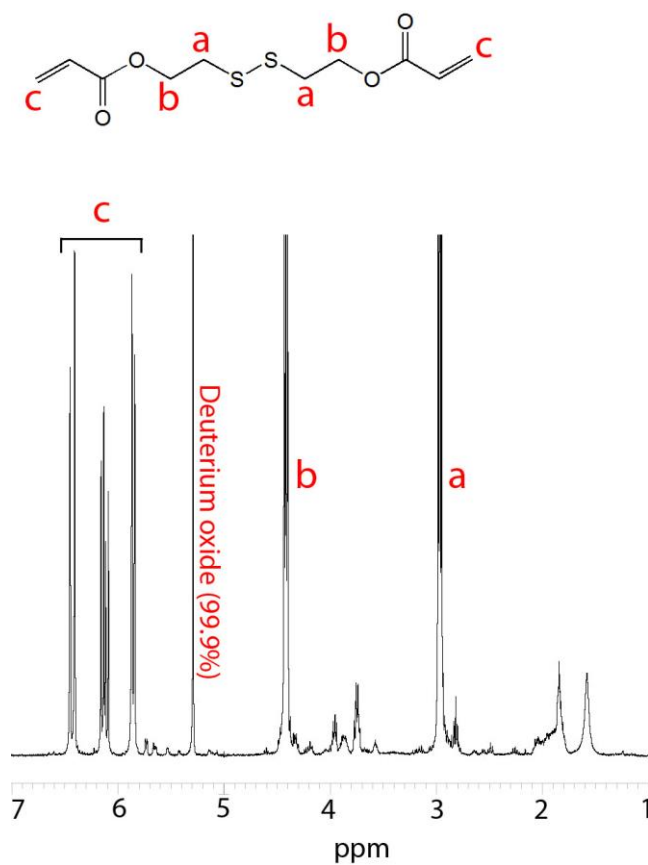
Figure 2.5: H^1 NMR spectrum of the disulfide monomer showing the peaks that represent the hydrogen atoms and their positions within the monomer.
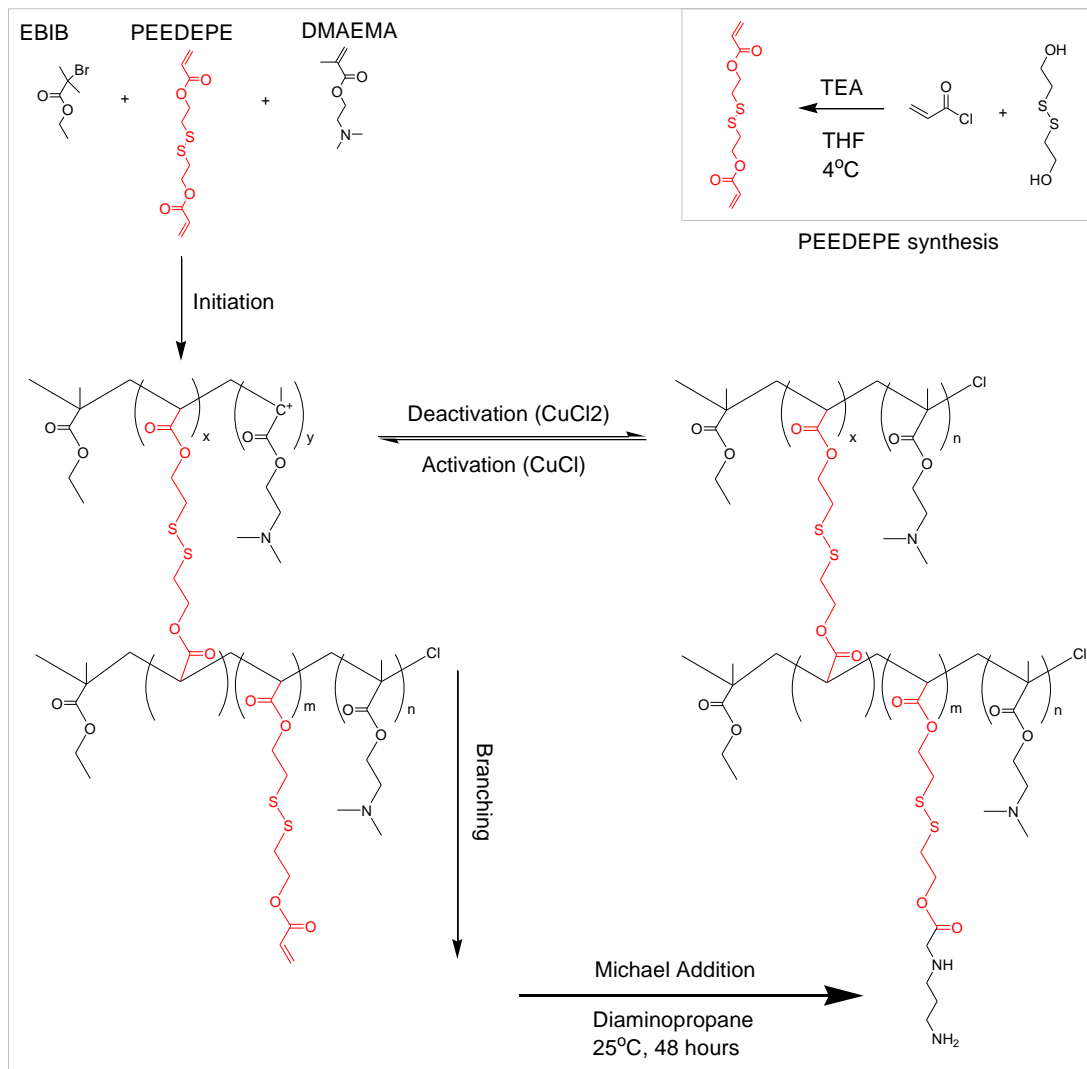
Figure 2.6: Synthesis and characterization of propenoyloxy ethyl disulfanyl ethyl propenoate (PEEDEPE) monomer and 'multi-knot' polymer. The structural components of the polymer include the initiator ethylbromoisobutyrate (EBIB), PEEDEPE and dimethyl amino ethyl methacrylate (DMAEMA). Initiation progresses towards linear propagation then branching both of which can be deactivated/activated during synthesis. Knotting occurs during linear propagation and branching. Unreacted vinyl groups were terminated with diaminopropane by Michael addition reaction.
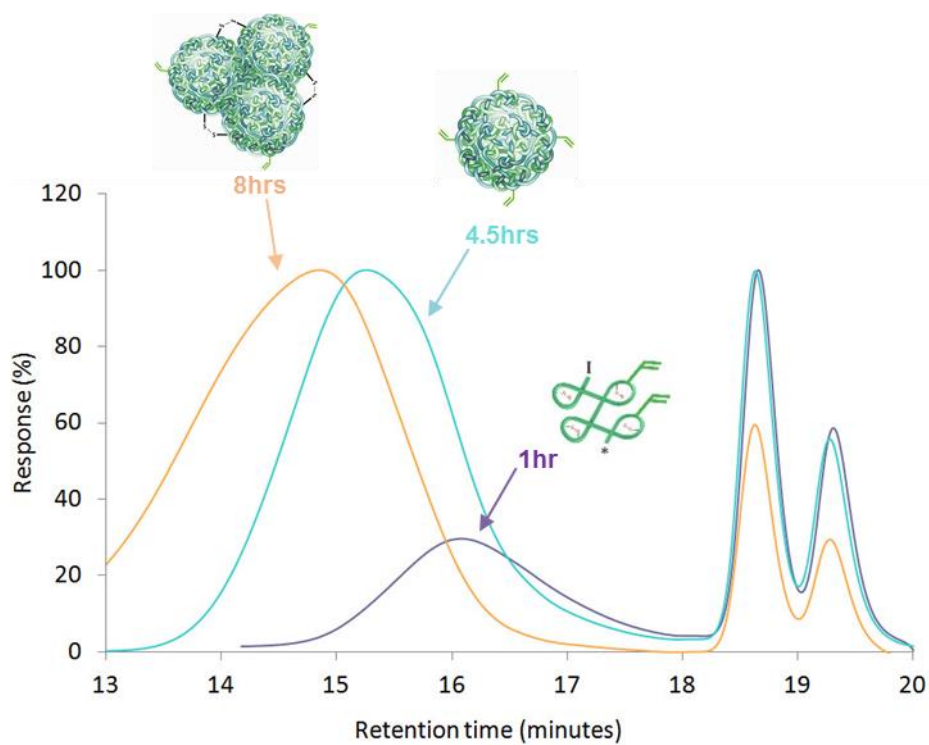
Figure 2.7: GPC trace of polymer synthesis. Each peak represents a sample taken at different time point of the reaction. The formation of the multi-knot polymer occurs when a number of knotted polymer molecules combine during a reaction lasting 8 hours. A GPC plot is given to show the difference between the polymer sizes at three different time points of the reaction.

Table 2.4: Increase in number average molecular weight (M_n), weight average molecular weight (M_w), polydispersity index and percentage monomer to polymer conversion over the reaction lifetime of the polymer. The reaction was stopped after 7 hours to obtain a polymer with final M_w of 42kDa.

Entry	Time (hrs)	M_n (g/mol)	M_w (g/mol)	PDI	Conversion (%)
H1	1	9.3	12.9	1.4	76.3
H2	2	10.6	15.0	1.4	78.0
H5	5	17.1	30.3	1.8	91.0
H7	7	19.9	42.1	2.1	92.2
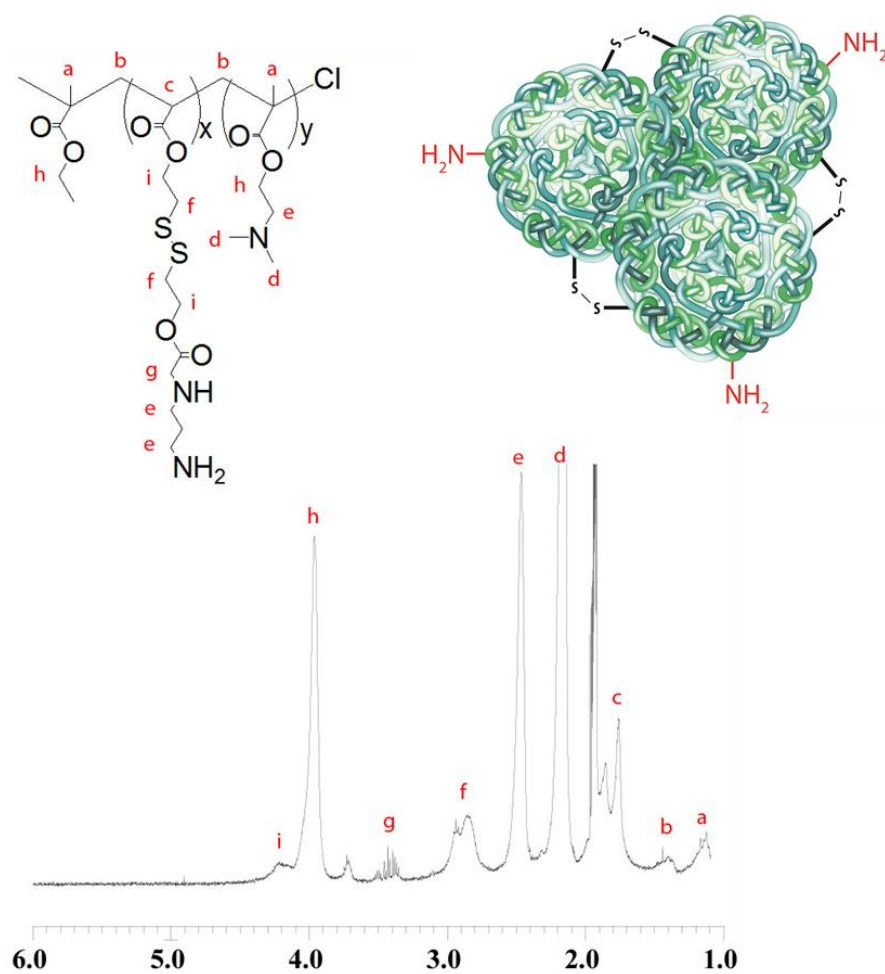
Figure 2.8: Final structure of the multi-knot polymer after diamine termination of the vinyl groups (-NH$_2$) as determined by H^1 NMR.
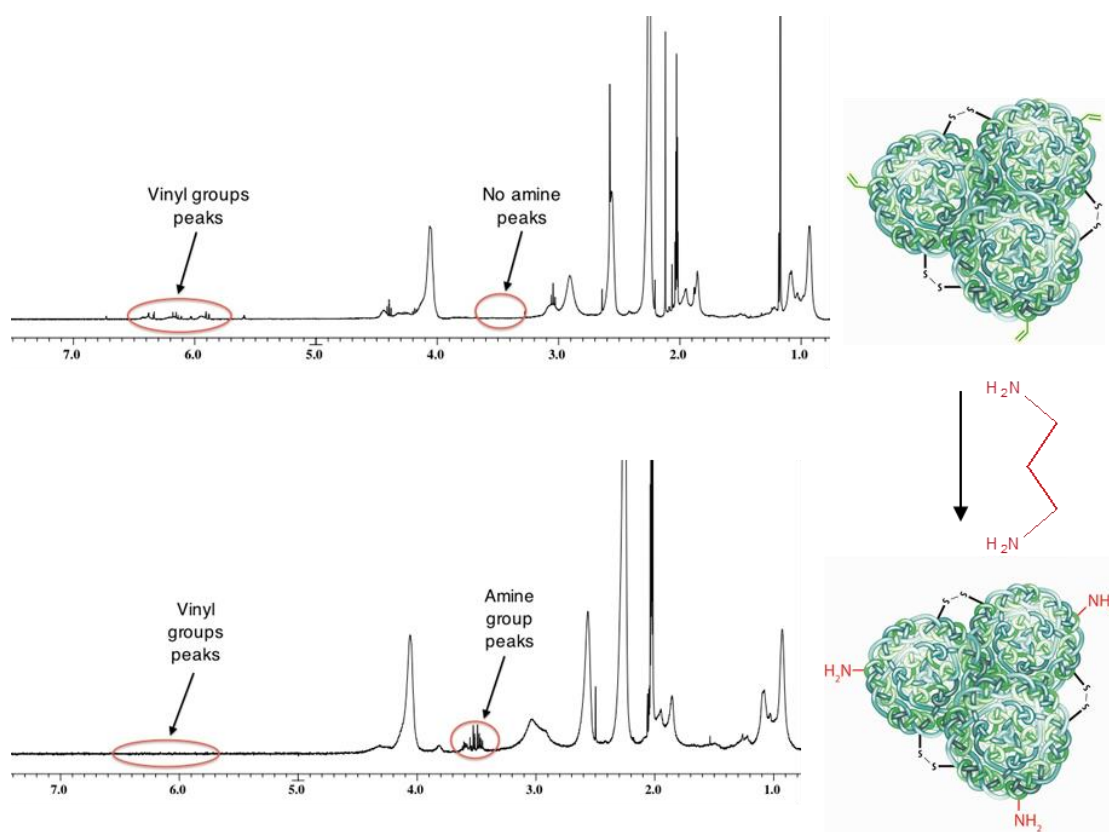
Figure 2.9: H^1 NMR spectra of the multi-knot polymer before (top) and after (bottom) Michael addition of diaminopropane.
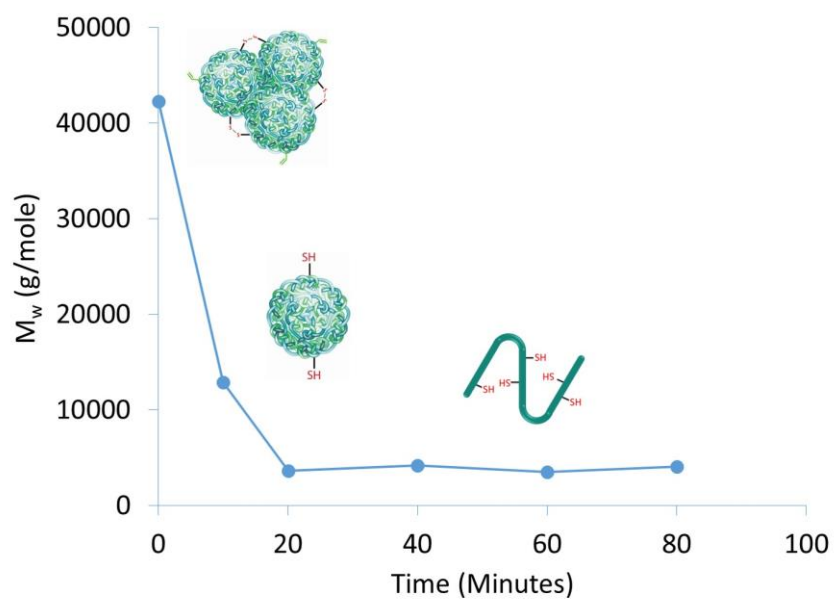
Figure 2.10: Disulfide reduction of the polymer in 5mM glutathione showing complete degradation (M_w=3400 Da) after 20 minutes of incubation at 37˚C.
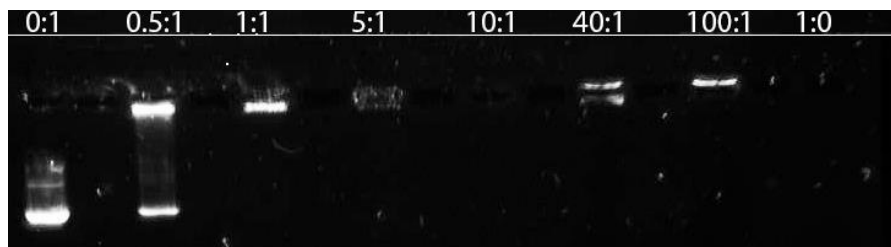
Figure 2.11: Polyplexes at different polymer: DNA ratios were run through agarose gel to determine binding efficiency.
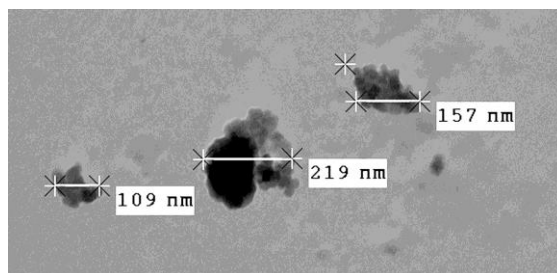
Figure 2.12: TEM of the polyplexes formed at polymer to DNA ratio of 10:1.
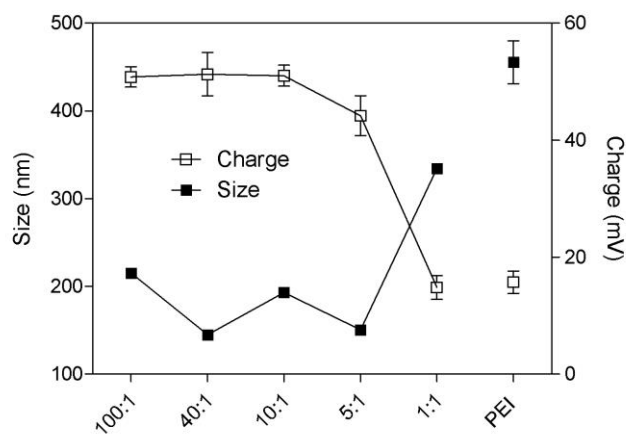
Figure 2.13: Average charge and average size of nanoparticles formed by the polymer with luciferase plasmid at different polymer to plasmid ratios. Error bars represent upper and lower values of standard deviation as mean ± S.D. (*n*=3). One way ANOVA was used for statistical analysis.
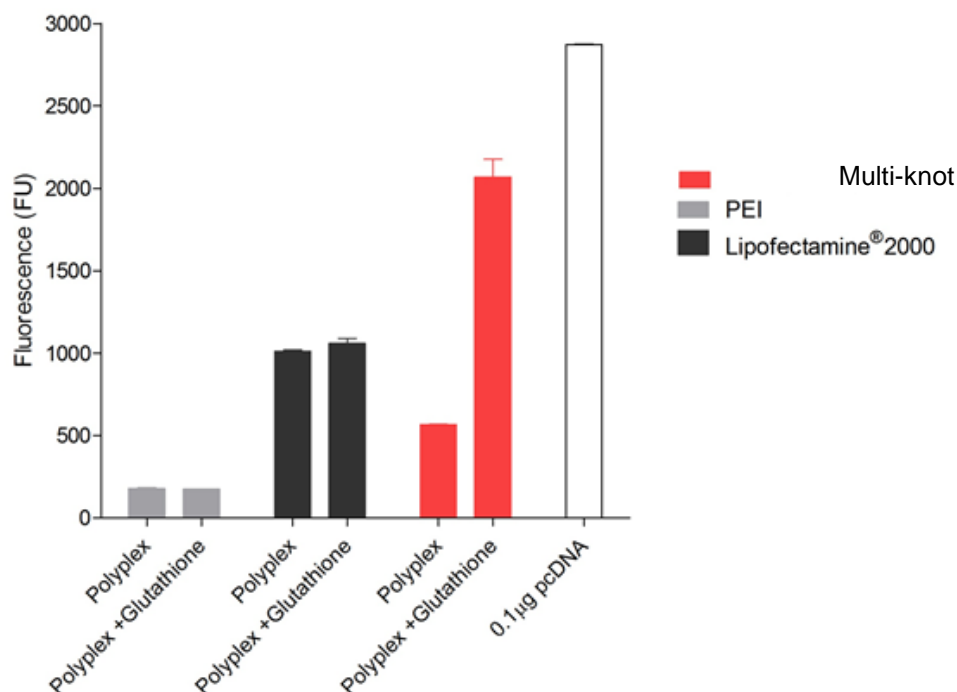
Figure 2.14: PicoGreen® can selectively identify pure DNA. When the DNA is complexed with the polymer, the signal is significantly reduced. Addition of glutathione to the polyplexes reduces the disulfide bonds of the polymer, allowing the DNA to be detected by the PG. Error bars represent upper and lower values of standard deviation expressed as mean ± S.D. (n=3). The one way ANOVA was used for statistical analysis.
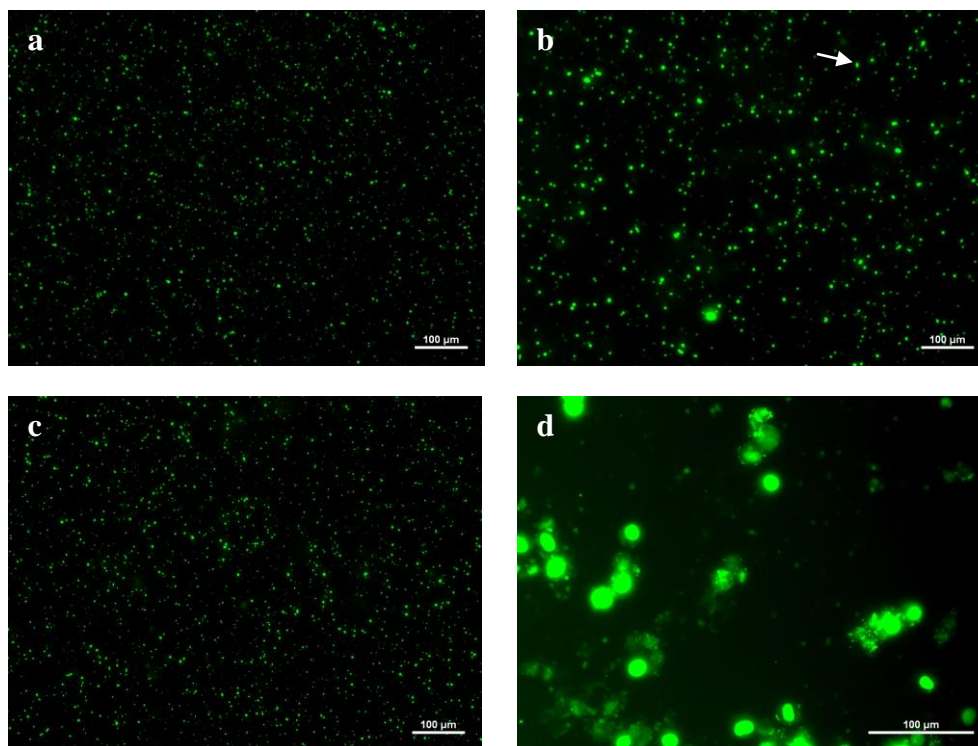
Figure 2.15: Multi-knot polyplexes after incubation with PG for 5 minutes at weight ratio **a**. 10 (20x), **b**. 15 (20x), and **c**. 30 (20x). **d**. Multi-knot polyplexes at weight ratio 10 incubated with HeLa Cells and labelled with PG (40x).
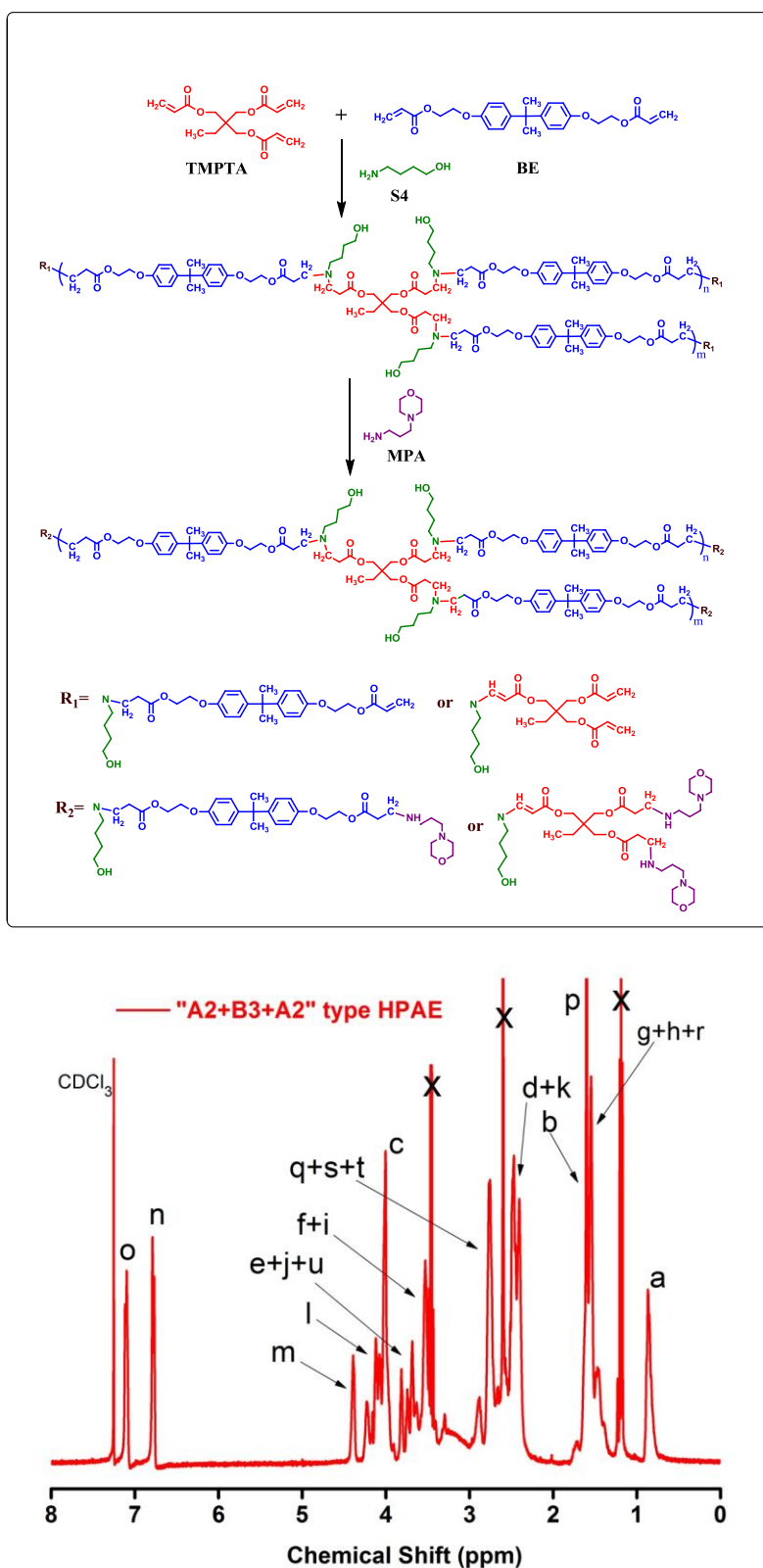
Figure 2.16: Schematic of the synthesis and chemical structures of "A2+B3/B2" type HPAE (above) and the 1H NMR spectrum of the same polymer (below). "**X**" refers to signals assigned to solvents of dimethyl sulfoxide (DMSO) and diethyl ether.
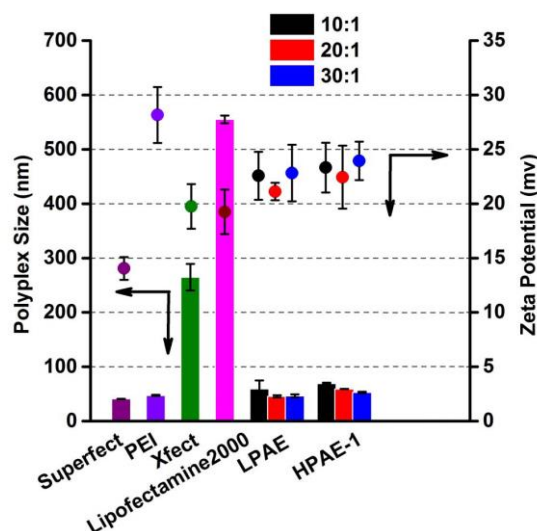
Figure 2.17: Polyplex sizes (bars), size distribution and zeta potentials (circles) measured by dynamic light scattering (DLS) in pH 5.2, 0.025 M sodium acetate buffer. At different w/w ratios, LPAE, "A2+B3/B2" type hybrid HPAE condense DNA into polyplexes with diameter in 50~130 nm and zeta potential of +14~25 mv.

2.5.   Conclusion

In conclusion, we proceeded beyond the single cyclized knot polymer to a unique higher and more complex multi-knot structure. This was achieved by delaying the onset of gelation in a one-pot in situ DE-ATRP reaction. This polymer displayed high charge density but fast biodegradation which is driven by biological reducing agents that cleave the disulfide bridge of the MVM. Its unique structure combines these two properties in one vector for efficient DNA packaging and swift DNA release, both of which raise the transfection traits of the current polymer above the 'gold' standard PEI and Lipofectamine®2000. In addition, a second polymer, synthesized by Michael addition, was characterized and placed as a 'backup-up' polymer in *ex vivo* and *in vivo* transfection studies described in the final chapter.

95

2.6. References

1. Ren, Y., X.A. Jiang, D. Pan, and H.Q. Mao, Charge Density and Molecular Weight of Polyphosphoramidate Gene Carrier Are Key Parameters Influencing Its DNA Compaction Ability and Transfection Efficiency. *Biomacromolecules*, 2010. 11: p. 3432.

2. Kim, T., T. Rothmund, T. Kissel, and S.W. Kim, Bioreducible polymers with cell penetrating and endosome buffering functionality for gene delivery systems. *J Control Release*, 2011. 152: p. 110.

3. Ouyang, D., N. Shah, H. Zhang, S.C. Smith, and H.S. Parekh, Reducible Disulfide-Based Non-Viral Gene Delivery Systems. *Mini-Rev Med Chem*, 2009. 9: p. 1242.

4. Schallon, A., V. Jerome, A. Walther, C.V. Synatschke, A.H.E. Muller, and R. Freitag, Performance of three PDMAEMA-based polycation architectures as gene delivery agents in comparison to linear and branched PEI. *React Funct Polym*, 2010. 70: p. 1.

5. Green, J.J., G.T. Zugates, N.C. Tedford, Y.H. Huang, L.G. Griffith, D.A. Lauffenburger, J.A. Sawicki, R. Langer, and D.G. Anderson, Combinatorial modification of degradable polymers enables transfection of human cells comparable to adenovirus. *Adv. Mater.*, 2007. 19: p. 2836.

6. Anderson, D.G., A. Akinc, N. Hossain, and R. Langer, Structure/property studies of polymeric gene delivery using a library of poly(beta-amino esters). *Mol Ther*, 2005. 11: p. 426.

7. Godbey, W.T., K.K. Wu, and A.G. Mikos, Size matters: Molecular weight affects the efficiency of poly(ethylenimine) as a gene delivery vehicle. *J Biomed Mater Res*, 1999. 45: p. 268.

8. Cai, J.G., Y.A. Yue, D. Rui, Y.F. Zhang, S.Y. Liu, and C. Wu, Effect of Chain Length on Cytotoxicity and Endocytosis of Cationic Polymers. *Macromolecules*, 2011. 44: p. 2050.

9. Kunath, K., A. von Harpe, D. Fischer, H. Peterson, U. Bickel, K. Voigt, and T. Kissel, Low-molecular-weight polyethylenimine as a non-viral vector for DNA delivery: comparison of physicochemical

properties, transfection efficiency and in vivo distribution with high-molecular-weight polyethylenimine. *J Control Release*, 2003. 89: p. 113.

10. Breunig, M., U. Lungwitz, R. Liebl, and A. Goepferich, Breaking up the correlation between efficacy and toxicity for nonviral gene delivery. *P. Natl. Acad. Sci. USA*, 2007. 104: p. 14454.

11. Newland, B., Y. Zheng, Y. Jin, M. Abu-Rub, H. Cao, W. Wang, and A. Pandit, Single cyclized molecule versus single branched molecule: a simple and efficient 3D "knot" polymer structure for nonviral gene delivery. *J Am Chem Soc*, 2012. 134: p. 4782.

12. Wang, W.X., Y. Zheng, E. Roberts, C.J. Duxbury, L.F. Ding, D.J. Irvine, and S.M. Howdle, Controlling chain growth: A new strategy to hyperbranched materials. *Macromolecules*, 2007. 40: p. 7184.

13. Zheng, Y., H. Cao, B. Newland, Y. Dong, A. Pandit, and W. Wang, 3D Single Cyclized Polymer Chain Structure from Controlled Polymerization of Multi-Vinyl Monomers: Beyond Flory-Stockmayer Theory. *J Am Chem Soc*, 2011.

14. Sunshine, J.C., S.B. Sunshine, I. Bhutto, J.T. Handa, and J.J. Green, Poly(beta-amino ester)-nanoparticle mediated transfection of retinal pigment epithelial cells in vitro and in vivo. *PLoS One*, 2012. 7: p. e37543.

15. Min, K., H.F. Gao, and K. Matyjaszewski, Preparation of homopolymers and block copolymers in miniemulsion by ATRP using activators generated by electron transfer (AGET). *J Am Chem Soc*, 2005. 127: p. 3825.

16. Wang, W., H. Liang, R.C. Al Ghanami, L. Hamilton, M. Fraylich, K.M. Shakesheff, B. Saunders, and C. Alexander, Biodegradable Thermoresponsive Microparticle Dispersions for Injectable Cell Delivery Prepared Using a Single-Step Process. *Adv. Mater.*, 2009. 21: p. 1809.

17. Li, Y.T. and S.P. Armes, Synthesis and chemical degradation of branched vinyl polymers prepared via ATRP: Use of a cleavable

disulfide-based branching agent. *Macromolecules*, 2005. 38: p. 8155.

18. Iwata, S., A. Takabayashi, and Y. Yamaoka, Modulation of intracellular glutathione concentration alters dehydropyrimidine dehydrogenase activity in peripheral blood mononuclear cells. *Clin Exp Med*, 2002. 2: p. 99.

19. Beach, L., C. Schweitzer, and J.C. Scaiano, Direct determination of single-to-double stranded DNA ratio in solution using steady-state fluorescence measurements. *Org Biomol Chem*, 2003. 1: p. 450.

20. Dragan, A.I., J.R. Casas-Finet, E.S. Bishop, R.J. Strouse, M.A. Schenerman, and C.D. Geddes, Characterization of PicoGreen interaction with dsDNA and the origin of its fluorescence enhancement upon binding. *Biophys J*, 2010. 99: p. 3010.

21. Batchelor, R., D. Hagen, I. Johnson, and J. Beechem, A fluorescent high-throughput assay for double-stranded DNA: the RediPlate PicoGreen assay. *Comb Chem High Throughput Screen*, 2003. 6: p. 287.

22. Ahn, S.J., J. Costa, and J.R. Emanuel, PicoGreen quantitation of DNA: effective evaluation of samples pre- or post-PCR. *Nucleic Acids Res*, 1996. 24: p. 2623.

23. Chen, H.H., Y.P. Ho, X. Jiang, H.Q. Mao, T.H. Wang, and K.W. Leong, Quantitative comparison of intracellular unpacking kinetics of polyplexes by a model constructed from quantum Dot-FRET. *Mol Ther*, 2008. 16: p. 324.

24. Debus, H., P. Baumhof, J. Probst, and T. Kissel, Delivery of messenger RNA using poly(ethylene imine)-poly(ethylene glycol)-copolymer blends for polyplex formation: Biophysical characterization and in vitro transfection properties. *J Control Release*, 2010. 148: p. 334.

CHAPTER 3

Polymer transfection efficiency analysis *in vitro*

3.1.   Introduction

Transfection is the process of delivering nucleic acids to cells for the purposes of gene knockdown (gene silencing) [1] or alternatively, synthesis of new proteins [2]. Both approaches involve genetic manipulation of the cells protein production line in many cases creating genetically modified cells. For gene silencing, interfering RNAs are used to increase or decrease the expression of certain or a group of proteins [3]. Interfering RNAs are a class of small RNA sequences that bind to messenger RNAs to alter their function. Interest in the small interfering RNA (siRNA) and micro-RNA (miRNA), the two main subgroups investigated, has grown rapidly in recent years thanks to their great therapeutic potential in many diseases [4, 5] including solid tumors [6], thanks to their knock-down ability of cancer-related genetic transcripts. Delivery of interfering RNAs has been achieved in many ways with liposome, polymer or viral vectors being the most successful [7, 8].

Protein expression motivated transfection can be considered the opposite of gene slicing as the final outcome always leads to new or increased production of a protein. Long term genetic change can be achieved through integration of the delivered nucleic acid to the host genome creating what is known as stable transfection [9]. Once integrated, the information can be passed down to the cells progeny for lasting expression. Although this has been the ultimate goal for many gene therapy based trails, drawbacks such as insertional mutagenesis [10] and difficulty to replicate with non-viral gene delivery vectors has made transient expression the more dominant mechanism of transfection.

Short term (transient) expression can be regularly achieved by direct application of the genetic sequence in the form of a plasmid DNA on its own or coupled in or with a biological/chemical carrier. Biological carriers mainly encompass viral vectors. However their success has been limited by major drawbacks such as toxicity and production difficulties which deterred a lot of investigators from using them in therapeutic applications. This provided a new opportunity for

non-viral vectors, especially polymer and liposome based agents, to be further advanced for gene therapy.

Advances in non-viral gene therapy have been slow because of the lack of efficient analytical techniques of the intracellular mechanisms leading to protein expression. Contemporary methods that strive to predict cellular response to nanoparticles such as mathematical models [11] and three dimensional particle tracking [12] to predict endocytosis could hold the key to understanding the mechanisms of internalisation and transfection in different cell types. Additionally, complex fluorescence based detectors in flow cytometry offer a variety of parameters to be tested in one experiment such as determination of transfection efficiency, cell health and morphology [13]. At the same time, using fluorescence-activated cell sorting (FACS), transfected cells can be isolated from the entire cell population and cultured separately to create stably transfected cells.

It is well documented that different cell types respond to transfection vectors differently, in fact, even the passage number has been reported to have notable influences on protein expression with lower passage number cells showing significantly higher protein expression than higher passage cells. The greatest variation is seen with dividing versus non-dividing cells. The source of the variation is the breakdown of the nuclear membrane during mitosis that permits the entry of genetic material into the nucleus, a process nonexistent in non-dividing cells such as neurons. To cross the nuclear membrane is one of the greatest hurdles facing current non-viral gene delivery. Recent investigations on the transfection efficiency of non-viral gene carriers have identified internalizations pathways as the main contributors to variations in efficiency seen between different cell lines [14].

Other notable influences on transfection efficacy are easier to control. Cell culture conditions such as cell number, presence of serum in the media and amount of DNA delivered to the cells can be optimized to increase transfection efficiency. In many cases, the presence of serum during DNA delivery can

hinder transfection as serum proteins tend to bind to the positively charged DNA carriers such as liposomes or polymers in their complexed form. This can be overcome by using more neutral gene carriers [15] or simply removing serum from the culture medium provided the cells can survive in such conditions for the time it is required to achieve transfection. The transfection procedure varies for viral, chemical and physical methods with the most basic being direct application of naked DNA to cells. In the less conventional polycation based transfection, the DNA is mixed with the synthetic vector and applied to the cells for a period of time to achieve maximum transfection (Figure 3.1).

In the past decade, a large number of non-viral transfection products have emerged to address the growing demand for genetic cell modulation and drug discovery. The global transfection market has grown tremendously and has been valued at US $385 million in 2012 and is expected to reach US $601 million by 2017 growing at a compound annual growth rate (CAGR) of 9.32% [16]. Originally used for gene therapy, the majority of the newly developed transfection agents have expanded their range of applications to include modulation of gene and protein expression, drug discovery and generation of induced pluripotent stem cells [17].

Because they are easy to generate and modify, synthetic polymers have attracted a lot of attention in the area of gene therapy [18]. In response to the increasing demand, a wide range of transfection reagents have emerged on the market to suit the needs of many areas of study. Altogen Biosystems have a range of *in vivo* reagents for siRNA and plasmid DNA delivery. They are lipid based, polymer based, nanoparticle based and PEGliposome based: all of which have been functionally tested on mice, have efficient delivery to pancreas, liver, kidney, spleen and certain tumor types and displaying minimal toxicity. Thermo Scientific carry two *in vivo* transfection reagents: ExGen 500 and TurboFect™ which provide gene delivery via multiple routes of administration and reproducible results. Thermo Scientific also provide *in vitro* transfection reagents with minimal cytotoxicity, ready-to-use reagents with high transfection

efficiency on a wide variety of cell types. Polyplus provide JetPEI® agents which are compatible with serum and antibiotics, has a broad cell-line spectrum and a straightforward protocol. InvivoGen claims to have the first lyophilized-based cationic lipid-based transfection reagent, LyoVec™. It is rapid and easy to use with an optimized procedure and a long shelf-life. Pierce Protein provides optimum delivery in 3 to 4 hours after incubation. SignaGen Laboratories have PepJet™ DNA and GenJet™ DNA which claim to have high *in vivo* transfection efficiency and give good renilla luciferase expression in lung, liver, spleen and kidney. T-Pro Biotechnology provides the T-Pro G-Fect Transfection Reagent which is suitable for DNA administration via various routes.

SuperFect and FuGENE® are now hugely important tools for R&D scientists. Some other companies and their products include INVITROGEN: Lipofectin, CLONTECH: Clonefectin; STRATAGENE: GeneJammer, LipoTAXI; GENE THERAPY SYSTEMS: GenePORTER. Indeed, Lipofectamine® reagents, owned by Life Technologies, have become the most referenced transfection reagents with over 42,000 citations to date. Despite market saturation, limitations in terms of transfection efficiency, cellular toxicity and clinical application mean the improvement drive is ongoing. The advantages of non-viral polymer/liposome reagents are; they consist of simple components, many are commercially available and they exhibit fewer biosafety problems. Although the current commercial non-viral transfections have shown great potential in gene delivery, their relatively low transfection capabilities in combination with high toxicity have significantly hampered and limited their applications. Moreover, the above mentioned transfection vectors have failed to achieve good transfection efficacy in non-dividing cells. Additionally, a major drawback of all current non-viral agents is their cytotoxicity, which has limited their application *in vivo* and halted progress to clinical trials [19].

In the previous chapter, we show the synthesis and characterization of degradable multi-knot polymeric gene vectors. The unique polymer vectors were synthesized from an adjusted deactivation enhanced strategy for ATRP

that efficiently delayed the point of gelation in the homopolymerization of PEEDEPE to over 60% monomer conversion in a concentrated polymerization system [20, 21] and post-functionalized by 1,3-diaminopropane. Our research suggests that marked improvements can stem from the dense multi-knot architecture and degradable property, which facilitates strong binding and better DNA release of the plasmid, respectively. In this chapter we analyze the transfection properties of various multi-knot polymers designed to overcome the problems associated with current polymer and lipid based vectors. In parallel, we will also demonstrate the transfection efficiency of the hyperbranched poly (β-amino esters) from experiments carried out by my colleague, Dr. Dezhong Zhou. We will examine protein expression efficiency and cell viability after treatment with the multi-knot and HPAE vectors on common cell types such as HeLa and 3T3 Fibroblasts, and RDEB keratinocyte cell lines generated from RDEB patients.

3.2. Methods

3.2.1. Plasmid amplification

Transformation:

Gaussia princeps luciferase (Newengland Biolabs, UK), green fluorescent protein (eGFP-pcDNA3, BD Biosceinces, UK) and COL7A1 (Division of cancer research, University of Dundee) expression plasmids were amplified to cover the large number of transfection studies. One microgram of the plasmid (either g-luc or GFP) was mixed with 50µl of XL1 Blue bacteria on ice then warmed up to 42°C to induce transformation. The bacteria was then mixed with LB Broth free of antibiotics for 35-45 minutes at 37°C before it was spread on sterile ampicillin or kanamycin (10-20µg/ml) containing agar plates and incubated overnight at 37°C.

Propagation:

A fresh colony was picked from the plate and inoculated into a starter culture of 2.5-5ml LB broth which was incubated at 37°C for ~8 hours under vigorous

shaking. This was then added to 2.5 LB with antibiotics and incubated for 12-16 hours. Centrifugation was then used to collect pellets of the bacteria containing the DNA. The bacteria were then resuspended in Giga prep kit buffer (Qiagen). Subsequent steps of the DNA isolation are described.

Isolation:

The bacteria were lysed using the standard buffers provided with the kit. A foamy solution is obtained that was allowed to settle before it was passed through a filter to remove the precipitates. Additional buffers are added to lyse the bacteria. To elute the DNA, 70ml isopropanol was added to the solution and then centrifuged. The pellet is washed with endotoxin free 70% ethanol, centrifuged then resuspended in the appropriate buffer.

3.2.2. Transfection of cell lines

This protocol applies for HeLa, 3T3, and hADSCs (also applies for fibroblasts and keratinocytes in the next chapter) using the GFP or the *gaussia* luciferase plasmids. The cells were seeded on the relevant well plate. For 96-well plate, the number of cells seeded range from 5,000-20,000 depending on the proliferation capacity of cells. For example, HeLa cells typically have a high proliferation capacity, so they would be at the lower range of the seeding number. One microgram of luciferase or GFP plasmids were mixed with the appropriate amount of polymer solution, in water, depending on the weight ratios used (3:1-15:1 ratios generally preform best depending on the cell type). The polymer/DNA mix was incubated at room temperature for 45-60 minutes, the time required for the multi-knot polymer and DNA to form polyplexes. For commercial transfection agents such as Lipofectamine®2000, the transfection procedure was carried out according to the manufacturer's guidelines. The polyplexes were diluted in serum-free media and applied directly to the cells. A minimum incubation period of 4 hours is required to achieve maximum transfection [22]. The polyplexes were pipetted out and serum containing media is added to the cells. Forty eight hours post-transfection, protein expression was analyzed with one of the procedures outlined below.

DMSO and Glycerol treatments:

One hundred microliters (or enough to cover the well) of 10% DMSO or glycerol was added to the well of 96-well plate of cells after the four hour incubation with polyplexes. The DMSO or glycerol solutions were incubated with the cells at room temperature for no more than 2 minutes, after which, the cells were washed with HANKs buffer solution (Sigma) and incubated with growth media for 48 hours or more (for longer time point studies).

For full detailed procedure of transfection see Appendix J.

3.2.3. Measurement of transfection efficiency

Gaussia luciferase assay:

After the cell incubation period, 20µl of the media was collected and pipetted into a black 96-well plate. Fifty microliters of the diluted luminescent *Biolux* gaussia luciferase agent (New England Biolabs, UK) was added to the cell media sample. The luminescence intensity was then measured (within less than 10 seconds after applying the agent) using a microplate reader at 1 second measurement time.

3.2.4. Analysis of GFP expression

Flow cytometry:

Forty eight hours post transfection; cells were washed with PBS, trypsinized and incubated with 4% paraformaldehyde (PFA) at 37°C for 30 minutes. Cells were then resuspended in 3% BSA and stored on ice prior to FACS analysis. Flourescent measurements were taken using the Becton Dickinson FACSCanto™ flow cytometer equipped with blue 488nm laser and utilizing the FITC flourochrome filter settings (530/30nm). Data was recorded linearly from 10,000 events and gated using cell count and side scatter parameters to exclude debris and dead cells.

Microscopy:

Again, 48 hours post transfection, flasks containing the GFP transfected cells were visualized directly under a fluorescent microscope using the Fluorescein Isothiocyanate (FITC) channel. Alternatively, if the cells were seeded on glass chamber slides, they were fixed with 4% PFA, washed with phosphate buffer saline and counterstained with -diamidino-2-phenylindole (DAPI) (Life Technologies, Ireland) at 1:200 dilution. Images were taken with 20x magnification using an Olympus IX81 inverted microscope.

3.2.5. Measurement of cell viability

The cytotoxicity of the polymer and cell metabolic activity of the cells after transfection was analyzed by alamarBlue® assay (Invitrogen). Fifteen microliters/well (96-well plate) of alamarBlue® was added to transfected and untreated (control) cells in 150µl/well of media and incubated at 37°C for 4 hours. Microplate (Thermo Scientific, Varioskanflash multimode reader) fluorescence measurements were then taken at 560EX nm/590EM nm filter settings. Results were obtained as the mean and standard deviation from triplicate values and displayed as percentage relative to untreated control cells.

3.3. Results and discussion

3.3.1. Transfection properties of the multi-knot polymers in cell lines

The ability of this polymer to efficiently induce transfection was examined in two popular cell lines (HeLa cells and 3T3 mouse fibroblasts) and human adipose derived stem cells (hADSCs). In the mouse fibroblasts, the polymer was able to induce protein expression levels comparable to Lipofectamine®2000, but it maintained 2-fold higher cell viability (Figure 3.2). In hADSCs, the expression levels were much lower than Lipofectamine®2000 but comparable to PEI. Interestingly, the multi-knot polymer induced minimal cytotoxicity in this cell type (Figure 3.3).

The HeLa cell line, derived from the epidermoid carcinoma of the cervix [23], is a well-established and studied cell line characterized by its infinite proliferation potential and high tolerance to genetic modifications for gene expression and drug discovery [24]. This cell line was used to test the newly developed multi-knot polymers for their efficiency as gene delivery vectors. We found that these cells were not very difficult to transfect using these polymers as they were able to induce high levels of *gaussia* luciferase expression using 1 µg DNA and 3, 4, 5, and 6 µg of the polymer without inducing cytotoxicity (Figure 3.4; Figure 3.5). The protein expression level was significantly lower than that of Xfect^TM at their optimal dose. However, the cytotoxicity of both commercial agents, Xfect^TM and Lipofectamine®2000 (LP2), was evident and may be a limiting factor for clinical application.

Increasing the molecular weight from 15kDa to 40kDa seems to have a positive effect on gene expression (Figure 3.6; Figure 3.7). We saw a significant increase in luciferase expression using the higher molecular polymer which proves the effect of molecular weight has on transfection efficiency. Interestingly, however, there was no difference in terms of cell viability as both of the polymers showed little to no cytotoxicity at the optimal transfection doses.

3.3.2. Effect of DNA dose on transfection properties

The optimal DNA per 20,000 cells was found to be higher than predicted and showed gene expression higher than that of the commercial agents. At the optimal DNA dose of 1.5µg, maximum luciferase expression was seen with little cytotoxicity, relative to Xfect[TM] and LP2 (Figure 3.8; Figure 3.9). Higher DNA dose did not show an increase but rather a decrease in expression as cell viability seems to drop below 80% especially with higher weight ratios.

Interestingly, however, we found that the same results could not be repeated using the green fluorescent protein (GFP). Figure 5 shows the contradicting results that imply huge influence of DNA vector on transfection. The optimal ratio for the multi-knot polymer was more difficult to pinpoint in this case, however, it was clear that the low dose of 0.1µg was the best for Xfect[TM]. Cytotoxicity issues become evident with higher ratios.

3.3.3. Effect of DMSO treatment on transfection properties

Dimethyl sulfoxide (DMSO) is an organic, sulfur containing compound used as a solvent of polar and non-polar compounds. More importantly, it has been previously reported to increase transfection efficiency by improving uptake of the complexed DNA [25]. Taking this into consideration, we shocked the polyplex treated HeLa cells with 10% DMSO for 2 minutes and we found that the treatment increased luciferase expression of the lower DNA doses but not the higher doses (Figure 3.10-Figure 3.12). The higher doses might not be influenced by the DMSO shock because the chances of uptake increase, but other barriers, such as nuclear membrane, prevent further increase in protein expression. The treatment had a devastating effect on HeLa cells with a 5-fold decrease in cell viability. The higher molecular weight polymer showed the same effect (Figure 3.13).

3.3.4. Transfection efficiency of the hyperbranched poly (β-amino esters)

The transfection efficiency of the HPAE polymers was tested on HeLa cells and RDEB keratinocytes. *Gaussia* luciferase expression levels in both cells show

HPAE efficiency to be similar to or better than other commercial transfection vectors (Figure 3.15). Figure 3.16 shows the GFP expressing cells after transfection with various agents. It is clear from this image that the best transfection agent is the HPAE. This is contrary to the *gaussia* luciferase expression but is a better representative of the number of cells transfected rather than the amount of protein produced after transfection. These results encouraged us to use the HPAE in the *in vivo* experiment as demonstrated later on in Chapter 4.
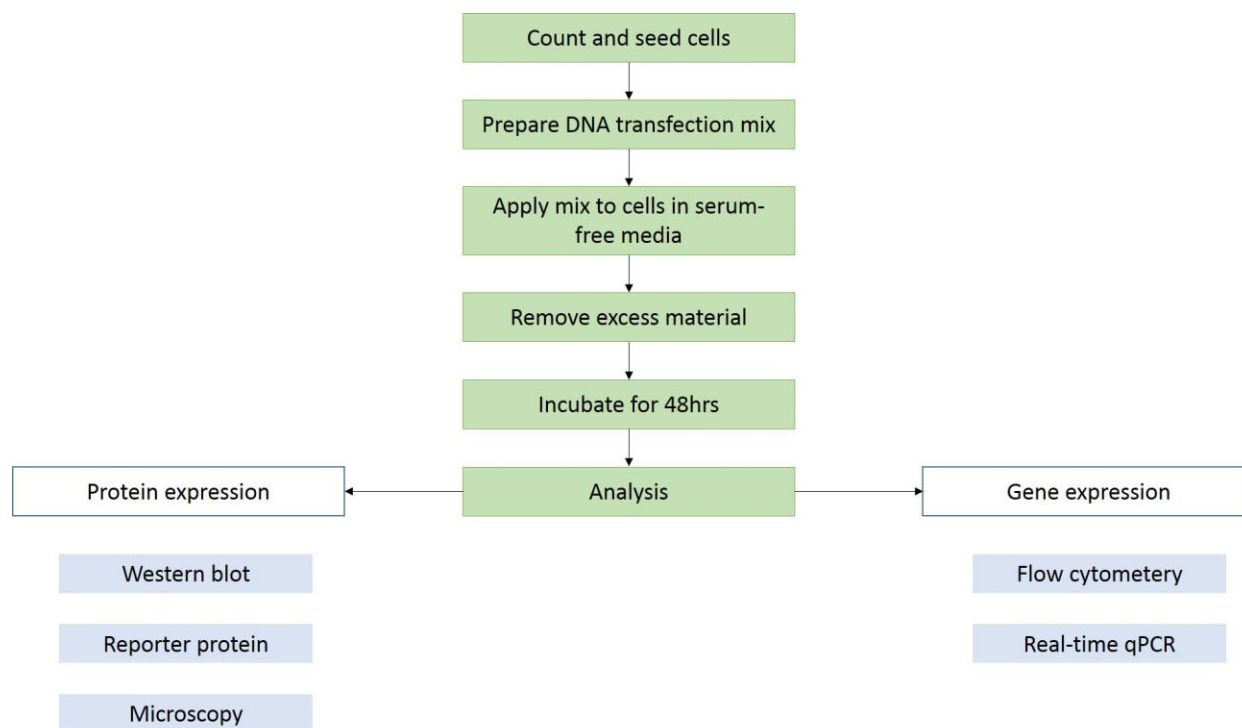
Figure 3.1: A flowchart diagram that outlines the workflow of polycation based transfection on a 96 well plate. Three methods can be used to quantify protein expression and two methods can be used to determine or quantify gene expression.
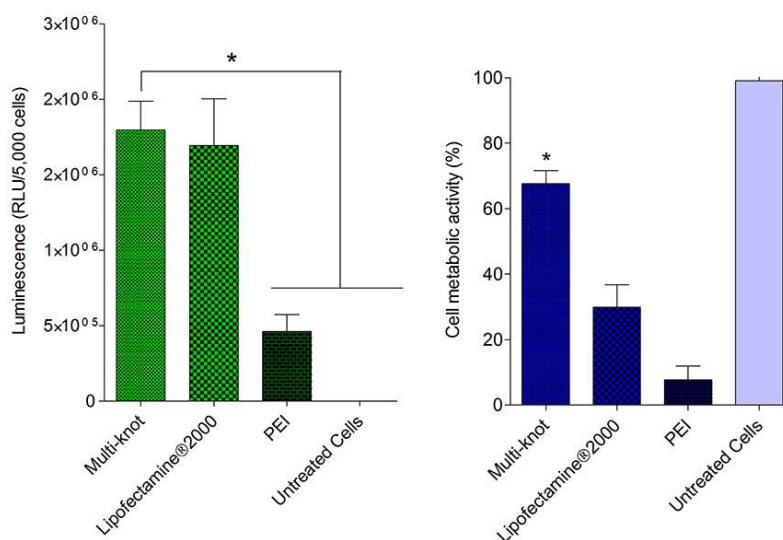
Figure 3.2: Luciferase expression levels and cell metabolic activity graphs comparing the transfection properties of the multi-knot polymer to other commercial agents in 3T3 fibroblasts. Error bars represent upper and lower values of standard deviation as mean ±S.D. Asterisk represents significant difference (n=3, p<0.05). One way ANOVA (Fisher) was used for statistical analysis.
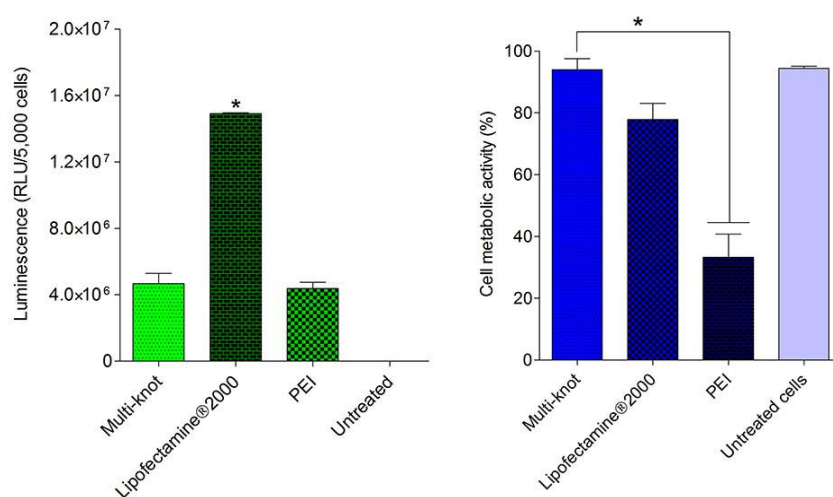
Figure 3.3: Luciferase expression levels and cell metabolic activity graphs comparing the transfection properties of the multi-knot polymer to other commercial agents in hADSCs. Error bars represent upper and lower values of standard deviation as mean ±S.D. Asterisk represents significant difference (n =3, p<0.05). One way ANOVA (Fisher) was used for statistical analysis.
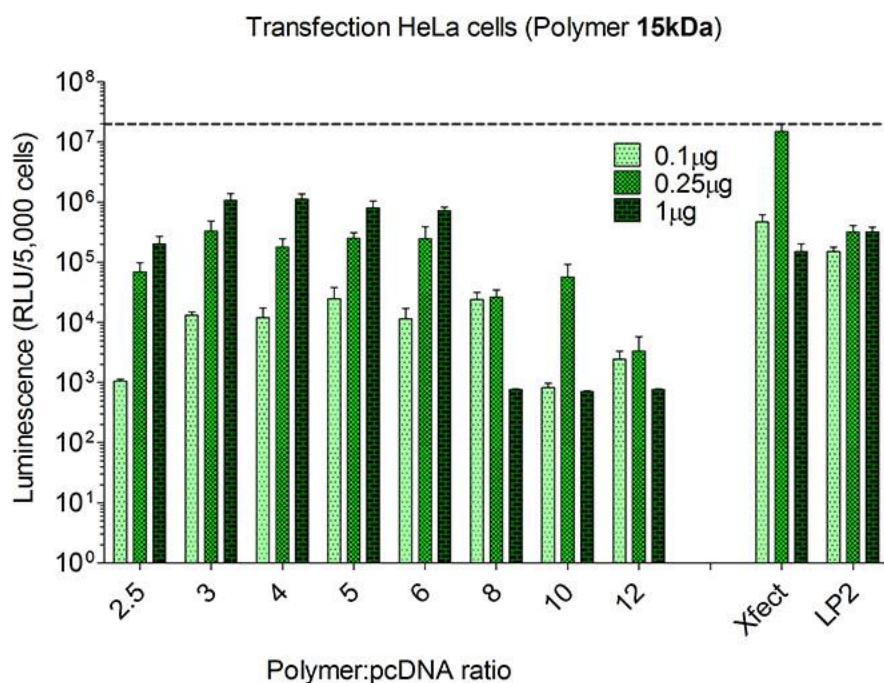
Figure 3.4: Luciferase expression levels in HeLa cells transfected with luciferase plasmid delivered using a 15kDa multi-knot polymer. Error bars represent upper and lower values of standard deviation as mean ±S.D. (*n* =3, p<0.05). One way ANOVA (Fisher) was used for statistical analysis.
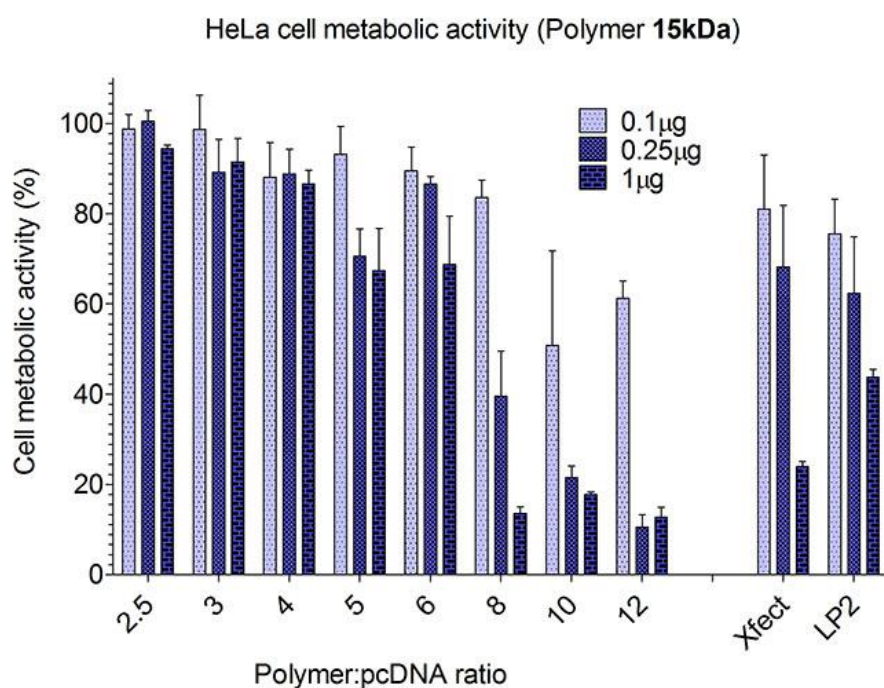
Figure 3.5: Cell metabolic activity (measured using alamarBlue®) of HeLa cells transfected with different amounts of luciferase plasmid and delivered using a 15kDa multi-knot polymer. Error bars represent upper and lower values of standard deviation as mean ±S.D. (*n*=3, $p < 0.05$). One way ANOVA (Fisher) was used for statistical analysis.
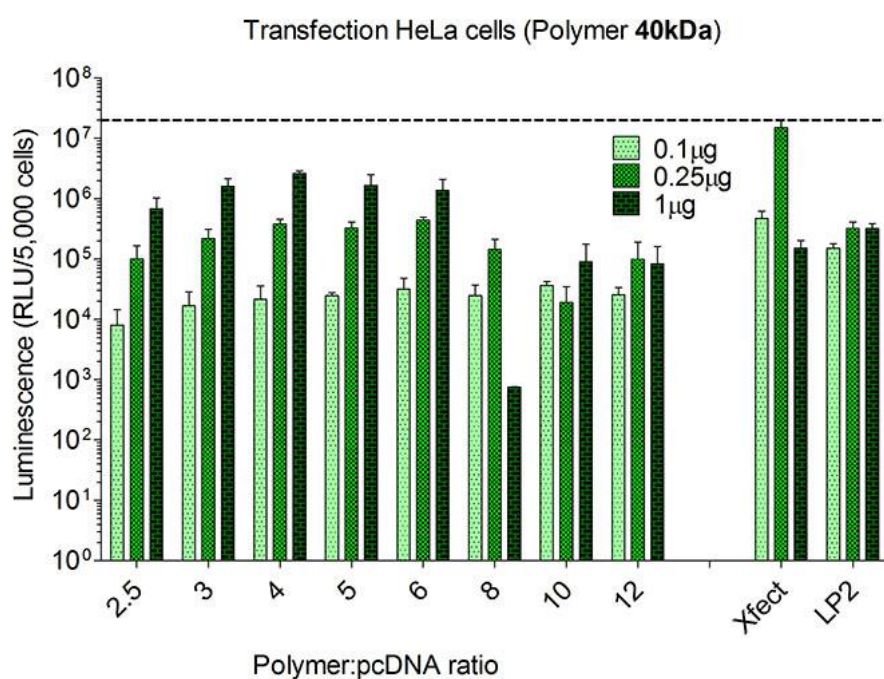
Figure 3.6: Luciferase expression levels in HeLa cells transfected with different amounts of luciferase plasmid and delivered using a 40kDa multi-knot polymer. Error bars represent upper and lower values of standard deviation as mean ±S.D. (*n*=3, p<0.05). One way ANOVA (Fisher) was used for statistical analysis.
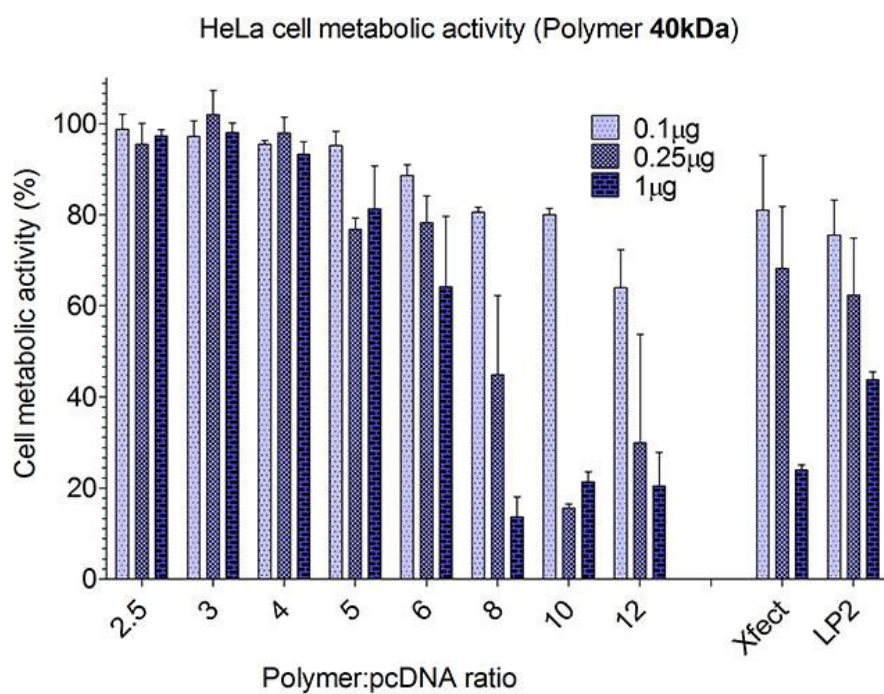
Figure 3.7: Cell metabolic activity (measured using alamarBlue®) of HeLa cells transfected with different amounts of luciferase plasmid and delivered using a 40kDa multi-knot polymer. Error bars represent upper and lower values of standard deviation as mean ±S.D. (*n*=3, p<0.05). One way ANOVA (Fisher) was used for statistical analysis.
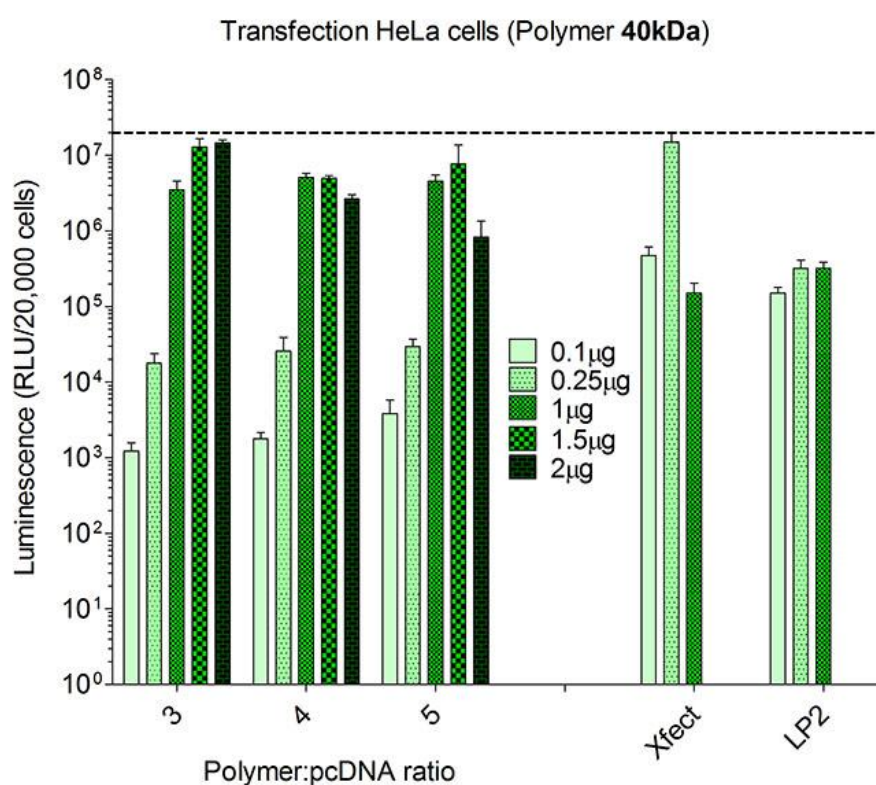
Figure 3.8: Effect of doubling polyplex dose on luciferase expression levels in HeLa cells. Error bars represent upper and lower values of standard deviation as mean ±S.D. (*n*=3, p<0.05). One way ANOVA (Fisher) was used for statistical analysis.
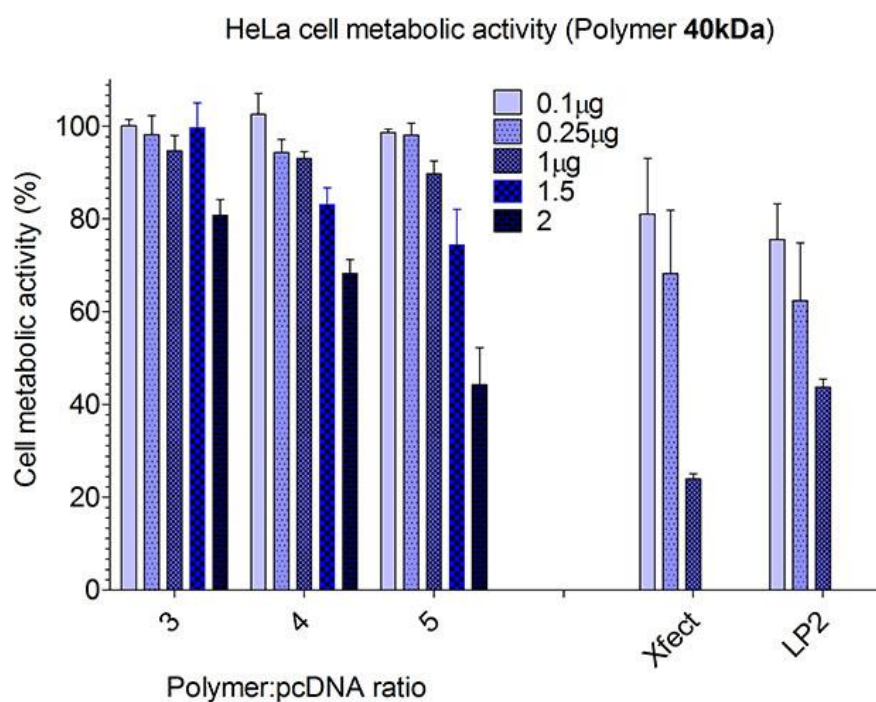
Figure 3.9: Effect of doubling polyplex dose on HeLa cells metabolic activity. Error bars represent upper and lower values of standard deviation as mean ±S.D. (*n*=3, p<0.05). One way ANOVA (Fisher) was used for statistical analysis.

Multi-knot polymer (40kDa)

0.1µg	0.25µg	1µg

1.5µg	2µg
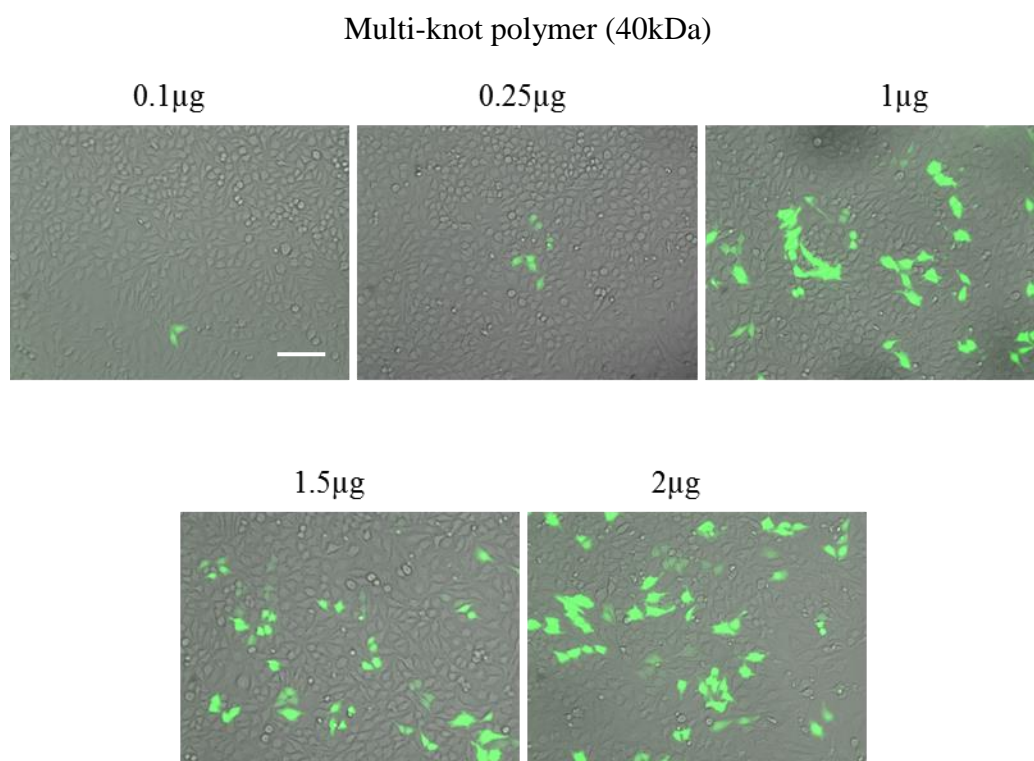
Figure 3.10: GFP expression in HeLa cells transfected with the 40 kDa multi-knot polymer with increasing amount of plasmid Images were taken 48 hours post transfection and at 20x magnification. Scale bar represents 100µm.

Xfect^{TM}
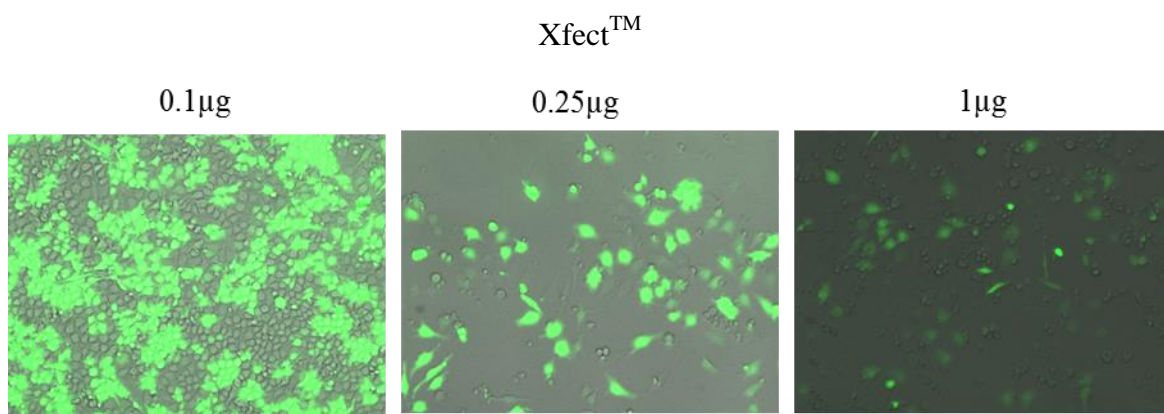
Figure 3.11: GFP expression in HeLa cells transfected with the Xfect® with increasing amount of plasmid DNA. Higher amounts of DNA resulted in complete cell death.
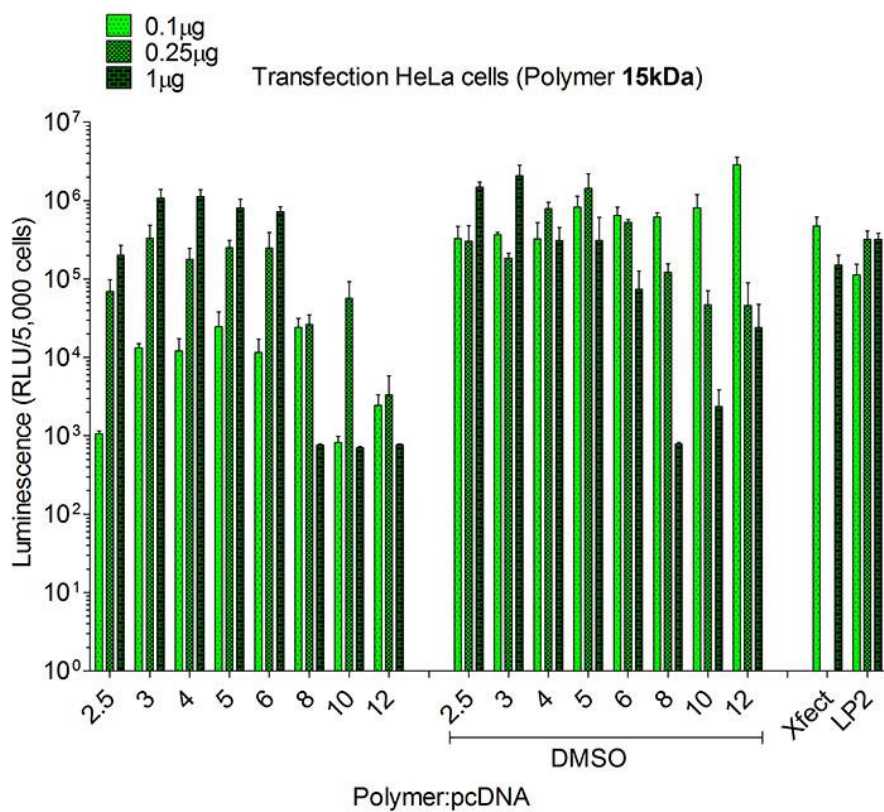
Figure 3.12: Effect of DMSO on luciferase protein expression after treatment with different complex ratios of 15 kDa multi-knot compared to commercial agents Xfect® and Lipofectamine®2000 (LP2). Error bars represent upper and lower values of standard deviation as mean ±S.D. (*n*=3, p<0.05). One way ANOVA (Fisher) was used for statistical analysis.
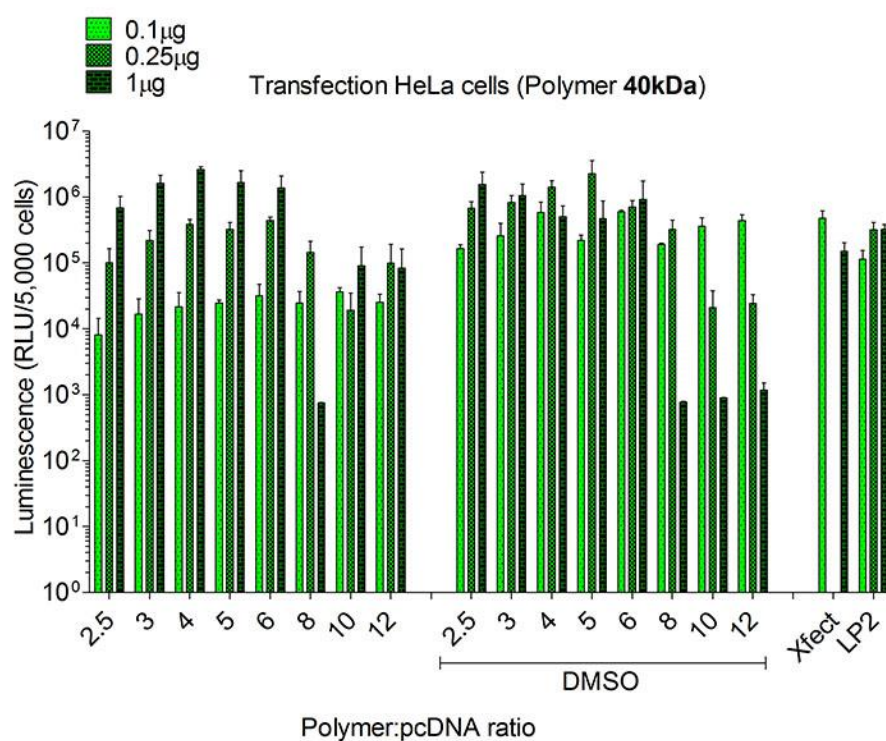
Figure 3.13: Effect of DMSO on luciferase protein expression after treatment with different complex ratios of 40 kDa multi-knot compared to commercial agents Xfect™ and Lipofectamine®2000 (LP2). Error bars represent upper and lower values of standard deviation as mean ±S.D. (*n*=3, p<0.05). One way ANOVA (Fisher) was used for statistical analysis.
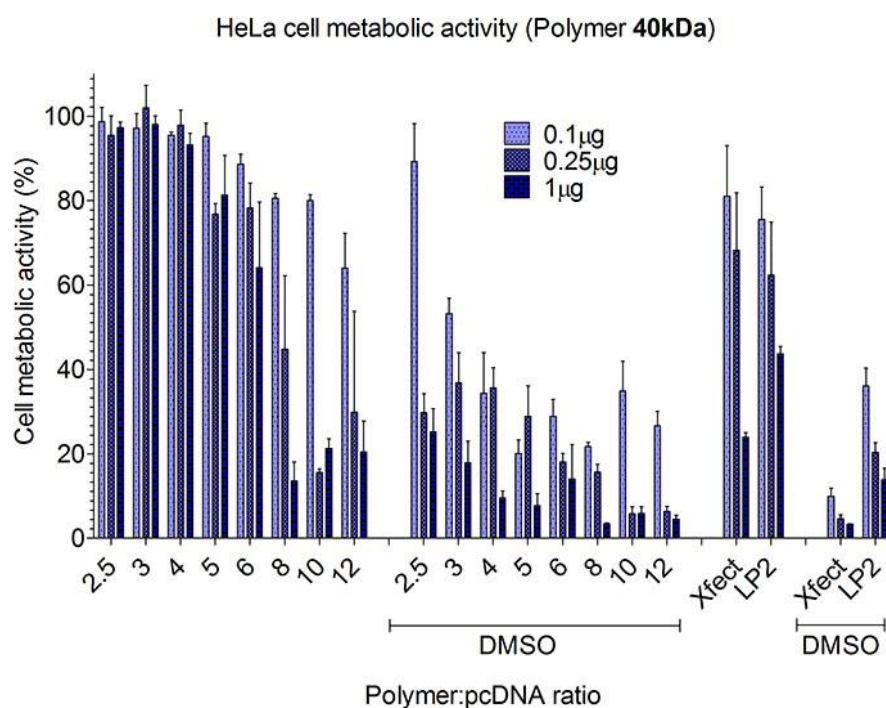
Figure 3.14: Effect of DMSO on cell metabolic activity after treatment with different complex ratios of 40 kDa multi-knot (not different from 15kDa) compared to commercial agents Xfect™ and Lipofectamine®2000 (LP2). Error bars represent upper and lower values of standard deviation as mean ±S.D. (*n*=3, $p < 0.05$). One way ANOVA (Fisher) was used for statistical analysis.
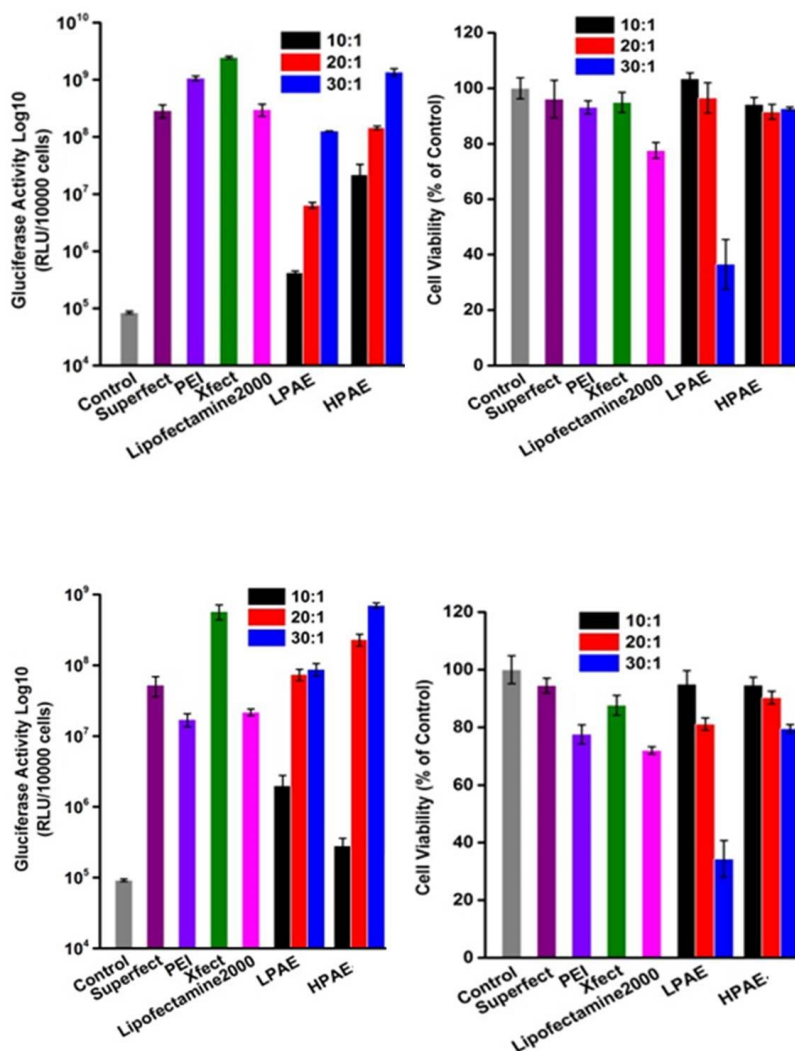
Figure 3.15: Cytotoxicity (a) and *in vitro* transfection capability (b) of LPAE, "A2+B3/B2" type hybrid HPAE at different weight w/w ratios (10:1, 20:1 and 30:1) over Hela (top panels), RDEBK (bottom panels) cell lines are evaluated and compared with that of the commercial Superfect, PEI, Xfect and Lipofectamine®2000 by alamarBlue assays and G-luciferase activity analysis respectively.
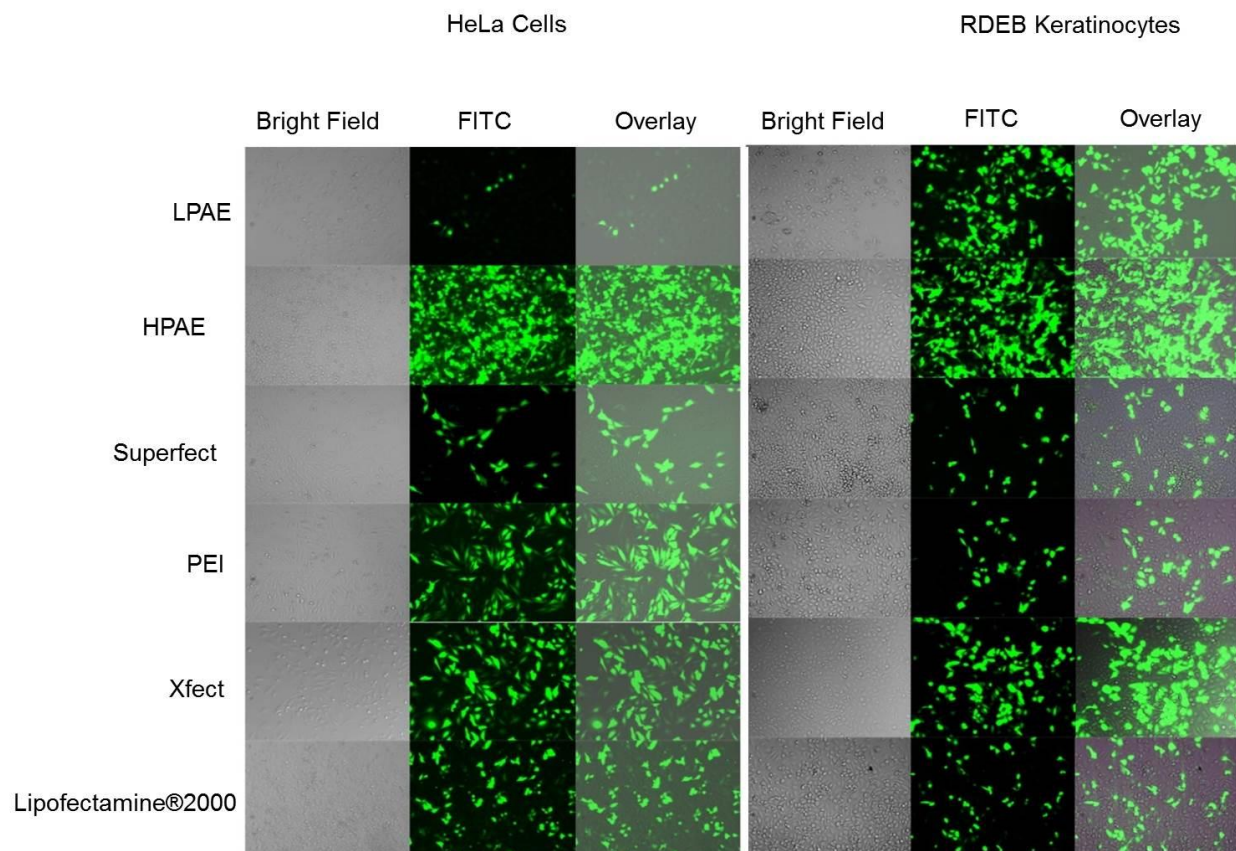
Figure 3.16: Representative fluorescent images of Hela (left panels) and RDEBK (right panels) cells transfected with LPAE at w/w ratio of 30:1, HPAE-1 at w/w ratio of 30:1 and commercial transfection vectors Superfect, PEI, Xfect and Lipofectamine®2000 at their optimized w/w ratios at 48 h post transfection. Images were taken at 10x magnification.

3.4. Conclusion

The transfection properties of the newly synthesized multi-knot polymer have been clearly demonstrated in this chapter. High transfection capability, specifically in 3T3 mouse fibroblasts, HeLa cells and RDEB keratinocytes, proves the first part of this chapter's hypothesis, in its simplified form: high charge density of the multi-knot polymer can provide sufficient transfection efficiency. The observed low cytotoxicity in all tested cell lines in agreement with the second hypothesis; incorporation of disulfide bonds will introduce faster degradation property for efficient DNA release and reduce cytotoxic. Unfortunately, low transfection efficiency in hADSCs demonstrates lack of nucleus penetration of the reporter plasmid in slow dividing cells. This can pose significant challenges *in vivo* since proliferating cells can take up to 14 hours to complete a single mitotic cycle [26]. Further *in vitro* imaging analysis is required to understand the mechanism of nuclear import and how the polymer agents can be modified to overcome such barrier. However, the HPAE polymers demonstrated very high transfection efficiency in the GFP transfection experiments indicating that it is a viable 'fail-safe' agent for the *in vivo* experiments.

3.5. References

1. Vicentini, F.T.M.D., L.N. Borgheti-Cardoso, L.V. Depieri, D.D. Mano, T.F. Abelha, R. Petrilli, and M.V.L.B. Bentley, Delivery Systems and Local Administration Routes for Therapeutic siRNA. *Pharm Res-Dordr*, 2013. 30: p. 915.

2. Manfredsson, F.P., D.C. Bloom, and R.J. Mandel, Regulated protein expression for in vivo gene therapy for neurological disorders: Progress, strategies, and issues. *Neurobiol Dis*, 2012. 48: p. 212.

3. Whitehead, K.A., R. Langer, and D.G. Anderson, Knocking down barriers: advances in siRNA delivery. *Nat Rev Drug Discov*, 2009. 8: p. 129.

4. Castanotto, D. and J.J. Rossi, The promises and pitfalls of RNA-interference-based therapeutics. *Nature*, 2009. 457: p. 426.

5. Leachman, S.A., R.P. Hickerson, M.E. Schwartz, E.E. Bullough, S.L. Hutcherson, K.M. Boucher, C.D. Hansen, M.J. Eliason, G.S. Srivatsa, D.J. Kornbrust, F.J.D. Smith, W.H.I. McLean, L.M. Milstone, and R.L. Kaspar, First-in-human Mutation-targeted siRNA Phase Ib Trial of an Inherited Skin Disorder. *Mol Ther*, 2010. 18: p. 442.

6. Davis, M.E., J.E. Zuckerman, C.H.J. Choi, D. Seligson, A. Tolcher, C.A. Alabi, Y. Yen, J.D. Heidel, and A. Ribas, Evidence of RNAi in humans from systemically administered siRNA via targeted nanoparticles. *Nature*, 2010. 464: p. 1067.

7. Mahato, M., P. Kumar, and A.K. Sharma, Amphiphilic polyethylenimine polymers mediate efficient delivery of DNA and siRNA in mammalian cells. *Mol Biosyst*, 2013. 9: p. 780.

8. Malamas, A.S., M. Gujrati, C.M. Kummitha, R. Xu, and Z.R. Lu, Design and evaluation of new pH-sensitive amphiphilic cationic lipids for siRNA delivery. *J control release,* 2013. 171: p. 296.

9.   Will, A., M. Rollinghoff, and A. Gessner, Stable transfection of cloned murine T helper cells. *J Immunol Methods*, 1995. 188: p. 139.

10. Howe, S.J., M.R. Mansour, K. Schwarzwaelder, C. Bartholomae, M. Hubank, H. Kempski, M.H. Brugman, K. Pike-Overzet, S.J. Chatters, D. de Ridder, K.C. Gilmour, S. Adams, S.I. Thornhill, K.L. Parsley, F.J.T. Staal, R.E. Gale, D.C. Linch, J. Bayford, L. Brown, M. Quaye, C. Kinnon, P. Ancliff, D.K. Webb, M. Schmidt, C. von Kalle, H.B. Gaspar, and A.J. Thrasher, Insertional mutagenesis combined with acquired somatic mutations causes leukemogenesis following gene therapy of SCID-X1 patients. *J Clin Invest*, 2008. 118: p. 3143.

11. Jin, H., D.A. Heller, R. Sharma, and M.S. Strano, Size-Dependent Cellular Uptake and Expulsion of Single-Walled Carbon Nanotubes: Single Particle Tracking and a Generic Uptake Model for Nanoparticles. *Acs Nano*, 2009. 3: p. 149.

12. Zhang, B.L., Y.Q. Li, C.Y. Fang, C.C. Chang, C.S. Chen, Y.Y. Chen, and H.C. Chang, Receptor-Mediated Cellular Uptake of Folate-Conjugated Fluorescent Nanodiamonds: A Combined Ensemble and Single-Particle Study. *Small*, 2009. 5: p. 2716.

13. Landi, A., L.A. Babiuk, and S.V. Littel-van den Hurk, High transfection efficiency, gene expression, and viability of monocyte-derived human dendritic cells after nonviral gene transfer. *J Leukocyte Biol*, 2007. 82: p. 849.

14. Izumisawa, T., Y. Hattori, M. Date, K. Toma, and Y. Maitani, Cell line-dependent internalization pathways determine DNA transfection efficiency of decaarginine-PEG-lipid. *Int J Pharmaceut*, 2011. 404: p. 264.

15. Luo, X.H., F.W. Huang, S.Y. Qin, H.F. Wang, J. Feng, X.Z. Zhang, and R.X. Zhuo, A strategy to improve serum-tolerant transfection activity of polycation vectors by surface hydroxylation. *Biomaterials*, 2011. 32: p. 9925.

16.   Markets, M.a., Global Transfection Market (2012 - 2017) (Gene Delivery, DNA Delivery, Protein Delivery, SiRNA Delivery) Technologies (Lipofection, Calcium Phosphate, Electroporation, Nucleofection, Magnetofection, Gene Gun, Viral). 2012.

17.   Yu, F., L.J. Ding, G.B. Sun, P.X. Sun, X.H. He, L.G. Ni, and B.C. Li, Transgenic Sperm Produced by Electrotransfection and Allogeneic Transplantation of Chicken Fetal Spermatogonial Stem Cells. *Mol Reprod Dev*, 2010. 77: p. 340.

18.   Boussif, O., F. Lezoualch, M.A. Zanta, M.D. Mergny, D. Scherman, B. Demeneix, and J.P. Behr, A Versatile Vector for Gene and Oligonucleotide Transfer into Cells in Culture and in-Vivo - Polyethylenimine. *P Natl Acad Sci USA*, 1995. 92: p. 7297.

19.   Moghimi, S.M., P. Symonds, J.C. Murray, A.C. Hunter, G. Debska, and A. Szewczyk, A two-stage poly(ethylenimine)-mediated cytotoxicity: Implications for gene transfer/therapy. *Mol Ther*, 2005. 11: p. 990.

20.   Zheng, Y., H. Cao, B. Newland, Y. Dong, A. Pandit, and W. Wang, 3D Single Cyclized Polymer Chain Structure from Controlled Polymerization of Multi-Vinyl Monomers: Beyond Flory-Stockmayer Theory. *J Am Chem Soc*, 2011. 133: p. 13130

21.   Newland, B., Y. Zheng, Y. Jin, M. Abu-Rub, H. Cao, W. Wang, and A. Pandit, Single cyclized molecule versus single branched molecule: a simple and efficient 3D "knot" polymer structure for nonviral gene delivery. *J Am Chem Soc*, 2012. 134: p. 4782.

22.   Rehman, Z.U., D. Hoekstra, and I.S. Zuhorn, Mechanism of Polyplex- and Lipoplex-Mediated Delivery of Nucleic Acids: Real-Time Visualization of Transient Membrane Destabilization without Endosomal Lysis. *Acs Nano*, 2013. 7: p. 3767.

23.   Scherer, W.F., J.T. Syverton, and G.O. Gey, Studies on the propagation in vitro of poliomyelitis viruses. IV. Viral multiplication in a stable strain of human malignant epithelial cells (strain HeLa) derived from an epidermoid carcinoma of the cervix. *J Exp Med,* 1953. 97: p. 695.

24. Tao, M., N. Miyano-Kurosaki, K. Takai, and H. Takaku, Specific inhibition of human telomerase activity by transfection reagent, FuGENE6-antisense phosphorothioate oligonucleotide complex in HeLa cells. *Febs Lett*, 1999. 454: p. 312.

25. Villa-Diaz, L.G., J.L. Garcia-Perez, and P.H. Krebsbach, Enhanced Transfection Efficiency of Human Embryonic Stem Cells by the Incorporation of DNA Liposomes in Extracellular Matrix. *Stem Cells Dev*, 2010. 19: p. 1949.

26. Weinstein, G.D., J.L. McCullough, and P. Ross, Cell proliferation in normal epidermis. *J Invest Dermatol*, 1984. 82: p. 623.

CHAPTER 4

Ex vivo and *in vivo* analysis of gene delivery efficacy

4.1.   Introduction

Epidermolysis Bullosa is a group of heritable skin diseases, defined by chronic fragility and blistering of the skin and mucous membranes. One of the most severe variants, RDEB, is characterized by a lack of adhesion of the epidermis to the dermis [1]. This condition has a high personal, medical and socio-economic impact as people with RDEB require a broad spectrum of medications and specialized care. The scope of this project is focused on the severe form of RDEB, severe generalized (RDEB-sv), which is distinguishable from other forms of EB by the presence of severe erosions and blisters on the mucosal membrane and the skin of newborns. These erosions and blisters are a result of loss-of-function mutations in the collagen type VII (COL7A1) gene [2, 3]. These mutations lead to severely reduced expression of C7, a major anchoring component of the basement membrane zone (BMZ), as mentioned in the introductory chapter. The mutations in C7 lead to formation of nonfunctional anchoring fibrils which contributes to the loss of adherence between the epidermis and the dermis.

Intensive efforts are being made to restore the anchoring protein at the BMZ as means of providing a lasting cure for the disease. One of the methods examined as potential therapy utilizes viral vectors for genetic correction of the C7 expressing cells [4]. However, toxicity and immunogenicity concerns have slowed any progress using viral vectors [5]. As a result, non-viral methods of delivery have attracted great interest as a replacement. In this project, we report on one of the more versatile methods of non-viral based delivery that utilizes a dense polycation synthesized from DE-ATRP (Chapter 2). The polymer was created to deliver the functional but large C7 plasmid DNA sequence that includes the CMV promoter to RDEB keratinocytes and fibroblasts. Skin fibroblasts, keratinocytes and endothelial cells have been reported to express C7 in the epidermal-dermal membrane [6, 7]. However, our focus was mainly on keratinocytes and fibroblasts since they are the predominant cells found in the upper dermis and epidermis, and possibly contribute more to C7 expression

than any other group of cells. These cells were used for transfection studies *in vitro* and *ex vivo*. The cells were isolated from RDEB patients with or without squamous carcinoma (Appendix L).

RDEB keratinocytes and fibroblasts are morphologically different from normal keratinocytes and fibroblasts [8]. They are polymorphic, elongated and enlarged compared to normal keratinocytes and fibroblasts. In addition, RDEB cells have higher motility, lower attachment to fibronectin, collagen type I, IV and VII, and abnormal proliferation rate compared with normal cells [9].

We successfully used these cells to build 3D skin equivalents (SE) for *ex vivo* transfection analysis. Tissue engineering of these substitutes involves seeding cells in a biodegradable matrix or scaffold providing an adequate three dimensional structure of the wanted tissue (Figure 4.1). The proliferating cells produce extracellular matrix to replace the degrading scaffold, eventually creating a functional or partly functional tissue [10]. The tissue is formed under regulated environment of growth factors and chemical compounds. In the case of RDEB SEs, epithelial growth factor, insulin and sodium pyruvate are required for adequate proliferation and ECM deposition (see Appendix M for full list of materials).

Skin equivalents (SEs) are being used to test for toxicity and effectiveness of many drugs, reducing the need for pre-clinical trials. They also provide more controlled environment for drug testing and screening than *in vivo* models eliminating variations such as age, gender and health. Unfortunately, SEs do not fully replicate natural tissues, as mentioned previously, as the latter lack the complexity and array of cells and proteins found in natural tissue. In addition, the presence of immune response capability and blood circulation in pre-clinical models will give a more accurate account of the drug's safety. This encouraged us to test the effectiveness of polymer vectors for COL7A1 delivery in an *in vivo* pre-clinical model of RDEB. Collagen VII alpha one null RDEB (Col7α1-/-) knockout mice have been previously developed from immunocompetent mice by targeted inactivation of Col7α1 [11]. Clinically, these mice showed

severe blistering and detachment of the epidermis from the dermis after birth because they have extremely reduced C7 protein at the BMZ of their skin and complete absence of functional anchoring fibrils. The mouse phenotype is not different from the human phenotype especially in the paws, where trauma induced blisters are more likely to occur. The mothers of the RDEB mice are fed high calorie and protein diet in the form of a gel (ClearH$_2$O dietGel® 76A) since the RDEB pups die early after birth due to slow growth attributed to malnutrition.

The recapitulating clinical, genetic and ultrastructural features in knockout mice encouraged us to use this model for testing the gene therapy efficiency of the multi-knot and the HPAE polymers.

It is hypothesized that three major milestones can be achieved using the polymer technology platform developed at Dr. Wang's group. Firstly, using a polymer vector (multi-knot or poly β amino ester, HPAE) carrying the COL7A1 gene, it is possible to transfect RDEB keratinocytes and fibroblasts and restore C7 expression in those cells. Secondly, this can be achieved *ex vivo* in SEs created from RDEB keratinocytes and fibroblasts seeded in and on top of a fibrin gel, respectively. Finally, intradermal injection of the therapeutic COL7A1 carried by the multi-knot polymer or HPAE in a Col7α1-/- knockout mouse (RDEB) model can restore C7 expression in the cells near the injection region.
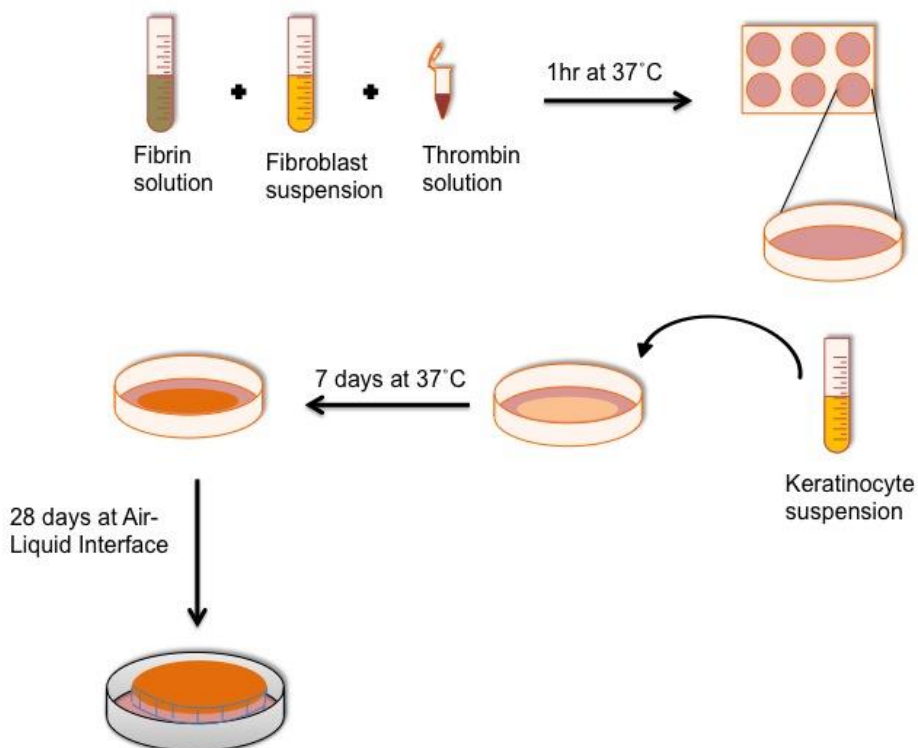
Figure 4.1: Construction of skin equivalents from RDEB or normal or RDEB keratinocytes and fibroblasts. The dermal fibroblasts are seeded in a fibrin gel and epidermal keratinocytes are cultured on the surface of the same gel. The keratinocytes are lifted and exposed to air for 28 days.

4.2. Materials and reagents

Hyperbranched poly-β-aminoester (HPAE) was kindly provided by Dr. Dezhong Zhou (The Charles Institute of Dermatology School of Medicine and Medical Science University College of Dublin, Dublin, Ireland). RDEB mice and normal mice were kindly provided by Dr. Olga Igoucheva and Prof. Jouni Uitto (Department of Dermatology and Cutaneous Biology, Thomas Jefferson University Hospital).

4.3. Methods

4.3.1. Polyplex preparation

The multi-knot polyplexes were prepared in water. 10mg was dissolved in 10ml of water, of which 30μl was mixed with 10μ of 1μg/μl COL7A1 plasmid DNA and incubated for 45 minutes before injection. To prepare HPAE polyplexes, 7.5mg is dissolved in 1ml of 25mM sodium acetate and mixed with equal volume of 0.25μg/μl COL7A1 plasmid DNA also diluted in sodium acetate.

4.3.2. *In vitro* transfection of keratinocytes and fibroblasts

For *in vitro* transfection methods, measurement of cell viability and culture conditions of RDEB keratinocytes and fibroblasts refer to the methods section of Chapter 3 and Appendix J, respectively.

4.3.3. Generation of skin equivalents

Briefly, the dermal part of the fibrin gel matrix is created by mixing fibrinogen with 38,000 skin fibroblasts in DMEM with trasylol and thrombine. To create the epidermis and stratum corneum, 60,000 RDEB or normal epidermal keratinocytes are seeded on top of the fibrin gel. The keratinocytes are exposed to air using special air-liquid interface inserts. (See Appendix M).

4.3.4. Generation of knockout mice

To generate RDEB mice, a targeting vector was used to replace the exons 46-69 of the COL7A1 with the neomycin-resistance gene resulting in elimination of most of domain 1 of the collagen. This created Col7α1 heterozygous (+/-) mice.

It is only after mating the heterozygous mice that the complete Col7α1-/- mice are born [11].

4.3.5. Experimental groups

Three RDEB mice were injected in the paws with Multi-knot/COL7A1 plasmid DNA, HPAE/COL7A1 plasmid DNA, PBS, while the fourth paw remained untreated. An additional injection of HPAE/COL7A1 plasmid DNA was made in the dorsal skin to investigate the transfection efficiency and immune response in that region.

4.3.6. Genotyping of the mice

To provide evidence of missing Col7α1 gene in knockout mice, we analyzed the genetic make-up of the RDEB mice and wild-type mice using the platinum® Taq DNA polymerase kit. Primers, 1: 5′ AGG TAT CAT ACT TCC TGG CAG A 3′; 2: 5′ AAG GCT ATC AAT ACT AGA ACC AG 3′; 3: 5′ CCT TCT TGA CCA GTT CTT CTG A 3′.

4.3.7. Injection procedure

The knockout mice were treated one day or eight days after birth. Five micrograms of complexed col7α1 pcDNA delivered by the hyperbranched poly-β-aminoester (synthesized in house) using a 30:1 ratio, was intradermally injected into the paws and up to 20µg into the dorsal or ventral regions. A tracing dye (Vybrant®) was used to locate the area of injection.

4.3.8. Sacrifice

Six mice were sacrificed 24 hours post last treatment, 3 wild type and 3 RDEB mice. Mice were put to sleep using isoflurane gas before cervical dislocation. Using an *in vivo* fluorescence microscope, images were taken of the area of dorsal injection where a dye was used to trace the polyplexes before it was excised and cryosectioned. For detailed protocol refer to Appendix X.

4.3.9. Indirect immunofluorescence staining

Cells and sections from skin equivalents were fixed with 4% paraformaldehyde

and permeabilized with 0.1% triton-x 100 before blocking (see Appendix S). Animal tissue sections are blocked without fixation or permeabilization. LH7.2 monoclonal antibody (Sigma Aldrich, Ireland) (see appendix Y: materials and reagents) was used to detect the human C7 and a rabbit polyclonal (Merick Millipore, UK) was used to detect mouse C7. Mouse collagen IV (C4) was detected using the rabbit polyclonal anti-C4.

4.3.10. Western blot

Forty-eight hours post transfection; the cell media is collected, filtered and stored at -20°C in the presence of protease inhibitors. The samples were concentrated and total protein was measured using a Bio-Rad protein assay. The sample was then run on 4 -12% SDS gel. This was then transferred to a protein membrane (400mA for 2 hours) before it was blocked with 3% BSA. The membrane was then incubated with primary antibody (LH7.2 at 1:1000 dilutions) for 3 hours, washed with TBS-Tween® 20 and incubated with secondary HRP for 2 hours at RT. Finally, the membrane was incubated with SuperSignal® substrate for 5 minutes before visualization.

For detailed protocol refer to Appendix U.

4.3.11. RNA extraction

Total RNA was extracted from cells and tissue using the Qiagen RNeasy® mini kit. The RNA template was then run using Verso one-step RT-PCR (ThermoScientific) according to manufacturer's guidelines. Refer to Appendices P and Q for full protocol.

4.4.   Results and discussion

4.4.1. Transfection properties of the multi-knot polymer in skin cells

The high charge density and fast degradability are important characteristics in gene delivery to cells especially in the case of polymer based gene carriers [12, 13]. The structure of the multi-knot polymer of dense cyclized chains creates a high concentration of amine groups providing the elevated charge density

required upon protonation. The degradability is through disulfide reduction. We found this polymer capable of transfecting a range of cell types with high efficiency including skin keratinocytes and fibroblasts. As a result, we examined its efficiency for gene therapy in the skin disease RDEB.

The majority of terminally differentiated cells that reside in the epidermal and dermal regions are fibroblasts and keratinocytes. Of the two, keratinocytes are the main producers of type VII collagen [14]. Although, genetically corrected fibroblasts on their own have been shown to produce sufficient type VII collagen and restore structural integrity in skin of RDEB patients after intradermal injection [15].

Collagen type VII-null fibroblasts extracted from squamous cell carcinoma of RDEB patients were transfected with the *Gaussia* luciferase plasmid using the multi-knot polymer or PEI (Figure 4.2). Under normal transfection conditions, multi-knot treated cells did not show any protein expression but this changed once uptake was improved by using glycerol and DMSO. We found that glycerol treatment significantly enhanced protein expression of the multi-knot treated cells but not the PEI treated cells. Likewise, DMSO had little influence on cells treated with PEI polyplexes, but gene expression of the multi-knot treated cells increased by more than 20-fold compared to the glycerol treated cells (Figure 4.3). Moreover, only glycerol was found to have a significant influence on cell viability, but only with higher weight ratios of polyplexes. The findings were consistent over different cell types including keratinocytes (Figure 4.4). We then focused on keratinocytes because they produce more than 90% of skin's collagen VII [7]. Keratinocytes treated with multi-knot polymer carrying the COL7A1 therapeutic plasmid showed high expression of the protein 48 hours post transfection (Figure 4.5 a). Additionally, cell extracted protein analysis with immunoblotting showed bands for collagen VII just above the 250 kDa marker in multi-knot transfected cells. Lower levels were seen in normal human keratinocytes with no trace of the protein band being detected in the untreated RDEB keratinocytes (Figure 4.5 b).

4.4.2. Transfection efficiency of the multi-knot polymer in skin equivalents (SEs)

Gene therapy offers a great potential for the treatment of RDEB which is why we used this non-immunogenic approach to test the feasibility of this hypothesis. Three-dimensional skin cultures were generated using fibrin as a scaffold. Type VII collagen-deficient fibroblasts were embedded into the matrix and immersed in growth media. On the surface of the scaffold, type VII collagen-null keratinocytes were seeded. The keratinocytes were in air-liquid interphase where they form a crest representing the upper layer of the epidermis after 28 days. These cultures were then transfected by topical application of the polyplex solution containing the multi-knot polymer and col7α1 plasmid. Figure 4.7 shows a cross section of the 3D skin cultures. Expression of collagen VII in transfected cells was visualized using an affinity-purified antibody to the NC2 domain of the type VII collagen. Normal keratinocytes show a green stain for collagen VII at the dermal-epidermal junction (DEJ) where it normally resides [16]. Signs of early protein homing to the DEJ in multi-knot polymer treated cultures is evident in the presence of collagen VII at the same region where the protein generally forms triple helical trimmers and anchoring fibrils [1]. Although the amount of protein released is low, these results are still very encouraging and prove the feasibility of using non-viral gene therapy for treating RDEB patients. Furthermore, the levels of col7α1 mRNA extracted from 3D skin equivalents, were significantly higher in the multi-knot treated cultures than in the untreated RDEB and , surprisingly, in the normal human skin cultures (Figure 4.6). These results critically demonstrate the effectiveness of the multi-knot as a gene delivery vector *ex vivo*.

4.4.3. Identification of the col7α1-/- mouse using phenotype and genotype analysis

Three primers were used to screen for the wild type (WT) (+/+), Heterozygote (HD) (+/-) and knockout (RDEB) (-/-) mice. Primer 1 and 2 amplify a 650 bp region of the normal type VII collagen, while primers 1 and 3 amplified a 490 bp region between the type VII collagen and the mutant genes. Using specific primers (section 4.3.6) [11], it is easy to distinguish between the normal and mutant genes (Figure 4.8, a). The heterozygote sample from the mouse carrying the mutation (HD +/-) is detected by both primer sets.

Phenotypically, RDEB mice are significantly smaller in size. Blistering in epithelial tissue of mucosal surfaces often leads to scarring within the mouth and gastrointestinal tract. This creates difficulties with digestion and limits nutrient absorption often leading to chronic malnutrition [17], the main cause of growth retardation. Even at 11 days old (Figure 4.9), the RDEB mouse was less than half of the weight of the wild type mouse of the same age. Blistering of the skin was noted at birth or shortly after in the RDEB mice with striking resemblance to human RDEB phenotype [18]. A hematoxylin and eosin stained cross section of a one day old mouse pup revealed prominent blistering in areas of high mobility such as the limbs, mouth and neck (Figure 4.10). Stained sections of the dorsal region showed little to no blistering in comparison to a section of the paws (Figure 4.11) confirming the impact of mobility and external trauma on the formation of the blisters. Immunofluorescence staining of an RDEB paw cross section revealed complete lack of mouse C7 in the basement membrane zone and clear presence of collagen type IV (C4) in the same region. Normal paw showed presence of both the mouse C7 and C4 at the BMZ (Figure 4.12). The lack of the structural C7 protein resulted in the detachment of the epidermis from the dermis leading to the formation of trauma-induced-blisters in the RDEB mouse paw [19].

4.4.4. Restoration of C7 expression in Col7α1-/- mouse using HPAE

The regions of injection were selected based on the size of the area and presence of blisters (Figure 4.10). The polyplexes were intradermally injected into the paws as well as the dorsal and ventral regions. They were then sacrificed 24 hours post last injection, as repetitive injections over three days were used in some experiments. A fluorescent DNA stain (Vybrant®) was used to trace the polyplexes post injection to make it easier to identify the region of injection (Figure 4.16 a). Areas of injection were then cryosectioned and examined for C7 production using indirect immunofluorescence staining. No human C7 was detected in the mouse dorsal region at any time post injection. This could be attributed to gravity acting on the polyplexes and preventing them from reaching dermal and epidermal cells. Additionally, the multi-knot polymer did not transfect any of the *in vivo* cells (results not shown) and thus was made redundant for the rest of the experiments. On the other hand, hyperbranched poly(β-amin ester) (HPAE) polymer (synthesized in house) was successfully used to transfect primary mouse cells *in vitro* and *in vivo*. Furthermore, two different time-points of sacrifice were studied in two separate experiments; the first experiment involved injecting the polyplexes on the first day (typically two or three days after birth) and sacrificing the animal on the second day. This allowed sufficient time for the cells in the injected region to be transfected and to express the protein. Human C7 was detected in and around the injected area of the paw (Figure 4.13). Understandably, the protein did not accumulate in the BMZ in such a short time and no human C7 was detected in and around the ventral injected site.

In the second experiment, the animals were sacrificed 96 hours post first injection and three injections were done in the paws and ventral area over a period of three days. Significant amount of C7 was immobilized in the BMZ near the injection sites in both cases (Figure 4.14 and Figure 4.15). Although there was significant presence of human C7 in the treated sections, there still remain large sections of the BMZ that did not have the protein and the figures

represent the small segments of the BMZ where the protein was restored after treatment.

4.4.5. Polyplexes ignite inflammatory response in injected skin of Col7α1- /- mouse

Although there was human C7 expression post treatment, toxicity and immunogenicity induced inflammatory response quickly became apparent in the injected tissue. Inflammatory response is well documented and characterized event being labelled as acute or chronic. In this study, the inflammation type can be described as acute since the majority of external triggers, such as the nanomaterials used for gene delivery [20], do not induce sustained immune cell mediated inflammatory response. We used image analysis of H&E stained sections or indirect immunofluorescence staining of inflammatory markers to detect early (24 hours post injection) and acute inflammation. Visual examination revealed inflammation 48 hours post polyplex injection (Figure 4.16 a). Epidermal inflammation was confirmed in H&E stained sections of the area (Figure 4.16 b). Primary antibodies for mouse CD45, CD44, CD11b and Ly6G were used to estimate the expression levels in wild type mouse and in RDEB mouse injected with the polyplexes.

Protein tyrosine phosphatase, receptor type, C (CD45) is a leukocyte common antigen involved in B and T-cell antigen receptor signaling and negative regulation of cytokine production [21]. High levels of this protein were detected in the area of treatment in RDEB mouse indicating early cellular response to the injected material (Figure 4.17). This is in parallel with exaggerated expression levels of CD11b [22] (expressed on the surface of the innate immune system cells such as monocytes, granulocytes, macrophages and natural killer cells) and Ly6g [23] (predominantly expressed in neutrophils) in the same region. The inflammatory response can be attributed to immediate toxicity associated with free polymer and delayed toxicity from cell processing of the polyplexes [24]. In addition, the transgene product (human C7) can induce immunogenicity in the host tissue as revealed in studies on protein replacement gene therapy in

some genetic diseases where neutralizing antibodies to the therapeutic products can be formed [25].
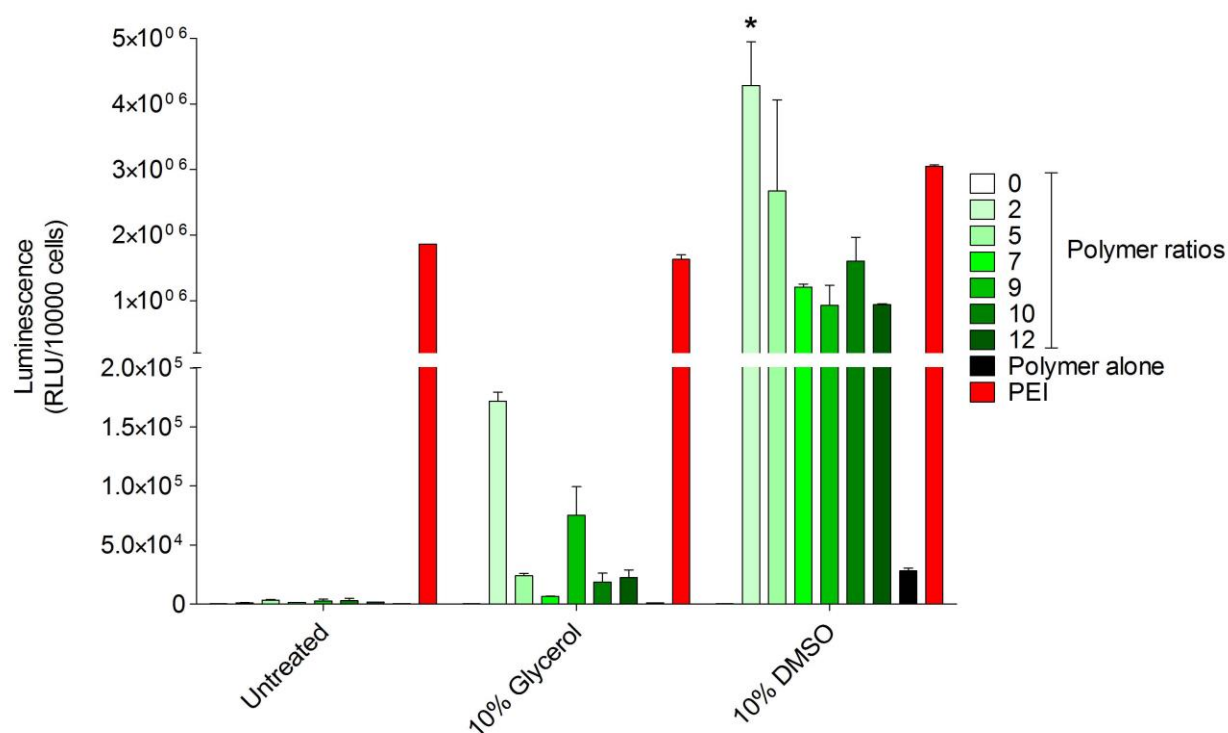
Figure 4.2: Luciferase expression levels in RDEB fibroblasts. Cells were either untreated or transfected with luciferase carried by the multi-knot polymer at different polymer to DNA weight ratios. Branched PEI (M_w=25 kDa) was used as control. Cells were incubated with 10% DMSO, 10% glycerol or left untreated. Asterisk represents statistical significance. Results are expressed as mean ± S.D. (n=3, p<0.05)). One way ANOVA (Fisher) was used for statistical analysis.
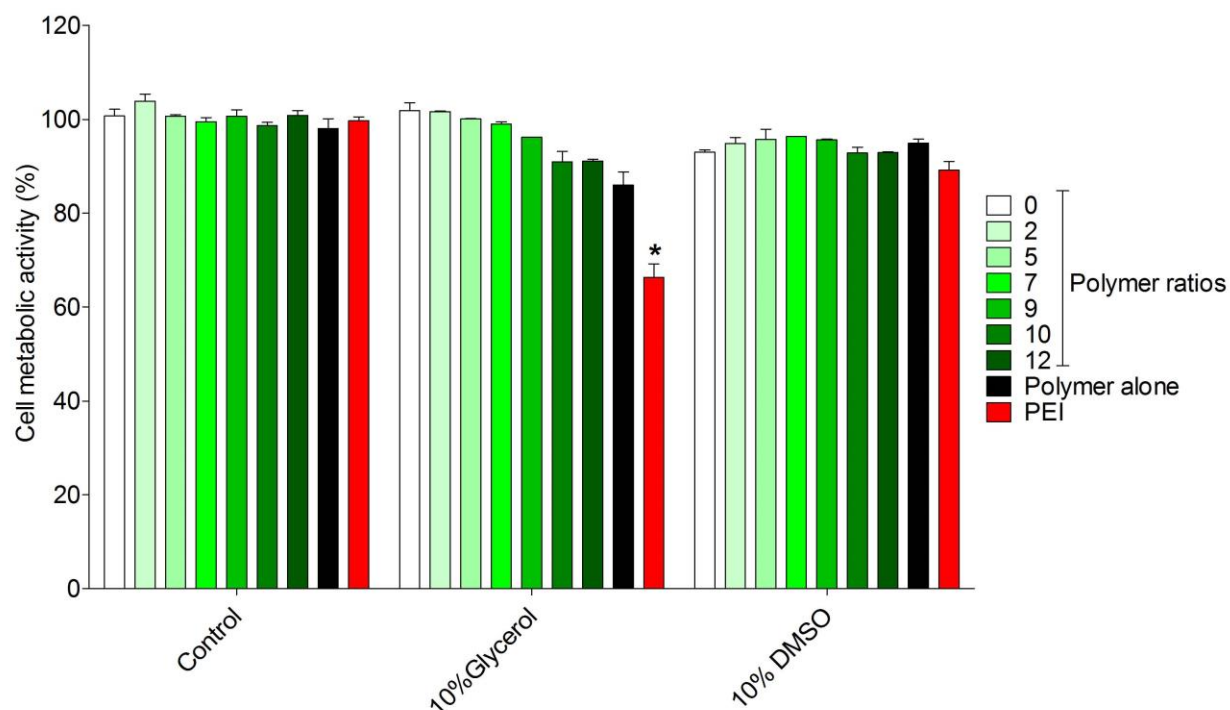
Figure 4.3: Cell metabolic activity of RDEB fibroblasts. Cells were either untreated or transfected with luciferase carried by the multi-knot polymer at different polymer to DNA weight ratios. Branched PEI (M_w=25 kDa) was used as control. Cells were incubated with 10% DMSO, 10% glycerol or left untreated. Asterisk represents statistical significance. Results are expressed as mean ±S.D. (n=3, p<0.05). One way ANOVA (Fisher) was used for statistical analysis.
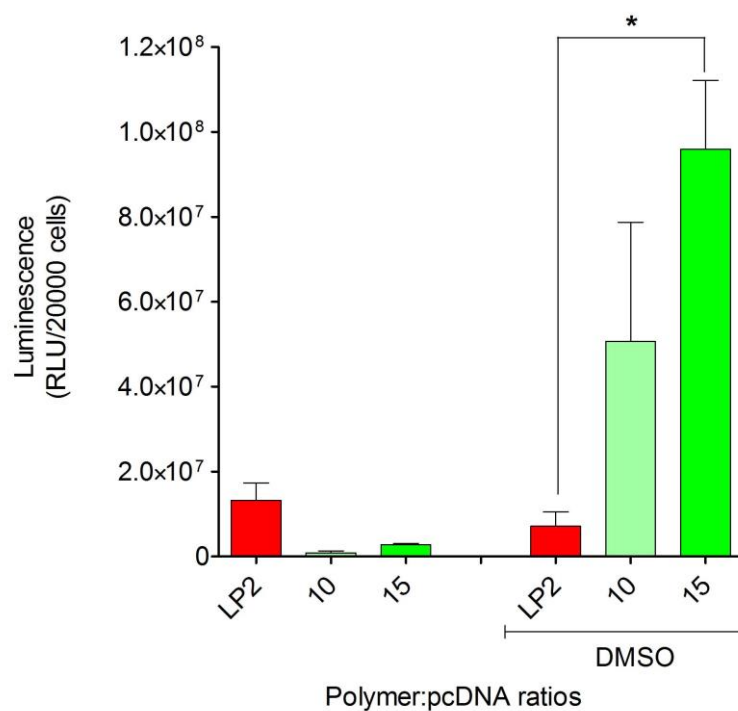
Figure 4.4: Luciferase expression levels in RDEB keratinocytes. Cells were transfected with luciferase carried by the multi-knot polymer at different polymer to DNA weight ratios. Lipofectamine2000® (LP2) was used as control. Cells were incubated with 10% DMSO or left untreated. The cell metabolic activity was unchanged for both treatments (results no shown). Asterisk represents statistical significance. Results are expressed as mean ±S.D. (n=3, p<0.05). One way ANOVA (Fisher) was used for statistical analysis.

a

b
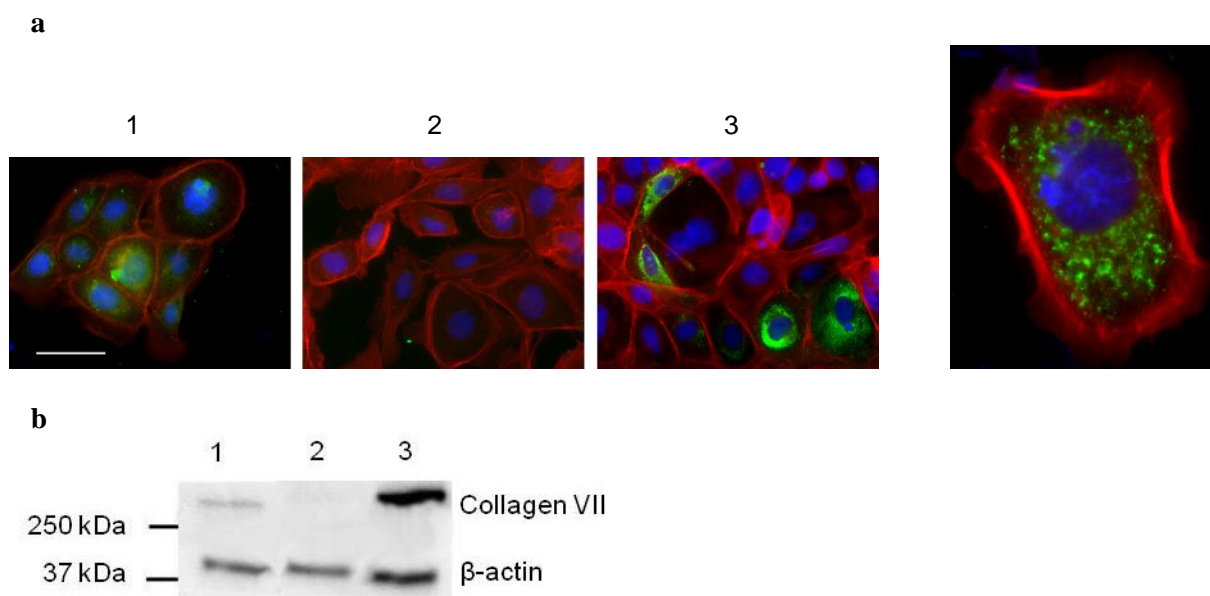
Figure 4.5: **a**. Immunofluorescence images of normal human keratinocytes (NHK) (1), RDEB keratinocytes (2) and RDEB keratinocytes corrected with multi-knot polymer carrying the COL7A1 gene (3). C7: green, actin filaments: red and DAPI: blue. Scale bar represent 50μm. **b**. Western blot showing bands for C7 in normal human keratinocytes (lane 1) and RDEB keratinocytes transfected with multi-knot polymer carrying the COL7A1 gene (lane 3). Only β-actin was detected in RDEB keratinocytes, (lane 2).
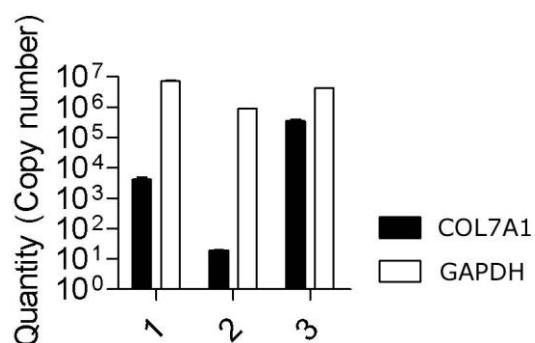
Figure 4.6: Real time quantitative PCR graph showing relative COL7A1 and GAPDH mRNA copy number extracted from normal human keratinocyte skin equivalents (1) RDEB keratinocyte SEs (2) and RDEB keratinocyte SEs transfected with Multi-knot polymer carrying the COL7A1 gene (3). Results are expressed as mean ±S.D. ($n =3$, $p<0.05$). The one way ANOVA (Fisher) was used for statistical analysis.
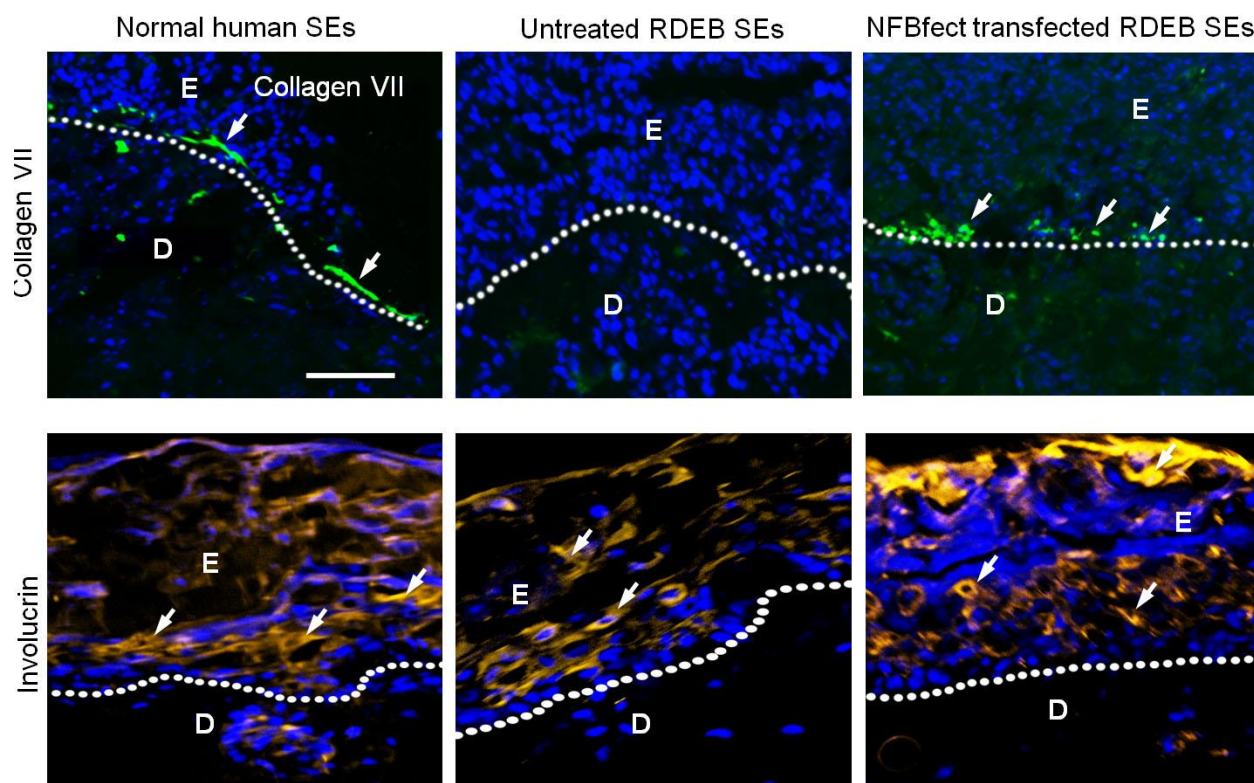
Figure 4.7: Immunofluorescence images of SE sections taken from normal human keratinocyte (NHK) cultures, RDEB keratinocyte cultures and RDEB keratinocyte cultures transfected with multi-knot polymer carrying the COL7A1 gene. Top: stains for collagen VII (green) and DAPI (blue). Bottom: stains for involucrin (amber) and DAPI (blue). Mouse anti-human was used to detect C7. Images were taken at 20x magnification. Scale bar represents 100μm.
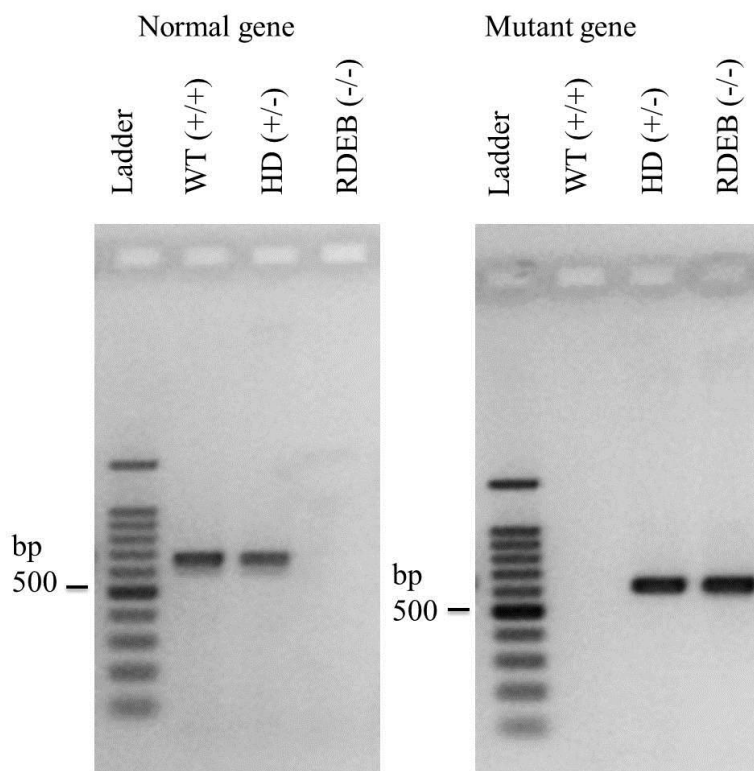
Figure 4.8: Gel electrophoresis of RT-PCR products of genomic DNA from wild type (WT +/+), Heterozygote HD +/-) and RDEB (-/-) mouse tissue. Using primers that amplify the normal or mutant gene, it is possible to distinguish between the three types of mice.

a **b**
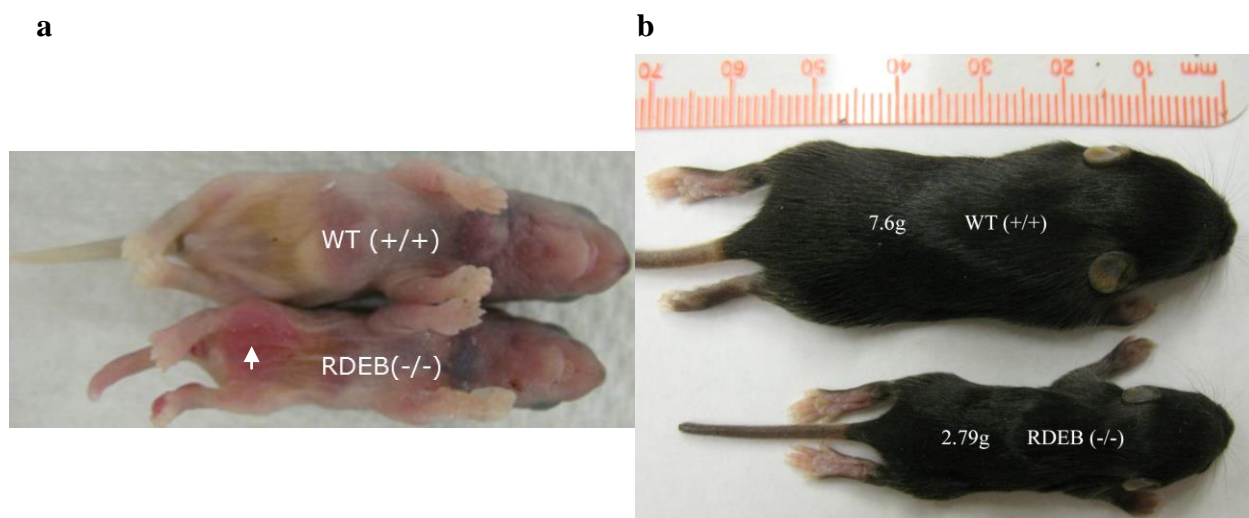
Figure 4.9: Side by side comparison of wild type mouse and RDEB mouse. **a**. Both mice at 2 days old, of which the RDEB mouse shows a large blister in the abdominal viscera (arrow). **b**. Different mice at 11 days old showing size difference between the wild type and RDEB mouse. The wild type is more than twice the weight of its counterpart.
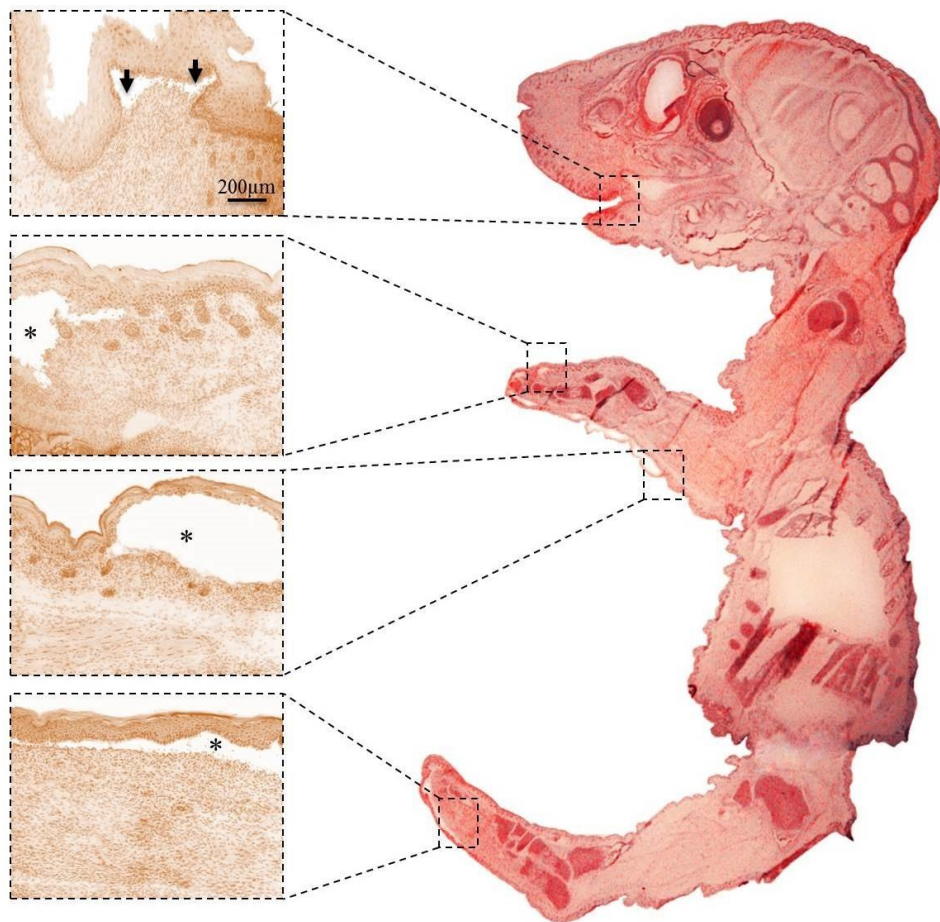
Figure 4.10: A hematoxylin and eosin stained cross section of a one day old RDEB (-/-) mouse. The mouse shows typical RDEB features of microblisters (arrows) and blisters (asterisk) in the regions of high mobility such as the front and hind limbs. Images were taken at 4x and 20x magnification.
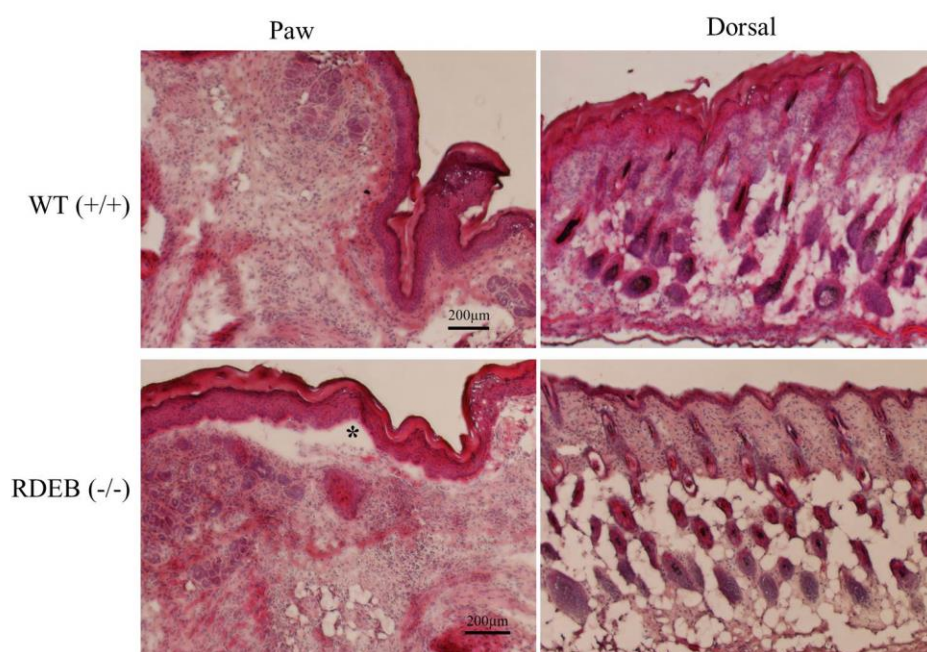
Figure 4.11: Hematoxylin and eosin stained cross sections of wild type and RDEB mouse skin taken from either the underside of the paw or from the dorsal area. Trauma induced blistering in the paw is attributed to structural instability due to the lack of C7 in RDEB mice. Images were taken at 20x magnification.
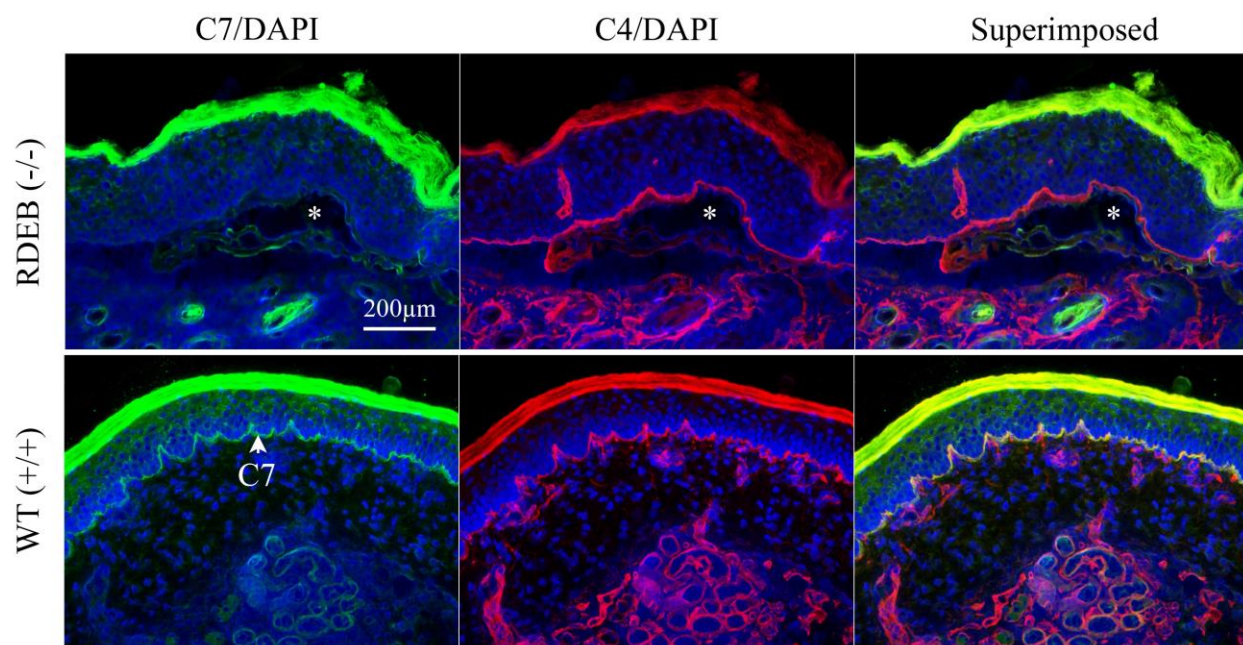
Figure 4.12: Immunofluorescence stained sections of wild type (WT) and RDEB mouse paw tissue. Lack of C7 in the BMZ is evident while there is abundance of the protein in the wild type which overlaps well with the C4 protein. Goat anti-mouse C7 and rabbit anti-mouse C4 were used. Images were taken at 20x magnification.
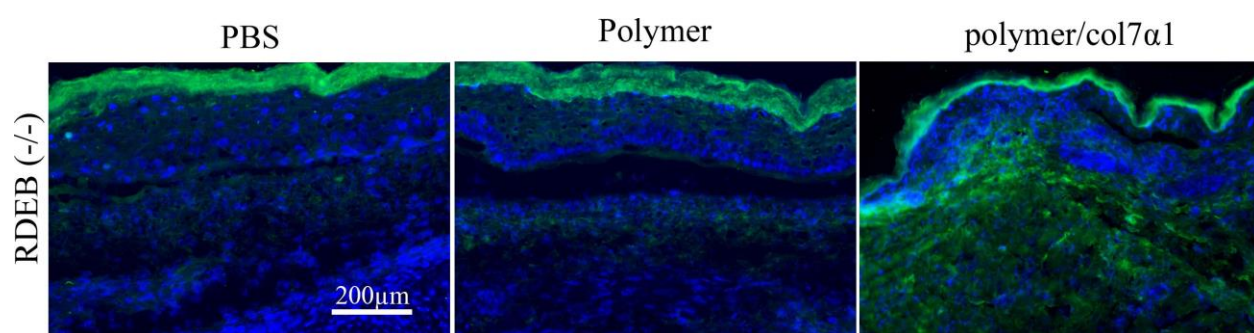
Figure 4.13: Immunofluorescence staining for human C7 in RDEB (-/-) mouse paws 24 hours post single injection. The paws were intradermally injected with PBS, polymer alone or polypexes (30:1). Sections were stained with LH7.2 mouse anti-human C7 and DAPI and images were taken at 20x magnification.
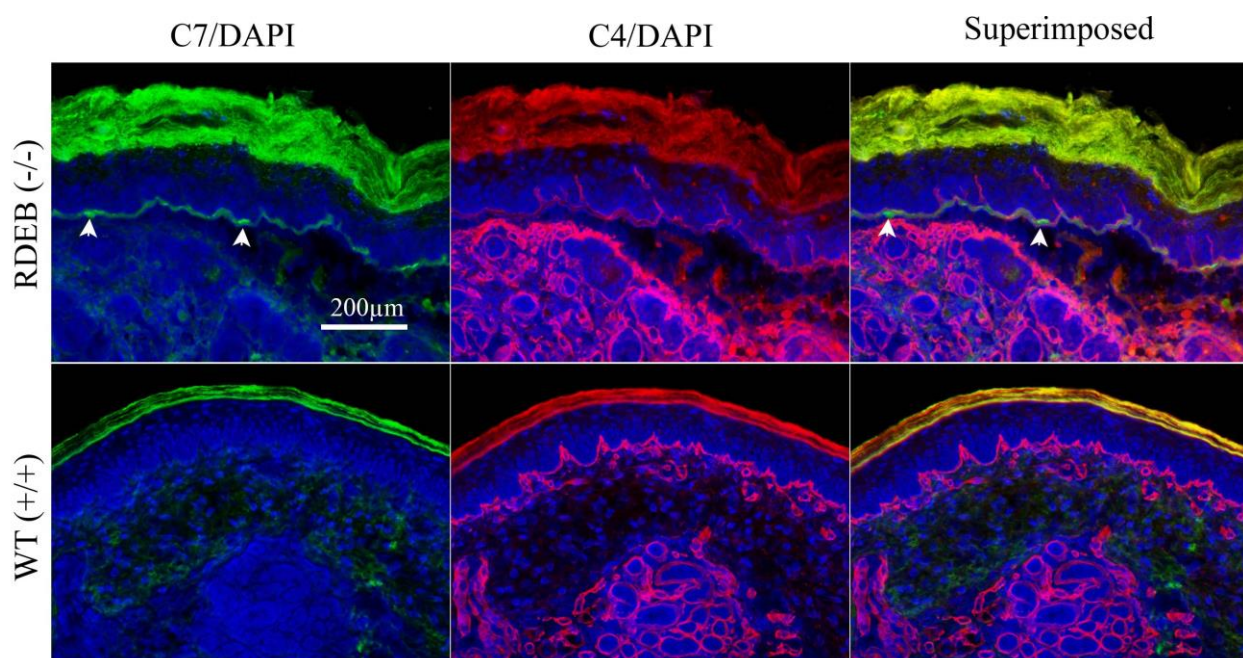
Figure 4.14: Immunofluorescence staining of RDEB (-/-) mouse paw injected with HPAE/COL7A1 plasmid DNA polyplexes compared to wild type paw. The animals were sacrificed 96 hours post first injection. Sections were stained with mouse anti-human C7 or rabbit anti-mouse C4. Arrows indicate human C7 in the BMZ of mouse. Images were taken at 20x magnification.
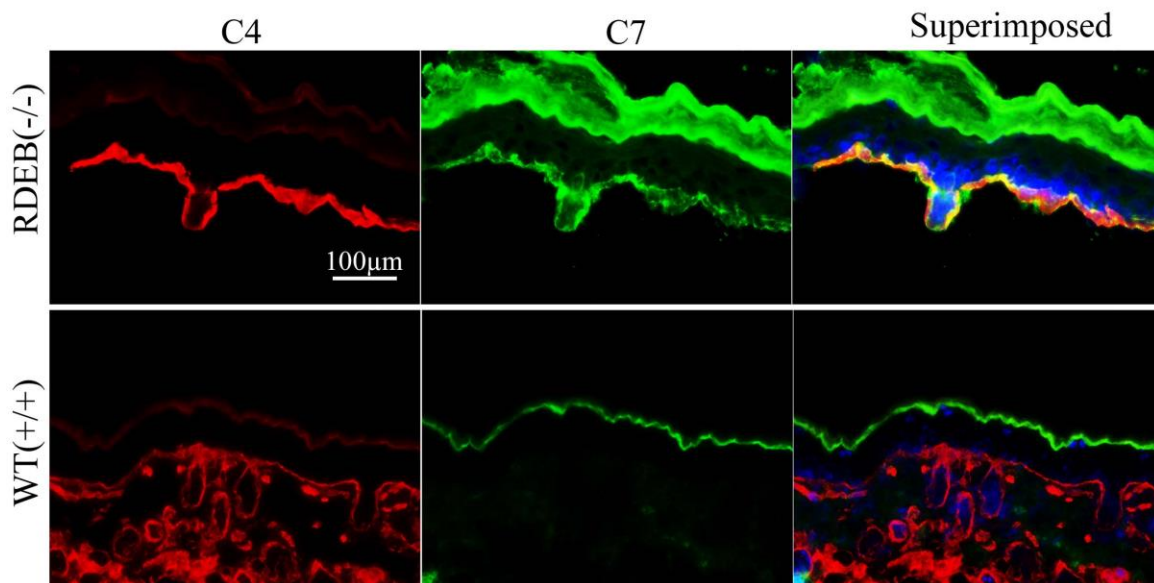
Figure 4.15: Immunofluorescence stained sections of RDEB (-/-) mouse ventral area injected with HPAE/COL7A1 plasmid DNA polyplexes and untreated wild type. The animals were sacrificed 96 hours post first injection. Sections were stained with goat anti-human C7, rabbit anti-mouse C4 and DAPI. Images were taken at 40x magnification.
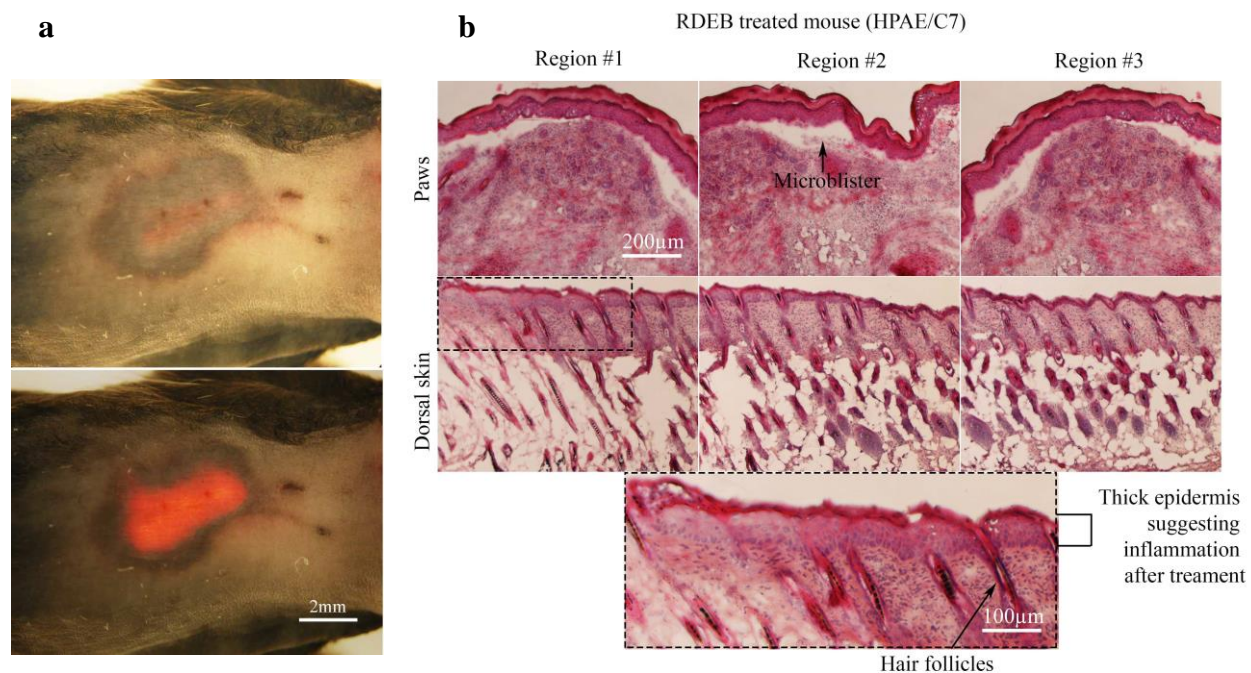
Figure 4.16: Polyplexes injected in the intradermal region induced epidermal inflammation and tissue necrosis. **a**. images of RDEB mouse dorsum taken using standard Nikon camera. The Vybrant® DNA dye can be seen through the skin under bright-field along with the inflamed area where the polyplex solution dispersed. **b**. Hematoxylin and eosin stained tissue sections of the paws and dorsum showing inflammation of the skin especially in the dorsum. Images were taken at 20x magnification.
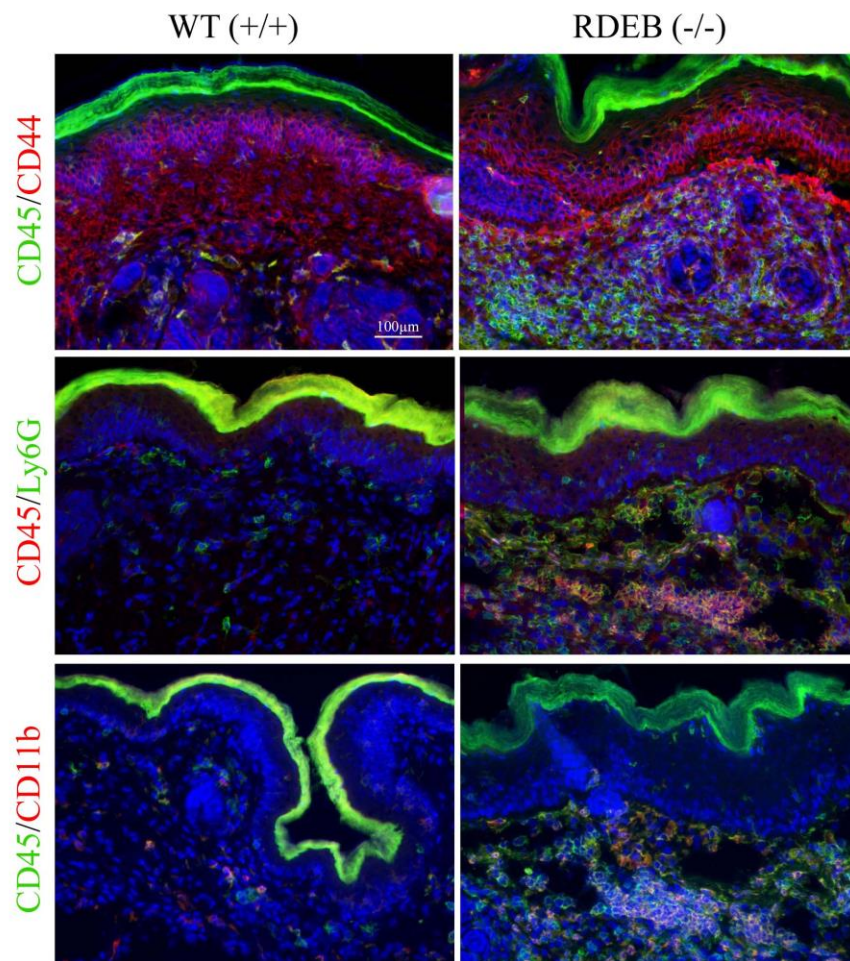
Figure 4.17: Immunofluorescence stained sections from mouse paws reveal elevated expression of cytokines and chemokines of the inflammatory response in the RDEB (-/-) treated area of the skin. Sections were stained with antibodies against four inflammatory cytokines all of which were up regulated in the area of injection. Images were taken at 20x magnification.

4.5.   Conclusion

In conclusion, we went beyond the single cyclized knot polymer to a unique higher and more complex multi-knot structure. This was achieved by delaying the onset of gelation in a one-pot *in situ* DE-ATRP reaction as outlined in chapter one. As a proof of concept, RDEB was selected for a number of *in vitro* and *ex vivo* studies. Successful transfection of RDEB keratinocytes with COL7A1 lead to the expression of recombinant protein faithful to the native showing signs of a possible treatment of the disease. Although the multi-knot polymers showed minor success *ex vivo*, only the HPAEs showed transfection capability *in vivo*. Human C7 expression was achieved 24 hours post injection of HPAE/COL7A1 polyplexes in the skin of RDEB (Col7α1-/-) knockout mice. The protein co-localized with C4 in the BMZ of the RDEB mice after 96 hours. However, elevated expressions of inflammatory markers such as CD45, CD44, Ly6G and CD11β point to acute inflammation and a natural response of the tissue to foreign materials such as the HPAE/COL7A1 complexes. The benign nature of this potential gene therapy make it a valid option, allowing the reparative gene to be repeatedly applied. The C7 protein (known to have a long half-life) would hopefully build up in the tissue and over time provide structural integrity to reverse the RDEB phenotype.

4.6.   References

1.   Bruckner-Tuderman, L., Can Type VII Collagen Injections Cure Dystrophic Epidermolysis Bullosa? *Mol Ther*, 2009. 17: p. 6.

2.   Dang, N. and D.F. Murrell, Mutation analysis and characterization of COL7A1 mutations in dystrophic epidermolysis bullosa. *Exp Dermatol*, 2008. 17: p. 553.

3.   Woodley, D.T., Y. Hou, S. Martin, W. Li, and M. Chen, Characterization of molecular mechanisms underlying mutations in dystrophic epidermolysis bullosa using site-directed mutagenesis. *J Biol Chem*, 2008. 283: p. 17838.

4.   Baldeschi, C., Y. Gache, A. Rattenholl, P. Bouille, O. Danos, J.P. Ortonne, L. Bruckner-Tuderman, and G. Meneguzzi, Genetic correction of canine dystrophic epidermolysis bullosa mediated by retroviral vectors. *Hum Mol Genet*, 2003. 12: p. 1897.

5.   Kay, M.A., J.C. Glorioso, and L. Naldini, Viral vectors for gene therapy: the art of turning infectious agents into vehicles of therapeutics. *Nat Med*, 2001. 7: p. 33.

6.   Chen, Y.Q., A. Mauviel, J. Ryynanen, S. Sollberg, and J. Uitto, Type VII collagen gene expression by human skin fibroblasts and keratinocytes in culture: influence of donor age and cytokine responses. *J Invest Dermatol*, 1994. 102: p. 205.

7.   Ryynanen, J., S. Sollberg, M.G. Parente, L.C. Chung, A.M. Christiano, and J. Uitto, Type VII collagen gene expression by cultured human cells and in fetal skin. Abundant mRNA and protein levels in epidermal keratinocytes. *J Clin Invest*, 1992. 89: p. 163.

8.   Chen, M., E.A. O'Toole, M. Muellenhoff, E. Medina, N. Kasahara, and D.T. Woodley, Development and characterization of a recombinant truncated type VII collagen "minigene". Implication for gene therapy of dystrophic epidermolysis bullosa. *J Biol Chem*, 2000. 275: p. 24429.

9.   Chen, M., N. Kasahara, D.R. Keene, L. Chan, W.K. Hoeffler, D. Finlay,

M. Barcova, P.M. Cannon, C. Mazurek, and D.T. Woodley, Restoration of type VII collagen expression and function in dystrophic epidermolysis bullosa. *Nat gen*, 2002. 32: p. 670.

10.   Langer, R. and J.P. Vacanti, Tissue engineering. *Science*, 1993. 260: p. 920.

11.   Heinonen, S., M. Mannikko, J.F. Klement, D. Whitaker-Menezes, G.F. Murphy, and J. Uitto, Targeted inactivation of the type VII collagen gene (Col7a1) in mice results in severe blistering phenotype: a model for recessive dystrophic epidermolysis bullosa. *J Cell Sci*, 1999. 112 (Pt 21): p. 3641.

12.   Jones, C.H., C.K. Chen, M. Jiang, L. Fang, C. Cheng, and B.A. Pfeifer, Synthesis of cationic polylactides with tunable charge densities as nanocarriers for effective gene delivery. *Mol Pharm*, 2013. 10: p. 1138.

13.   Zhang, G., J. Liu, Q. Yang, R. Zhuo, and X. Jiang, Disulfide-Containing Brushed Polyethylenimine Derivative Synthesized by Click Chemistry for Nonviral Gene Delivery. *Bioconjugate Chem*, 2012. 23: p. 1290.

14.   Ryynanen, J., S. Sollberg, M.G. Parente, L.C. Chung, A.M. Christiano, and J. Uitto, Type VII collagen gene expression by cultured human cells and in fetal skin. Abundant mRNA and protein levels in epidermal keratinocytes. *The J Clin Invest*, 1992. 89: p. 163.

15.   Wong, T., L. Gammon, L. Liu, J.E. Mellerio, P.J.C. Dopping-Hepenstal, J. Pacy, G. Elia, R. Jeffery, I.M. Leigh, H. Navsaria, and J.A. McGrath, Potential of fibroblast cell therapy for recessive dystrophic epidermolysis bullosa. *J Invest Dermatol*, 2008. 128: p. 2179.

16.   Yan, W.F. and D.F. Murrell, Fibroblast-based cell therapy strategy for recessive dystrophic epidermolysis bullosa. *Dermatol Clin*, 2010. 28: p. 367.

17.   Fine, J.D. and J.E. Mellerio, Extracutaneous manifestations and complications of inherited epidermolysis bullosa: part I. Epithelial associated tissues. *J Am Acad Dermatol*, 2009. 61: p. 367.

18.   Fritsch, A., S. Loeckermann, J.S. Kern, A. Braun, M.R. Bosl, T.A. Bley,

H. Schumann, D. von Elverfeldt, D. Paul, M. Erlacher, D. Berens von Rautenfeld, I. Hausser, R. Fassler, and L. Bruckner-Tuderman, A hypomorphic mouse model of dystrophic epidermolysis bullosa reveals mechanisms of disease and response to fibroblast therapy. *J Clin Invest*, 2008. 118: p. 1669.

19.   Christiano, A.M., J.A. McGrath, and J. Uitto, Influence of the second COL7A1 mutation in determining the phenotypic severity of recessive dystrophic epidermolysis bullosa. *J Invest Dermatol*, 1996. 106: p. 766.

20.   Nunes, A., K.T. Al-Jamal, and K. Kostarelos, Therapeutics, imaging and toxicity of nanomaterials in the central nervous system. *J Control Release*, 2012. 161: p. 290.

21.   De Dios, I., L. Ramudo, J.R. Alonso, J.S. Recio, A.C. Garcia-Montero, and M.A. Manso, CD45 expression on rat acinar cells: involvement in pro-inflammatory cytokine production. *FEBS Lett*, 2005. 579: p. 6355.

22.   Solovjov, D.A., E. Pluskota, and E.F. Plow, Distinct roles for the alpha and beta subunits in the functions of integrin alphaMbeta2. *J Biol Chem*, 2005. 280: p. 1336.

23.   Mishalian, I., R. Bayuh, E. Eruslanov, J. Michaeli, L. Levy, L. Zolotorov, S. Singhal, S.M. Albelda, Z. Granot, and Z.G. Fridlender, Neutrophils recruit regulatory T-cells into tumors via secretion of CCL17 - a new mechanism of impaired anti-tumor immunity. *Int J Cancer*, 2014.

24.   Godbey, W.T., K.K. Wu, and A.G. Mikos, Poly(ethylenimine)-mediated gene delivery affects endothelial cell function and viability. *Biomaterials*, 2001. 22: p. 471.

25.   Fields, P.A., D.W. Kowalczyk, V.R. Arruda, E. Armstrong, M.L. McCleland, J.N. Hagstrom, K.J. Pasi, H.C. Ertl, R.W. Herzog, and K.A. High, Role of vector in activation of T cell subsets in immune responses against the secreted transgene product factor IX. *Mol Ther*, 2000. 1: p. 225.

CHAPTER 5

Summary and future directions

5.1.   Introduction

The progress towards finding a long term solution to the genetic skin condition, recessive dystrophic epidermolysis bullosa, is slow with little to no evidence of effective long term treatment being proposed aside from the highly invasive bone marrow transplantation. The reason behind this is the low prevalence of the disease which has been categorized as a rare genetic disease by the National Institutes of Health. The condition, attributed to mutations in the COL7A1 gene [1], affects the skin and internal mucosa covering a wide surface area making it difficult to treat. One of the more promising methods of treatment is bone marrow transplantation [2]. In this major study, scientists proposed the idea of using allogeneic bone marrow stem cells to revert the RDEB phenotype. They found that transplantation of these cells into the RDEB patients restore C7 deposition with noticeable improvements in wound healing and reduced blistering. Unfortunately, two of the seven patients enrolled in the trials died sometime after the procedure. The high risk, cost and ethical issues retracted many RDEB patients from the procedure.

Other proposed treatments include; injection of allogeneic fibroblasts [3], injection of recombinant C7 protein [4] and *ex vivo* cell correction of patient's cells [5-7]. All these publications reported encouraging signs of C7 restoration post treatment. However, many of them have not been fully tested and those that have only restored structural and mechanical stability partially while having a limited time of restoration. These methods have also been tested in other diseases, of which viral vector based therapy showed the greatest potential because of their high gene delivery efficiency.

Viral vectors have been at the forefront in terms of transfection efficiency since their inception as gene delivery vectors. Their major drawback is that they carry the risk of inducing severe toxicity and immunogenicity. Non-viral gene delivery has emerged as a more risk free method. However, despite the recent expansion of non-viral gene delivery vectors, they are still limited in terms of efficiency. Polymeric vectors are among the more versatile of non-viral gene

167

delivery vectors offering great composition versatility and more controllable synthesis [8] in addition to have low production costs. The overall aim of this study was to design a cationic polymer vector with biodegradable property for efficient gene delivery of COL7A1 to RDEB skin cells.

5.2. Summary

The objective of phase I (**Chapter 2**) was to synthesis a cationic polymer with high charge density and fast degradation capability. These two properties were found to be highly influential in determining the transfection efficiency and cytotoxicity [9, 10]. To increase the charge density of the polymer, we went beyond the single knot polymer [11] to the denser and more complex multi-knot polymer structure. This was achieved by delaying the onset of gelation in a one-pot *in situ* DE-ATRP reaction. At the same time, we introduced a disulfide based cross-linker in the reaction as opposed to the conventional EGDMA monomer. The disulfide link is commonly broken in the presence of thiol reducing agents such as glutathione [12, 13], a chemical present in high concentrations in cellular vesicles [14]. This disulfide containing crosslinker was synthesized in house by mixing acroylyl chloride with triethyleamine and hydroxy ethyl disulfide under argon. The monomer was then purified before being used in the multi-knot synthesis reaction. By using *in situ* DE-ATRP [15] under a high polymer concentration system and delaying the onset of gelation (beyond the single knot structure), a high molecular weight, and multi-knot structured polymer was obtained. Characterization of the polymer post DNA interaction revealed the formation of polyplexes with sizes ranging from 100-200 nm and a positive charge reaching 50mV after protonation. In the presence of 5mM glutathione, the polymer degraded within minutes allowing for efficient DNA escape (80% efficiency) as determined by the PicoGreen® assay.

In the second phase of the study, the polymer was optimized for reporter gene delivery and tested for cytotoxicity in common cell lines (**Chapter 3**). In primary cells, the multi-knot polymer and commercial vector treated cells expressed similar levels of the luciferase protein expression. The polymer was

less efficient in transfection human ADSCs. In HeLa cells, expression levels of the protein were dramatically increased (100-fold) after increasing the DNA amount to 1µg. This was achieved at a polymer/DNA ratio of 3, much lower than what was predicted to be an optimal ratio. Increasing the polymer DNA further reduced the cell viability. The results were reproduced using GFP reporter gene. Although the number of transfected cells using the multi-knot polymer was significantly lower than of those transfected with the commercial agent, Xfect®. Interestingly, the fluorescence intensity in the multi-knot transfected cells was significantly higher. When the same experiments were repeated in the presence of 10% DMSO (2 minute incubation with cells), luciferase levels were again higher than the untreated cells. This indicates involvement of the uptake levels in determining the transfection efficiency [16]. The treatment, however, had a catastrophic effect on cell viability where more than 90% of the cells died at high polymer/DNA ratios.

Phase III involved the *in vitro*, *ex vivo* and *in vivo* testing of the polymer platform in RDEB skin cells and an RDEB mouse model (**Chapter 4**). Efficient transfection of the RDEB fibroblasts using the multi-knot polymer was only achieved after DMSO treatment. We focused on the transfection of RDEB keratinocytes since they are the main source of collagen type VII [17]. We discovered that, although DMSO treatment increased luciferase expression in multi-knot treated keratinocytes, it did not influence expression levels of C7. Using a polymer/col7α1 ratio of 3, the transfected cells expressed a significant amount of C7 as determined by immunohistochemistry and western blotting. Transfection of 3D skin equivalents (composed of fibroblasts and keratinocytes) was also possible, even though the amount of C7 produced was much lower than what is seen in normal skin. Additionally, lack of hair follicles, stem cells and inflammatory cells in the skin equivalents prompted us to test this polymer *in vivo* by intradermal injection of the polyplexes in an RDEB mouse model. This model was developed at the Thomas Jefferson University with a similar phenotype to human [18]. The mice develop blisters immediately after birth

with noticeable scarring thereafter. Genotyping of the mouse revealed absence of the correct COL7A1 coding sequence. Staining of the mouse skin tissue revealed wide spread blistering in the paws, ventral side and mouth, areas where friction is more prevalent. Immunostaining revealed complete lack of the C7 protein in the BMZ of these mice. Upon intradermal injection of various gene delivery vectors carrying the COL7A1 gene into the skin of these mice, we found that out of the polymers tested; only the hyperbranched poly (β-amino ester) (HPAE) induced minute human C7 production in the injected region. We found the human C7 in the dermal tissue below the basement membrane zone (BMZ) 24 hours post injection and the protein was only detected in the BMZ 96 hours post first injection. The results pointed towards slow migration of the C7 from its source to the BMZ.

Examination of the tissue (H&E) revealed epidermal inflammation in the injected site with elevated expression of CD11b, CD45 and Ly6g which indicates to a major inflammatory response in the area. The levels of these markers were higher than in PBS injected control (results not shown). It is assumed that the inflammation is caused by polymer toxicity and not the transgene product.
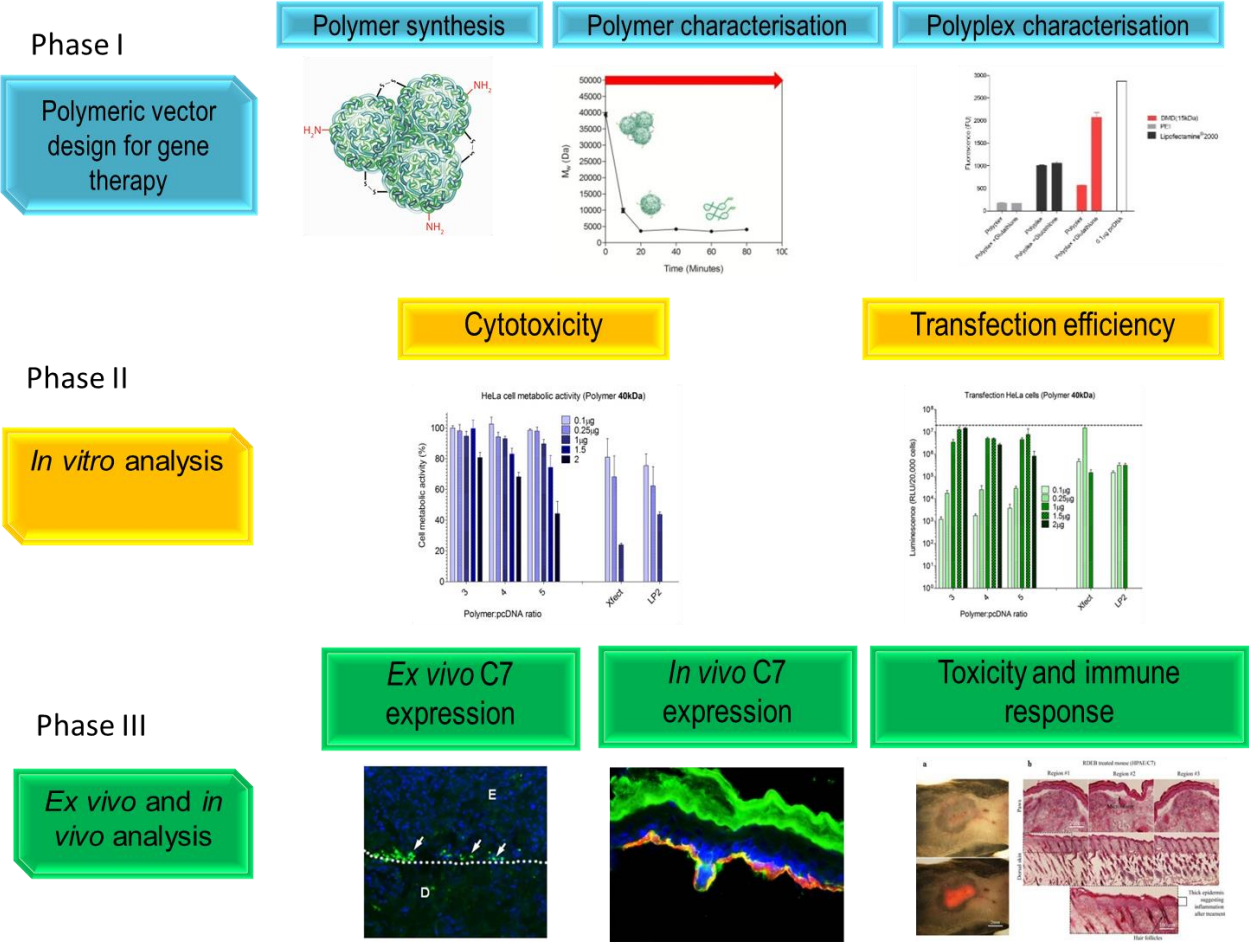
Figure 5.1: Summary of the main outcomes of each phase of this thesis.

5.3.   Limitations

Transfection efficiency in primary cells was significantly lower than in cell lines because of the slow proliferation rate of primary cells. This is the case for all the tested transfection vectors including the commercial agents and for many of the cell types that we tested including human adipose derived stem cells (hADSCs), human keratinocyte and fibroblasts (NHKs and RDEBFs) (Figure 5.2 and Figure 5.3). This poses a universal problem for all transfection agents. Primary cells pose more of a challenge because they divide less often, making it difficult for the reporter or therapeutic plasmids to enter the nucleus. Overcoming this limitation requires further understanding of the nuclear import mechanism and what molecules or agents are required to enhance nuclear entry of the polyplexes. Once these molecules are identified they can be easily mounted to the multi-knot polymer, since this polymer has unique post-synthesis modifiable reactive species in the form of vinyl groups.

Another limitation concerns the cells used in the construction of the skin equivalents (SEs). The nature of the method required to construct the SEs made it difficult to prevent contamination since the SEs are suspended in the liquid-air interface. Eventually, contamination was controlled by using a higher antibiotic concentration. On several occasions the density of the cells (high density of cells is required to construct the SEs) also resulted in cell death but that did not affect the experiment because the growth medium was changed on regular basis.

Regarding the animal studies, there was a limited amount of polyplexes delivered to the paws (15µl) because of the small surface area. The new born pups have very small paws and injecting any kind of solution into them proved to be a huge task. Additionally, the injections caused bruises (Figure 5.4) and bleeding in the paws which might have influenced the transfection efficiency. It was easier to inject the polyplexes into the ventral and dorsal regions where there is more surface area.

Despite finding the transgene product, human C7, in the BMZ near the injected site, there was not sufficient amount of the structural protein to restore adherence of the epidermis to the dermis. This was seen in almost all HPAE/col7α1 injected sites. This indicates to a limited number of transfected cells which reflect the number of transfected primary cells *in vitro* (Figure 5.3). Finally, we predicted that the time from injection to sacrifice is not long enough for the C7 to form anchoring fibrils and restore the structural stability of the skin. This remains to be tested.

5.4. Future directions

Based on the outcomes and limitations of the project, the following section is devoted to outlining the potential alternatives to the pitfalls encountered and the possible future directions the project may follow. Four different but related approaches are described in this section.

5.4.1. Poly(β-amino esters) for RDEB gene therapy

Linear poly (β-amino esters) (PAEs) have been previously reported by Langer *et al*. in which a library of PAEs was synthesized and end modified with amines. They have discovered a robotic method of synthesizing thousands of different PAEs in a single reaction. This method helped define the polymer composition and molecular weight ideal for transfection. Some of these polymers have comparable transfection levels to lentiviruses and adenoviruses in HUVECs [19]. The polymers were also used successfully *in vivo* [20] thus giving a glimpse of hope for the future of polymers in gene therapy. In Chapter 4, a hyperbranched poly (β-amino esters) (HPAE) was used to correct the skin cells of an RDEB (Col7α1-/-) mouse. This polymer was in fact synthesized in house as we discovered that it had higher transfection levels than the commercially available PAE, Xfect® in RDEB keratinocyte cell lines (Figure 5.5). For future polymer gene delivery projects, it is recommended that HPAE is tested more thoroughly in terms of polyplex forming capability, transfection efficiency in RDEB primary and stem cells with GFP and COL7A1, and toxicity levels *in vivo*.

5.4.2. Optimizing polymer vectors for primary and stem cell transfection

Primary cells are more representative of the main functional component of the tissue from which they are derived in comparison to immortalized or tumor derived cell lines which have undergone multiple population doublings [21]. As demonstrated in the limitations section of this chapter, they are much harder to transfect than immortalized cells due to their slow proliferation rate [22], and higher extracellular matrix (ECM) deposition significantly reducing transfection efficiency. The ECM traps the polyplexes in a web like structure preventing them from accessing the cellular membrane. While slow proliferation is a problem for non-viral gene delivery because mitosis occurs less frequently in primary cells meaning that the nuclear membrane remains intact for longer periods of time. This limits the access of the therapeutic gene to the host genome. Stem cells are just as hard to transfect but hold potential for differentiation and proliferation. Stem cells, such as embryonic and induced pluripotent stem cells hold great promise for disease treatment because they can differentiate into any cell type [23]. This is in addition to having potentially infinite proliferative capacity which means it is possible to induce long lasting transgene expression in progeny cells after stable transfection of the parent cells. Thus, it is important to focus the vector design and optimization around the cellular uptake and nuclear import mechanisms of primary and stem cells. This will inevitably uplift the transfection of non-viral vectors *in vivo* and in the clinic.

Here are a number of important considerations to take into account when designing and optimizing a non-viral gene vector for primary and stem cell transfection:

Small and homogenous polyplexes

A key aspect we have discussed in Chapter 2 is the characterization of the polypelxes in terms of size and charge. Uneven distribution or aggregation of polyplexes significantly lowers transfection efficiency. This can be caused by unbalanced polymer/DNA ratio or by the buffer solution the polyplexes made in

174

[24]. To identify the best polyplex formulation, polyplex sizes ranging from 10nm to 200 nm should be tested in addition to examining the influence of excess polymer on the transfection efficiency. The sizes of the polyplexes can be determined using Dynamic Light Scattering (DLS) or Gel Permeation Chromatography (GPC). The excess polymer can be eliminated from the polyplexes by filtration or by drop-wise addition of the polymer to DNA solution such that all the polymer molecules are bound to a DNA molecule.

Determining the optimal polyplex weight ratio and DNA dose

Establishing a clear basic requirement for maximum transfection efficiency such as the polyplex weight ratio and DNA dose per a certain number of cells is important and has to be carried out for each cell type as both parameters change accordingly [25]. Other controllable influences on the outcome of transfection should be taken into account and they include; polyplex incubation period with cells, pH of the media, condition of the cells and level of confluency.

Understanding and overcoming the physiological environment of the cells

Different cell types require different culture conditions. Primary human keratinocytes, for example require specific supplements such as epidermal growth factor (EGF), insulin and cholera toxin for optimal growth and proliferation. On the other hand, primary fibroblasts can be grown in bovine serum which contains proteins that might interfere with the polyplexes [26]. Thus, a gene delivery system should have a strategy that prevents unfavorable protein interaction.

5.4.3. Genetically modified stem cell therapy for RDEB

A hugely attractive feature of stem cells is their capability to seemingly divide indefinitely and enabling to generate a wide range of cell types from the originating organ or even regenerate the entire organ [27-29]. Correcting stem cells means that the entire cell's progeny will carry the correct genetic sequence. Both keratinocytes and fibroblasts have the capability of secreting collagen type VII (C7) and both cell types can be used to restore the mechanical

stability of the skin in RDEB patients. However, considering the rapid turnover of the skin, genetically modified fibroblasts and keratinocytes are quickly lost. The ideal therapy would be to target the epidermal stem cells to have a long lasting and sustained therapeutic effect. Although allogeneic bone marrow stem cells have been used to ameliorate the manifestations of RDEB in mice and humans [2, 30], other more convenient stem cells sources are currently being examined. The known stem cells that have the potential to be used in autologous cell therapy for RDEB are listed in Table 5.1. Epidermal stem cells localized to the basal layer of the epidermis or the ones residing in the bulge area of the hair follicle are some of the more ideal cells that can be used for such application.

5.4.4. A thorough approach for analyzing C7 expression *in vivo*

Cell and tissue laboratory analysis techniques are constantly being used in clinical and pre-clinical settings to understand diseases and find the effect of new therapies on the micro and cellular biology of the mammalian tissues and organs. It is vital that these techniques are used in the appropriate setting to reach a conclusive result about the test. In testing the appropriate therapy method for RDEB, one must examine the expression patterns of the therapeutic gene (COL7A1) using comprehensive methods such as immunofluorescence staining; quantitative real-time PCR, transmission electron microscopy and mechanical testing of the skin after treatment. Combining all the mentioned methods will provide a clear insight into C7 expression levels, migration of C7 into the basement membrane zone (BMZ), formation of anchoring fibrils and structural stability of the skin.

In Chapter 4 of this thesis, we discussed the C7 expression patterns in the treated mouse tissue after immunofluorescence staining with antibodies specific for mouse or human C7 (Figure 5.6). The stained tissues showed clear presence of C7 in the injected area and BMZ. However, it was not possible to learn whether the protein subsequently formed functional anchoring fibrils and if it had restored the mechanical stability of the treated section of the skin. These

questions can only be answered after thorough analysis of the tissue using TEM and mechanical stress testing. These answers will provide a comprehensive conclusion about the feasibility of using polymer gene therapy for RDEB.
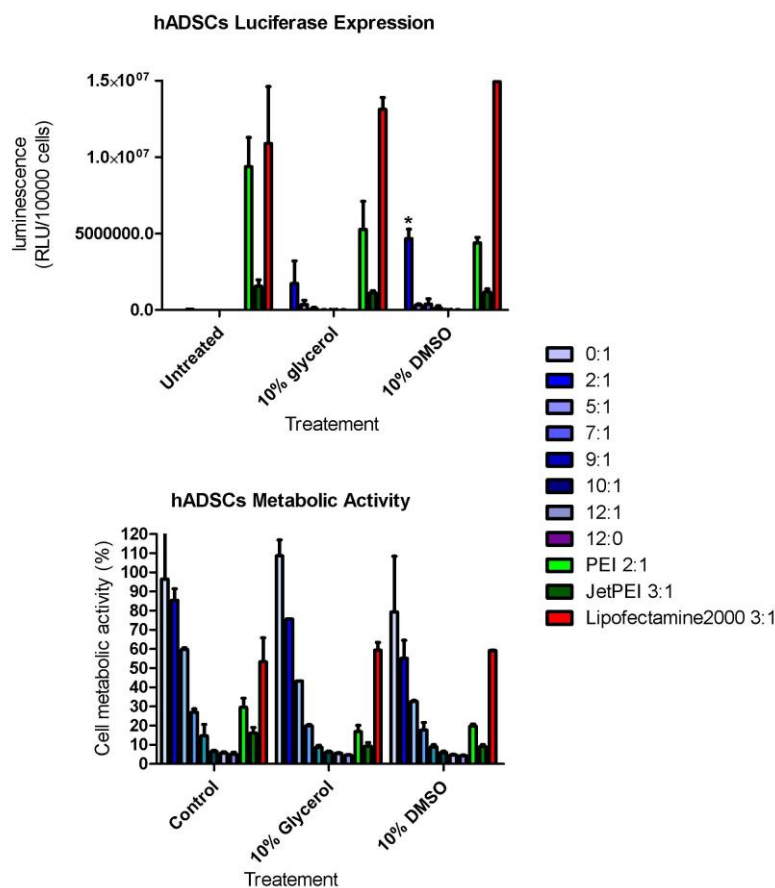
Figure 5.2: Luciferase expression levels and cell viability in human adipose derived stem cells (hADSCs) transfected with various ratios of multi-knot polymer compared to PEI, JetPEI® and Lipofectamine®2000. Results are expressed as mean ± S.D. (n=3, p<0.05). One way ANOVA (Fisher) was used for statistical analysis.
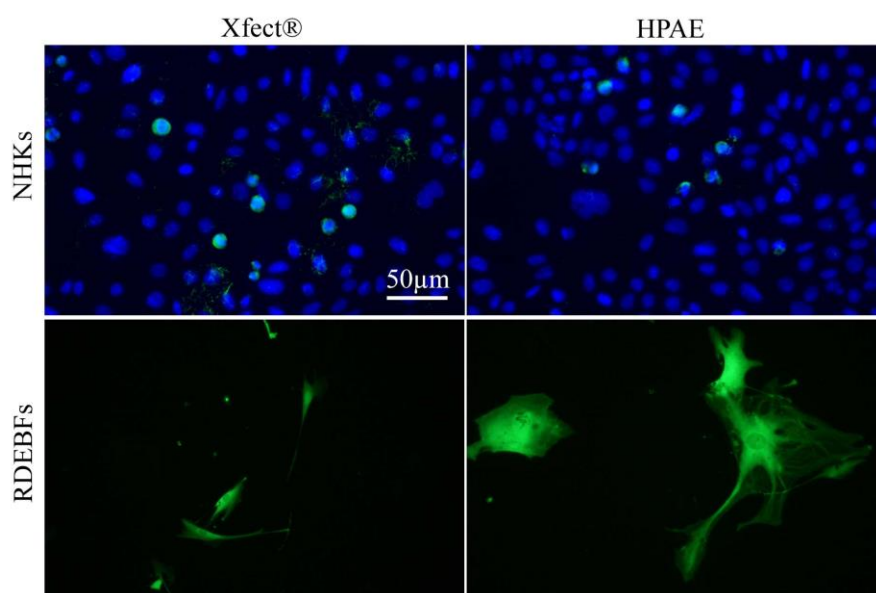
Figure 5.3: GFP expression in normal human keratinocytes (NHKs) and RDEB human fibroblasts (RDEBFs) transfected with either Xfect® or hyperbranched poly (β-amino esters).
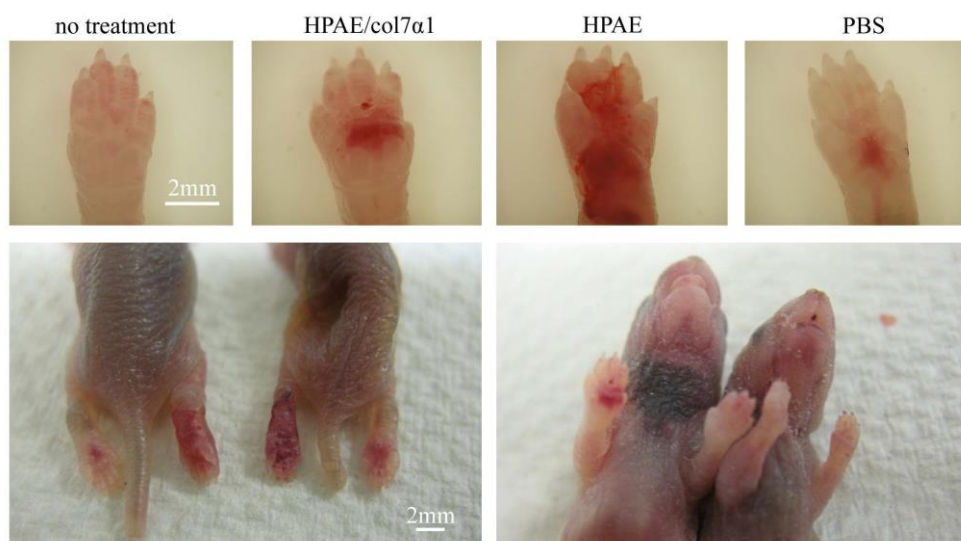
Figure 5.4: Images of RDEB mouse paws after intradermal injections. The bruises formed by the hypodermic needle injection were damaging to the immunostaining and immunohistochemistry analysis.
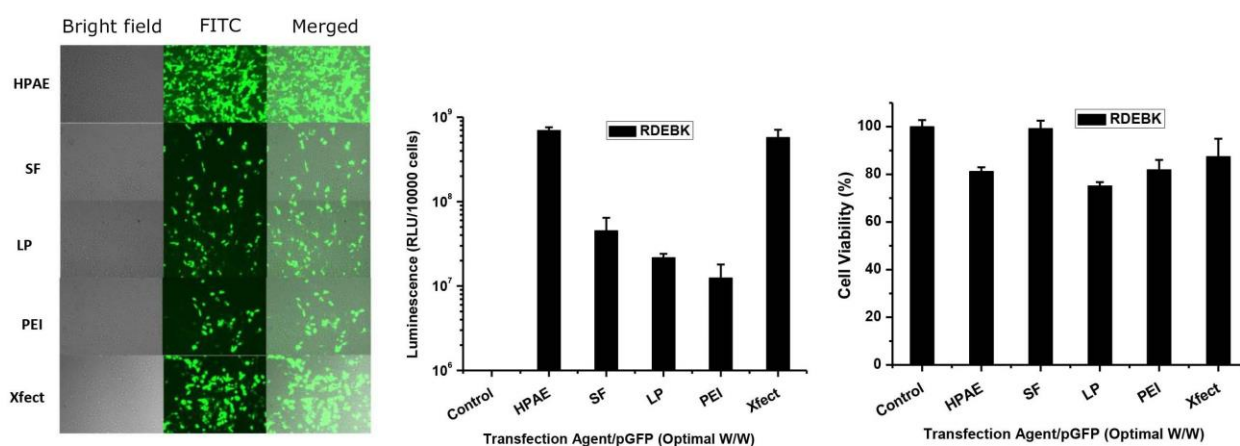
Figure 5.5: Transfection efficiency of the hyperbranched PAE compared to commercial vectors SuperFect (SF), Lipofectamine®2000 (LP), PEI and the linear PAE (Xfect®) in RDEB keratinocyte cell lines. Results are expressed as mean ± S.D. (n=3). One way ANOVA was used for statistical analysis. Images were taken at 20x magnification.
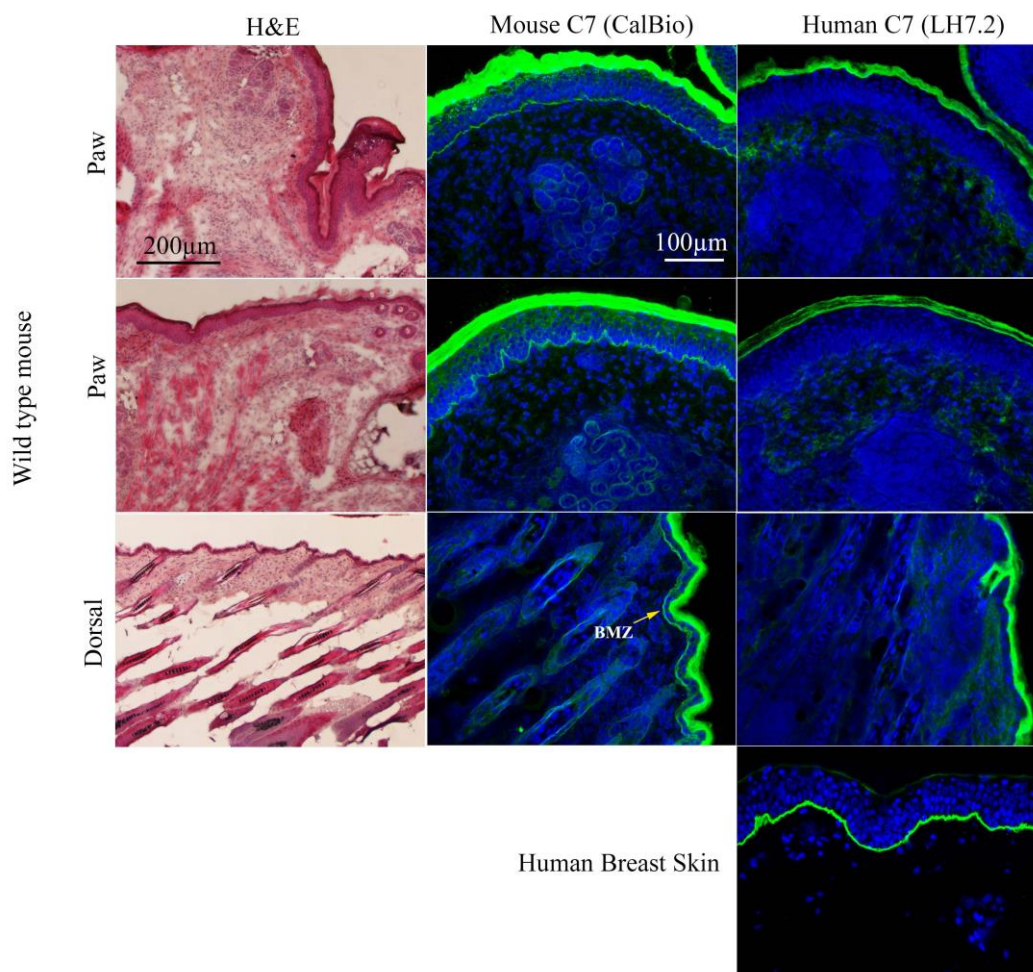
Figure 5.6: Hematoxylin and Eosin stained sections from wild type mouse tissue (left) and immunofluorescence staining of the same with an additional human breast skin tissue stained with an antibody specific for human C7 (LH7.2, Sigma) (right). This method segregates between the human transgene product and the wild type mouse protein. Images were taken at 10x and 20x magnification.

Table 5.1: Possible sources of stem cells that can be genetically modified and used for autologous cell therapy.

Stem cell sub-class	Name or Source	Classification	Reference
	Interfollicular	Somatic adult stem cell	[31]
Epidermal stem cells	Bulge area	Somatic adult stem cell	[32]
	Isthmus	Somatic adult stem cell	[33]
	Hair follicle dermal sheath	Somatic adult stem cell	[34]
Dermal stem cells	Skin-derived precursors: hair follicle dermal papillae	Somatic adult stem cell	[35]
	Dermal mesenchymal	Somatic adult stem cell	[36]
	Bone marrow-derived	Somatic adult stem cell	[37]
Mesenchymal stem cells	Adipose tissue-derived	Somatic adult stem cell	[38]
	Umbilical cord-derived	Somatic adult stem cell	[39]
Hematopoietic stem cells	Bone marrow-derived	Somatic adult stem cell	[40]
	Umbilical cord blood-derived	Somatic adult stem cell	[41]
	Human embryo	Human embryonic stem cells	[42]
Pluripotent stem cells	Induced pluripotent	Terminally differentiated human cells	[43]

5.5.   Conclusions

The ultimate goal of the project is to develop a safe and efficient polymer based gene delivery method to encourage the production of functional collagen type VII protein in RDEB skin using a polymer gene delivery vector.

The conclusions of this project can be summarized to the following:

Phase I: Synthesis and optimization of a cationic polymer for the purpose of gene delivery (Chapter 2)

1. A multi-knot polymer with high charge density composed of amine and disulfide monomers was successfully synthesized from DE-ATRP.

2. The polymer was able to bind to DNA efficiently forming nanoscale polyplexes.

3. The polymer degrades within minutes under physiological environment. This is a result of the incorporation of the bio-reducible disulfide links into the polymer's structure.

Phase II: Polymer transfection efficiency analysis *in vitro* (Chapter 3)

1. The optimal polymer/DNA ratio was found to be between 3 and 5 at which no cytotoxicity was observed.

2. Protein expression levels increased well above the levels observed using commercial agents when 4-fold DNA dose is used.

3. Protein expression levels rose significantly when the cells were permeablized with Dimethyl Sulfoxide.

Phase III: *Ex vivo* and *in vivo* analysis of the polymer gene delivery efficacy in RDEB skin (Chapter 4)

1. Collagen type VII expression in RDEB keratinocyte cell lines was restored using the multi-knot polymer

2. Partial restoration of C7 expression was achieved in skin equivalents made of human RDEB keratinocytes and fibroblasts.

184

3. Only the hyperbranched poly (β-amino ester) was used successfully to restore C7 expression in the BMZ of RDEB (Col7α1-/-) mouse after intradermal injection into the paws and ventral region.

5.6.   References

1.   Sakai, L.Y., D.R. Keene, N.P. Morris, and R.E. Burgeson, Type-Vii Collagen Is a Major Structural Component of Anchoring Fibrils. *J Cell Biol*, 1986. 103: p. 1577.

2.   Wagner, J.E., A. Ishida-Yamamoto, J.A. McGrath, M. Hordinsky, D.R. Keene, D.T. Woodley, M. Chen, M.J. Riddle, M.J. Osborn, T. Lund, M. Dolan, B.R. Blazar, and J. Tolar, Bone marrow transplantation for recessive dystrophic epidermolysis bullosa. *N Engl J Med*, 2010. 363: p. 629.

3.   Venugopal, S.S., W. Yan, J.W. Frew, H.I. Cohn, L.M. Rhodes, K. Tran, W. Melbourne, J.A. Nelson, M. Sturm, J. Fogarty, M.P. Marinkovich, S. Igawa, A. Ishida-Yamamoto, and D.F. Murrell, A phase II randomized vehicle-controlled trial of intradermal allogeneic fibroblasts for recessive dystrophic epidermolysis bullosa. *J Am Acad Dermatol*, 2013. 69: p. 898.

4.   Remington, J., X. Wang, Y. Hou, H. Zhou, J. Burnett, T. Muirhead, J. Uitto, D.R. Keene, D.T. Woodley, and M. Chen, Injection of recombinant human type VII collagen corrects the disease phenotype in a murine model of dystrophic epidermolysis bullosa. *Mol Ther*, 2009. 17: p. 26.

5.   Titeux, M., V. Pendaries, M.A. Zanta-Boussif, A. Decha, N. Pironon, L. Tonasso, J.E. Mejia, A. Brice, O. Danos, and A. Hovnanian, SIN retroviral vectors expressing COL7A1 under human promoters for ex vivo gene therapy of recessive dystrophic epidermolysis bullosa. *Mol Ther*, 2010. 18: p. 1509.

6.   Mecklenbeck, S., S.H. Compton, J.E. Mejia, R. Cervini, A. Hovnanian, L. Bruckner-Tuderman, and Y. Barrandon, A microinjected COL7A1-PAC vector restores synthesis of intact procollagen VII in a dystrophic epidermolysis bullosa keratinocyte cell line. *Hum Gene Ther*, 2002. 13: p. 1655.

7.   Ortiz-Urda, S., B. Thyagarajan, D.R. Keene, Q. Lin, M. Fang, M.P. Calos, and P.A. Khavari, Stable nonviral genetic correction of inherited human skin disease. *Nat Med*, 2002. 8: p. 1166.

8.   Putnam, D., Polymers for gene delivery across length scales. *Nat Mater*, 2006. 5: p. 439.

9.   Rezvani Amin, Z., M. Rahimizadeh, H. Eshghi, A. Dehshahri, and M. Ramezani, The effect of cationic charge density change on transfection efficiency of polyethylenimine. *Iran J Basic Med Sci*, 2013. 16: p. 150.

10.   Yan, Y., A.P. Johnston, S.J. Dodds, M.M. Kamphuis, C. Ferguson, R.G. Parton, E.C. Nice, J.K. Heath, and F. Caruso, Uptake and intracellular fate of disulfide-bonded polymer hydrogel capsules for Doxorubicin delivery to colorectal cancer cells. *ACS Nano*, 2010. 4: p. 2928.

11.   Zheng, Y., H. Cao, B. Newland, Y. Dong, A. Pandit, and W. Wang, 3D single cyclized polymer chain structure from controlled polymerization of multi-vinyl monomers: beyond Flory-Stockmayer theory. *J Am Chem Soc*, 2011. 133: p. 13130.

12.   Kim, T.I. and S.W. Kim, Bioreducible polymers for gene delivery. *React Funct Polym*, 2011. 71: p. 344.

13.   Ryu, K. and T.I. Kim, Therapeutic gene delivery using bioreducible polymers. *Arch Pharm Res*, 2014. 37: p. 31.

14.   Wen, H.Y., H.Q. Dong, W.J. Xie, Y.Y. Li, K. Wang, G.M. Pauletti, and D.L. Shi, Rapidly disassembling nanomicelles with disulfide-linked PEG shells for glutathione-mediated intracellular drug delivery. *Chem Commun (Camb)*, 2011. 47: p. 3550.

15.   Tai, H., W. Wang, T. Vermonden, F. Heath, W.E. Hennink, C. Alexander, K.M. Shakesheff, and S.M. Howdle, Thermoresponsive and photocrosslinkable PEGMEMA-PPGMA-EGDMA copolymers from a one-step ATRP synthesis. *Biomacromolecules*, 2009. 10: p. 822.

16.   Melkonyan, H., C. Sorg, and M. Klempt, Electroporation efficiency in mammalian cells is increased by dimethyl sulfoxide (DMSO). *Nucleic Acids Res*, 1996. 24: p. 4356.

17. Ryynanen, J., S. Sollberg, M.G. Parente, L.C. Chung, A.M. Christiano, and J. Uitto, Type VII collagen gene expression by cultured human cells and in fetal skin. Abundant mRNA and protein levels in epidermal keratinocytes. *J Clin Invest*, 1992. 89: p. 163.

18. Heinonen, S., M. Mannikko, J.F. Klement, D. Whitaker-Menezes, G.F. Murphy, and J. Uitto, Targeted inactivation of the type VII collagen gene (Col7a1) in mice results in severe blistering phenotype: a model for recessive dystrophic epidermolysis bullosa. *J Cell Sci*, 1999. 112 (Pt 21): p. 3641.

19. Green, J.J., R. Langer, and D.G. Anderson, A combinatorial polymer library approach yields insight into nonviral gene delivery. *Acc Chem Res*, 2008. 41: p. 749.

20. Anderson, D.G., W. Peng, A. Akinc, N. Hossain, A. Kohn, R. Padera, R. Langer, and J.A. Sawicki, A polymer library approach to suicide gene therapy for cancer. *Proc Natl Acad Sci U S A*, 2004. 101: p. 16028.

21. Pan, C., C. Kumar, S. Bohl, U. Klingmueller, and M. Mann, Comparative proteomic phenotyping of cell lines and primary cells to assess preservation of cell type-specific functions. *Mol Cell Proteomics*, 2009. 8: p. 443.

22. Gniadecki, R., Regulation of keratinocyte proliferation. *Gen Pharmacol*, 1998. 30: p. 619.

23. Massumi, M., E. Hoveizi, P. Baktash, A. Hooti, L. Ghazizadeh, S. Nadri, F. Pourasgari, A. Hajarizadeh, M. Soleimani, M. Nabiuni, and M.R. Khorramizadeh, Efficient programming of human eye conjunctiva-derived induced pluripotent stem (ECiPS) cells into definitive endoderm-like cells. *Exp Cell Res*, 2014.

24. Kwoh, D.Y., C.C. Coffin, C.P. Lollo, J. Jovenal, M.G. Banaszczyk, P. Mullen, A. Phillips, A. Amini, J. Fabrycki, R.M. Bartholomew, S.W. Brostoff, and D.J. Carlo, Stabilization of poly-L-lysine/DNA polyplexes for in vivo gene delivery to the liver. *Biochim Biophys Acta*, 1999. 1444: p. 171.

25.   Kim, T.K. and J.H. Eberwine, Mammalian cell transfection: the present and the future. *Anal Bioanal Chem*, 2010. 397: p. 3173.

26.   Cherng, J.Y., P. van de Wetering, H. Talsma, D.J. Crommelin, and W.E. Hennink, Effect of size and serum proteins on transfection efficiency of poly ((2-dimethylamino)ethyl methacrylate)-plasmid nanoparticles. *Pharm Res*, 1996. 13: p. 1038.

27.   Leong, K.G., B.E. Wang, L. Johnson, and W.Q. Gao, Generation of a prostate from a single adult stem cell. *Nature*, 2008. 456: p. 804.

28.   Takebe, T., N. Koike, K. Sekine, M. Enomura, Y. Chiba, Y. Ueno, Y.W. Zheng, and H. Taniguchi, Generation of functional human vascular network. *Transplant Proc*, 2012. 44: p. 1130.

29.   Badylak, S.F., D. Taylor, and K. Uygun, Whole-organ tissue engineering: decellularization and recellularization of three-dimensional matrix scaffolds. *Annu Rev Biomed Eng*, 2011. 13: p. 27.

30.   Tolar, J., A. Ishida-Yamamoto, M. Riddle, R.T. McElmurry, M. Osborn, L. Xia, T. Lund, C. Slattery, J. Uitto, A.M. Christiano, J.E. Wagner, and B.R. Blazar, Amelioration of epidermolysis bullosa by transfer of wild-type bone marrow cells. *Blood*, 2009. 113: p. 1167.

31.   Li, A., P.J. Simmons, and P. Kaur, Identification and isolation of candidate human keratinocyte stem cells based on cell surface phenotype. *Proc Natl Acad Sci U S A*, 1998. 95: p. 3902.

32.   Cotsarelis, G., Epithelial stem cells: a folliculocentric view. *J Invest Dermatol*, 2006. 126: p. 1459.

33.   Jensen, U.B., X. Yan, C. Triel, S.H. Woo, R. Christensen, and D.M. Owens, A distinct population of clonogenic and multipotent murine follicular keratinocytes residing in the upper isthmus. *J Cell Sci*, 2008. 121: p. 609.

34.   Gharzi, A., A.J. Reynolds, and C.A. Jahoda, Plasticity of hair follicle dermal cells in wound healing and induction. *Exp Dermatol*, 2003. 12: p. 126.

35.   Biernaskie, J., M. Paris, O. Morozova, B.M. Fagan, M. Marra, L. Pevny,

and F.D. Miller, SKPs derive from hair follicle precursors and exhibit properties of adult dermal stem cells. *Cell Stem Cell*, 2009. 5: p. 610.

36.   Soma, T., J. Kishimoto, and D. Fisher, Isolation of mesenchymal stem cells from human dermis. *Methods Mol Biol*, 2013. 989: p. 265.

37.   Wu, Y., L. Chen, P.G. Scott, and E.E. Tredget, Mesenchymal stem cells enhance wound healing through differentiation and angiogenesis. *Stem Cells*, 2007. 25: p. 2648.

38.   Brzoska, M., H. Geiger, S. Gauer, and P. Baer, Epithelial differentiation of human adipose tissue-derived adult stem cells. *Biochem Biophys Res Commun*, 2005. 330: p. 142.

39.   Lee, O.K., T.K. Kuo, W.M. Chen, K.D. Lee, S.L. Hsieh, and T.H. Chen, Isolation of multipotent mesenchymal stem cells from umbilical cord blood. *Blood*, 2004. 103: p. 1669.

40.   Wilson, A. and A. Trumpp, Bone-marrow haematopoietic-stem-cell niches. *Nat Rev Immunol*, 2006. 6: p. 93.

41.   Liu, S.S., C. Zhang, X. Zhang, and X.H. Chen, Human umbilical cord blood-derived stromal cells: A new source of stromal cells in hematopoietic stem cell transplantation. *Crit Rev Oncol Hematol*, 2013.

42.   Park, S.J., S.H. Moon, H.J. Lee, J.J. Lim, J.M. Kim, J. Seo, J.W. Yoo, O.J. Kim, S.W. Kang, and H.M. Chung, A comparison of human cord blood- and embryonic stem cell-derived endothelial progenitor cells in the treatment of chronic wounds. *Biomaterials*, 2013. 34: p. 995.

43.   Tolar, J., L. Xia, M.J. Riddle, C.J. Lees, C.R. Eide, R.T. McElmurry, M. Titeux, M.J. Osborn, T.C. Lund, A. Hovnanian, J.E. Wagner, and B.R. Blazar, Induced pluripotent stem cells from individuals with recessive dystrophic epidermolysis bullosa. *J Invest Dermatol*, 2011. 131: p. 848.

APPENDICES

A. Gel permeation chromatography

1. While bubbling under argon, draw out 100μl from polymer solution during or after polymer reaction using a glass syringe.

2. Dilute the sample in 2 ml dimethylformamide (DMF)

3. Pass the diluted sample through aluminum oxide and cotton wool to remove the copper

4. Filter the solution through 0.2μm filter to remove aluminum oxide

5. Run GPC for 25 minutes using DMF with 0.1% Lithium Bromide of final volume.

B. Proton nuclear magnetic resonance

1. Polymer is resuspended in Deuterium Oxide (or other hydrogen free solvent) to a final concentration of 5mg/ml

2. This solution is then pipetted into special ^{1}H NMR tubes

3. The ^{1}H NMR spectrum is analysed using the DELTA processing software

C. Zetasizer

1. Weigh out 2mg of the polymer and resuspend in distilled water to make 2mg/ml stock solution

2. Make up 0.1mg/ml of DNA (GFP or G-luciferase) stock solution

3. Make up the following polymer to DNA ratios:
   1:1, 2:1, 5:1, 10:1, 15:1, 20:1, 40:1, 100:1

4. Mix 0.1mg of gaussia luciferase in water with 0.1mg of polymer in water to get a ratio of 1:1

5. A minimum of 1ml is required to fill a standard potential or size measurement tube

6. Measure using Zetasizer Nano-ZS90

D. Transmission electron microscopy

1. From the polymer and DNA stock solutions mix 0.5μg of DNA with 0.5μg polymer in distill water to get 1:1 ratio.

2. Make up different ratios (refer to zetasizer protocol)

3. Pipette 10μl of polyplexes onto graphene grids and let it dry

4. Visualize the polyplexes using Hitachi H-7500 TEM and 80kV accelerating voltage

E. PicoGreen® assay

Preparation:

1. On the day of the experiment, prepare an aqueous working solution of the Quant-iTTM PicoGreen® reagent by making a 200-fold dilution of the concentrated DMSO solution in TE. For example, to prepare enough working solution to assay 20 samples in a 2 mL final volume, add 100 μL Quant-iTTM PicoGreen® dsDNA reagent to 19.9 mL TE. Protect the working solution from light by covering it with foil or placing it in the dark, as the Quant-iTTM PicoGreen® reagent is susceptible to photodegradation.

DNA Standard Curve:

- For the high-range standard curve, dilute the 2 μg/mL DNA stock solution into disposable cuvettes (or plastic test tubes for transfer to quartz cuvettes) as shown in Table 1. Then add 1.0 mL of the aqueous working solution of Quant-iTTM PicoGreen® reagent to each cuvette. Mix well and incubate for 2 to 5 minutes at room temperature, protected from light.

Table 1: Preparing standard curve with DNA

Volume (µl) of TE	Volume (µl) of 2 µg/ml DNA stock	Volume (µl) of diluted PicoGreen® Reagent	Final DNA concentration in PicoGreen ® Assay
0	1000	1000	1 µg/ml
900	100	1000	100 ng/ml
990	10	1000	10 ng/ml
999	1	1000	1 ng/ml
1000	0	1000	blank

Polyplex measurement:

1. Prepare polyplex samples using 0.5μg DNA and 1, 5, 7.5, or 15 μg of polymer

2. Optimal ratios are used for lipofectamine^{TM}2000 (3:1), and PEI (2:1).

3. Dilute the polyplexes in TE buffer (provided with kit) to obtain a DNA final concentration of 0.001μg/μl.

4. Add equal-volume of the aqueous working solution of Quant-iTTM PicoGreen® reagent.

5. Mix well and incubate for 2 to 5 minutes at room temperature, protected from light.

6. After incubation, measure the sample fluorescence using a spectrofluorometer or fluores- cence microplate reader and standard fluorescein wavelengths (excitation ~480 nm, emission ~520 nm).

F. NanoDrop®

1. Weigh out 0.5mg of the polymer and resuspend in 0.5ml of DNAse/RNAse free water

2. Mix 0.5μg DNA and polymer at different ratios in DNAse/RNAse free water

3. Vortex and pipette 10μl of the polyplex solution onto the NanoDrop detector and measure absorbance.

G. Agarose Gel Electrophoresis

Materials needed: Agarose

TAE Buffer

6X Sample Loading Buffer

DNA ladder standard

Electrophoresis chamber

Power supply

Gel casting tray and combs

DNA stain

TAE Buffer: 4.84 g Tris Base

1.14 ml Glacial Acetic Acid

2 ml 0.5M EDTA (pH 8.0)

Bring the total volume up to 1L with water

Add Tris base to ~900 ml H_2O. Add acetic acid and EDTA to solution and mix. Pour mixture into 1 L graduated cylinder and add H_2O to a total volume of 1 L.

6X Sample Loading Buffer:

> 1 ml sterile H_2O
>
> 1 ml Glycerol

enough bromophenol blue to make the buffer deep blue (~ 0.05 mg)

SYBR®Safe DNA gel stain

Preparing the agarose gel:

1. Measure 0.7 g Agarose powder and add it to a 100 ml TAE Buffer
2. Melt the agarose in a microwave or hot water bath until the solution becomes clear. Usually 2 minutes in microwave.
3. Let the solution cool to about 50-55°C, swirling the flask occasionally to cool evenly.
4. Add 10μl of SYBR®Safe DNA stain when solution has cooled to ~ 40°C
5. Place the combs in the gel casting tray.
6. Pour the melted agarose solution into the casting tray and let cool until it is solid (appear as milky white solution).
7. Place the gel in the electrophoresis chamber.
8. Add TAE Buffer so that there is about 2-3 mm of buffer over the gel.

Loading and running the gel

1. Add 6 μl of 6X Sample Loading Buffer to each 25 μl sample
2. Record the order each sample will be loaded on the gel, controls and ladder.
3. Carefully pipette 20 μl of each sample/Sample Loading Buffer mixture into separate wells in the gel.
4. Pipette 10 μl of the DNA ladder standard into at least one well
5. Connect the positive electrode to the positive inlet (red) and negative electrode to the negative inlet (black).
6. Run the gel at 80V for 30-45 minutes depending the size of the DNA
7. Bubbles should be seen rising from both sides of the chamber indicating that the setup is working.
8. The bands should be visible and checked every 10 minutes.
9. Visualize the bands under short wave bypass on G-Box.

H. Cell splitting

1. Pre-warm trypsin to 37°C in water bath

2. Sterilize all equipment, flasks, pipettes and falcon tubes before placing them in the culture hood

3. Remove culture media and wash cells once with Hanks buffer

4. Add 6 ml of pre-warmed trypsin to the flask and incubate for 2 minutes
   Note: incubation time is cell type dependent.

I. Cell freezing and thawing

1. Pre-warm growth media in 37°C water bath

2. Thaw frozen cells in water bath until only 3/4th of the cells are in solution

3. Quickly spry with 70% IMS and place in culture hood

4. After the solution is completely thawed, pipette the complete cell suspension into a 15ml tube

5. Slowly add the pre-warmed media into the 15ml tube and centrifuge at 1200rpm for 5 minutes.

6. Discard

J. Transfection of cultured cells: (6-well plate)

Cells should be transfected when they are 60-80% confluent

1. Prepare 1 μg/μl of polymer stock solution in distilled water
   Note: When using commercial transfection agents follow protocol provided by manufacturer

2. Prepare 0.1 μg/μl of DNA in DNAse/RNAse free water.

3. Mix 40 μl of DNA with 40 μl of Polymer to obtain 10:1 ratio polymer:DNA
   For higher ratios use more polymers.

4. Vortex the solution and incubate at RT for 45-60 minutes.

5. Dilute the mixture by adding 420 μl DMEM containing 1% antibiotics (penicillin/streptomycin).

6. Remove cell media from wells and wash once with Hanks buffer

7. Add the diluted polyplex solution to the cells and incubate at 37°C, 5% CO_2 for 4 hours.

8. After the incubation period. Remove the polyplex solution from the cells and wash cells and add pre-warmed serum/growth medium.

   For DMSO shock, add 10% filtered DMSO to cells for 2-3 minutes and wash with Hanks before adding growth medium.

9. Incubate the cells for 48 hours and measure protein expression

K. AlamarBlue® protocol for cell viability: (6-well plate)

1. Prepare alamarBlue® working solution by adding 800 µl of the alamarBlue® to 10 ml of Hanks buffer.

2. Remove growth media from the cells and wash once with Hanks buffer

3. Add 1 ml of alamarBlue® working solution to each well and incubate at culture conditions for 1-4 hours.

4. Pipette out 100 µl of the solution into a clear 96-well plate after the time has elapsed.

5. Measure absorbance at ex: 550nm and em: 595nm

6. Subtract the absorbance values of Hank's balanced salt solution only from the absorbance values of the alamarBlue® in Hank's balanced salt solution (ratio 1:9).

   Refer to Alamar Blue® guidelines for instructions on calculating reduction values.

L. RDEB Keratinocytes (RDEBK) source and culture

1. Skin punch-biopsies from patients with RDEB

2. SV40 immortalized passage 4 (called LCT on frozen vial, 3 frozen vials left labeled: RDEBK Ahmed, one A and two C, Rack 4 Box 5)

3. Mutation: homozygous 6527ins, TAA stop 337bp downstream (2176) in axon 80

M. Green media preparation for NHKs, RDEB keratinocytes and skin equivalents

   Different amounts used depending on requirement

Table 2: Solutions required for Green media

DMEM (ml)	60	120	180	240	300
Ham F-12	30	60	90	120	150
FCII	10	20	30	40	50
L-Glutamine 4mM final	2	4	6	8	10
Na Pyruvate 1mM final	1	2	3	4	5
Vol. final	100	200	300	400	500

Add the following:

Adenine: Solution 500X (70.8 mM)

1. Resuspend 191 mg of Adenine in 20 ml of sterile H_2O (pre-warmed to 60°)

2. Add drop by drop 14 µl of 32% HCl

3. Filter sterilize through 0.22µm

4. Aliquote 1ml in cryovials (white)

5. Write 500X onto the cap

6. Store at −20°C (3 month)

Insulin: Solution 1000X (5 mg/ml) same for RM Medium

1. Prepare 0.05N HCl in 1X sterile PBS

2. Resuspend the lyophilized powder in 20ml of 0.05N HCl (c= 5mg/ml)

3. Filter sterilize through 0.22µm

4. Aliquote 1ml in cryovials (green)

5. Store at −20°C (1 month maximum)

Hydrocortisone: Solution 500X (0.2 mg/ml) for RM: 4 mg/ml

1. Prepare stock solution

2. Add 10ml 95% ethanol to the tube (5mg/ml)

3. Write the date onto the tube

4. Aliquote 1ml in cryovials (blue)

5. Store at 4°C for 1 year

   Prepare aliquots ready to use (500X)

6. Add 24ml of DMEM to 1ml stock solution (0.2mg/ml)

7. Filter sterilize through 0.22µm

8. Write 500X onto the cap

9. Aliquote 1ml in cryovials (blue)

10. Store at −20°C (3 month)

Cholera Toxine: Solution 1000X (47 µg/ml)

1. Prepare stock solution

2. Resuspend the lyophilized powder in 11.8ml of sterile ddH_2O

   (Dilute the powder first in 5ml and transfer into a 15ml tube, then rinse the

   tube with 6,8 ml H_2O)

3. Filter sterilize through 0.22µm

4. Aliquote 2ml in cryovials (pink)

5. Store at 4°C for 1 year

Prepare aliquots ready to use (1000X)

6. Add 18ml of DMEM to 2ml stock solution

7. Filter sterilize through 0.22μm

8. Aliquote 1ml in cryovials (pink)

9. Store at –20°C (1 year)

Triodothyronine: Solution 1000X (1.37 ng/ml)

1. Prepare stock solution (20μg/ml)

2. Resuspend 1mg T3 with DMEM basic (1ml 0.001N NaOH+49ml DMEM)

3. Aliquot 2.5ml stocks (yellow)

4. Store at –20°C (1 year)

   Prepare aliquots ready to use (1000X)

5. Dilute 2.5ml stock solution in 34ml DMEM (total volume: 36.5ml)

6. Filter sterilize through 0.22μm

7. Aliquote 1ml in cryovials (yellow)

EGF: Solution 1000X (10μg/ml) same for RM Medium

1. Prepare a stock solution of 1mg/ml by adding 100 μl of 10 mM HCl to the vial

   a. (Stock solution can be stored for at least 3 month at –20°C or –70°C

   b. Avoid repeated freeze-thaw cycles.)

2. Resuspend 100 μl of EGF stock solution in 10 ml 10mM HCl

   a. (Final concentration of stock is 10μg/ml = 1000X)

3. Filter sterilize through 0.22μm

4. Aliquote 1ml in cryovials

5. Store at –20°C

N. PromoCell media for high passage cell lines

Keratinocyte growth medium 2: Add the following into pre-warmed kerationcyte
basal medium

Table 3: PromoCell supplement mix

Bovine Pituitary Extract	0.004 ml / ml
Epidermal Growth Factor (recombinant human)	0.125 ng / ml
Insulin (recombinant human)	5 μg / ml
Hydrocortisone	0.33 μg / ml
Epinephrine	0.39 μg / ml
Transferrin, holo (human)	10 μg / ml
$CaCl_2$	0.06 mM

O. Skin equivalents perpetration and culture

Material:

- Fibrinogen

- Thrombine

- CaCl$_2$ 25 mM, sterile

- NaCl 0.9 %, sterile

- Trasylol (Aprotinin)

- 12-well plates

- BioCoat 6 well deep well plate (BD Cat.No: 355467)

- Cell Culture Inserts, 3 μm pore size, PET-track-etched membrane, 6 well formats.

Preparation:

Fibrinogen

1. Thaw the vial at RT

2. Put 20 ml NaCl 0.9 % into the vial (15 ml + 5 ml): final concentration: 25 mg/ml

3. Incubate at 37°C for 1h without agitation

4. Filter through 0.22 μm

5. Aliquote 0.5 ml (15 ml Greiner)

6. Store at –20°C

Thrombine

1. Put 1ml CaCl$_2$ 25 mM

2. Filter through 0.22 μl

3. Aliquote in 1.5 ml tubes 120 μl

4. Store at –20°C

Table 4: Special media components

DMEM (HyClone)	130 ml
Ham F-12 (HyClone)	60 ml
FCII (HyClone)	1 ml
10% BSA in PBS	3.2 ml
Glutamine stock: 200mM	4 ml
NaPyruvate stock: 100mM	1.3 ml
Hydrocortisone stock 500x	400 µl
Insulin stock 1000x	200 µl
Vitamin C stock 1000x	200 µl

Preparation of Dermis:

In a 15 ml tube, add:

1. 500 µl Fibrinogen

2. 1 ml Fibroblasts in DMEM (38,000 c/ml)

3. 100 µl trasylol

4. 100 µl thrombine

5. Mix gently by pipetting up and down, avoiding bubble formation

6. Put it to the bottom of the well without bubble formation

7. Let it polymerize for 1h at 37°C (incubator)

8. If the keratinocytes are not seeded 1h later, cover the matrix with Green-medium

Seeding of keratinocytes:

1. Seed 60,000 cells onto the dermal matrix (in 1 ml Green - EGF)

2. Change medium 48 h later into Green + EGF and let the cells grow to confluence (~6-7 days) (all green+EGF was used all the time or with only DMEM 1%PS).

Lifting to the air-liquid interface:

At confluence lift the SE to the air-liquid interface. Detach the skin equivalents using forceps and place it onto an insert in a deep-well plate with keratinocytes on the top. Put Green+ medium incl. P/S into the bottom of the well covering the filter but not the skin (~8-10 ml). Change the medium every other day.

After one week use special medium and change it every other day. Add 1x Vitamin C separately every day.

P. RNA extraction and preparation for PCR

Extraction of total RNA from skin equivalents

1. Cut skin equivalents into 30mg sections by weighing them in RNase/DNase free conditions and store in RNA*later*® stabilisation reagent.

2. Wash tissue by the medium Hanks' balanced salt solution before the next step.

3. Homogenization of tissue by 1 mL Trizol onto the scaffold by a TissueLyser LT (Qiagen).

4. Store homogenate for 5 minutes at RT (complete dissociation of nucleoprotein complexes).

Phase separation

1. Add 0.2 ml of Chloroform per 1 ml of Trizol

2. Shake vigorously for 15 seconds by inversion

3. Incubate for 15 minutes at RT

4. Centrifuge at 12 000 g max (tr/min) for 15 minutes at 4°C

5. Following the centrifugation, 3 phases:

    - a lower red phenol-chloroform phase

    - an interphase

    - an aqueous phase (translucent)

6. Remove clear upper aqueous phase (~ 650µl) and add in a fresh tube

7. Slowly add 1 volume (Equal vol) of 70% ethanol (in 3 equal aliquots) mixing by inversion.

8. Apply 700µl sample from 3. to RNeasy column, centrifuge for 15s at 8 000g and discard flow-through. Repeat for remaining sample.

9. Add 350 µl of RW1 buffer to centre of column, centrifuge for 15s at 8 000g, discard flow-through.

10. Add 10µl DNase stock solution to 70 µl Buffer RDD and add the DNase incubation mix directly onto the RNeasy column. Incubate at RT for 15 min (for genomic)

11. Add 350 µl of RW1 buffer to centre of column, centrifuge for 15s at 8 000g, discard flow-through.

12. Transfer column to new 2ml collection tube. Add 500 µl RPE to centre of column, centrifuge for 15s at 8 000 g, discard flow-through.

13. Add 500 µl of RPE buffer to centre of column, centrifuge for 15s at 8 000g, discard flow-through, centrifuge for a further 2 minutes at 8 000g.

14. Transfer column to new 1.5 ml tube , add 30 µl RNase-free water onto the column, incubate at RT for 1 min, centrifuge for 1 minute at 8 000g.

15. Add a further 30 µl RNase-free water onto the column, incubate at RT for 1 min, centrifuge for 1 minute at 8 000g.

16. Take back the 30 µl of eluate and add again onto the column, incubate at RT for 1 min, centrifuge for 1 minute at 8 000g.

17. Split up in 3 the eluate

18. Determine the concentration at the nanodrop and freeze at -80°C.

RNA quantification and purity determination:

Quantification: Dilution of RNA 1/50 or 1/100 in water RNase Free. Measure the absorbance at 260 nm. *(Calibration of the spectrometer with water)*

1 unit of A_{260} = 40 µg/ml of RNA

Concentration of RNA sample = 40 * A260 * dilution factor = x µg/ml

Quantity of RNA = concentration * volume of sample in ml = x µg

Purity: Ratio between A260 and A280.

If the ratio A260/A280 is superior at 1, 8-1, 9 obtaining of a pure RNA (max of the ratio 2, 2).

The ratio of reading at A260/A280 provides an estimate of the purity of RNA with the respect to contaminants that absorb in the UV, such as protein. It's influenced by the pH. Since water is not buffered, the pH and the resulting A260/A280 ratio can vary greatly. But the extinction coefficient is calculated in water, so for the concentration it's better to calculate in water.

Agilent RNA 6000 Nano Assay Protocol – RNA purity measurement:

Preparing the Gel

1. Pipette 550 µl of RNA 6000 Nano gel matrix (red) into a spin filter.
2. Centrifuge at 1500 g ± 20 % for 10 minutes at room temperature.
3. Aliquot 65 µl filtered gel into 0.5 ml RNase-free microfuge tubes. Use filtered gel within 4 weeks.

Preparing the Gel-Dye Mix

1. Allow the RNA 6000 Nano dye concentrate (blue) to equilibrate to room temperature for 30 min.
2. Vortex RNA 6000 Nano dye concentrate (blue) for 10 seconds, spin down and add 1 µl of dye into a 65 µl aliquot of filtered gel.
3. Vortex solution well. Spin tube at 13000 g for 10 min at room temperature. Use prepared gel-dye mix within one day.

Loading the Gel-Dye Mix

1. Put a new RNA 6000 Nano chip on the chip priming station.
2. Pipette 9.0 µl of gel-dye mix in the well-marked G.
3. Make sure that the plunger is positioned at 1 ml and then close the chip priming station.
4. Press plunger until it is held by the clip.
5. Wait for exactly 30 seconds then release clip.

6. Wait for 5 s. slowly pull back plunger to 1ml position.

7. Open chip priming station and pipette 9.0 μl of gel-dye mix in the wells marked G.

8. Discard the remaining gel-dye mix.

Loading the Agilent RNA 6000 Nano Marker

1. Pipette 5 μl of RNA 6000 Nano marker (green) in all 12 sample wells and in the well-marked ladder.

Loading the Ladder and Samples

1. Pipette 1 μl of prepared ladder in well-marked.

2. Pipette 1 μl of sample in each of the 12 sample wells. Pipette 1 μl of RNA 6000 Nano Marker (green) in each unused sample well.

3. Put the chip horizontally in the adapter of the IKA vortexer and vortex for 1 min at 2400 rpm.

4. Run the chip in the Agilent 2100 bioanalyzer within 5 minutes.

Note: after total RNA extraction, samples can be directly used in a PCR reaction using the Verso one-step RT-PCR kit from thermo scientific

Q. Reverse transcription of extracted RNA sample

Note: Manipulation still in RNase free conditions

Gloves, Nuclease Free Water

Note: contaminations

Prepare RNA Target and Primers:

Use sterile, nuclease-free, tubes, pre-chilled on ice

1. For 20μl reverse transcription reaction:
   - RNA Template up to 1μg
   - Primers Oligo (dT)$_{15}$ Primer and Random primer 0.5μg (see the concentration)
   - Nuclease free water to a final volume of 5μl

2. Incubate at 70°C for 5 minutes (denature the target and the primers)

3. Quick-chill at 4°C for 5 minutes and hold on ice (or direct in the bath of ice)

(Let on ice during the preparation of reverse transcription mix)

Table 5: Reverse transcription components

Component	Volume per 1 RT (µl)	Final Concentration
Nuclease-free water	5,6	
ImProm-IITM 5X Reaction Buffer	4	1X
MgCl2, 25mM	2,4	3mM
dNTP mix (10mM each dNTP)	1	0.5mM
Recombinant RNasin Ribonuclease Inhibitor (20/40u per µl)	1	1u/µl
ImProm-IITM Reverse Transcriptase	1	
Final Volume RT Mix per 20µl reaction	15	

Prepare Reverse transcription Mix:

1. Begin with the biggest volume

2. Add the reverse transcriptase last

3. Keep mix and products and all manipulation products on ice before incubation

4. Vortex gently to mix

5. Dispense 15µl aliquots into reaction tubes

Add Template + primers to the reaction mix:

1. Add for each individual reaction 5 µl of the appropriate template + primers in the 15µl of reverse transcription mix.

2. Add the RNA template + primers mix immediately prior to incubation

Reverse transcription: Table below

Table 6: Reverse transcription program

Step	Temperature	Time
Annealing	25°C	5 minutes
Extension	42°C	60 minutes
Heat-inactivation Reverse transcriptase	70°C	15 minutes

After, analyse cDNA, proceed with PCR or store frozen.

R. Polymerase Chain Reaction

Reverse transcription was carried out using the GoTaq® qPCR Master Mix (Promega, UK) using the COL7A1 forward primer (5'-gagcctgtggccttgatgga-3') and the reverse primer (5'-gcacagcatggagctgggag-3') with GAPDH being the endogenous housekeeping control (forward: 5'-tgcaccaccaactgcttagc-3'; reverse: 5'-ggcatggactgtggtcatgag).

1. Thaw the PCR Master Mix at room temperature.
2. Vortex the Master Mix and then spin it briefly in a micro centrifuge to collect the material in the bottom of the tube.
3. Prepare one of the following reaction mixes on ice

Table 7: Component and amount required for 25µl reaction

Component	*Volume*	*Final Conc.*
PCR Master Mix, 2X	12.5µl	1X
upstream primer, 10µM	0.25–2.5µl	0.1–1.0µM
downstream primer, 10µM	0.25–2.5µl	0.1–1.0µM
DNA template (or standards)	1–5µl	<250ng
Nuclease-Free Water	to 25µl	N.A.

S. Immunofluorescence staining of cells

Cells were cultured at 20000 cells/well in 4 well- chamber slides with 500µl of media per well:

DMEM 500ml

10% FBS 50ml (filtered, 0.20µm filter)

1% penicillin/Streptomycin (P/S) 5ml

Keratinocyte growth medium supplement (promoCell)

For transfection, the following were used: (in 200µl water and 400µl media)

COL7A1 (Plasmid)   8µg

Polymer   80µg

PEI   16µg

Superfect   80µg

Lipofectamine®2000   80µg

Normal Human keratinocytes (same growth media)

Untreated RDEB keratinocytes

Staining protocol:

1. Fix cells in 4% paraformaldhyde for 30 minutes at 25°C

2. Wash three times with PBS for 5min each

3. Permeablise cells with PBS 0.1% Triton-x 100 for 5 minutes at 25°C

4. Wash three times with PBS for 5 minutes each

5. Incubate with 50 mM NH_4Cl for 15 minutes at 25°C

6. Wash three times with PBS for 5min each

7. Block with 3% BSA PBS for 30 minutes at 25°C

8. Incubate with primary (monoclonal antibody LH7.2 mouse anti-human collagen VII) diluted in 3% BSA PBS (1:1000) overnight at 4˚C.

9. Wash 3 times with PBS for 5 minutes each

10. Incubate with:

Secondary AlexaFlour 488 Donkey anti-mouse   1.25µl

DAPI   5µl

Rhodamine-Philliodin/cellMask^{TM} 5µl

PBS   990µl

For 1-2 hrs at 25˚C

11. Wash 3 times with PBS for 5 minutes each

12. Add mounting medium to cover slide and visualise

T. Immunofluorescence staining of tissue sections

1. Leave slides to dry

2. Block in 1% BSA for 10 minutes at 42°C

3. Incubate with primary at RT for 1 hour (1:1000 in PBS)

4. Wash three times for 5 minutes with PBS

5. Incubate with secondary (1:200 in PBS) and add DAPI (1:1000 in PBS) or the last 2 minutes

6. Wash 2 times for 5 minutes with dH$_2$O

7. Air dry and add flouroSafe® mounting medium.

Primaries: C7: Sigma Lh7.2 anti-human produced in mouse

        C4: Millipore GT x anti-mouse produced in goat

Secondary: C7: Invitrogen molecular probes Alexafluor 488 goat anti-mouse

        C4: Invitrogen molecular probes alexafluor 594 donkey anti-goat

U. Western blot

Keratinocyte culture and transfection

Because Collagen VII is an extracellular protein, we used the serum free media of the cultured and transfected cells to test for the presence of the protein.

1. RDEB keratinocytes and normal human keratinocytes are cultured in T-25 flasks

2. Use a cell density of 800,000 cells per flask

3. Cells are transfected when they reach 60-80% confluency

4. Use polyplexes containing 20μg col7a1 DNA

   Weight ratios:

   DMD   10:1

   PEI   2:1

   Superfect   5:1

   Lipofectamine®2000 3:1

5. Make a 1mg/ml stock solution of ascorbic acid (AA) in water and filter the solution using a 0.2μm filter.

6. After transfection, add 500μl of the AA to 10ml of the free serum PromoCell media in the T-25 cell flask

7. Change the media with new AA every day.

8. After 48 hours of incubation, aspirate the media into new 15 ml tubes by passing it through 40µm cell sorters.

9. To each sample add 1:100 protease inhibitor cocktail and store at -20°C for short term storage and -80°C for long term storage.

10. If extracting proteins from cells then use celLytic M lysis buffer, pass through 40µm cell sorters and add 1:100 protease Inhibitor Cocktail and store same as above.

Total protein quantification using Biorad protein assay:

1. Dilute 1 part Dye reagent in 4 parts distilled water. 2.5ml dye and 7.5ml water

2. Prepare bovine serum albumin standards: 0.1mg/ml, 0.25mg/ml, 0.5mg/ml, 1mg/ml and 2mg/ml.

3. Use n=3 and 10µl of each sample

4. Add 200µl of dye reagent to each sample and incubate at RT for 5 minutes
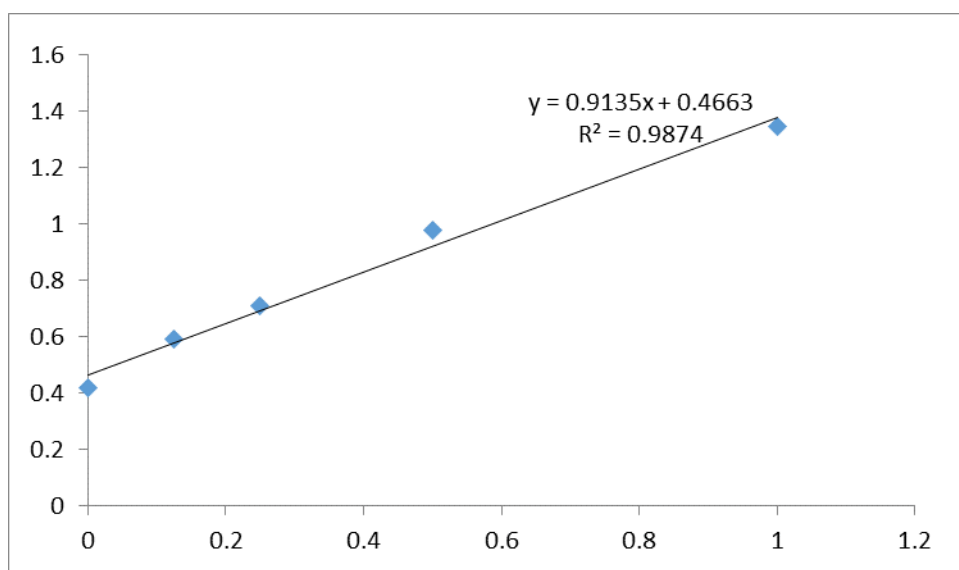
5. Measure absorbance at 595nm

Figure i: Standard protein curve using bovine serum albumin

Concentrating media samples using the Amicon® Ultra-15 Centrifugal filters:

> The samples have to be concentrated prior to western blot as the protein concentration is too dilute to be detected in this condition. This is not required for cell lysates.

1. Add samples to center of the tubes and spin at 4000g for 15 minutes
2. Repeat if required to concentrate more
3. 500µl should be obtained from the first run
4. Multiple the concentration by the dilution factor to obtain new concentration

SDS-page:

Running buffer (10x):

1.	25mM Tris Base	30g
2.	192mM Glycin	144g
3.	SDS	10g
4.	dH$_2$O	1L

Transferring from gel to cellulose membrane (1x transfer buffer)

1.	25 mM Tris base, pH 8.9	3g
2.	192 mM Glycin	14.4g
3.	0.05% SDS	0.5g
4.	Methanol	100ml
5.	dH$_2$O	1L
6.	Run at 75mV for 30 min and 120mV for 1hour	

TBS-Tween 20 (1x, 1L)

1.	Trizma base	2.43g
2.	Tween20	1ml (0.1%)
3.	dH$_2$O	1L

Blocking buffer (500ml)

1.	TBS-Tween20	500ml
2.	3% BSA	15g
3.	Filter and incubated at 4˚C overnight or RT	

Immunoblotting:

1. Prepare Primary antibody solution

TBS-Tween® 20	10ml
3% Bovine Serum Albumin	1.5g
1:1000 primary	10µl

2. Prepare goat anti-rabbit IgG (H+L) Secondary Antibody, HRP conjugate (1:10000, Thermo scientific, RT for 1hr) diluted in TBS-Tween® 20

3. SuperSignal® West Dura Extended Duration Substrate (Thermo Scientific, UK, for 5 min)

4. Chemiluminescence measured using Synegene G: Box for 1min-1hr.

For immunoblotting of housekeeping gene β-actin

1. Wash membrane with TBS-Tween® 20 three times for 10 minutes

2. Incubate with primary monoclonal anti-β-Actin antibody produced in mouse

3. SuperSignal® West Dura Extended Duration Substrate (Thermo Scientific, UK, for 5 min)

Table 8: Standards and samples concentrations measured from Bio-Rad protein assay.

	BSA 1mg/ml	BSA 0.5mg/ml	BSA 0.25mg/ml	BSA 0.1mg/ml	BSA 0.05mg/ml	Untreated RDEB keratinocytes	DMD	PEI	Lipofectamine™2000
Absorbance units	0.96	0.55	0.26	0.13	0.053	1.59	1.57	1.61	1.56
mg/ml	1	0.5	0.25	0.1	0.05	0.38	0.41	0.46	0.45

V. Histochemical Staining using Hematoxylin and Eosin

1. For slides that have been frozen, remove from -20°C and bring to RT.

2. Fix slides in 2 parts ETOH and 1 part acetic acid for 15 minutes at -20°C. For fication use glass container for slides. Make sure slides are not touching each other

3. After fixation, transfer slides from the glass container to a plastic slide holder

4. Rinse slides 2-3 times in water. (can use tab water stream)

5. Stain slides in hematoxylin for 5 minutes. After staining, let excess of hematoxylin to drip down to the paper towel.

6. Wash 2-3 times in water. Let slides sit for 3-5 minutes for each wash.

7. If adequate nuclear staining is required, dip slides in Bluing solution for 30 secs after washes.

8. Dip slides in 75% ETOH for 30 sec-1 min.

9. Dip slides in 95% ETOH for 30 sec-1 min.

10. Stain slides in Eosin for 3 minutes. Let excess of Eosin drip down to paper towel.

11. Dip in 75% ETOH for 30 sec-1 min.

12. Dip in 100% ETOH for 1 min.

13. Dip in 75% ETOH for 1 min.

14. Dip in 95% ETOH for 1 min.

15. Repeat step 14 in fresh container of 95% ETOH.

16. Dip slides in 100% ETOH for 1 min.

17. Dip slides in fresh container of 95% ETOH.

18. Dip in Xylene for 5 minutes. Repeat in fresh container of Xylene (In fume hood).

19. Let the slides air dry.

20. Add permount mounting media to slides and cover with coverslips.

W. *In vivo* injection of polyplexes

Mouse: RDEB col7a1-/- (knockout)

DOB: 25/11/2013

Days of injection: eight, nine and ten days after-birth

Material injected: HPAE polymer/col7α1 pcDNA (30:1 polymer: DNA weight ratio) or multi-knot polymer (3:1).

Areas injected: Intradermal injections. Front paws, 5µg of DNA per paw (10µl solution)

Dorsal region (below the neck), 20µg of DNA (40µl solution)
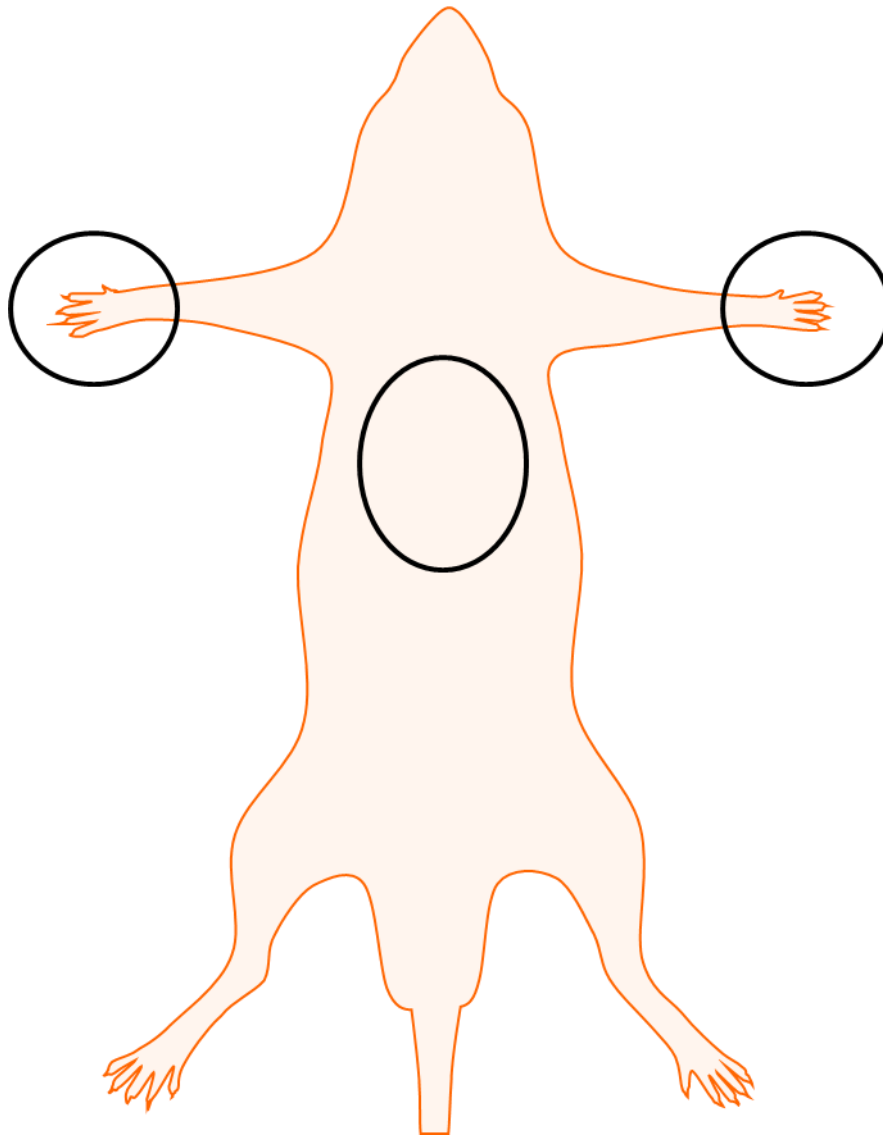
Figure ii: Areas of intradermal injection in RDEB (col7α1-/-) mice.

X. Sacrifice and excision

Mice sacrificed at day 11 after birth and one day post third treatment

Three mice were sacrificed per group

      Group #1: RDEB (col7a1-/-) mouse

      Group #2: wild type mouse

1. Mouse were put to sleep using isoflurane gas before cervical dislocation

2. Using an in vivo fluorescence microscope, images were taken of the area of dorsal injection where a dye was used to trace the polyplexes

3. The fingers were cut and the both paws were placed under OCT compound

4. The mice were shaved and the hair was removed using hair removing lotion

5. The dorsal area of injection was then excised out and placed in OCT compound for cryosectioning

Y. Materials and Reagents

Material	Supplier
Acryloyl Chloride	Sigma-Aldrich
2-Hydroxyethyl disulfide	
Triethylamine	
Magnesium sulphate	
Ethyl-α-bromoisobutyrate (Initiator)	
2-(Dimthylamino)ethyl methacrylate (DMAEMA)	
N,N,N',N'',N''-Pentamethyldiethylenetriamine (Ligand)	
Copper (II) Chloride	
[1,2-dihydroxyethyl]-3,4-dihydroxyfuran-2-one (L-Ascorbic acid)	
1, 3-Diaminopropane (M_w=74.13, ≥99%)	
Ethylenediamine (M_w=60.10, ReagentPlus® 99%)	
Deuterium oxide	
Deuterated acetone	
Deuterated chloroform	
Deuterated Dimethyl sulfoxide	
Sodium carbonate	
Dichloromethane	
ethylenediamine	
Polyethylenimine	
DMEM: Hyclone	
Ham F-12: Hylcone	
Fibrinogen	
Thrombine	
Trasylol	
L-Glutamine	
NaPyruvate	

Appendices

Adenine	
Insulin	
Hydrocortisone	
Cholera Toxin	
Triodothyronine	
CelLytic M cell lysis buffer	
Protease Inhibitor Cocktail	
Monoclonal Anti-Collagen, Type VII antibody produced in mouse clone LH7.2 in ascites fluid	
TBS-Tween® 20	
Monoclonal anti-β-actin antibody produced in mouse	
CellMask™ membrane stain	
Secondary AlexaFlour 594 Donkey anti-rabbit	Invitrogen, Life technologies
Serum FCII: Hyclone	
Epidermal Growth Factor	
TRIzol®	
Secondary alexaFlour 488 donkey anti-mouse IgG (H+L)	
Alamar Blue®	
Anti-CD103 (hamster)	
Vybrant® dye cycle	
Lipofectamine®2000	
Anti-CD 44 (Rat)	Abcam®
Anti-CD11B (Rat)	
Anti-CD45 (Goat)	
Anti-Ly6g (Rat)	
GoTaq® qPCR Mastr Mix	Promega
goat anti-mouse horseradish peroxidase (HRP) secondary	
SuperSignal® West Dura Extended	Thermo scientific

Duration Substrate	
Verso one-step RT-PCR kit	
Precast gels	Bio-Rad
Hybond-C extra cellulose membrane	
Bio-Rad protein assay kit	
Keratinocyte Growth Medium 2 SupplementPack and basal medium	PromoCell
BioLux® *Gaussia* luciferase kit	New England BioLabs® Inc.
BioCoat 6 well deep well plate	Bd biosciences
Cell Culture Inserts, 3 μm pore size, PET-track-etched membrane, 6 well format	
Amicon® Ultra-15 Centrifugal Filters 10,000 NMWL	MILLIPORE
Rabbit anti-collagen IV polyclonal	
Rabbit anti-collagen VII polyclonal	
Xfect®	Clontech
RNeasy® mini kit	Qiagen

Z. Conference Proceedings, Journal Publications and Patents

Conference proceedings

- **Aied A.,** <u>Zao T.</u>, Mauerer E., South A., Carroll O., Greiser U., Pandit A., and Wang W. 'Knotted polymer structure: Efficient nucleic acid delivery agents'. Podium presentation at the annual conference of the *European Society for Biomaterials,* 2013, Madrid, Spain.

- **Aied A.,** Mauerer E., South A., Carroll O., Greiser U., Pandit A., and Wang W. 'Knotted Polymer Structures: Efficient Nucleic Acid Delivery Agents'. Podium presentation at the annual conference of the *Tissue Engineering and Regenerative Medicine International Society-EU,* 2013, Istanbul, Turkey.

- **Aied A.,** Murauer E., Carroll O., Cutlar L., Zheng Y., South A., Pandit A., and Wang W. 'Restoration of Collagen Type VII Expression in Recessive Dystrophic Epidermolysis Bullosa using a Cationic Polymer'. Poster presentation at the *Epidermolysis Bullosa 2012 conference,* Marbella, Spain.

- **Aied A.,** Murauer E., Carroll O., Cutlar L., Zheng Y., South A., Pandit A., and Wang W. 'Restoration of Collagen Type VII Expression in Recessive Dystrophic Epidermolysis Bullosa using a Cationic Polymer'. Poster presentation at the annual meeting of *European Society for Dermatological Research,* 2012, Venice, Italy.

- **Aied A.,** Cao H., Dong Y., Zheng Y., Pandit A., and Wang W. 'Biodegradable Disulfide-Cationic Polymer for the Gene Therapy of Recessive Dystrophic Epidermolysis Bullosa'. Podium presentation at the annual conference of the *European Society for Biomaterials*, 2011, Dublin, Ireland.

- **Aied A.,** Cao H., Dong Y., Zheng Y., Pandit A., and <u>Wang W</u>. 'Biodegradable Disulfide-Cationic Polymer for the Gene Therapy of Recessive Dystrophic Epidermolysis Bullosa'. Podium presentation at the annual conference of the *Tissue Engineering and Regenerative Medicine International Society-EU*, 2011, Granada, Spain.

- **Aied A.,** Glynn B., Tai H., Newland B., Saeed A., and Wang W. 'Direct Detection of Model Target MicroRNA Using a DMAEMA-EGDMA Dendritic Polymer DNA Probe Complex for Clinical Applications'. Poster presentation at 23rd annual conference of the *European Society for Biomaterials*, 2010, Finland.

- **Aied A.,** Glynn B., Tai H., Newland B., Saeed A., and Wang W. 'Detection of Model Target MicroRNA Using a DMAEMA-EGDMA Dendritic Polymer Complexes DNA Probe for Clinical Application'. Poster presentation annual Meeting & Exposition of the *Controlled Release Society* (CRS), 2010, Portland, USA.

Peer-reviewed articles

- **Ahmed Aied**, Udo Greiser, Abhay Pandit and Wenxin Wang. 'Polymer gene delivery: Overcoming obstacles'. *Drug Discovery Today*. 2013, in press. DOI: 10.1016/j.drudis.2013.06.014. (IF: 6.5)

- Yixiao Dong, **Ahmed Aied,** Junming Li, Qi Wang, Xuejun Hu, Wenxin Wang. 'An *in vitro* approach for production of non-scar minicircle DNA vectors'. *Journal of Biotechnology*. 2013, 166, 84-87. (IF: 3.18)

- Sandra Ganly, Sean O. Hynes, Faisal Sharif, **Ahmed Aied**, Valerie Barron, Karl McCullagh, Jill McMahon, Peter McHugh, Jim Crowley, Wenxin Wang, Timothy O'Brien, Udo Greiser. 'Liposomal surface coatings of metal stents for efficient non-viral gene delivery to the injured vasculature'. *Journal of Controlled Release.* 2012, 167, 109-119. (IF: 7.6)

- **Ahmed Aied,** Yu Zhneg, Abhay Pandit and Wenxin Wang. 'DNA 'Immobilization on cellulose paper using a grown cationic polymer via ATRP'. *ACS applied materials and interfaces* 2012, 4, 826-831. (IF: 5.008)

- **Ahmed Aied**, Barry Glynn, Ben Newland, Hongliang Cao, Hongyun Tai, Abhay Pandit and Wenxin Wang. 'A fluorescently labelled hyperbranched polymer synthesized from DE-ATRP for the detection of DNA hybridization' *Polymer chemistry* 2012, 3, 332-334. (IF: 5.2)

Patents

- **Ahmed Aied,** Wenxin Wang and Abhay Pandit. 'Disulfide based cationic polymer synthesised from controlled living polymerisation and synthesis of disulfide monomer'. Patent No. 12187515.7-1217.